Jesús Salgado Benito

Sustitución metálica en proteínas azules de cobre

Propiedades químicas y estructurales de las azurinas de níquel y cobalto

Tesis Doctoral

Universitat de València

Burjassot (València), 1995.

ProQuest LLC
789 East Eisenhower Parkway
P.O. Box 1346
Ann Arbor, MI 48106-1346

Metal substitution in blue copper proteins

Chemical and structural properties of cobalt and nickel azurins

s Químicas

This research has been supported in part by the Conselleria de Educació i Ciència (Generalitat Valènciana).

Departament de Química Inorgànica
Facultat de Química

Universitat de València

JOSEP-MARIA MORATAL i MASCARELL, Catedràtic de Química Inorgànica de la Universitat de València,

CERTIFICA: Que En Jesús Salgado i Benito, Llicenciat en Biología, ha realitzat als laboratoris del Departament de Química Inorgànica de la Universitat de València, i baix la meua direcció, el treball que per a optar al Grau de Doctor ací es presenta, amb el titol de: *"Sustitución metálica en proteínas azules de cobre: propiedades químicas y estructurales de las azurinas de nickel y cobalto"*.

I per a que així conste, signe aquest certificat, en Burjassot a dèneu de Setembre de mil noucents noranta cinc.

Josep-Maria Moratal i Mascarell

But is not an event all the more significant and privileged the more chances are necessary to produce it ?. Only chance can appear before us like a message. What happens of necessity, what is expected, what is repeated every day, is mute. Only chance talks to us. We try to read it as gypsies read the figures formed by the coffee dregs on the bottom of a cup.

Milan Kundera (1984) *"Nesnesitelná lehkost bytí"*
(*The unbearable levity of the being*), 2nd part: *Soul and body*, 9.

... You can only depend on one thing, You need a Busload of Faith to get by.

Lou Reed (1989) *New York: "Busload of Faith"*.

A mi familia,
por estar siempre ahí

Abbreviations.

1D	one-dimensional
2D	two-dimensional
Ade	*Alcaligenes denitrificans*
C112D	Cys112→Asp
COSY	correlation spectroscopy
cyt	cytochrome
EPR	electron paramagnetic resonance
ESE	electron self-exchange
ET	electron transfer
IEF	iso-electric focusing
IPTG	isopropyl-β-D-thiogalactopyranoside
LF	ligand field
LMCT	ligand-to-metal charge transfer
M121Q	Met121→Gln
NMR	nuclear magnetic resonance
NiR	cytochrome-cd_1 nitrite reductase
NOE	nuclear Overhauser effect
NOESY	nuclear Overhauser effect spectroscopy
Pae	*Pseudomonas aeruginosa*
PAGE	polyacrylamide gel electrophoresis
r.m.s	root-mean-square
TPPI	time-proportional phase increment
TOCSY	total correlation spectroscopy
WEFT	water-eliminated Fourier transformation.

Table of Contents

hapter **1**

ZURIN, METAL SUBSTITUTION AND PARAMAGNETIC-NMR: eneral aspects and objective of this work. 1

I. Introduction and objective..... 1

II. Azurin and the blue-copper proteins. 5

a) Types of copper site in biological systems: the type 1 site. 5

The type 1 copper-proteins family..... 6

b) The function of blue-copper proteins. 10

c) Structural, spectroscopic and redox properties. 12

The crystal structure of azurin. 12

Electronic and Raman spectra. 16

EPR spectroscopy..... 18

Redox and electron-transfer properties. 19

III. The genetic approach..... 23

a) Site directed mutagenesis and structure/function relation-ships in azurin..... 24

Mutations in the metal site. The minimum requirements for a blue-copper site..... 24

Studying docking patches and electron-transfer pathways..... 25

IV. Metal substitution and spectroscopic probes..... 27

a) Why replacing metals in metalloproteins?..... 27

b) Metal substitution in blue-copper proteins. 28

V. NMR of paramagnetic molecules. 31

a) The NMR phenomenon and the paramagnetic effect. Disadvantages and virtues. 31

The hyperfine shift. 32

Paramagnetic relaxation..... 35

b) The unpaired-electron relaxation: a determining factor. 37

c) Paramagnetic-NMR and copper proteins..... 38

d) Probing the blue-copper site by NMR on the cobalt and nickel derivatives. 39

Cobalt(II) in paramagnetic-NMR. 39

Nickel(II) in paramagnetic-NMR. 41
NMR investigations on nickel and cobalt derivatives of blue-copper proteins. 43
e) Assignment of paramagnetic signals: a limiting step. 43

Chapter **2**

EXPERIMENTAL METHODOLOGY. 47
I. Obtaining and preparing the protein samples 47
a) Bacterial growth. 47
b) Protein isolation and purification. 48
Pseudomonas aeruginosa azurin. 48
Alcaligenes denitrificans azurin. 50
c) Metal replacement and preparation of samples 52
II. NMR spectroscopy: measurements and calculations 55
a) Performing the spectra 55
b) Determining relaxation times. 56
c) Analyzing pH dependent effects. 60
pH titrations: determining the pK_a. 60
Exchange rates of conformational transitions 61
d) Proton exchange analysis. 62
e) Determining inter-proton distances from 1D NOE data. 63
f) Analyzing temperature dependence of the isotropic shifts. 66
g) Assigning paramagnetic NMR signals 67
III. Other techniques 69
a) Electronic spectroscopy 69
b) EPR spectroscopy. 69
c) Magnetic measurements. 69
d) X-ray diffraction analysis. 70

Chapter **3**

***Pseudomonas aeruginosa* NI(II)-AZURIN: a nickel substituted blue copper protein 73**
I. Characterization of nickel azurin by paramagnetic NMR 73
RESULTS 73
a) The ^1H NMR spectrum 73
b) Assignment of the isotropically-shifted signals 77
c) Other assignments. 82
DISCUSSION 85
a) The analysis of the NMR spectra. 85
b) The nickel-azurin metal site. 88
c) pH dependent structural variations 89
II. The X-ray structure of nickel-azurin 95
RESULTS 95

DISCUSSION.....101
a) The structure of the Ni(II)–azurin metal site..... 101
b) Binding of different metals to azurin..... 102
III. Magnetic susceptibility of Ni(II)-azurin.....107
RESULTS AND DISCUSSION.....107
IV. Concluding remarks.....111

Chapter **4**

CHARACTERIZATION OF CO(II)-AZURIN FROM *P. aeruginosa* 115
I. Paramagnetic-NMR study.....115
RESULTS.....115
a) The ^{1}H NMR spectrum of Co(II)-azurin..... 115
b) Assignment of the ^{1}H NMR signals..... 120
c) Additional assignments..... 130
DISCUSSION.....135
a) The assignments..... 135
b) NMR properties: interpretation and consequences..... 137
Metal coordination..... 137
His35 and the effect of pH in the azurin structure..... 141
Exchange of the His117 $N_{\varepsilon 2}H$ proton..... 142
II. EPR spectroscopy of Co(II)-azurin.....147
RESULTS AND DISCUSSION.....147
III. Concluding remarks.....151

Chapter **5**

***Alcaligenes denitrificans* AZURIN AND ITS M121Q MUTANT:**
^{1}H NMR Study of the cobalt and nickel derivatives.....157
RESULTS.....157
a) UV-Vis spectra of Co(II) and Ni(II) derivatives of wild type and M121Q azurins.157
b) ^{1}H NMR spectra of the Ni(II) metalloderivatives..... 158
Wild-type nickel azurin..... 158
M121Q nickel azurin..... 161
c) ^{1}H NMR spectra of the Co(II) metalloderivatives..... 167
wild-type cobalt azurin..... 167
M121Q cobalt azurin..... 169
DISCUSSION.....173
a) Absorption spectra..... 173
b) ^{1}H NMR spectra of wt and M121Q azurin metalloderivatives..... 174
c) The Met121Gln azurin mutant and the stellacyanin metal site..... 178
CONCLUDING REMARKS.....181

Chapter **6**

FINAL CONCLUSIONS 183
Cobalt and nickel as NMR-probes for the azurin copper site 183
The structure of the metal site 184
Other investigated properties of azurin 186

SUSTITUCIÓN METÁLICA EN PROTEÍNAS AZULES DE COBRE: propiedades químicas y estructurales de las azurinas de níquel y cobalto 189

I. Introducción y objetivos 191

II. Breve revisión sobre la azurina 195
a) La azurina: una proteína azul de cobre 195
b) Estructura de la azurina 196
c) Relaciones estructura/función en azurina: estudios de mutagénesis dirigida 198

III. Experimental 201
a) Obtención de azurina y preparación de muestras 201
Extracción y purificación de azurina 201
Preparación de los derivados metálicos 202
b) Métodos físicos 202
Espectroscopia UV-vis 202
Espectros de EPR 202
Medidas magnéticas 203
Resonancia magnética nuclear 203
Cristalografía de rayos X 205

IV. Resultados 207
a) Azurina de níquel(II) 207
Espectros RMN de protón 207
Estructura de rayos X 210
Medidas de susceptibilidad magnética 210
b) Azurina de cobalto(II) 211
RMN de protón 211
Espectros de EPR 213

V. Discusión 215
a) Cobalto y níquel como sondas espectroscópicas de las proteínas azules de cobre 215
b) El centro metálico en las azurinas de níquel y cobalto 216
c) Cambio conformacional y otros efectos asociados al pH 218
d) El mutante M121Q y el centro metálico en estelacianina 220

VI. Conclusiones 221

AGRADECIMIENTOS • ACKNOWLEDGMENTS 223

Chapter **1**

Azurin, metal substitution and paramagnetic-NMR:

general aspects and objective of this work.

I. Introduction and objective.

Blue copper proteins have been an exciting matter for scientists from the very moment of the discovery of laccase, isolated from the Japanese lacquer tree more than a century ago[1]. Many years later, stellacyanin was found also in lacquer tree extracts[2]. But the investigation of the blue-copper proteins expands from mid fifties, with the discovery of azurin from *Pseudomonas aeruginosa* bacteria[3] and plastocyanin from spinach leaves[4]. Promptly characterized as copper proteins with an electron transfer function[3c,5,6], they immediately attracted the attention of chemists and biochemists due to their unusual spectroscopic features, never found before in any other known copper complexes. An abnormally intense blue color was from the beginning their principal characteristic, which became part of their name, either as a general type of copper proteins: the "blue-copper proteins"

---

[1] Yosida, H. (1883) *J. Chem. Soc. 43*, 472.

[2] Keilin, D. & Mann, T. (1940) *Nature 145*, 304.

[3] a) Verhoeven, W. & Takeda, Y. (1956) in *Organic Nitrogen Metabolism* (McElroy, W.D. & Glass, W.B., ed.) p. 159, The Johns Hopkins Press, Baltimore. b) Horio, T. (1958) *J. Biochem. 45*, 195 c) Horio, T. (1958) *J. Biochem. 45*, 267.

[4] Kato, S. & Takamiya, A. (1961) *Nature 189*, 665.

[5] a) Nakamura, T. (1958) *Biochim. Biophys. Acta 30*, 44. b) Yamanaka, T., Kiyimoto, S. & Okunuki, K. (1963) *J. Biochem. 53*, 256.

[6] Ambler, R.P. & Brown, L.H. (1967) *Biochem. J. 104*, 784.

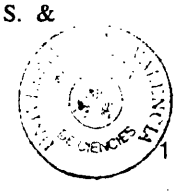

(also called later type 1 copper proteins or cupredoxins), or as a subtype of them: the "azurins"[7].

The fifties were also the beginning of the *Bioinorganic Chemistry*, a new discipline born in the interface between Chemistry and Biology which then expanded and established during the sixties and the seventies[8]. A large number of metalloenzymes and metalloproteins were found in living organisms, in which metals, despite being minority atoms, monopolize the principal roles and are capable of binding and activating substrates or mediate fundamental reactions like electron transfer[8]. Many of the researchers who contributed to the development of this new interdisciplinary field, E.I. Solomon, B.G. Malmström, H.B. Gray and H.A.O. Hill among others, centered an important part of their activity in the blue-copper proteins. Their spectroscopic, structural and functional investigations gave an early explanation to the distinctive features of these metal sites[9]. Parallel, the idea that the protein environment imposes unusual geometric and electronic structures on the metal ions, which are in turn essential for the development of their biological function, spread and became familiar to the bioinorganic chemistry community[10]. Other different types of blue-copper proteins were purified from bacterial and plant sources, and the structure of some of them was solved by X-ray crystallography[11]. As the structural knowledge of these proteins grew, they became one of the preferred model systems, together with the small cytochromes *c*, for the study of biological electron transfer[12]. More recently, the application of genetic techniques has made available a large number of site-directed mutated blue-copper proteins. It has permitted to check the actual importance of individual

---

[7] The name "Azurin" was proposed by Sutherland and Wilkinson, who showed that these proteins were widely distributed in the genera *Pseudomonas, Bordetella* and *Alcaligenes* (Sutherland, I.W. & Wilkinson, J.F. (1963) *J. Gen. Microbiol. 30*, 105).

[8] Eichhorn, G.L., ed. (1973) *Inorganic Biochemistry* , Elsevier, Amsterdam.

[9] a) Peisach, J., Aisen, P. & Blumberg, W.E., eds. (1966) *The Biochemistry of Copper*, Academic Press, New York. b) Malkin, R. & Malmström (1970) *Adv. Enzymol 33*, 177. c) Gray, H.B. & Solomon, E.I. (1981) in *Copper proteins* (Spiro, T.G., ed) p. 1, Wiley, New York.

[10] a) Williams, R.J.P. (1963) in *Molecular bases of enzyme action and inhibition* (Desnuelle, P.A.E., ed.) p. 133, Pergamon Press, Oxford. b) Malmström, B.G. (1965) in *Oxidases and related redox systems* (King, T.E., Mason, H.S. & Morrison, M., eds.) vol. 1, p. 207, Wiley, New York. c) Vallee, B.L. & Williams, R.J.P. (1968) *Proc. Natl. Acad. Sci. U.S.A. 59*, 498. d) Gray, H.B. & Malmström, B.G. (1983) *Comments Inorg. Chem. 2*, 203.

[11] a) Colman, P.M., Freeman, H.C., Guss, J.M., Murata, M., Norris, V.A., Ramshaw, J.A.M. & Venkatappa, M.P. (1978) *Nature 272*, 319. b) Adman, E.T. Stenkamp, R.E., Sieker, L.C., & Jensen, L.H. (1978) *J. Mol. Biol. 123*, 35.

[12] a) Canters, G.W. & van de Kamp, M. (1992) *Curr. Opin. Struct. Biol. 2*, 859. b) Wuttke, D.S. & Gray, H.B. (1993) *Curr. Opin. Struct. Biol. 3*, 555.

aminoacid residues in the general spectroscopic, structural and functional properties of the protein, and to investigate defined electron transfer pathways and docking patches[12,13].

Metal substitution, as one of the main approaches for the investigation of metalloproteins, has been also used in the case of blue-copper proteins. Copper has been replaced by cobalt, nickel, manganese, mercury and cadmium[14], among others, and the study of the corresponding metalloderivatives have been important to characterize the structural and spectroscopic features of the blue copper site. This thesis deals with the study of nickel and cobalt metallosubstituted azurin. The structural characteristics of the substituted metal site are investigated by means of different techniques, being paramagnetic-NMR[15] the most notable. The scope of this work is double. On one hand, we intend to set up the basis for the use of paramagnetic probes and paramagnetic NMR in the investigation of blue-copper proteins, as it has been extensively done in the case of zinc enzymes[16]. On the other hand, it is also our intention to contribute with this approach to a better understanding of the blue-copper proteins, taking azurin as an example.

The question of the protein-controlled metal coordination in azurin will be addressed. Thus, the study of the metallosubstituted azurin site will allow us to test its flexibility. The modes of metal coordination found here will be analyzed and compared with the structure of the native copper-azurin[17,18], as well as with the structure of other azurin metalloderivatives studied elsewhere[19], using both X-ray crystallographic data and spectroscopic data in solution (principally from NMR). Additionally, we will pay also attention to some other important topics of azurin, particularly, those dynamic aspects that can be better studied in solution by NMR due to the improvement of the observation conditions introduced by the

---

13 Canters, G.W. & Gilardi, G. (1993) *FEBS Lett. 325*, 39.

14a) McMillin, D.R., Rosemberg, R.C. & Gray, H.B. (1974) *Proc. Natl. Acad. Sci. USA 71*, 4760. b) Tennent, D.L. & McMillin, D.R. (1979) *J. Am. Chem. Soc. 101*, 2307. c) Mitra, S. & Bersohn, R. (1982) *Proc. Natl. Acad. Sci. U.S.A. 79*, 6807. d) Engeseth, H.R., McMillin, D.R. & Otvos, J.D. (1984) *J. Biol. Chem. 259*, 4822.

15Bertini, I. & Luchinat, C. (1986) *NMR of Paramagnetic Molecules in Biological Systems*, The Benjamin/Cummings Publishing Company, Menlo Park.

16Bertini, I & Luchinat, C. (1986) in *Zinc Enzymes* (I. Bertini, C. Luchinat, W. Maret, M. Zeppezauer eds.) p. 27, Birkhäuser, Boston.

17Baker, E.N. (1988) *J. Mol. Biol. 203*, 1071.

18Nar, H., Messerchmidt, A., Huber, R., van de Kamp, M. & Canters, G.W. (1991) *J. Mol. Biol. 221*, 765.

19Nar, H., Huber, R., Messerschmidt, A., Filippou, A.C., Barth, M., Jaquinod, M., van de Kamp, M. & Canters, G.W. (1992) *Eur. J. Biochem. 205*, 1123.

paramagnetic probe, like structural transitions and proton exchange. Finally, one of the many azurin mutants obtained in the last few years, the Met121Gln azurin[20], will be also studied here. The Co(II) and Ni(II) derivatives of this mutant will be characterized as an example of an important sub-family of the blue-copper proteins: the so called stellacyanin-like, which present an axial glutamine coordinated to the metal instead of a methionine.

[20]Romero, A., Hoitink, C.W.G., Nar, H., Huber, R., Messerschmidt, A. & Canters, G.W. (1993) *J. Mol. Biol. 229,* 1007.

II. Azurin and the blue-copper proteins.

a) Types of copper site in biological systems: the type 1 site.

Copper is one of the most widely distributed metal ions in the living world[9,21]. Copper-containing proteins appear in plants, animals, bacteria and archaea and participate in important metabolic processes as oxygen transport, oxidative catalysis and electron transfer[21]. Particular arrangements of the copper site in each of these systems, confer on them the pertinent chemical properties needed for the perfect development of their function. The very early investigated copper proteins laccase and ceruloplasmin present various forms of copper sites[10b]. They can be distinguished from their spectroscopic features, which were the basis for their classification in three main types[10b,22,23]:

Type 1 Cu(II), EPR detectable, reoxidizable and responsible for the strong blue color. Its distinctive spectral features are an intense absorption band around 600 nm ($\varepsilon \geq 1500\ M^{-1}cm^{-1}$), and very small parallel hyperfine splitting constants ($A_{\parallel} \leq 60 \times 10^{-4}\ cm^{-1}$) and small g values in the EPR spectrum, compared with other copper complexes.

Type 2 Cu(II), EPR detectable but non-blue and non-reoxidizable. Its spectroscopic characteristics can be considered normal in copper coordination chemistry. Its EPR spectrum presents large parallel hyperfine splitting constants ($A_{\parallel} \geq 140 \times 10^{-4}\ cm^{-1}$) and $g_{\parallel} > g_{\perp} > 2.00$, and the visible bands in the electronic spectrum have very low extinction coefficients ($\varepsilon \leq 100\ M^{-1}cm^{-1}$).

Type 3 Cu(II), antiferromagnetically coupled pair of Cu(II) ions non-detectable by EPR. The spin-pairing between the electrons of the two Cu(II) ions is due to the presence of a bridging ligand. Its visible spectrum is characterized by a strong absorption around 300 nm.

This classification of the laccase copper sites was later the origin of a general classification of the copper proteins on the basis of their spectral features[21,24]. Thus, azurins and blue-copper proteins in general, whose

---

[21] **a)** Sigel, H., ed. (1981) *Metal ions in Biological systems*, vol. 13: *Copper proteins*, Marcel Dekker, New York. **b)** Spiro, T.G., ed. (1981) *Copper proteins*, Wiley, New York. **c)** Adman, E.T. & Turley, S. (1993) in *Bioinorganic chemistry of copper.* (Karlin, K.D. & Teyklar, Z., eds.) Chapman & Hall, New Yok.

[22] Malkin, R., Malmström, B.G. & Vänngård, T. (1969) *Eur. J. Biochem. 7*, 253.

[23] **a)** Vänngård, T. (1972) in *Biological Applications of Electron Spin Resonances* (Schwartz, ed.) p. 441, Wiley, New York. **b)** Fee, J.A. (1975) *Struct Bonding 23*, 2.

[24] Solomon, E.I., Penfield, K.W. & Wilcox, D.E. (1983) *Struct. Bonding 53*, 1.

spectroscopic characteristics are very similar to those of the type 1 copper site in laccase and ceruloplasmin, constitute the family of type 1 copper proteins, also called cupredoxins. They are generally small, contain a single copper site and function as electron carriers[21,25]. The typical example of a type 2 copper protein is superoxide dismutase[26], where the copper site is involved in the binding and catalytic removal of superoxide. Tyrosinase and Hemocyanin contain a type 3 copper site which can bind dioxygen[27]. And multicopper oxidases, which include laccase, ceruloplasmin and ascorbate oxidase, contain the three types of copper[28]. However, in this last group of proteins the type 2 and type 3 sites form a trinuclear cluster, called type 4 copper site, which functions as a unit in the multielectron reduction of O_2 to H_2O[28]. There is finally a type of copper site whose spectroscopic characteristics do not fit to any of the aforementioned three types. It is the so called Cu_A or purple copper, found in the cytochrome *c* oxidase subunit II and in nitrous oxide reductase[29]. This is a binuclear mixed-valence copper center[29a] in which a direct copper-copper metal bond seems to be present[29d,30].

The type 1 copper-proteins family.

To this group belong a large number of proteins which have been classified according to their sequence, structure and presumed physiological function[25]. Many of them are bacterial, like azurin[3,5,6,31], pseudoazurin[32], amicyanin[33],

---

[25]a) Adman, E.T. (1985) *Top. Mol. Struct. Biol. 6*, 1. **b)** Adman, E.T. (1991) *Adv. Protein Chem. 42*, 145. **c)** Chapman, S.K.(1991) in *Perspectives on Bioinorganic Chemistry* (Hay, R.W., Dilworth, J.R. & Nolan, K.B., eds.) vol 1, p. 95, Jai Press Ltd, London. **d)** Sykes, A.G. (1991) *Adv. Inorg. Chem. 36*, 377. **e)** Lappin, G.A. (1981) in *Metal ions in Biological Systems* (Sigel, H., ed.) vol. 13, p. 15, Marcel Dekker, Inc, New York.

[26]Valentine, J.S., & Pantoliano, M.W. (1981) in *Copper proteins* (Spiro, T.G., ed.) p. 291, Wiley, New York.

[27]a) Lontie, R. & Witters, R. (1981) in *Metal ions in biological systems* (Sigel, H., ed.) vol. 13, p. 229, Marcel Dekker, New York. **b)** Lerch, K. (1991) in *Metal ions in biological systems* (Sigel, H., ed.) vol. 13, p. 143, Marcel Dekker, New York.

[28]Messerschmidt, A., Ladenstein, R., Huber, R., Bolognesi, M., Avigliano, L., Petruzzelli, R., Rossi, A. & Finazzi-Agró, A. (1992) *J. Mol. Biol. 224*, 179.

[29]a) Antholine, W.E., Kastrau, D.H.W., Steffens, G.C.M., Buse, G., Zumft, W.G. & Kroneck, P.H.M. (1992) *Eur. J. Biochem. 209*, 875. **b)** Malmström, B.G. & Aasa, R. (1993) *FEBS Lett. 325*, 49. **c)** Kelly, M., Lappalainen, P., Talbo, G., Haltia, T., van der Oost, J. & Saraste, M. (1993) *J. Biol. Chem. 268*, 16781. **d)** Iwata, S., Ostermeier, C., Ludwig, B. & Michel, H. (1995) *Nature 376*, 660.

[30]Blackburn, N.J., Barr, M.E., Woodruff, W.H., van der Oost, J. & Devries, S. (1994) *Biochemistry, 33*, 10401.

[31]a) Ambler, R.P. & Tobari, J. (1989) *Biochem. J. 261*, 495. **b)** Groeneveld, C.M., Aasa, R.

rusticyanin[34], auracyanin[35] and halocyanin[36]. Other are found in plants, like plantacyanin[37] and cucumber basic blue protein, CBP[38]; or in photosynthetic plants and cyanobacteria, like plastocyanin[39]. Finally, there are various

Reinhammar, B. & Canters, G.W. (1987) *J. Inorg. Biochem. 31*, 143. **c)** Ainscough, E.W., Bingham, A.G., Brodie, A.M., Ellis, W.R., Gray, H.B., Loehr, T.M., Plowman, J.E., Norris, G.E. & Baker, E.N. (1987) *Biochemistry 26*, 71. **d)** Canters, G.W. (1987) *FEBS Lett. 212*, 168. **e)** Groeneveld, C.M. & Canters, G.W. (1988) *J. Biol. Chem. 263*, 167. **f)** Zumft, W.G. Gotzmann, D.J. & Kroneck, P.M.H. (1987) *Eur. J. Biochem. 168*, 301. **g)** Causer, M.J., Hopper, D.J., McIntire, W.S. & Singer, T.P. (1984) *Biochem. Soc. Trans. 12*, 1131. **h)** Broman, L., Malmström, B.G., Aasa, R. & Vänngård, T (1963) *Biochim. Biophys. Acta 75*, 365. **i)** Hutnik, C.M. & Szabo, A.G. (1989) *Biochemistry 28*, 3923. **j)** Martinkus, K., Kennelly, P.J., Rea, T. & Timkovich, R. (1980) *Arch. Biochem. Biophys. 199*, 465.

[32] **a)** Kakutani, T., Watanabe, H., Arima, K. & Beppu, T. (1981) *J. Biochem. 89*, 463. **b)** Liu, M.Y., Liu, M.C., Payne, W., LeGall, J. (1986) *J. Bacteriol. 166*, 604. **c)** Yamamoto, K., Uozumi, T., Beppu, T. (1987) *J. Bacteriol. 169*, 5648. **d)** Adman, E.T., Turley, S., Bramson, R., Petratos, K., Banner, D., Tsernoglou, D., Beppu, T. & Watanabe, H. (1989) *J. Biol. Chem. 264*, 87. **e)** Petratos, K., Dauter, Z., Wilson, K.S. (1988) *Acta Cryst. B44*, 628.

[33] **a)** Ambler, R.P. & Tobari, J. (1985) *Biochem. J. 232*, 451. **b)** van Houwelingen, T., Canters, G.W., Stobbelaar, G., Duine, J.A., Frank, J.Jzn. & Tsugita, A. (1985) *Eur. J. Biochem. 153*, 75. **c)** Husain, M. & Davidson, V.L. (1985) *J. Biol. Chem. 260*, 14626. **d)** Dinarieva, T. & Netrusov, A. (1989) *FEBS Lett. 259*, 47. **e)** Lommen, A. & Canters, G.W. (1990) *J. Biol. Chem. 265*, 2768. **f)** Kalverda, A.P., Wymenga, S.S., Lommen, A., van de Ven, F.J.M., Hilbers, C.W. & Canters, G.W. (1994) *J. Mol. Biol. 240*, 358. **g)** Romero, A., Nar, H., Messerschmidt, A., Kalverda, A., Canters, G.W., Durley, R. & Mathews, F.S. (1994) *J. Mol. Biol. 236*, 1196. **h)** Ubbink, M., van Kleef, M.A.G., Kleinjan, D.J., Hoitink, C.W.G., Huitema, F., Beintema, J.J., Duine, J.A. & Canters, G.W. (1991) *Eur. J. Biochem. 202*, 1003. **i)** Chen, L., Durley, R., Poliks, B.J., Hamada, K., Chen, Z., Mathews, F.S., Davidson, V.L., Satow, Y., Huizinga, E., Vellieux, F.M.D. & Hol, W.G.J. (1992) *Biochemistry 31*, 4959.

[34] **a)** Cox, J.C. & Boxer, D.H. (1978) *Biochem. J. 174*, 497. **b)** Yano, T., Fukumori, Y. & Yamanaka, T. (1991) *FEBS Lett. 288*, 159.

[35] Trost, J.T., McManus, J.D., Freeman, J.C., Ramakrishna, B.L. & Blankenship, R.E. (1988) *Biochemistry 27*, 7858.

[36] Scharf, B. & Engelhard, M. (1993) *Biochemistry. 32*, 12894.

[37] **a)** Aikazyan, V.T. & Nalbandyan, R.M. (1975) *FEBS Lett. 55*, 272. **b)** Nersissian, A.M.& Nalbandyan, R.M. (1988) *Biochim. Biophys. Acta 957*, 446.

[38] **a)** Murata, M., Begg, G.S., Lambrov, F., Leslie, B., Simpson, R.J., Freeman, H.C. & Morgan, F.J. (1982) *Proc. Natl. Acad. Scien. U.S.A. 79*, 6434. **b)** Guss, J.M., Merritt, E.A., Phizackerley, R.P., Hedman, B., Murata, M., Hodgson, K.O. & Freeman, H.C. (1988) *Science 241*, 806.

[39] **a)** Guss, J.M. & Freeman, H.C. (1983) *J. Mol. Biol. 169*, 521. **b)** Hervás, M., Navarro, F., Navarro, J.A., Chávez, S., Díaz, A., Florencio, F.J. & de la Rosa, M.A. (1993) *FEBS Lett. 319*, 257. **c)** Moore, J.M., Case, D.A., Charzin, W.J., Gippert, G.P., Havel, T.F., Powls, R. & Wright, P.E. (1988) *Science 240*, 314. **d)** Sykes, A.G. (1991) *Struct. Bonding 75*, 175. **e)** Redinbo, M.R., Yeates, T.O. & Merchant, S. (1994) *J. Bioenerg. Biomembr. 26*, 49. **f)** Penfield, K.W., Gay, R.R., Himmelwright, R.S., Eickman, N.C., Norris, V.A., Freeman, H.C. & Solomon, E.I. (1981) *J. Am. Chem. Soc. 103*, 4382.

glycosylated plant blue-copper proteins, like stellacyanin[40], umecyanin[41], mavicyanin[42] and cucumber peeling cupredoxin, CPC (also called stellacyanin-like cucumber protein, SLCP)[43]. For a detailed list of them, see Table 1:1.

As we have seen above, the type 1 site can be also found in multicopper proteins, such as the plant blue oxidases ascorbate oxidase[28] and laccase[44], ceruloplasmin from blood-plasma[45] and some bacterial nitrite reductases[46]. On the other hand, type 1 binding motifs are present in many proteins like the bacterial H8 outer membrane proteins[47], and the human coagulation factor VIII[48]. Finally, the so-called cupredoxin folding is present in the subunit II of cytochrome *c* oxidases and quinol oxidases[29d,49].

[40a] Peisach, J., Levine, W.G. & Blumberg, W.E. (1967) *J. Biol. Chem. 242*, 2847. **b)** Malmström, B.G., Reinhammar, B. & Vänngård, T. (1970) *Biochim. Biophys. Acta 205*, 48. **c)** Feiters, M.C., Dahlin, S. & Reinhammar, B. (1988) *Biochim. Biophys. Acta 955*, 250. **d)** Fields, B.A., Guss, J.M. & Freeman, H.C. (1991) *J. Mol. Biol. 222*, 1053. **e)** Ferris, N.S., Woodruff, W.H., Rodabacher, D.B., Jones, T.E. & Ochrymowycz, L.A. (1978) *J. Am. Chem. Soc. 100*, 5939. **f)** Thomann, H., Bernardo, M., Baldwin, M.J., Lowey, M.D. & Solomon, E.I. (1991) *J. Am. Chem. Soc. 113*, 5911.

[41a] Stigbrand, T. (1971) *Biochim. Biophys. Acta 236*, 246. **b)** Stigbrand, T. (1972) *FEBS Lett 23*, 41. **c)**van Driessche, G., Dennison, C., Sykes, A.G. & van Beeumen, J. (1995) *Protein Science 4*, 209.

[42]Marchesini, A., Minelli, M., Merkle, H. & Kroneck, P.M.H. (1979) *Eur. J. Biochem. 101*, 77.

[43a] Aikazyan, V.T. & Nalbandian, R.M. (1979) *FEBS Lett. 104*, 127. **b)** Mann, K., Schafer, W., Thoenes, U., Messerchmidt, A., Mehrabian, Z.B. & Nalbandian, R.M. (1992) *FEBS Lett. 314*, 220.

[44]Reinhammar, B. (1984) in *Copper proteins and copper enzymes* (Lontie, L., ed.) vol. 3, p. 1, CRC Press Inc, Boca Raton, Florida.

[45]Linder, M.C. (1991) *Biochemistry of copper*, Plenum, New York.

[46a] Kakutani, T., Watanabe, H., Arima, K. & Beppu, T. (1981) *J. Biochem. 89*, 453. **b)** Zumft, W.G., Goztmann, D.J. & Kroneck, P.M.H. (1987) *Eur. J. Biochem. 168*, 301.

[47]Cannon, J.C. (1989) *Clin. Microbiol. Rev. 2*, 1.

[48]Vehar, G.A., Keit, B., Eaton, B., Rodriguez, H., O'Brien, D.P., Rotblat, F., Opperman, H., Keck, R., Wood, W.I., Harkins, R.N., Tuddenham, E.G.D., Lawn, R.M. & Capon, D.G. (1984) *Nature 312*, 337.

[49a] Saraste, M. (1990) *Quart. Rev. Biophys. 23*, 332. b) van der Oost, J., Lappalainen, P., Musacchio, A., Warne, A., Lemieux, L., Rumbley, J., Gennis, R.B., Aasa, R., Pascher, T., Malmström, B.G. & Saraste, M. (1992) *EMBO J. 11*, 3209.

Table 1:1. The family of blue-copper proteins.

subclass	biological origin
azurin	*Pseudomonas aeruginosa* *aereofacients* *denitrificans* *fluorescens* *Alcaligenes denitrificans* *faecalis* spp. *Bordetella bronchiseptica* *Methylomonas J*
pseudoazurin	*Achromobacter cycloclastes* *Alcaligenes faecalis* S6 *Methylobacterium extorquens* AM1
amicyanin	*Methylobacillus flagellatum* KT *Methylobacterium extorquens* AM1 *Methylomonas* spp. *Paracoccus denitrificans* *Thiobacillus versutus*
rusticyanin	*Thiobacillus ferrooxidans*
auracyanin	*Chloroflexus aurantiacus*
halocyanin	*Natronobacterium pharaonis*
plantacyanin (CBP)	*Cucumis sativus* *Spinacea oleracea*
plastocyanin	*Anabaena variabilis* *Enteromorpha prolifera* *Microcystus aeruginosa* *Phaseolus vulgaris* *Populus nigra* *Scenedesmus obliquus* *Spinacea oleracea* *Synechocystis 6830*
stellacyanin	*Rhus vernicifera*
umecyanin	*Armoracia laphatifolia*
mavicyanin	*Cucurbito pepo medullosa*
cucumber peeling cupredoxin (CPC)	*cucumis sativus*

b) The function of blue-copper proteins.

Whatever the biological origin of a blue-copper protein is, it is always considered as an electron-transfer protein[25]. More difficult is to specify the precise process in which the protein is involved, i.e. the electron-transfer chain in which it participates and its redox partners. In some cases the function seems to be clear. Thus, plastocyanin participates in the photosynthesis redox-chain transferring electrons between cytochrome f and the P-700 system[39], amicyanin mediates electron transport in the methylamine dehydrogenase (MADH) redox chain of methylotrophic bacteria[33], and rusticyanin seems to be a component of the *Thiobacillus ferrooxidans* respiratory chain where Fe(II) is oxidized to Fe(III)[34]. In other cases, like pseudoazurin, stellacyanin, plantacyanin, CBP, auracyanin, halocyanin, umecyanin, CPC and mavicyanin[32,35-38,40-43], many of them recently discovered, the concrete function is uncertain.

A special case is azurin. Different physiological functions have been proposed for this protein depending on the microorganism from which it is extracted. Thus, *Pseudomonas putida* azurin would participate as an electron donor of *p*-cresol methylhydrolase[31f], and methylamine dehydrogenase has been reported to be the redox partner of *Methylomonas* azurin[31a]. But generally azurin has been associated for a very long time with the anaerobic respiratory chain of dissimilatory denitrification (Fig. 1:1). It is due to the fact that *Pseudomonas aeruginosa* (*Pae*) azurin is obtained together with nitrite reductase (cytochrome cd_1, NiR) and cytochrome c_{551} (cytc_{551}) when the bacteria is grown in the presence of nitrate and in anaerobic conditions[50]. Moreover, both NiR and cytc_{551} are good redox partners of azurin *in vitro*[51]. This led to the suggestion that both azurin and cytc_{551} would be the physiological redox partners of NiR *in vivo*[52]. The DNA sequence of the azurin gene seems to be in agreement with such function[31d]. The presence of a signal peptide in this sequence indicate that the final location of the mature protein is the periplasm, and this is also the case of the NiR and cytc_{551} genes[53]. Additionally, the azurin promoter sequence contain *fnr* and *rpoN* boxes, which seem to be an indication that the expression

---

[50]Parr, S.R., Barber, D., Greenwood, C., Phillips, B.W. & Melling, J. (1976) *Biochem. J. 157*, 423.

[51]Silvestrini, M.C., Brunori, M., Wilson, M.T. & Darley-Usmar, V.M. (1981) *J. Inorg. Biochem. 14*, 327.

[52]Zannoni, D. (1989) *Biochim. Biophys. Acta 975*, 299.

[53]Silvestrini, M.C. Galeotti, C.L., Gervais, M., Schininà, E., Barra, D., Bossa, F. & Brunori, M. (1989) *FEBS Lett. 254*, 33.

is activated in presence of nitrate and anaerobic conditions[54]. However, *Pae* azurin can also be expressed, although in less amount, in aerobic conditions[50], and NiR accepts electrons more efficiently from cytc_{551}[51], whose gene seems to be organized in an operon together with the NiR gene[53]. Recently, the physiological function of *Pae* azurin has been investigated *in vivo* by following the expression of the azurin gene in *Pae* at different metabolic conditions, and studying the anaerobic growth rate in presence of nitrate or nitrite by disrupting the azurin gene and/or the cytc_{551} gene[55]. The results demonstrate that: i) the azurin expression is not ligated to the presence of nitrate or nitrite in the medium and ii) is cytc_{551} and not azurin which is essential for the electron-transfer from the cyt *bc* complex to NiR[55].

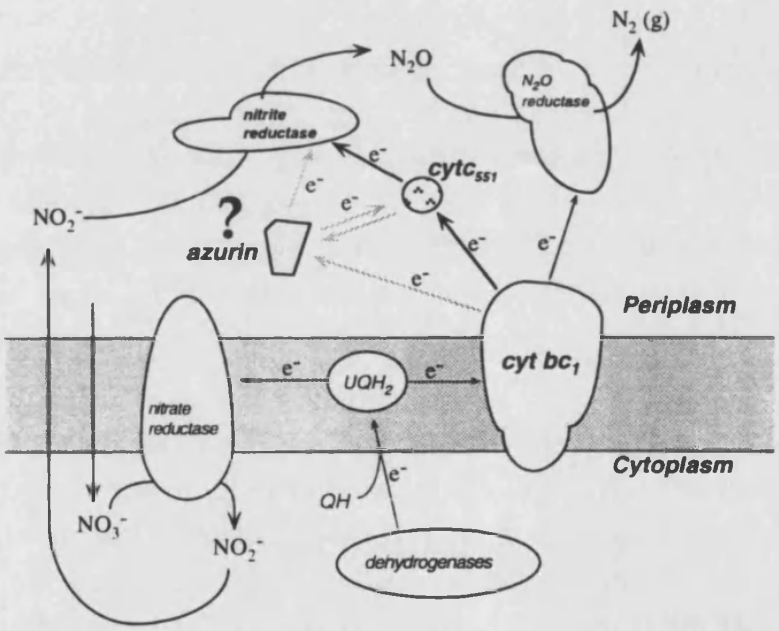

Fig. 1:1 A scheme of the anaerobic dissimilatory nitrate/nitrite respiratory chain in *Pseudomonas aeruginosa*. The enzymes and electron-transfer proteins supposedly involved in this process are showed[52]. It was until very recently assumed that azurin participates, together with cytochrome c_{551} mediating the flow of electrons form the cytochrome bc_1 to nitrite reductase in this chain. However, this role of azurin (gray arrows) has been questioned by recent *in vivo* investigations[55].

[54]Arvidsson, R.H.A., Nordling, M. & Lundberg, L. (1989) *Eur. J. Biochem. 179*, 195.

[55]Vijgenboom, E., Busch, J.E. & Canters, G.W. (1995) *J. Inorg. Biochem. 59 (Abstracts of the seventh International Conference on Bioinorganic Chemistry, ICBIC-7)* 720.

c) Structural, spectroscopic and redox properties.

The crystal structure of azurin.

The crystal structure of *Pae* Cu(II)-azurin was first solved by Adman, et al. at 2.7 Å resolution[11b,56]. Later on, the structures of azurins from other sources appeared, like azurins from *Alcaligenes denitrificans* (*Ade*)[17] and *Paracoccus denitrificans*[57], and the structure of *Pae* azurin was solved up to 1.93 Å resolution at pH 5.5 and pH 9.0[18]. In all these cases, the structure encountered is very similar to the structures of other blue copper proteins, like plastocyanin and amicyanin[11a,33g]. The molecule is a β-barrel made of eight β-strands and contains only an α-helical section (Fig. 1:2A). The metal site is buried under the surface of a hydrophobic patch. Ligands from five aminoacid residues interact with the copper. Three of them, the thiolate S^{γ} of Cys112 and the imidazole $N^{\delta 1}$ of both His46 and His117, are strongly coordinated to it (2.0-2.2Å) and form an equatorial trigonal plane (N_2S). Two additional ligands, the Met121 S^{δ} and the Gly45 carbonyl oxygen, are weakly coordinated in axial positions (Fig. 1:2B). The metal site geometry has been described as trigonal bipyramidal, but, since the Cu-O_{Gly} distance is significantly large, this coordination bond may be not considered and the metal site can be described as a trigonal pyramid[17,58]. The copper is almost in the N_2S plane, a structural fact which seems to have important spectroscopic and functional implications, as we are going to discuss below.

Additionally, the structures of the reduced Cu(I)-azurin[59] and the apo-azurin[60] have been also solved by X-ray crystallography. In the Cu(I)-azurin, the structure of the metal site is almost identical to the corresponding structure of the oxidized azurin[59]. Moreover, the extraction of the metal provokes minimal changes in the metal binding site (<0.2Å)[60]. These data are consistent with the idea that the blue-copper site is defined by the constraints of the polipeptide chain. Thus, the structure surrounding the metal site is the most tightly constrained, less flexible part of the molecule, due to an extensive network of

---

[56]Adman, E.T. & Jensen, L.H. (1981) *Isr. J. Chem. 21*, 8.

[57]Korszun, Z.R. (1987) *J. Mol. Biol. 196*, 413.

[58]Lowery, M.D. & Solomon, E.I. (1992) *Inorg. Chim. Acta 198-200*, 233.

[59]Shepard, W.E.B., Anderson, B.F., Lewandoski, D.A., Norris, G.E. & Baker, E.N. (1990) *J. Am. Chem. Soc. 112*, 7817.

[60]a) Shepard, W.E.B., Kingston, R.L., Anderson, B.F. & Baker, E.N. (1993) *Acta Crystallogr. D49*, 331. b) Nar, H., Messerschmidt, A., Huber, R., van de Kamp, M. & Canters, G.W. (1992) *FEBS Lett. 306*, 119-124.

hydrogen bonds and van der Waals interactions[17]. The structure of various azurin metalloderivatives is also in agreement with this view[61]. In these cases, the metal site remains almost the same as in the Cu(II)-azurin, except that the position of the metal ion with regard to the equatorial plane and the axial ligands changes and the geometry becomes more tetrahedral. Thus, in the zinc and nickel azurins, is the Met121 S^{δ} which falls too far to be coordinated, while the Gly45 O makes a closer contact with the metal and is now considered a regular ligand[61a,b].

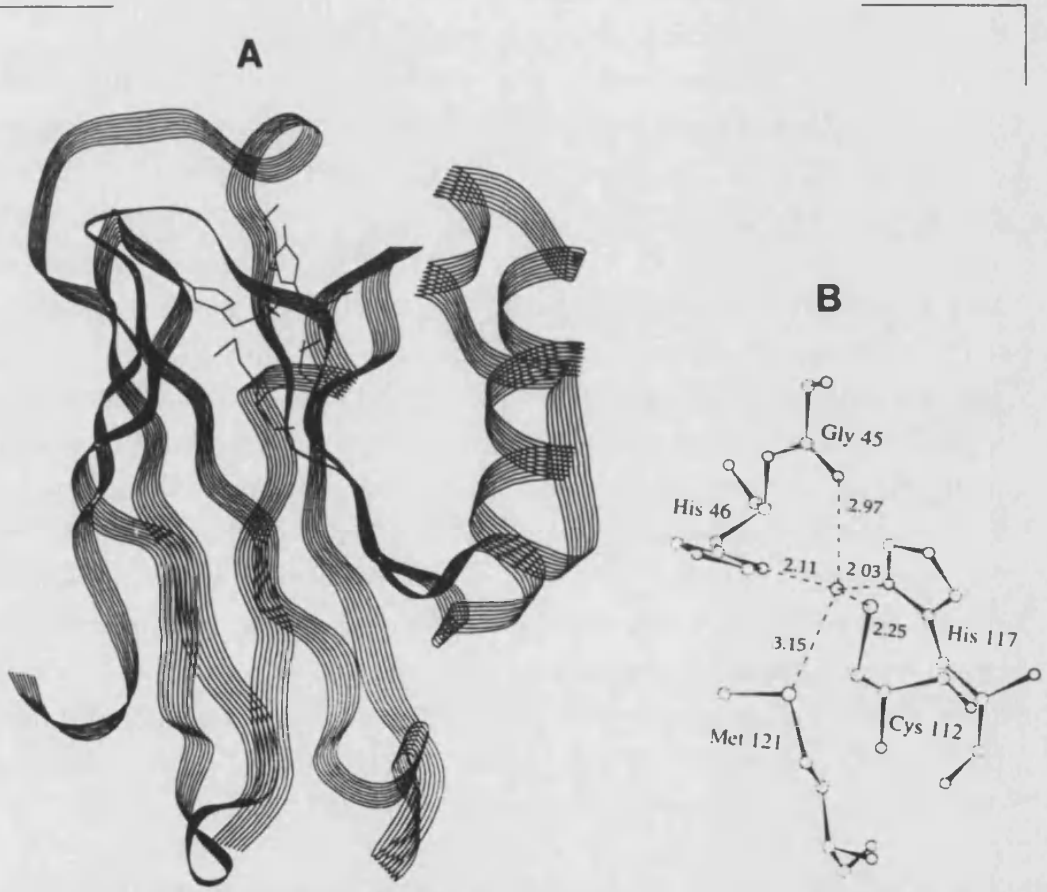

Fig. 1:2. The structure of *Pseudomonas aeruginosa* azurin as determined by X-ray crystallography[18]. Ribbon representation of the azurin structure (A) and scheme of the coordination of copper (B)

Besides the metal site, a comment should be made also on the structure of possible docking patches in the surface of the molecule. A hydrophobic patch is

[61] a) Nar, H., Huber, R., Messerschmidt, A., Filippou, A.C., Barth, M., Jaquinod, M., van de Kamp, M. & Canters, G.W. (1992) *Eur. J. Biochem. 205*, 1123. **b)** Moratal, J.M., Romero, A., Salgado, J., Perales-Alarcón, A. & Jiménez, H.R. (1995) *Eur. J. Biochem. 228*, 653. **c)** Blackwell, K.A., Anderson, B.F. & Baker, E.N. (1994) *Acta Crystallogr. D50*, 263.

the most distinctive surface feature[17,18,62]. It is situated just above the copper site, surrounding the imidazole ring of one of the ligands, His117, which is placed in a surface depression (see Fig. 3:12). The $N_{\varepsilon 2}H$ group of this residue is pointing towards the solvent and interacts through a proton bridge with a water molecule[62]. It has been demonstrated that the hydrophobic patch is the relevant docking zone used by azurin to interact with other redox proteins, like NiR and cytc_{551}[63], as well as in the azurin-azurin electron self-exchange reaction[64]. Additionally, a mechanism, has been proposed in which the Cu-His117-H_2O arrangement would constitute a through H-bonds pathway for the electron-transfer process[62].

A second relevant zone in the azurin structure is the region around the His35. The pH dependent behavior of *Pae* azurin, which was connected with the ionization of His35[65], appeared related with the pH dependence of the midpoint potential (a 60 mV E_m decrease from pH 5 to 8)[66], and with the observation of a slow reaction coupled with a fast one in the electron transfer kinetics between azurin and cytochrome c_{551}[67]. Additional experiments using Cr-labeled azurin led to postulate the existence of a His35 patch, used for the reaction of azurin with cytochrome c_{551}, apart from the hydrophobic patch, which would be responsible for the reaction with nitrite reductase[68]. However, site directed mutagenesis later demonstrated that the hydrophobic patch is the only relevant surface zone for the reaction of azurin with its redox partners, while the His35 is not functionally essential[63,64]. The X-ray diffraction study at different pH conditions agreed with the existence and origin of the pH induced structural change, but showed that it affects only a local zone close to the His35 residue[18]. Thus, at pH 5.5, the protonated His35 imidazole ring is anchored through two proton bridges formed by the $N_{\varepsilon 2}H$ and $N_{\delta 1}H$ groups of this residue with the

---

[62]Nar, H., Messerchmidt, A., Huber, R., van de Kamp, M. & Canters, G.W. (1991) *J. Mol. Biol. 218*, 427.

[63]van de Kamp, M., Silvestrini, M.C., Brunori, M., van Beeumen, J., Hali, F.C., Canters, G.W. (1990) *Eur. J. Biochem. 194*, 109.

[64] van de Kamp, M., Floris, R., Hali, F.C. & Canters, G.W. (1990) *J. Am. Chem. Soc. 112*, 907.

[65]Adman, E.T., Canters, G.W., Hill, H.A.O. & Kitchen, N.A. (1982) *FEBS Lett. 143*, 287.

[66]Strong, C., Ellis, W.R. & Gray, H.B. (1992) *Inorg. Chim. Acta 191*, 149.

[67]**a)** Rosen, P. & Pecht, I. (1976) *Biochemistry 15*, 775. **b)** Silvestrini, M.C., Brunori, M., Wilson, M.T. & Darley-Usmar, V. (1981) *J. Inorg. Biochem. 14*, 327. **c)** Corin, A.F., Bersohn, R. & Cole, P.E. (1983) *Biochemistry 22*, 2032.

[68]**a)** Farver, O. & Pecht, I. (1981) *Israel J. Chem. 21*, 13. **b)** Farver, O., Blatt, Y. & Petch, I. (1982) *Biochemistry 21*, 3556.

O44, and O36, respectively. At high pH, the His35 $N_{\delta 1}H$ group deprotonates, while the $N_{\varepsilon 2}H$-O44 interaction is conserved. Additionally, a flip of the Pro36-Gly37 peptide, together with a 0.2 Å shift of the His35 ring, facilitates the formation of a weak hydrogen-bond between the His35 $N_{\delta 1}$ and the Gly37 amide hydrogen. Despite these rearrangements, the structure of the metal center suffers only minimal changes which are below the 0.1 Å resolution limit[18].

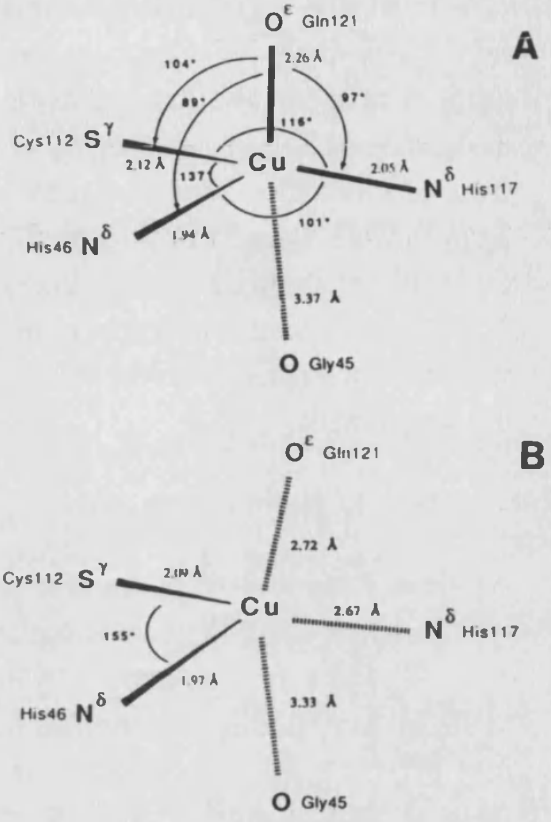

Fig. 1:3. The coordination geometry in oxidized (A) and reduced (B) copper–Met121Gln azurin[20].

Finally, some azurin mutants have been also crystallized and their structure solved[62,20]. We will just add some comments about the structure of the M121Q mutant[20] since this protein has been object of the present work. This azurin mutant is also relevant because it has been proposed as a possible model for the stellacyanin copper site, whose structure is unknown[69]. As the spectroscopic properties of this azurin mutant (visible and EPR spectra) resemble those of stellacyanin, it was proposed that the metal site in both proteins has to be very similar[20]. The structure of the Cu(II)-M121Q azurin metal site (Fig. 1:3A) is clearly tetrahedral with a short Cu(II)-O^{ε}_{Gln121} distance (2.26 Å). The Cu(II)-O_{Gly45} distance (3.37 Å) is too long for a coordination bond. The strong axial bond, stretches the metal out of the equatorial plane, something which seems to be in good

[69]Since stellacyanin lacks methionine in its sequence, much speculation has appeared in the literature about the nature of the axial (fourth) ligand in this protein. Early studies proposed that this fourth ligand is a sulfur provided by a S-S bridge[40e]. However, more recent investigations based on sequence alignment[41c], structure prediction[40d], ENDOR spectroscopy[40f], and site-directed mutagenesis of azurin[20], indicate that the stellacyanin axial ligand is most probably the Gln97 side-chain carbonyl oxygen. This last hypothesis has been recently confirmed with the solution of the crystal structure of a cucumber stellacyanin-like copper protein (SLCP) obtained from the heterologous expression of the gene in *E. coli* (Nersissian, A.M., Nalbandyan, R.M., Herrmann, R.G. & Valentine, J.S. unpublished results).

agreement with the presence of a rhombic EPR spectrum and with the $\varepsilon_{452}/\varepsilon_{610}$ ratio[20] (see below). Upon reduction of the copper, however, the metal site changes considerably[20] as a difference with regard to the wt azurin[59]. Thus, in the Cu(I)-M121Q metal site, an almost linear coordination is adopted, with strong coordination bonds between the Cu(I) and the Cys112 S^{γ} and His46 $N^{\delta 1}$ ligands, while the rest of possible ligands (His117 $N^{\delta 1}$, Gln121 O^{ε} and Gly45 O) are placed farther away and interact only weakly with the metal (Fig. 1:3B). This effective twofold coordination is preferred by Cu(I), what could explain why the redox potential in the M121Q mutant is only 25 mV lower than that for the wt azurin[20].

Electronic and Raman spectra.

As already mentioned, azurin presents the spectroscopic features typical of the type 1 copper sites. They are summarized in Table 1:2. The electronic spectrum of Cu(II)-azurin is characterized by the strong absorption at ~620 nm (ε=1.5-5.7 x 10^3 $M^{-1}cm^{-1}$). This spectrum has been gaussian-resolved by Solomon, et al. in four bands at 780, 619, 560 and 460 nm [70], which have been assigned in the case of plastocyanin[71]. The last three bands correspond to ligand-to-metal charge-transfer transitions (LMCT). Although σ charge-transfer transitions are expected to be more intense than π ones, here the strong band at ~620 nm corresponds to the $S_{Cys}\pi \rightarrow Cu\, d_{x^2-y^2}$ transition, while the weaker absorption at ~560 nm is due to a $S_{Cys}\sigma \rightarrow Cu\, d_{x^2-y^2}$ transition. It means that the $d_{x^2-y^2}$ orbital must be rotated in the *xy* plane to favor the overlap with the thiolate π orbital[71]. Additionally, the band at ~460 nm is assigned to a $N_{His}\pi \rightarrow Cu\, d_{x^2-y^2}$ charge-transfer transition[71]. So, the most distinctive characteristic of azurin (and the blue-copper sites in general) is due to an abnormally efficient overlap between the ground state Cu(II)-$d_{x^2-y^2}$ orbital and the excited state S *3p* π orbital, which originates from the particular geometry of the type 1 site. The $d_{x^2-y^2}$ orbital in the N_2S equatorial plane is highly covalent and the delocalization in the $p\pi$ orbital of the thiolate S is strongly anisotropic[72a]. It converts the Cu-S_{Cys} interactions in a very significant structural feature of the

[70]Solomon, E.I., Hare, J.W., Dooley, D.M., Dawson, J.H., Stephens, P.J. & Gray, H.B. (1980) *J. Am. Chem. Soc. 102*, 168.

[71]Gewirth, A.A. & Solomon, E.I. (1988) *J. Am. Chem. Soc. 110*, 3811.

[72a]) Solomon, E.I. & Lowery, M.D. (1993) *Science 259*, 1575. b) Guckert, J.A., Lowery, M.D. & Solomon, E.I. (1995) *J. Am. Chem. Soc. 117*, 2817.

blue-copper sites, not only to explain their spectroscopic properties, but also to understand their functionality[72].

Table 1:2. The spectroscopic features of some azurins and other blue-copper proteins.

protein and source	λ_{max}, nm (ε_{max}, M^{-1} cm^{-1})	$g_{\|\|}$ (z)	g_y	$g_\perp$	g_x	$A_{\|\|}$ $cm^{-1}x10^4$
Azurin[31,70]						
P. aeruginosa	628 (5700)	2.258		2.057		58
P. fluorescens	620 (3500)	2.261		2.052		58
A. denitrificans	619 (5100)	2.256		2.059		62
Pa. denitrificans	595 (1500)	2.290		2.052		77
P. aerofaciens	624 (2500)	2.266		2.056		58
B. bronchiseptica	625 ---	2.273		2.049		60
Plastocyanin[39]						
P. nigra	597 (4700)	2.226		2.053		—
Stellacyanin[40]						
R. vernicifera	604 (4100)	2.287	2.077		2.018	35
Amicyanin[33]						
T. versutus	596 (3900)	2.239		2.046		56
Pseudoazurin[32]						
A. cycloclastes	596 (3700)	2.200	2.090		2.020	55
Rusticyanin[34]						
T. ferrooxidans	597 (2100)	2.229	2.064		2.019	45
CBP[38]						
C. sativus	593 (2900)	2.220	2.070		2.020	60
Umecyanin[41]						
A. laphatifolia	610 (3300)	2.317		2.050		35
Auracyanin[35]						
C. aurantiacus	596 (3000)	2.210	2.062		2.018	47
Mavicyanin[42]						
C. pepo	600 (5000)	2.287	2.077		2.025	35

Thus, every distortion affecting the Cu $d_{x^2-y^2}$–S *3p* π overlap, such as a stronger interaction of the Cu with the axial ligand which displaces it out of the N_2S equatorial plane, influences the optical and redox properties of the metal site[72]. This possible connection between the spectroscopic and structural data has been addressed by correlating the axial displacement of the copper from the trigonal N_2S plane with the ratio of absorption intensities in the 440-480 nm and 580-630 nm spectral regions[73].

[73]Han, J., Loehr, T.M., Lu, Y., Valentine, J.S., Averill, B.A. & Sanders-Loehr, J. (1993) *J. Am. Chem. Soc. 115*, 4256.

The resonance Raman (RR) spectrum of azurin is also a direct consequence of the structure of the metal site, specially of the Cu-S_{Cys} bond and the coplanar Cu–S_γ–C_β–C_α–N arrangement[74]. Up to 12 vibrational modes between 250 and 500 cm^{-1} come up upon excitation in the 625 nm band, which are believed to originate from kinematic and vibronic coupling of the Cu-S_{Cys} stretch with vibrational motions of the Cys and His ligands[75]. These spectra are particularly sensitive to the length of the Cu-S_{Cys} bond, being a good method to fingerprint the coordination geometry in azurin mutants[76].

EPR spectroscopy.

Azurin presents an axial EPR spectrum ($g_z > g_y \approx g_x$) with a small $A_{||}$=55-75 x 10^4 cm^{-1} as corresponds to a blue-copper protein (Table 1:2). As in the case of the optical properties, these EPR features have been attributed to the coordination geometry of the metal site: three strongly coordinated ligands with the copper placed almost in the plane formed by them. The delocalization of the unpaired electron in the $d_{x^2-y^2}$ orbital into the equatorial ligands, specially on the S_{Cys} $p\,\pi$ orbital, seems to be the responsible for the small parallel hyperfine splitting observed[72,77]. Being the planar arrangement in the equatorial plane so determinant, variations in the axial interactions significantly affect the EPR spectra. Thus, a correlation between the $A_{||}$ and $g_{||}$ values is found[78]. Additionally, the rhombicity of the EPR spectrum is related with the displacement of the copper out of the N_2S plane and the strength of the axial interaction[20]. Proteins with a close coordination to the axial ligand (around 2.6 Å), like pseudoazurin, CBP or the M121Q azurin mutant, have rhombic EPR spectra, while those with a weak axial coordination (2.9-3.1 Å), like azurin and plastocyanin, present axial EPR spectra[20].

---

[74]Han, J., Adman, E.T., Beppu, T., Codd, R., Freeman, H.C., Huq, L., Loehr, T.M., & Sanders-Loehr, J. (1991) *Biochemistry 30*, 10904.

[75]Blair, D.F., Campbell, G.W., Schoonover, J.R., Chan, S.I., Gray, H.B., Malmström, B.G., Pecht, I., Swanson, B.I., Woodruff, W.H., Cho, W.K., English, A.M., Fry, H.A., Lum, V. & Norton, K.A. (1985) *J. Am. Chem. Soc. 107*, 5755.

[76]den Blaauwen, T., Hoitink, C.W.G., Canters, G.W., Han, J., Loehr, T.M. & Sanders-Loehr, J. (1993) *Biochemistry 32*, 12455.

[77]Shadle, S.E., Penneer-Hahn, J.E., Schugar, H.J., Hedman, B., Hodgson, K.O. & Solomon, E.I. (1993) *J. Am. Chem. Soc. 115*, 767.

[78]den Blaauwen, T. & Canters, G.W. (1993) *J. Am. Chem. Soc. 115*, 1121.

Redox and electron-transfer properties.

The blue-copper proteins have relatively high midpoint redox potentials (E_m=180-680 mV; 230-348 mV for azurins)[25,79] compared with the Cu(I)/Cu(II) pair (148 mV) and most model complexes. It has been proposed that a stabilization of the Cu(I) state could originate from a combination of *Cu → ligand* back-bonding and a weak ligand-field[10d]. Other factors like the number and strength of NH···S$^{\gamma}$ hydrogen bonds[80] have been also related with the value of the potential. The axial ligand, a Met S$^{\delta}$ in most blue copper proteins, seems to be important also to tune the potential[10d,72b]. Thus, electronic structure calculations of the reduced Cu(I)-plastocyanin, indicate that the long Cu-thioether axial bond destabilizes the oxidized state of copper and is a key determining factor in the high reduction potential[72b]. However, site-directed mutagenesis have demonstrated that the actual factors which determine the midpoint potential are difficult to be defined[81]. Thus, some mutations out of the coordination sphere induce changes in the potential which are larger than those corresponding to some substitutions of the coordinated ligands[80-82].

The influence of electrostatic interactions in the redox potential seems to be more clear[82a,83,84]. In this sense, the potential can be determined by the burial of the copper in a low-dielectric protein environment and possible interactions with polar groups. Azurins provide a good example in which these effects can be tested. Thus, *Pae* azurin presents two ionizable histidine residues, His35 and His83, and the former one is relatively close to the copper. In *Ade* azurin, however, the His35 residue does not titrate. This difference between the two azurins is clearly reflected in the pH dependence of the reduction potentials: a ~60 mV E_m decrease from pH 5 to 8 for *Pae* azurin, but only a ~20 mV decrease in the case of *Ade* azurin[66]. Site-directed mutagenesis demonstrates that the

---

[79] Farver, O. & Pecht, I. (1984) in *Copper Proteins ans Copper Enzymes* (Lontie, R., ed.) vol. I, Ch. 7., CRC Press, Boca de Raton, FL.

[80] **a)** Karlsson, B.G., Aasa, R., Malmström, B.G. & Lundberg, L.G. (1989) *FEBS Lett. 253*, 99. **b)** Hoitink, C.W.G. & Canters, G.W. (1992) *J. Biol. Chem. 267*, 13836.

[81] Pascher, T., Karlsson, B.G., Nordling, M., Malmtröm, B.G. & Vänngård, T. (1993) *Eur. J. Biochem. 212*, 289.

[82] **a)** van de Kamp, M., Canters, G.W., Andrew, C.R., Sanders-Loehr, J., Bender, C.J. & Peisach, J. (1993) *Eur. J. Biochem. 218*, 229. **b)** Pascher, T., Bergström, J., Malmtröm, B.G., Vänngård, T. & Lundberg, L.G. (1989) *FEBS Lett. 258*, 266.

[83] Moore, G.R., Pettigrew, G.W. & Rogers, N.K. (1986) *Proc. Natl., Acad. Sci. U.S.A. 83*, 4998.

[84] **a)** Groeneveld, C.M., Ouwerling, M.C., Erkelens, C. & Canters, G.W. (1988) *J. Mol. Biol. 200*, 189. **b)** Bashford, D., Karplus, M. & Canters, G.W. (1988) *J. Mol. Biol. 203*, 507.

His35 ionization accounts for most of the E_m decrease (~50 mV) in *Pae* azurin[63,82a].

On the other hand, blue-copper proteins mediate efficient electron-transfer (ET) and are one of the favorite systems to study these fundamental reactions[12]. Various factors have been described that influence ET in proteins, like driving force, reorganization energy, distance and coupling between the redox centers; as well as the nature of the medium between them and the characteristics of the recognition and association processes between the redox partners[12a,85]. The driving force in ET processes is proportional to the difference in the midpoint potential between the proteins involved[86]. With regard to the reorganization energy, it is normally low in type 1 copper proteins[10d], which constitute a good example of the "entatic state" or rack-induced bonding"[10,87]. A very rigid protein matrix constrains the metal site to adopt a particular coordination geometry. This structure is indeed a compromise between those preferred by Cu(II) and Cu(I), and so, the alternation in the oxidation state of the copper occurs with minimal changes in the structure of the metal site and requires low activation energy[10d,59].

The distance and the medium between the redox centers have been object of intense research in the context of intramolecular protein-mediated electron transfer[12a]. Many recent investigations have faced the problem which has been analyzed according to two mechanisms[12a]: the organic glass mechanism[85b,88] and the superexchange mechanism[89,90]. The first one consider the protein matrix as an organic glass[91] representing a rather uniform electronic barrier, in such a way that ET does not proceed through concrete pathways. It has been mainly applied to the photosynthetic reaction centers[85b,88]. In contrast, the superexchange model states that electrons travel along specific paths. Thus, two

---

[85a] Marcus, R.A. & Sutin, N. (1985) *Biochim. Biophys. Acta 811*, 265. **b)** Moser, C.C. & Dutton, P.L. (1992) *Biochim. Biophys. Acta 1101*, 171. **c)** McLendon, G. & Hake, R. (1992) *Chem. Rev. 92*, 481. **d)** Pelletier, H. & Kraut, J. (1992) *Science 258*, 1748.

[86] Farver, O., Skov., L.K., van de Kamp, M., Canters, G.W. & Pecht, I. (1992) *Eur. J. Biochem. 210*, 399.

[87a] Lumry, R. & Eyring, H. (1954) *J. Phys. Chem. 58*, 110. **b)** Eyring, H., Lumry, R. & Spikes, J.D. (1954) in *The mechanism of enzyme action* (McElroy, W.D. & Glass, B., eds) p. 123, The Johns Hopkins Press, Baltimore. **c)** Malmström, B.G. (1994) *Eur. J. Biochem. 223*, 711.

[88] Moser, C.C., Keske, J.M., Warnicke, K., Faird, R.S. & Dutton, P.L. (1992) *Nature 355*, 796.

[89a] Beratan, D.N., Betts, J.N. & Onuchic, J.N. (1991) *Science 252*, 1285. **b)** Beratan, D.N., Onuchic, J.N., Winkler, J.R. & Gray, H.B. (1992) *Science 258*, 1740.

[90] Farver, O. & Pecht, I. (1992) *J. Am. Chem. Soc. 114*, 5764.

[91] Frauenfelder, H., Sligar, S.G. & Wolines, P.G. (1991) *Science 254*, 1598.

redox centers are coupled through some paths which connect them and are made of different steps called physical ET pathways[89]. The steps can be of three types: covalent bonds, hydrogen bonds or jumps through space, and their efficiency vary according to an attenuation factor[89]. It has been shown that only a limited number of paths are significant and it appears that α-helices are less efficient than β-sheets[89].

The superexchange model has been applied to analyze the intramolecular ET in azurin using different experimental strategies. RSSR* radicals can be generated by pulse-radiolysis, after which one electron is transferred to the copper[92]. Alternatively, solvent-exposed His residues have been modified with ruthenium, which then can be used to photo-initiate an ET reaction by either pulse-radiolysis or flash-photolysis[93]. Intramolecular rates of ET have been determined in wt and site-directed mutant-azurins from different species [12,86,92], and a good correlation has been found between the reaction rates and the driving force which agrees with the predictions based on the Marcus theory and a through-bound-coupling model[86,92b].

Intermolecular ET has been studied between azurin and other electron-transfer proteins and small inorganic complexes[12a,25e]. On the other hand, electron self-exchange (ESE) reactions have been studied in blue-copper proteins as a way to determine the intrinsic reactivity of these proteins, which is important in the context of the Marcus formalism[85a]. The second order bimolecular ESE rate constant (k_{ESE}) depends only on the association constant, K_A, and the reorganization energy, and there is no driving force[12a]. The ESE reaction of azurin is particularly well known[31e,94]. For *Pae* and *Ade* wt azurins, k_{ESE} is significantly large ranging from 4×10^5 to 1×10^6 M^{-1} sec^{-1} depending on the pH and temperature conditions. These values are independent on ionic strength suggesting that ET takes place in a complex in which two azurin molecules are associated by their hydrophobic patches[31e,94a]. Such interaction minimizes the Cu-Cu distance to around 15 Å. On the other hand, the association would be very weak ($K_A \leq 1 M^{-1}$) since no ESE complexes are observed in experimental conditions. This model has been successfully proved by studying the ESE in azurin mutants in which residues of the hydrophobic patch were substituted by charged residues, and the mutation resulted in a decrease of the k_{ESE} by 2-3

[92a] Farver, O. & Pecht, I. (1989) *Proc. Natl. Acad. Sci. U.S.A. 86*, 6868. **b)** Farver, O., Skov, L.K., Pascher, T., Karlsson, G., Nordling, M., Lundberg, L.G., Vänngård, T. & Pecht, I. (1993) *Biochemistry 32*, 7317.

[93] Winkler, J.R. & Gray, H.B. (1992) *Chem. Rev. 92*, 369.

[94a] Groeneveld, C.M. & Canters, G.W. (1985) *Eur. J. Biochem. 153*, 559. **b)** Groeneveld, C.M., Dahlin, S., Reinhammar, B. & Canters, G.W. (1987) *J. Am. Chem. Soc. 109*, 3247.

orders of magnitude[64,95] (see below). Moreover, as we have discussed above, crystallographic studies show that azurin molecules are packed as dimers interacting through the hydrophobic patches[17,18,62]. In the center of the interacting surfaces, the two coordinated His117 residues are connected through the H-bridges *via* two water molecules which are encapsulated by the dimer[62]. This arrangement is suggested as a molecular model for the ESE complex in which the His117 imidazole ligands and the two water molecules form an ET pathway connecting the two coppers[12a,62]. Recent quantum-mechanical calculations demonstrate that the involvement of the two water molecules in the ET pathway means an improvement the coupling between the two coppers[96].

[95]a) van Pouderoyen, G., Cigna, G., Andrew, C.R., Sanders-Loehr, J. & Canters, G.W. (1995) *J. Inorg. Biochem. 59 (Abstracts for the seventh International Conference on Bioinorganic Chemistry, ICBIC-7)* 660. b) van Pouderoyen, G., Mazundar, S., Hunt, N.I., Hill, H.A.O. & Canters, G.W. (1994) *Eur. J. Biochem. 222*, 583.

[96]Mikkelsen, K.V., Skov, L.K., Nar, H. & Farver, O. (1993) *Proc. Natl. Acad. Sci. U.S.A. 90*, 5443.

III.The genetic approach.

Molecular biology, extensively developed in the last decades, has became an essential tool in the many different areas of biochemical research. Thus, the investigation of any biochemical system experiences a giant step, when the gene (or genes) codifying for the proteins involved in that particular function are cloned and over-expressed. Apart from the information that can be extracted from the structure of the gene (presence of putative sequences, relationships with other genes in the chromosome) and the DNA sequence itself (sequence homology with regard to other genes), which usually have functional or evolutionary implications, an immediate advantage comes from the possibility of obtaining large amounts of protein in an easy way. This is particularly important for metalloproteins, since normally high sample concentrations are needed to perform most types of spectroscopic measurements. Additionally, these techniques have been of help to obtain the crystal structure of many proteins, where heterologous expression has been decisive to crystallize them. On the other hand, cloning and over-expression of genes allow one to produce isotopically enriched proteins[97], which is particularly important to perform some types of advanced spectroscopic experiments like ^{15}N-^{1}H and ^{13}C-^{1}H heterocorrelated NMR experiments. But perhaps the most significant advantage of having a gene cloned, is that it opens the possibility to perform very selective modifications in the protein sequence, by means of the so called site-directed mutagenesis[98]. Thus, new proteins, in which specific aminoacid residues have been replaced, can be obtained and studied, and very direct conclusions can be extracted about the structural and functional role of specific residues, the mechanism of action of the protein, etc.

---

[97]Muchmore, D.C., McIntosh, L.P., Russell, C.B., Anderson, D.E. & Dahlquist, F.W. (1989) *Methods Enzymol. 177*, 44.

[98]**a**) Kunkel, T.A. (1985) *Proc. Natl. Acad. Sci. U.S.A. 82*, 488. **b**) Saiki, R.K., Scharf, S., Faloona, F., Mullis, K.B., Horn, G.T., Ehrlich, H.A. & Arnheim, N. (1985) *Science 230*, 1350. **c**) Carter, P. (1986) *Biochem. J. 237*, 1. **d**) Smeekens, S. Bauerle, C., Hageman, J., Keegstra, K. & Weisbeg, P. (1986) *Cell 46*, 365.

a) Site directed mutagenesis and structure/function relationships in azurin

Mutations in the metal site. The minimum requirements for a blue-copper site.

Immediately after the azurin gene was cloned[31d,54,99,100] many different mutated proteins were expressed and studied in various groups. The metal ligands (Cys112, His46, His117 and Met121) were obvious targets for these experiments. They were individually replaced by other residues to study their role in the functional, structural and spectroscopic properties of the azurin metal center, and to find out which of these ligands are essential for a minimum type 1 copper site.

Replacement of the Met121 axial ligand to all other aminoacid residues shows that all 20 mutants exhibit the principal characteristics of the blue-copper proteins[20,80a,81,100,101]. These mutations and other site-directed replacements of the Cys112, His46 and His117 equatorial ligands[76,78,102,103], have demonstrated that the N_2S equatorial trigonal-planar entity is the minimum structure which defines a type 1 copper site. However, among the three equatorial ligands, only Cys112 is absolutely essential for a blue-copper center. Thus, the His46 position can be occupied by Asp and the protein still presents the spectral features typical of type 1 [103]. Additionally, replacement of His46 or His117 by Gly creates a "hole" in the metal site, which can be filled by added external ligands reconstituting the blue site[76,78,95a]. But when Cys112 is replaced by Asp the protein definitively loses the EPR and electronic spectral characteristics which define a type 1 copper site[102].

Being Met121 not essential, a question have risen concerning the specific role of this axial position[20,80a,81,100]. It seems that the most probable meaning

---

[99]Hoitink, C., Woudt, L.P., Turenhout, J.C.M., van de Kamp, M. & Canters, G.W. (1990) *Gene 90*, 15.

[100]Chang, T.C., Iverson, S.A., Rodrigues, C.G., Kiser, C.N., Lew, A.Y., Germanas, J.P. & Richards, J.H. (1991) *Proc. Natl. Acad. Sci. U.S.A. 88*, 1325.

[101]a) Karlsson, B.G., Nordling, M., Pascher, T., Tsai, L.C., Sjölin, L. & Lundberg, L.G. (1991) *Protein Eng. 4*, 343. b) Di Bilio, A.J., Chang, T.K., Malmström, B.G., Gray, H.B., Karlsson, B.G., Nordling, M., Pascher, T. & Lundberg, L.G. (1992) *Inorg. Chim. Acta 198-200*, 145. c) Murphy, L.M., Strange, R.W., Karlsson, B.G., Lundberg, L.G., Pascher, T., Reinhammar, B. & Hasnain, S.S. (1993) *Biochemistry 32*, 1965.

[102]Mizoguchi, T.J., Di Bilio, A.J., Gray, H.B. & Richards, J.H. (1992) *J. Am. Chem. Soc. 114*, 10076.

[103]Germanas, J.P., Di Bilio, A.J., Gray, H.B. & Richards, J.H. (1993) *Biochemistry 32*, 7698.

of this residue is to tune the redox potential of the blue-copper site[10d,72b,81] . Thus, substitutions in position 121 by hydrophobic aminoacids, mean an increase in potential, probably due to a reduction of the electronegativity in the metal site which destabilize Cu(II)[81]. However, other substitutions outside the coordination sphere also increase considerably the redox potential[80b,82], and additive effects are observed when two mutations are simultaneously present[81]. Finally, an interesting case of Met121 mutation is the Met121Gln azurin, since it presents the spectroscopic features of stellacyanin and stellacyanin-like proteins, whose sequence lacks methionine[20]. These characteristics are, essentially, a rhombic EPR spectrum, in contrast to the axial one of the wt azurin, and an increase in the ~450 nm absorption band and a blue-shift of the ~600 nm absorption band[20]. On these basis, it has been proposed that the axial ligand in stellacyanin is Gln97, in agreement with other investigations based on sequence alignment[41c], structure prediction[40e] or ENDOR spectroscopy[40f]. The crystal structure of a cucumber stellacyanin-like copper protein (SLCP) has recently confirmed this hypothesis[69].

Apart from the study of the functional significance of the metal ligands, their replacement by site directed mutagenesis have permitted to obtain novel copper proteins with exciting structural and spectroscopic characteristics[13,76,78,95a,104]. Among them, those originated by the substitution of some of the copper ligands by a glycine are particularly interesting because they create "holes" in the metal site and leave a position free. These vacant places can be occupied by added external ligands giving back the type site or creating new copper sites, in some cases with hitherto unknown properties[78,95a,104]. Obtaining and studying engineered metalloproteins using this approach, trying to find novel functional properties which can be of (academic, or even economic) interest is today an important research topic[13,105].

Studying docking patches and electron-transfer pathways.

As already pointed out, site-directed mutagenesis has proved valuable in understanding biological electron transfer at a molecular level. Thus, it has been used to identify specific docking surface zones and physical ET pathways which are relevant for intermolecular and intramolecular ET processes.

---

104 Vidakovic, M. & Germanas, J.P. (1995) *Angew. Chem. 34*, 1622.

105 a) Gilardi, G., den Blaauwen, T. & Canters, G.W. (1994) *J. Controlled Release 29*, 231. b) Canters, G.W. & van Pouderoyen, G. (1994) in *Proceedings of the Second CEC Workshop on Bioelectronics.*

It was for a long time thought that there were two important patches in the surface of azurin: the hydrophobic patch, placed above the metal site surrounding the His117 copper ligand, and the His35 patch[68]. The second one was supposed to be important due to the pH dependent behavior of *Pae* azurin, which, on one hand, means a local conformational change connected with the ionization of His35[18,65], and on the other hand, is related with the pH dependence of the midpoint potential[66,82a]. Additionally, the characteristics of the reaction between azurin and cytochrome c_{551}[67], and experiments made with Cr-labeled azurin led to suggest the existence of a His35 patch, used for the reaction of azurin with cytochrome c_{551}, different from the hydrophobic patch, which would be responsible for the reaction with nitrite reductase[68]. Replacement of Met44 residue in the hydrophobic patch of *Pae* azurin by Lys demonstrates that the hydrophobic patch is involved in the ET reactions of this protein with both cytochrome c_{551} and nitrite reductase, as well as in the azurin-azurin electron self-exchange reaction [63,64]. Other mutations which introduce charges in the hydrophobic patch also affect the electron self-exchange and the electrochemistry of azurin[95b]. Curiously, the simultaneous presence of a positive and a negative charge in this patch creates a dipole which does not affect significantly the electron self-exchange reaction[95a].

Conversely, the ET kinetics of the His35 mutants (where this residue is replaced by Phe, Leu or Gln) with cyt c_{551} and NiR is very similar to that of the wt azurin. It definitively roles out the possibility of a second (His35) patch in azurin[63]. However, these experiments also demonstrate that the slow relaxation phase observed in the reaction of *Pae* azurin with cyt c_{551}[67], as well as the pH dependent variations observed in the NMR spectra[65], are due to a conformational change involving His35[63,18].

On the other hand, intramolecular ET between the RSSR* radical an the Cu(II) has been investigated in various azurin mutants[12,86,90,92]. These experiments have been important to correlate the reorganization energies and coupling factors corresponding to the different mutants with the different ET rates observed[12,86,92]. Calculations show that two principal ET pathways may couple the disulfide bridge and the copper in azurin[86]. Interestingly, the results obtained with Trp48 mutants indicate that this residue does not play a significant role in mediating the ET[92a,90]. It seems that the coupling is determined by peptide backbone interactions better than by π systems, in line with a through-bound ET mechanism[90].

IV.Metal substitution and spectroscopic probes.

a) Why replacing metals in metalloproteins?

Substitution of the naturally occurring metals in metalloproteins is used as a common strategy in bioinorganic chemistry[8,16,106,107]. In a first approach it is a direct, and normally easy, way to test the essentiality of the metal ion itself. Changing a native metal, we can learn about its role in the system. Thus, if the metal has a structural function, the metalloprotein stability could be affected by its replacement. On the other hand, in most metalloenzymes the catalytic function is partially or totally lost upon metal substitution, and some times the enzyme acquire new catalytic properties[16]. These changes in the enzymatic activity can be used to elucidate the details of the reaction mechanism of the native enzyme. Additionally, metal replacement can give an idea of the metal site selectivity and structural rigidity, the mechanism of metal uptake and some general chemical properties of the metalloprotein. In all these cases, metal substitution can be considered a very specific "site-directed" modification, equivalent to a site-directed mutation on any of the aminoacid residues of the metalloprotein. Of course, we have first to be sure that the non-native metal occupies the same coordination position as the native one.

In some special cases, substitution of metal ions is used to probe the metal site[16,106,108]. This is possible when the chromophore that brings along the exogenous metal has peculiar spectroscopic properties, which can be exploited to get structural information or to follow dynamic processes affecting the metal site or its proximities. Thus, conformational changes, pH titrations, binding of ligands (inhibitors, activators or substrates) or the kinetics of the metalloprotein activity (provided the metalloderivative is active) can be monitored using spectroscopic methods. This approach is specially important when the native metal does not exhibit such potentially informative spectroscopic properties, as in the case of zinc, in zinc-metalloproteins and metalloenzymes[16,106a]. It is important to point out that, in order to be a good spectroscopic probe, a metal ion

---

[106a] a) Bertini, I. & Luchinat, C. (1984) in *Advances in Inorganic Biochemistry* (Eichorn, G.L. & Marzilli, L.G., eds.) p. 71, Elsevier, New York. b) Hauenstein, B.L. & McMillin, D.R. (1981) in *Metal ions in biological systems* (Sigel, H., ed.) vol. 13, p. 319, Marcel Dekker, New York.

[107] Hughes, M.N. *The Inorganic Chemistry of Biological Processes* (1972) p. 63, Wiley, New York.

[108] Donaire, A., Salgado, J., Jiménez, H.R. & J.M. Moratal (1995) in *Nuclear Magnetic Resonance of Paramagnetic Macromolecules, seriesC: Mathematical and Physicals Sciences*, (La Mar, G.N., ed.) vol. 457, p. 213, Kluwer Accademic Publishers, Dordrecht.

should fulfill as many as possible of the following requirements: 1) it should bind to the protein adopting a coordination geometry as similar as possible to the coordination of the native metal, 2) it should not provoke structural modifications or stress in the rest of the molecule, 3) it is also important that the new metal ion does not change the electrostatic balance of the protein, 4) the new metal ion should conserve as many as possible of the functional and functionally-related properties of the native protein, and it should not introduce new functional properties, and 5) the stability of the metal-protein complex should be large enough to exist without an excess of metal in solution.

The type of metal ion used as a spectroscopic probe depends on the physical technique chosen to explore the metal site and on the native metal ion which has to be replaced. Thus, cadmium has been employed to investigate zinc and copper sites by ^{113}Cd NMR[14d] and ^{111m}Cd perturbed angular correlation[109], and the use of copper as a substitute of zinc in zinc-enzymes like liver alcohol dehydrogenase has permitted to study this metalloenzymes by EPR and RR spectroscopy[110]. But among the different transition metal ions, nickel(II), and specially cobalt(II), have been the most widely used as substitutes of the native metals in zinc, copper, manganese and iron proteins[16,106,108,111]. Their spectroscopic features make them suitable for UV-Vis, EPR (not in the case of nickel), CD, MCD and RR spectroscopies; for magnetic susceptibility measurements and for (paramagnetic) Nuclear Magnetic Resonance (see next section)[14-16,106-108,111,112]. Additionally, they have flexible coordination-chemistry properties and an intermediate size, which generally permit them to obey many of the conditions required for a good probe.

b) Metal substitution in blue-copper proteins.

For the blue copper proteins, like azurin, the native copper(II) center has itself exciting spectroscopic properties which are singular and very informative[25]. They are principally EPR and electronic spectral characteristics whose extensive study throughout the last few decades has led to a detailed knowledge of type 1

---

[109]Danielsen, E., Bauer, R., Hemmingsen, L., Andersen, M.L., Bjerrum, M.J., Butz, T., Tröger, W., Canters, G.W., Hoitink, C.W.G., Karlsson, G., Hansson, Ö. & Messerschmidt, A. (1995) *J. Biol. Chem. 270*, 573.

[110]a) Maret, W., Dietrich, H., Ruf, H.H., & Zeppezauer, M. (1980) *J. Inorg. Biochem. 12*, 241. b) Maret, W., Shiemke, A.K., Wheeler, W.D., Loehr, T.M. & Sanders-Loehr, J. (1986) *J. Am. Chem. Soc. 108*, 6351.

[111]Bertini, I., Turano, P. & Vila, A. (1993) *Chem. Rev. 93*, 2833.

[112]Rosenberg, R.C., Root, C.A., Wang, R.H., Cerdonio, M. & Gray, H.B. (1973) *Proc. Natl. Acad. Sci. U.S.A. 70*, 161.

copper sites as we have summarized above[25]. But even in this case, metal substitution has proved to be very useful. Thus, it has been frequently used for the structural and spectroscopic characterization of the blue-copper sites by means of many different techniques[14,61,101b,103,113,114]. Zinc, nickel and cadmium azurins have been crystallized and their structures solved by X-ray diffraction[61]. In theses cases, the metal site is better defined as four-coordinated, due to the movement of the metal ion towards the carbonyl Gly45 ligand which leaves the Met121 sulfur practically out of the coordination sphere[61a,b] (Fig. 1:4).

Substitution of copper by cobalt (II) and nickel(II) has been done because of the singular spectroscopic properties of their metal complexes. In the early stages of the investigation of the cupredoxins, the nature of the strong visible absorption characteristic of these proteins was in doubt. At that point, copper replacement by cobalt(II) was of great help since LMCT and LF absorption systems are clearly separated in the cobalt metallo-derivatives[14a,112,115]. Thus, *Pae* Co(II)-azurin presents two strong bands at 330 and 375 nm (ε=4.0 x 10^3 $M^{-1}cm^{-1}$ and 1.5 x 10^3 $M^{-1}cm^{-1}$, respectively) and a group of moderately weak features (ε=150–

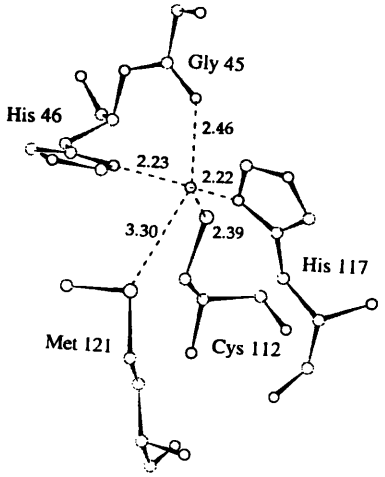

Fig. 1:4. The metal center in Ni(II)-azurin as seen in the X-ray crystal structure[61b].

[113a] Hill, H.A.O., Smith, B.E. & Storm, C.B. (1976) *Biochem. Biophys. Res. Commun. 70*, 783. b) Blaszak, J.A., Ulrich, E.L., Markley, J.L. & McMillin, D.R. (1982) *Biochemistry 21*, 6253. c) Dahlin, S., Reinhammar, B. & Ångström, J. (1989) *Biochemistry 28*, 7224.

[114a] Moratal, J.M., Salgado, J., Donaire, A., Jiménez, H.R. & Castells, J. (1993) *J. Chem. Soc. Chem. Commun.*, 110. b) Moratal, J.M., Salgado, J., Donaire, A., Jiménez, H.R., Castells, J. & Martínez-Ferrer, M[a].J. (1993) *Magn. Reson. Chem. 31*, 541. c) Moratal, J.M., Salgado, J., Donaire, A., Jiménez, H.R. & Castells, J. (1993) *Inorg. Chem. 32*, 3587. d) Salgado, J., Jiménez H.R., Donaire, A. & Moratal, J.M. (1995) *Eur. J. Biochem. 231*, 358. e) Piccioli, M., Luchinat, C., Mizoguchi, T.J., Ramírez, B.E., Gray, H.B. & Richards, J.H. (1995) Inorg. Chem. 34, 737. f) Vila, A.J. (1994) *FEBS Lett. 355*, 15.

[115] McMillin, D.R., Holwerda, R.A. & Gray, H.B. (1974) *Proc. Natl. Acad. Sci. U.S.A. 71*, 1974.

500 $M^{-1}cm^{-1}$) between 500 and 650 nm[14a,b] (Fig. 1:5B). The first two bands originate from S(Cys)-metal charge transfer transitions and correspond to the bands around 620 nm and 800 nm in Cu(II)-azurin, while the weak absorptions are due to d-d transitions[14b]. In the spectrum of Ni(II)-azurin, the LMCT bands are placed at lower energy (354 nm and 438 nm, ε = 1600 and 3300 $M^{-1}cm^{-1}$, respectively) and the d-d transitions, around 550 nm, are weaker and less resolved than in the cobalt derivative[14b, 101b] (Fig. 1:5A). Nowadays, this approach is still being used to reach a better understanding of some not very well known type 1 copper sites[116] and to characterize other new sites generated by site-directed mutagenesis[101b,102,103,114e]. The use of Co(II) or Ni(II) as spectroscopic probes for paramagnetic-NMR is discussed in the next section.

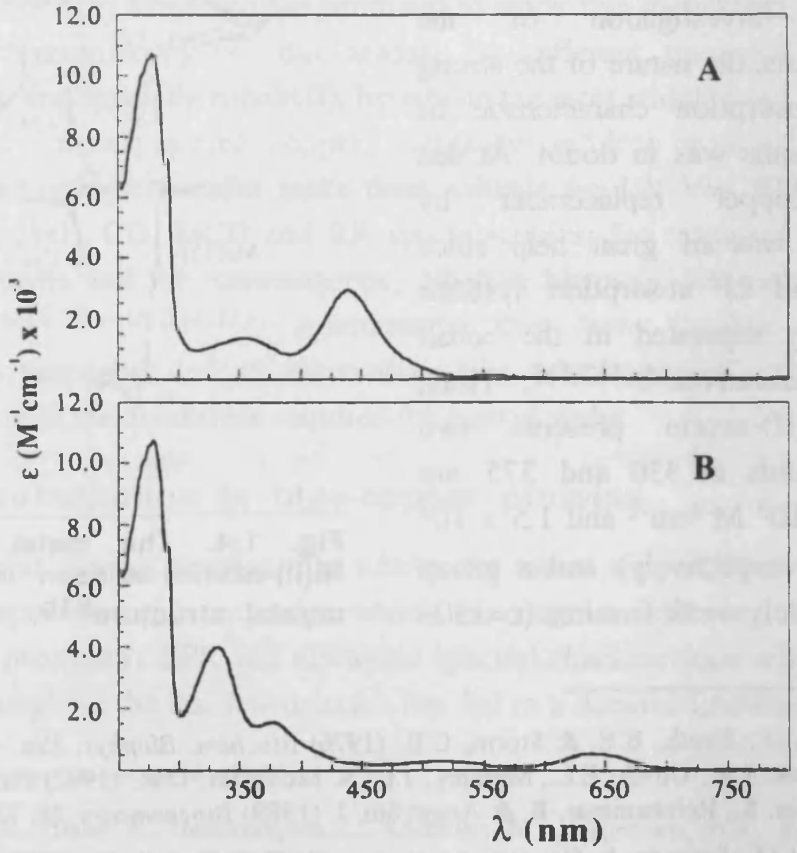

Fig. 1:5. The electronic spectra of *Pseudomonas aeruginosa* nickel(II)-azurin (A) and cobalt(II)-azurin (B).

[116]Strong, C., Harrison, S.L. & Wesley, Z. (1994) *Inorg. Chem. 33*, 606.

V. NMR of paramagnetic molecules.

As NMR has been the main technique used in this work, a brief introduction about it is presented here. Only general ideas will be discussed, especially those which introduce the blue-copper proteins and the cobalt and nickel metalloderivatives in the context of paramagnetic-NMR. Experimental aspects, related more directly with signal assignments and the analysis and interpretation of the data can be found in the next chapter.

a) The NMR phenomenon and the paramagnetic effect. Disadvantages and virtues.

For most of the NMR spectroscopists the presence of a paramagnetic center in the molecule is considered a big problem[117]. In fact it is, if we think on the "negative" consequences that it has on resonances feeling the paramagnetic effect: basically line broadening, which impair the signal/noise ratio making the signals difficult to be observed, and paramagnetic shift, which destroys completely the normal "topography" of the spectra and sends signals even some hundred ppms far away from their typical positions[15,111,118]. The insistence of a few groups (essentially I. Bertini's group and G.N. La Mar's group) during various decades, together with the technical improvement of the NMR apparatus, have made possible the development of experimental approaches which permit to board the study of the paramagnetic systems in a systematic and reliable way[111,118c,119]. The last few years have been particularly important for the development of this technique. Now, we can say that almost every type of NMR experiment can, in principle, be performed on a paramagnetic molecule using variations of the sequences employed in conventional diamagnetic NMR, or the same ones but choosing suitable values for the time parameters[119]. But which are the properties that can make attractive having a paramagnetic center in a system investigated by NMR. They are in essence the same that we have just described as drawbacks, i.e. paramagnetic relaxation and isotropic shifts, but

---

[117] Sanders, J.K.M. & Hunter, B.K. (1993) *Modern NMR Spectroscopy*, Oxford University Press, Oxford.

[118] **a)** Dwek, R.A. (1973) *Nuclear Magnetic Resonance in Biochemistry: Applications to Enzyme Systems*, Oxford University Press, London. **b)** La Mar, G.N., Horrocks, W.D. & Holm, R.H. (1973) *NMR of Paramagnetic Molecules*, Academic Press, New York. **c)** La Mar, G.N. & de Ropp, J.S. (1993) in *Biological Magnetic Resonance* (Berliner L.J. & Reuben , J., eds.) vol 12, p. 1, Plenum Press, New York.

[119] La Mar, G.N., ed. (1995) *Nuclear Magnetic Resonance of Paramagnetic Macromolecules, seriesC: Mathematical and Physicals Sciences*, vol. 457, Kluwer Accademic Publishers, Dordrecht.

with an appropriate experimental treatment they can be of great help for the NMR study of the system[15,111,118]. Thus, hyperfine shifts increase the resolution of the spectra and make the signals around the metal site (usually the active part of the metalloprotein) available to our direct observation out of the over-crowded diamagnetic region. Moreover, these signals become more sensitive to structural or chemical changes in the surroundings. Dynamic processes, like structural rearrangements, pH titrations or binding of ligands can be easily followed. On the other hand, the relaxation enhancement of protons around the paramagnetic center gives us the possibility to select them among the rest of some thousand diamagnetic signals using the pertinent NMR sequences[118c,119]. With a correct evaluation and interpretation of the paramagnetic relaxation and isotropic shifts, they become very powerful structural-related data[15,111,118c,119].

The hyperfine shift.

The resonating frequency (chemical shift) of a particular nucleus in an NMR spectrum is given by the following simple equation:

$$\omega = \gamma(B_0 - \sigma B_0) \qquad \text{Eq 1:1}$$

where γ is the magnetogyric ratio of the nucleus and σ is the so called screening constant. In diamagnetic systems[117], this chemical shift is principally due to the shielding effects of the electrons of the molecule in the presence of an external magnetic field. In paramagnetic systems[15], however, unpaired electrons have a large magnetic moment μ_S given by:

$$\mu_S = g\mu_S\sqrt{S(S+1)} \qquad \text{Eq 1:2}$$

where g is a proportionality parameter between the angular and magnetic moments whose value is g_e=2.0023 in the free electron case, μ_B is the Bohr magneton and S is the electron spin quantum number. This magnetic moment can be the main contributor to the screening constant, becoming the dominant factor determining the chemical shift. Since this contribution is due to the hyperfine coupling between the unpaired electrons and the resonating nucleus, it is normally called hyperfine shift[120]. It can be defined as the difference between the measured chemical shift of a nucleus in the paramagnetic compound and the shift of that nucleus in the same molecule if it were diamagnetic[15,120].

---

[120]Bertini, I. & Turano, P. (1995) in *Nuclear Magnetic Resonance of Paramagnetic Macromolecules, seriesC: Mathematical and Physicals Sciences* (La Mar, G.N., ed.) vol. 457, p. 29, Kluwer Accademic Publishers, Dordrecht.

The hyperfine coupling can be described using the spin Hamiltonian formalism as[15,120]:

$$\aleph = \hat{\mathbf{I}} \cdot \mathbf{A} \cdot \hat{\mathbf{S}} \qquad \text{Eq 1:3}$$

where $\hat{\mathbf{I}}$ and $\hat{\mathbf{S}}$ are the nuclear and electron spin operators, respectively, and $\mathbf{A}$ is the coupling tensor. This tensor contains a constant A_c which originates from the unpaired spin density sitting at the resonating nucleus[120]. It is related with the spin density ρ at the nucleus and does not depend on the molecular orientation, i.e. it is isotropic[15]. This constant A_c is called contact or Fermi-contact hyperfine coupling constant and is given by[120]:

$$A_c = \frac{\mu_0}{3S} \hbar \gamma_N g_e \mu_B \sum_i \rho_i \qquad \text{Eq 1:4}$$

where μ_0 is the magnetic permeability of vacuum and ρ_i is the spin density at the nucleus due to the i^{th} s orbital.

But the nuclear and electronic magnetic moments can also interact through space, and so the hyperfine coupling depends on the orientation of the $\hat{\mathbf{I}}$ and $\hat{\mathbf{S}}$ vectors. This effect of the unpaired spin density on the molecule over the resonating nucleus is dipolar in origin and can be represented by the dipolar tensor $\mathbf{A_{dip}}$, also contained in the coupling tensor $\mathbf{A}$ of Eq 1:3. If the system is characterized by an isotropic magnetic susceptibility, due to molecular tumbling in solution $\mathbf{A_{dip}}$ averages to zero. Conversely, in the presence of anisotropic magnetic susceptibility, the magnetic moment associated with $\hat{\mathbf{S}}$ changes with the orientation and the averaged $\mathbf{A_{dip}}$ is different from zero and amounts A_{pcon} [120]:

$$A_{pcon} = \frac{\mu_0}{4\pi} \frac{\hbar \gamma_N \mu_B}{3\bar{g}\mathbf{r}^3} \left\{ \left[\mathbf{g}_{zz}^2 - \frac{1}{2}\left(\mathbf{g}_{xx}^2 + \mathbf{g}_{yy}^2\right) \right] \left(3\cos^2\theta - 1\right) + \left[\frac{3}{2}\left(\mathbf{g}_{xx}^2 - \mathbf{g}_{yy}^2\right) \sin^2\theta \cos 2\varphi \right] \right\} \qquad \text{Eq 1:5}$$

where $\mathbf{r}$, θ and φ are the polar coordinates of the resonating nucleus with respect to the magnetic anisotropy tensor, and $\mathbf{g}_{ii}$ are the principal components of the $\mathbf{g}$ tensor. In this case, another contribution to the hyperfine shift appears, which due to its dipolar nature is often called dipolar shift[15]. However, in solution it is an averaged value, and as such is isotropic, so it should be better called pseudocontact shift[111].

Now we can also define the hyperfine shift as the algebraic sum of the Fermi-contact shift and the pseudocontact shift[15,111]. Since both terms are isotropic this sum is also called isotropic shift[15]. The contact and pseudocontact shifts are expressed by the following general equations, which take into account the zero-field splitting of an orbitally non-degenerated spin multiplet and the g and magnetic susceptibility, χ, anisotropy:

$$\left(\frac{\Delta\nu}{\nu_0}\right)^{con} = \frac{1}{\mu_0}\frac{A_c}{3\hbar\gamma_N\mu_B}\left(\frac{\chi_{xx}}{g_{xx}}\frac{\chi_{yy}}{g_{yy}}\frac{\chi_{zz}}{g_{zz}}\right) \qquad \text{Eq 1:6}$$

$$\left(\frac{\Delta\nu}{\nu_0}\right)^{pcon} = \frac{1}{4\pi}\frac{1}{3N_A}\left\{\left[\chi_{zz} - \frac{1}{2}(\chi_{xx}+\chi_{yy})\frac{3\cos^2\theta - 1}{r^3}\right] - (\chi_{xx}-\chi_{yy})\frac{\text{sen}^2\,\theta\cos 2\varphi}{r^3}\right\} \qquad \text{Eq 1:7}$$

where $\Delta\nu$ is the averaged isotropic shift, ν_0 is the resonance frequency of a reference nucleus at the magnetic field of the experiment, N_A is the Avogadro's constant, and χ_{ii} are the principal components of the magnetic susceptibility tensor.

Eq 1:7 is specially important since it relates a structural property, defined by the polar coordinates of the nucleus (r, θ and φ), with an observable value, $(\Delta\nu/\nu_0)$[15,111]. However, it is approximated because it is based on the assumption that the unpaired electron is fixed in a single position, which in a metalloprotein is identified with the metal ion (metal-centered point-dipole approximation). So, deviations from the values predicted by this equation can be severe in the presence of unpaired spin delocalization[15,111]. To factorize out the contact and pseudocontact contributions to the isotropic shift is difficult, because, in principle, the magnetic anisotropy and the orientation of the magnetic axes which define the magnetic susceptibility tensor need to be known[15]. Such geometrical coordinates could be determine by single-crystal magnetic susceptibility measurements, but this kind of experiments are not yet available for metalloproteins. Alternatively, the components of the magnetic susceptibility tensor can be estimated from single crystal EPR data[15,121]. The problem can be also tackled in the opposite way, i.e. using the hyperfine shifts of protons from non-coordinated residues, where these shifts are pure pseudocontact, to search

[121] Coremans, J.W.A., Poluektov, O.G., Groenen, E.J.J., Canters, G.W., Nar, H. & Messerschmidt, A. (1994) *J. Am. Chem. Soc. 116*, 3097.

for the magnetic anisotropy and the principal axes of the magnetic tensor[111]. This has been done successfully in the case of low-spin ferric hemoproteins[122] and in the cobalt(II) substituted carbonic anhydrase[123].

When it can be assumed that the magnetic anisotropy is small, the pseudocontact contribution may be neglected[15,111]. This is true when the ground state is orbitally non-degenerate, as in the case of six-coordinated Ni(II) in an octahedral symmetry[15]. In other cases, like low-spin Fe(III) and high-spin Co(II) complexes in some geometries, an orbitally degenerate ground state exists which accounts for large magnetic anisotropy, and so important pseudocontact contributions[122,123].

Paramagnetic relaxation.

The other important effect of the nucleus-unpaired electron hyperfine coupling is the paramagnetic relaxation enhancement[15,120,124]. It is due to the fluctuating magnetic fields provided by the unpaired electrons, which constitute an additional non-radiative relaxation pathway[15]. Three contributions are responsible for such fluctuating magnetic field: electron relaxation, molecular tumbling (in solution) and chemical exchange. To every of these contributions, corresponds a correlation time: τ_s, τ_r and τ_M, respectively[15,124]. In the general equations for the paramagnetic nuclear relaxation, it is expressed as a function of the correlation time τ_c, or time constant of the exponential process in which the nuclear and electron spins change their interaction energy[120]:

$$T_i^{-1} = \overline{E}^2 f_i(\tau_c, \omega_S, \omega_I); \; i = 1, 2 \qquad \text{Eq 1:8}$$

where $\overline{E}^2$ is the average of the squared coupling energy and ω_I and ω_S are the energies of the nuclear and electron transitions (the nuclear and electron Larmor frequencies, respectively). As in the case of the hyperfine shift, there are dipolar

---

[122]a) La Mar, G.N., Chen, Z. & de Ropp, J. (1995) in *Nuclear Magnetic Resonance of Paramagnetic Macromolecules, seriesC: Mathematical and Physicals Sciences* (La Mar, G.N., ed.) vol. 457, p. 55, Kluwer Accademic Publishers, Dordrecht. b) Rajarathman, K., La Mar, G.N., Chiu, M.L. & Sligar, S.G. (1992) *J. Am. Chem. Soc. 114*, 9048. c) La Mar, G.N., Chen, Z., Vyas, K. & McPherson, A.D. (1994) *J. Am. Chem. Soc. 117*, 411.

[123]Banci, L., Dugad, L.B., La Mar, G.N., Keating, K.A., Luchinat, C. & Pieratelli, R. (1992) *Biophys. J. 63*, 530.

[124]a) Banci L., Bertini, I., Luchinat, C. (1991) *Nuclear and Electron Relaxation*, VCH, Weinheim. b) Bertini, I., Luchinat, C. & Messori, L. (1987) in *Metal Ions in Biological Systems* (Sigel, H., ed.) vol. 21, p. 47, Marcell Dekker, New York.

and contact contributions to the paramagnetic relaxation. The corresponding values of $\overline{E}^2$ are given by the equations[120]:

$$\overline{E}^2_{cont} = \frac{2}{3}\left(\frac{A_c}{\hbar}\right)S(S+1) \qquad \text{Eq 1:9}$$

$$\overline{E}^2_{pcon} = \frac{2}{15}\left(\frac{\mu_0}{4\pi}\right)^2 \frac{\gamma_N^2 g_r^2 \mu_B^2 S(S+1)}{r^6} \qquad \text{Eq 1:10}$$

There is also a dipolar coupling energy between the electron magnetic moment induced by the external magnetic field and the nuclear magnetic moment. The corresponding relaxation mechanism is called Curie relaxation[15,120,124], and its average squared energy is given by[120]:

$$\overline{E}^2_{Curie} = \frac{2}{5}\left(\frac{\mu_0}{4\pi}\right)^2 \frac{\hbar^2 \gamma_N^2 g_e^2 \mu_B^2}{r^6} \qquad \text{Eq 1:11}$$

Since the induced magnetic moment is small, this energy is also small, but it increases with the external magnetic field and is modulated by the rotation which is slow in macromolecules. So, for the Curie relaxation the correlation time is τ_r. This relaxation mechanism is specially important on determining T_2 [15,124].

In the case of longitudinal relaxation times T_1, which are generally more relevant for the paramagnetic-NMR studies, the dipolar contribution is dominant[15, 111,120,124]. Such dipolar relaxation rate is normally expressed by the so-called Solomon equation[15,124,125]:

$$T_1^{-1} = \frac{2}{15}\left(\frac{\mu_0}{4\pi}\right)^2 \frac{\gamma_N^2 g_r^2 \mu_B^2 S(S+1)}{r^6}\left(\frac{7\tau_c}{1+\omega_S^2\tau_c^2} + \frac{3\tau_c}{1+\omega_I^2\tau_c^2}\right) \qquad \text{Eq 1:12}$$

where the $\omega_S \pm \omega_I$ energies are approximated to ω_S. The correlation time is given by:

$$\tau_c^{-1} = \tau_s^{-1} + \tau_r^{-1} + \tau_M^{-1} \qquad \text{Eq 1:13}$$

where the three contributing terms are related with the electron relaxation, molecular tumbling and chemical exchange processes as defined above. The

[125] a) Bloembergen, N., Purcell, E.M. & Pound, R.V. (1948) *Phys. Rev. 73*, 679. b) Solomon, I. (1955) *Phys. Rev. 99*, 559. c) Bloembergen, N. & Morgan, L.O. (1961) *J. Chem. Phys. 34*, 842. d) Koening, S.H. (1982) *J. Magn. Reson. 47*, 441.

fastest of these processes, usually the electron relaxation, will be dominant, and the corresponding correlation time become the τ_c of the dipolar relaxation[15,124].

Again, Eq 1:12 is only valid assuming the metal-centered approximation and deviations can be important when there is spin delocalization in the metal ligands[15,124]. However, these ligand-centered effects are difficult to be quantified because the spin distribution is normally not known with enough accuracy.

b) The unpaired-electron relaxation: a determining factor.

All we can get from the NMR spectra of a paramagnetic metalloprotein, depends on our faculty of observing, assigning and analyzing the paramagnetic signals[111,118c]. The relaxation enhancement on the observed nuclei, typically protons, due to coupling with the unpaired electrons of the paramagnetic metal center, should be large enough to make these nuclei distinguishable from the majority of the (diamagnetic) protons of the system, but small enough to permit their observation, assignment and study. It means that the line-width of the proton signals must be generally $\leq$ 1000 Hz, and the longitudinal relaxation times should be $\geq$ 0.5 ms.

According to the relaxation equations, is the electronic relaxation time of the unpaired electrons, τ_s, which determines the relaxation of the protons in a paramagnetic metalloprotein, since in these systems the rotation of the molecules is slow and $\tau_r \gg \tau_s$[15,124]. Thus, a paramagnetic metal ion is an adequate spectroscopic probe for the so-called paramagnetic-NMR when its unpaired electrons relax fast[111]. There is a qualitative statement, derived from the Solomon equation, that can be enunciated as follows: the shorter the electronic relaxation times of the metal ions, the sharper the NMR signals of the nuclei coupled to the unpaired electrons[15,118b]. As it can be observed in Table 1:3, at a 100 MHz field values of τ_s in the range of 10^{-10}-10^{-13} sec induce line broadening in the range of 1-1200 Hz on signals corresponding to protons placed at 5 Å from the metal center[15,111,]. So, nickel(II) and cobalt(II) are, together with low-spin iron(III), high spin iron(II) and most of the lanthanides, suitable for paramagnetic-NMR studies[15,111]. The actual τ_s values of these metal ions vary within a large interval, depending on the coordination geometries adopted in each case[15,124].

Table 1:3. Electron-relaxation times τ_S of some paramagnetic metal ions[15]. The line broadening $\Delta\nu$ is that induced at a 100 MHz field in NMR resonances of protons placed at 5 Å from the metal. $\Delta\nu$ values have been calculated using the relaxation equations for T_2^{-1}, considering metal-centered dipolar relaxation and no magnetic field effect on τ_S.

metal ion	τ_s (sec)	$\Delta\nu$ (Hz)
Ti^{3+}	$10^{-9} - 10^{-10}$	1000–100
V^{2+}	5×10^{-10}	2500
V^{3+}	5×10^{-12}	5
VO^{2+}	$10^{-8} - 10^{-9}$	10000–1000
Cr^{3+}	5×10^{-10}	2500
Cr^{2+}	10^{-11}	80
Mn^{3+}	$10^{-10} - 10^{-11}$	800–80
Mn^{2+}	$10^{-9} - 10^{-10}$	12000–1200
Fe^{3+} (HS)	$10^{-10} - 10^{-11}$	1200–120
Fe^{3+} (LS)	$10^{-11} - 10^{-12}$	10–1
Fe^{2+} (HS)	$10^{-11} - 10^{-12}$	80–10
Co^{2+} (HS)	$10^{-11} - 10^{-12}$	50–5
Co^{2+} (LS)	$10^{-9} - 10^{-10}$	1000–100
Ni^{2+}	$10^{-10} - 10^{-12}$	300–3
Cu^{2+}	$(1–3) \times 10^{-9}$	3000–1000
Ru^{3+}	$10^{-11} - 10^{-12}$	10–1
Re^{3+}	10^{-11}	30
Gd^{3+}	$10^{-8} - 10^{-9}$	4000000–60000
Dy^{3+}	8×10^{-13}	100
Ho^{3+}	8×10^{-13}	100
Tb^{3+}	8×10^{-13}	100
Tm^{3+}	8×10^{-13}	70
Yb^{3+}	1×10^{-12}	30

c) Paramagnetic-NMR and copper proteins.

Copper(II), a d^9 metal ion, is paramagnetic with S=1/2. However, Cu(II)-proteins are generally not adequate for paramagnetic-NMR since their τ_s is very large (1-3 x 10^{-9} sec) giving rise to very broad paramagnetic signals[15,111]. Two exceptions are found to this general rule. The first one is the case in which we have a polimetallic system where Cu(II) can magnetically couple with another paramagnetic metal ion with a much faster electron relaxation[120,111,124a]. This is the case of the copper-zinc metalloprotein superoxide dismutase[126] when zinc is replaced by Co(II) or Ni(II). The magnetic coupling between this new metal ion and Cu(II), through a common imidazole ligand, results in an increase of the

[126a] Bertini, I., Banci, L. & Luchinat, C. (1988) in *Metal clusters in proteins* (Que, L.Jr., ed.) p. 70, Am. Chem. Soc., Washington, DC. b) Bertini, I., Luchinat, C. & Piccioli, M. (1994) *Progr. in NMR spectr. 26*, 91.

relaxation rate of the copper unpaired electron, which takes advantage of the relaxation mechanisms operative in the cobalt or nickel ions[124a]. As a consequence, τ_s for copper decreases and relatively narrow signals from protons around both metal ions can be detected[126]. The second example has been observed in the blue copper proteins amicyanin and azurin[127]. As it is well known, these proteins undergo very quick electron self-exchange reactions (k_{ESE}=10^4-10^6 M^{-1} sec^{-1})[94]. Under this fast exchange conditions, in partially oxidized samples (3% to 15%), protons from the Cu(I) species close to the metal center have their relaxation times shortened, due to the paramagnetic effect that they experience whenever the copper gets oxidized[127]. This mixing of the relaxation times of the Cu(II) and Cu(I)-species occurs because the exchange rate is faster than the relaxation rate (the process is fast with regard to the relaxation rate time-scale)[128]. However, the process is slow in the chemical shift time-scale and the "paramagnetic" signals of the Cu(I)-species are observed in the same position as in the completely reduced samples, whatever the concentration of the Cu(II)-species is[127]. This fact permits the selective observation of signals from protons close to the metal center using experimental approaches designed for paramagnetic molecules, like the super-WEFT and WEFT-NOESY sequences[129]. In the completely oxidized sample, isotropically shifted signals corresponding to the coordinated residues can be observed. Although some of them are extremely broad, assignments have been made by means of WEFT-EXSY spectra on 50% oxidized samples[127].

d) Probing the blue-copper site by NMR on the cobalt and nickel derivatives.

Another approach to study the copper proteins by paramagnetic-NMR is to replace the slow-relaxing Cu(II) by a fast-relaxing metal ion like Co(II) or Ni(II)[113,114]. We are going to discuss now the electronic properties of these metal ions which make them suitable for this kind of experiments.

Cobalt(II) in paramagnetic-NMR.

Cobalt(II) is a d^7 ion which can be either high-spin (S=3/2) or low-spin (S=1/2), although the high-spin form is more common[15], being the low-spin one only found under strong-ligand conditions as in the case of planar cobalt-

---

[127]Kalverda, A.P., Salgado, J., Dennison, C. & Canters, G.W. (1995) *Biochemistry*, submitted.

[128]Sandström, J. (1982) *Dynamic NMR spectroscopy*, Academic Press, New York.

[129]a) Inubushi, T. & Becker, E.D. (1983) *J. Magn. Reson. 51*, 128. b) Chen, Z., de Ropp, J.S., Hernández, G. & La Mar, G.N. (1994) *J. Am. Chem. Soc. 116*, 8772.

porphyrins[130]. Thus, in most cobalt-substituted metalloproteins, Co(II) is found in the high-spin state[111]. It has usually short electron relaxation times which range from 10^{-11} to 10^{-12} sec, depending on the coordination geometry. Consequently, it is a good spectroscopic probe for NMR[15,111]. The lowest energy (ground) terms for a S=3/2 d^7 ion in octahedral, square pyramidal, trigonal bipyramidal and tetrahedral geometries are represented in Fig. 1:6.

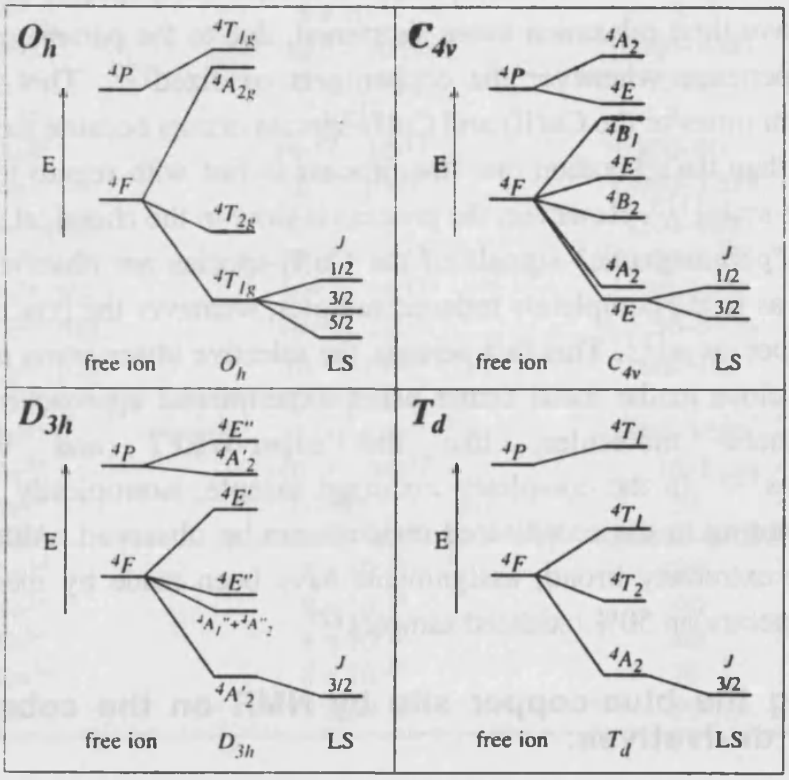

Fig. 1:6. Splitting and spin-orbit coupling of ion terms of high-spin cobalt(II) in different coordination geometries: octahedral (O_h), square pyramidal (C_{4v}), trigonal bipyramidal (D_{3h}) and tetrahedral (Td). The energy scaling is arbitrary.

Octahedral (O_h) high spin cobalt(II) presents a $^4T_{1g}$ ground state. Upon spin-orbit coupling, this triplet converts into three energy levels that give six Kramers' doublets. Due to this, electron relaxation in these systems is fast (in the order of 10^{-12} sec), and so, ^{1}H NMR signals are relatively narrow and easily observed[15,111]. High-spin cobalt(II) in five coordinated complexes also presents

[130] a) Shirazi, A. & Goff, H.M. (1982) *Inorg. Chem. 21*, 3420. b) Inubushi, T., Ikeda-Saito, M. & Yonetani, T. (1983) *Biochemistry 22*, 2904.

fast electronic relaxation times which depend on the geometry adopted. For a trigonal bipyramidal geometry (D_{3h}), the $^4A_2$ ground state is orbitally-non-degenerate and does not split, but the existence of low-lying excited states populated at room temperature makes the electron relaxation relatively fast[15,124a]. NMR signals are usually not very broad and they can be detected even when the electron relaxation is slower than in octahedral complexes. In the square pyramidal geometry (C_{4v}), the excited states lie closer to the ground state and exhibit electron relaxation intermediate between that corresponding to the O_h and D_{3h} geometries. Finally, for high spin cobalt(II) in a tetrahedral environment (T_d), the difference in energy between the first excited level and the non-degenerated $^4A_2$ ground state is higher than in five coordinated complexes. Therefore, four coordinated cobalt(II) has shorter electronic relaxation times (about 10^{-11} s)[15,124a]. However, even in this case, ^{1}H NMR lines are still sharp enough to be detected. To sum up, the electronic relaxation rates in high spin cobalt(II) complexes increase with the coordination number. Similarly, the relaxation times of protons coupled to the unpaired electrons are found to follow the same order. Thus, in these systems, signals are sharper and better resolved in the order: $O_h > D_{3h} > T_d$.

A comment must be made on the magnetic anisotropy of these systems. It arises from the existence of populations in different electronic states. Therefore, the magnetic anisotropy in Co(II) complexes follows the order: $O_h > D_{3h} > T_d$[15]. Likewise, as magnetic anisotropy increases, the dipolar term of the isotropic shift for protons near the metal ion also increases, and so, a large number of signals with pseudo-contact contribution to the hyperfine shift are observed[15,111].

Nickel(II) in paramagnetic-NMR.

The spin state of Ni(II), a d^8 ion, depends on its coordination geometry (Fig. 1:7) [15]. In octahedral or pseudo-tetrahedral coordination, it is paramagnetic with S=1, but it is low-spin diamagnetic when exhibits a tetragonal planar geometry. Five-coordinated nickel(II) can be either paramagnetic (high-spin) or diamagnetic (low-spin), depending on the nature of the donor atoms. In metalloproteins it is normally pseudo-tetrahedral (paramagnetic)[15,111].

The electron relaxation properties of nickel(II) complexes in octahedral and pseudo-tetrahedral environments follow an opposite pattern to that observed for cobalt(II)[15,124]. Six-coordinated nickel(II) complexes have an orbitally-non-degenerate $^3A_2$ ground state level, and the first excited state is some thousand wave numbers far away. So in these cases, broad signals in the NMR spectrum and no magnetic anisotropy are expected (except a small magnetic anisotropy due

to zero-field splitting)[15]. Conversely, in pseudo-tetrahedral symmetry, the electron relaxation is fast because there are closely spaced levels from a 3-fold orbitally-degenerated $^3T_1$ ground state. It means that NMR proton signals will be sharp and well resolved, and sizable pseudocontact contributions to the isotropic shifts must be present due to the existence of magnetic anisotropy[15].

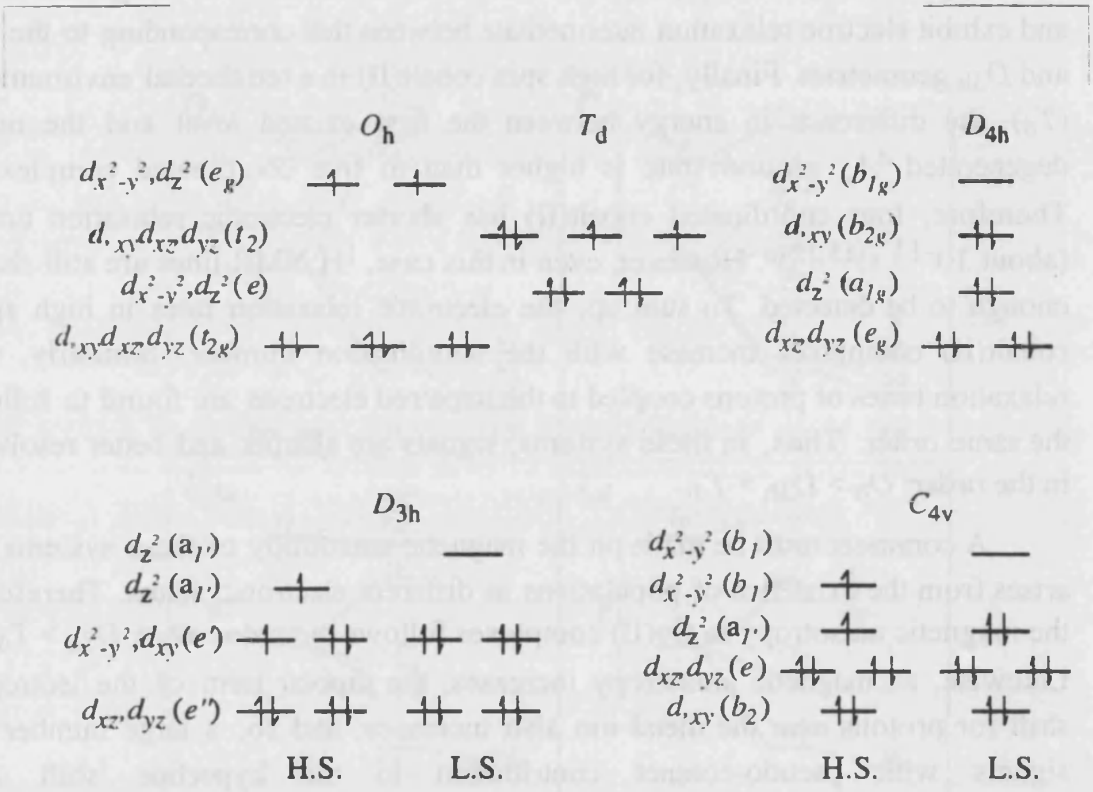

Fig. 1:7. The electronic configuration of nickel(II) in various coordination geometries[15].

The fact that the relaxation properties of nickel(II) and cobalt(II) are the opposite in similar coordination environments and geometries, make these metal ions complementary for paramagnetic-NMR investigations through metal substitution. Thus, the use of cobalt is generally more convenient when larger coordination numbers are expected, i.e. in the case of six-coordinated complexes. Nickel, on the contrary, should be better used in tetrahedral coordination sites. Penta-coordination, an intermediate case, is frequently found in metalloproteins, so the use of both metal ions as paramagnetic probes in these systems results very interesting.

NMR investigations on nickel and cobalt derivatives of blue-copper proteins.

The experimental approach of this work is mainly focused on using the properties of the Co(II) and Ni(II) to get information about azurin by means of NMR. Although this has been a common strategy in the case of the zinc proteins[16,106a,108,111] its use for the blue copper proteins has been until recently very limited[113,114]. Before 1993, only three examples on the application of paramagnetic-NMR on Co(II) or Ni(II)-derivatives of blue-copper proteins appeared in the literature[113]. In the first one, published in 1976 by Hill, et al.[113a], the ^1H NMR spectrum of *Pae* Co(II)-azurin at 270 MHz is reported. Although the quality of the spectra does not permit an adequate analysis of the isotropically shifted resonances, the authors point out the potentiality of this approach in order to get structural information about the type 1 metal site. The pH dependent conformational equilibrium is studied and a $pK_a \approx 6$ is estimated for the deprotonation of the His35 residue, whose imidazole signals are tentatively assigned. The second paper shows the ^1H NMR spectrum of *Pae* Ni(II)-azurin, but only the Met121 methyl signal is assigned in the basis of its three-fold area[113b]. Finally, a study of the metal site in cobalt-substituted stellacyanin by paramagnetic-NMR had been also published[113c], in which the assignments were based on distances calculated by means of the Solomon equation using T_1 relaxation data. The recent development of new assignment strategies for the NMR spectra of paramagnetic molecules, as well as the improvement of the commercial NMR spectrometers, have permitted in the last few years a more efficient use of the cobalt(II) and nickel(II) paramagnetic properties to probe the metal environment in blue-copper proteins[114]. Many of these new results will be presented here as part of this work.

e) Assignment of paramagnetic signals: a limiting step.

To have access to the potential information provided by a paramagnetic-NMR spectrum, we need a systematic strategy to perform unambiguous signal assignments[118c]. Early strategies were based on the comparison of the shifts of model compounds with those of the metalloprotein[131]. This method is normally unreliable due to the difficulty to select appropriate models. A more reliable method involves selective isotopic labeling (selective replacement of ^1H and ^{12}C by ^2H and ^{13}C), which however implies laborious synthetic work and is restricted to special reversibly removable prosthetic groups, like some types of

[131] La Mar, G.N. (1979) in *Biological Applications of Magnetic Resonance* (Shulman, ed.) p.305, Academic Press, New York.

heme groups[132]. A very widely applied strategy was the analysis of paramagnetic dipolar relaxation, assuming that the induced relaxivity is proportional to the inverse sixth power of the distance from the metal ion[15]. This method led very frequently to ambiguous situations and important errors in the assignments, since relaxation equations are approximate and deviations can be important in real cases, like when delocalization of the unpaired-electron density is present. However, it provided many of the assignments for non-heme paramagnetic proteins made before the application of modern 1D and 2D NMR methodologies.

Multidimensional NMR spectroscopy is an effective methodology applied to the assignment of resonances and structure determination in diamagnetic proteins since the early 80s[133]. But the application of these techniques to paramagnetic metalloproteins had to wait still some more years, until special strategies were developed to deal with broad signals and short relaxation times. Thus, 1D NOE dominated the assignment methodologies for paramagnetic signals in the 80s, being systematically introduced for many different hemoproteins in most accessible oxidation and spin states[134]. More recently, it has been extended to iron-sulfur proteins[135] and Co(II) or Ni(II) substituted zinc and copper proteins[114,123,136].

Reports on 2D NMR applied to paramagnetic systems started to appear in the mid 80s[137], but were the 90s which witnessed an authentic expansion and generalization of multidimensional NMR techniques in paramagnetic systems[119].

---

[132]a) La Mar, G.N., Budd, D.L., Viscio, D.B., Smith, K.M. & Langry, K.C. (1980) *J. Am. Chem. Soc. 102*, 1822. b) La Mar, G.N., Yamamoto, Y., Jue, T., Smith, K.M. & Pandey, R.K. (1985) *Biochemistry 24*, 3826.

[133]Wüthrich, K. (1986) *NMR of proteins and nucleic acids*, John Wiley & Sons, New York.

[134]a) Keller, R.M. & Wüthrich, K. (1978) *Biochem. Biophys. Res. Commun. 83*, 1132. b) Ramaprasad, S., Johnson, R.D. & La Mar, G.N. (1984) *J. Am. Chem. Soc. 106*, 5330. c) Unger, S., Lecomte, J.T.J. & La Mar, G.N. (1985) *J. Magn. Reson. 64*, 521. d) McLachlan, S.J., La Mar, G.N. & Lee, K.B. (1988) *Biochim. Biophys. Acta 957*, 430. e) Thanabal, V. & La Mar, G.N. (1989) *Biochemistry 28*, 7038. f) Satterlee, J.D. & Erman, J.E. (1991) *Biochemistry 30*, 4398.

[135]a) Cowan, J.A. & Sola, M. (1990) *Biochemistry 29*, 5633. b) Bertini, I., Briganti, F., Luchinat, I., Scozzafava, A. & Sola, M. (1991) *J. Am. Chem. Soc. 113*, 1237.

[136]a) Banci, L., Bertini, I., Luchinat, C. & Piccioli, M. (1990) *FEBS Lett. 272*, 175. b) Banci, L., Bencini, A., Bertini, I., Luchinat, C. & Piccioli, M. (1990) *Inorg. Chem. 29*, 4867. c) Moratal, J.M., Martínez-Ferrer, M.J., Donaire, A., Castells, J., Salgado, J. & Jiménez, H.R. (1991) *J. Chem. Soc. Dalton Trans.*, 3393. d) Bertini, I., Luchinat, C., Ming, L.J., Piccioli, M., Sola, M. & Valentine, J.S. (1992) *Inorg. Chem. 31*, 4433.

[137]a) Yu, C., Unger, S.W. & La Mar. G.N. (1985) *J. Magn. Reson. 67*, 346. b) Jenkins, B.G. & Lauffer, R.B. (1988) *J. Magn. Reson. 80*, 328.

2D dipolar correlation via NOESY experiments and scalar correlation by means of COSY have been applied first; specially to low-spin Fe(III) hemoproteins, but also to different types of Fe-S cluster protein and Co(II) and Ni(II) metallosubstituted proteins[111]. More recently, other pulse sequences normally used in conventional systems, like TOCSY, have been also tried[122a,129b]. It has been shown that, in general, all the pulse sequences initially developed for diamagnetic proteins can be applied in paramagnetic systems, with an appropriate choice of the time parameters taking into account the T_1 and T_2 of the paramagnetic signals[138,139]. However, some limitations inherent in these paramagnetic systems have been found, like cross-correlation effects between the inter-proton dipolar coupling and Curie relaxation inducing relaxation allowed coherence transfer, which give raise to "false" scalar couplings in the COSY spectra[140]. Additionally, new sequences like WEFT or DEFT-NOESY are being used[122a,129b] in which typical approaches developed for selecting paramagnetic signals in 1D NMR spectra (super-WEFT or mo-DEFT)[15,129a] are combined with a normal NOESY to give a very effective sequence for dipolar correlation in paramagnetic proteins. Nowadays, even sequences as complex as NOE-NOESY[141] and 3D NOE-NOE[142], as well as ^{15}N-^{1}H and ^{13}C-^{1}H heterocorrelated experiments (HMQC)[143], are being successfully applied to paramagnetic metallo-proteins and it has been shown that the determination of the tertiary structure of a paramagnetic metalloprotein by means of NMR is no longer an impossible task[144]. Among the principal limitations that still today can

---

[138]Banci, L., Bertini, I. & Luchinat, C. (1994) *Methods Enzymol. 239*, 485.

[139]Luchinat, C. & Piccioli, M. (1995) in *Nuclear Magnetic Resonance of Paramagnetic Macromolecules, seriesC: Mathematical and Physicals Sciences* (La Mar, G.N., ed.) vol. 457, p. 1, Kluwer Accademic Publishers, Dordrecht.

[140]**a)** Wimperis, S. & Bodenhausen, G. (1989) *Mol. Phys. 66*, 897. **b)** Bertini, I., Luchinat, C. & Tarchi, D. (1993) *Chem. Phys. Lett. 203*, 445. **c)** Qin, J., Delaglio, F., La Mar, G.N. & Bax, A. (1993) *J. Magn. Reson. Ser. B 102*, 332.

[141]Bertini, I., Dikiy, A., Luchinat, C., Piccioli, M. & Tarchi, D. (1994) *J. Magn. Reson. Ser. B 103*, 278.

[142]Banci, L., Bermel, W., Luchinat, C., Pierattelli, R. & Tarchi, D. (1993) *Magn. Reson. Chem. 31*, 3.

[143]**a)** Oh, B.H. & Markley, J.L. (1990) *Biochemistry 29*, 3993. **b)** Santos, H. & Turner, D.L. (1992) *Eur. J. Biochem. 206*, 721. **c)** Shiro, Y., Iizuka, T., Makino, R., Ishimura, Y. & Morishima, I. (1989) *J. Am. Chem. Soc. 111*, 7707. **d)** Bertini, I., Luchinat, C., Macinai, R., Piccioli, M. Scozzafava, A. & Viezzoli, M.S. (1994) *J. Magn. Reson. Ser. B 104*, 95. **e)** Bertini, I., Capozzi, F. Luchinat, C., Piccioli, M. & Vila, A.J. (1994) *J. Am. Chem. Soc. 116*, 651.

[144]**a)** Banci, L. & Pieratelli, R. (1995) in *Nuclear Magnetic Resonance of Paramagnetic Macromolecules, seriesC: Mathematical and Physicals Sciences* (La Mar, G.N., ed.) vol. 457, p.

be found in paramagnetic-NMR, the dependence on a crystal structure of a close analogue protein, to interpret some paramagnetic NOESY data in terms of specific assignments, is perhaps the most severe[139]. In a paramagnetic metalloprotein, there are always some protons from residues in the surroundings of the metal center which are lost in the 2D maps due to their short relaxation times (specially when these protons appear in the crowded region of the spectrum). This means that the usual strategies for sequential-specific assignment[133] can not be always applied in these cases, since some spin systems are "incomplete" on one hand, and is not possible to follow the complete protein sequences through $C_\alpha H$-NH dipolar correlations on the other hand.

281, Kluwer Accademic Publishers, Dordrecht. **b)** Banci, L., Bertini, I., Eltis, L.D., Felli, I.C., Kastrau, D.H.W., Luchinat, C., Piccioli, M., Pierattelli, R. & Smith, M. (1994) *Eur. J. Biochem. 225*, 715. **c)** Banci, L., Bertini, I., Dikiy, A., Kastrau, D., Luchinat, C. & Sompornpisut, P. (1995) *Biochemistry 34*, 206.

Chapter 2

Experimental methodology.

I. Obtaining and preparing the protein samples.

a) Bacterial growth.

Part of the azurin samples were extracted from *Pseudomonas aeruginosa* (*Pae*) bacteria. The strain 110 obtained from the "Colección Española de Cultivos Tipo" (CECT 110) was grown at 35 ºC in anaerobic conditions in a medium rich in KNO_3 salt as described by Parr et al[1]. For the large scale growth, a 400 ml culture grown overnight was used to inoculate 12 L of fresh medium in an automatic 14 L fermentor (New Brunswick Scientific Co. NB, USA.). Growth was maintained at 35 ºC in continuous agitation (100 rpm) with N_2 aeration to ensure anaerobic conditions. After 20 hours the bacteria were harvested by centrifugation and the wet cell paste obtained (4 g per liter of culture) was stored at –20 ºC.

Wild-type and mutated *Alcaligenes denitrificans* (*Ade*) azurins were obtained from the heterologous expression of the corresponding *azu* genes in *Escherichia coli* (K12, strain JM101)[2]. The expression plasmids used (pCH5 for the wt azurin and pCH6 for the M121Q azurin) had been constructed by Carla Hoitink and contained the wt or site-directed mutant *Ade azu* genes inserted

---

[1] Parr, S.R., Barber, D., Greenwood, C., Phillips, B.W. & Melling, J. (1976) *Biochem. J. 157*, 423.

[2] Hoitink, C. (1993) PhD Thesis, *Leiden University*, The Netherlands.

behind the *lac* promoter in a pUC19 plasmid[2,3]. Large scale bacterial growth was performed as follows. A 300 ml culture of *E. coli* cells, freshly-transformed with the corresponding expression plasmid, was grown overnight in LB medium[4] with ampicillin (50 μg/ml) and then used to inoculate 30 L of the same medium supplemented with $CuSO_4$ (0.1 mM), in a computer controlled 40 L fermentor (NBS MPP40, New Brunswick Scientific, New Brunswick, USA). Cells were grown at 37 °C until the oxygen consumption reaches a maximum. Then IPTG was added (up to 100 μM) and the culture was maintained for about 3 hours until the oxygen consumption sloped down. Bacteria were harvested by tangential filtration (Millipore) resulting in 4–5 g of wet cell paste per liter of culture.

b) Protein isolation and purification.

Pseudomonas aeruginosa azurin.

Pae azurin was purified according to the reported procedures[1,5] with minor modifications. 100 g of cell paste were defrozen and resuspended in 500 ml of 20 mM potassium phosphate buffer pH 7.0 at 4 °C. Cells were disrupted by ultrasonication of 100 ml batches of the cell suspension for 2 min at 140 W and 0 °C. The sonicated suspension was stirred vigorously and then centrifuged at 10,000 g for 20 min. The crude-extract supernatant, with a dark green-brown color, was decanted from the precipitated cell debris and fractionated by precipitation with $(NH_4)_2SO_4$ in two steps. In the first one it was brought to 45% saturation in $(NH_4)_2SO_4$ and a precipitate of unwanted proteins, obtained by centrifugation at 20,000 g for 20 min, was discarded. Then, the clear yellowish supernatant was brought to 95 % saturation in $(NH_4)_2SO_4$ and the pale yellow supernatant was discarded. The greenish precipitate was resuspended in a minimum volume of 20 mM sodium phosphate buffer, pH 7.0, and dialyzed overnight at 4 °C against 5 L of the same buffer. The dialyzed protein solution was applied to a 3cm x 50 cm DEAE-Sephacel column equilibrated with 20 mM-sodium phosphate buffer, pH 7.0. Under these conditions *Pae* respiratory proteins (nitrite reductase, cytochrome c_{551} and azurin) do not absorb to the gel and elute with the same buffer as a broad band of

---

[3] a) Hoitink, C., Woudt, L.P., Turenhout, J.C.M., van de Kamp, M. & Canters, G.W. (1990) *Gene 90*, 15. b) Romero, A., Hoitink, C.W.G., Nar, H., Huber, R., Messerschmidt, A. & Canters, G.W. (1993) *J. Mol. Biol. 229*, 1007.

[4] Sambrook, J., Fritsch, E.F. & Maniatis, T. (1989) *Molecular cloning, a laboratory manual*, Cold Spring Harbor, New York.

[5] Ambler, R.P. & Wynn, M. (1973) *Biochem. J. 131*, 485.

bright-green fractions. They were pooled and concentrated down to 10 ml by ultrafiltration in amicon cells (Amicon, MA, USA). Subsequently, the concentrated solution was applied to a Sephadex G-100 column (2.5cm x 90cm) equilibrated in 10 mM-Tris/HCl buffer, pH 7.5 and eluted with the same buffer at a 5 ml per hour elution rate. Three colored bands were collected from this column. The first one, of a clean bright-green color, showed the visible-spectrum of the *Pae* nitrite reductase (cytochrome cd_1)[6] (Fig. 2:1A). The second and the third bands were not clearly resolved. They displayed intense blue and orange colors, respectively, and their visible spectra corresponded to azurin and cytochrome c_{551}[7] (Fig. 2:2 and Fig. 2:1B), although the blue fractions appeared contaminated with cytochrome c, as judged by the existence of a small band at 410 nm in the visible spectrum (not shown). Fractions from the blue band were

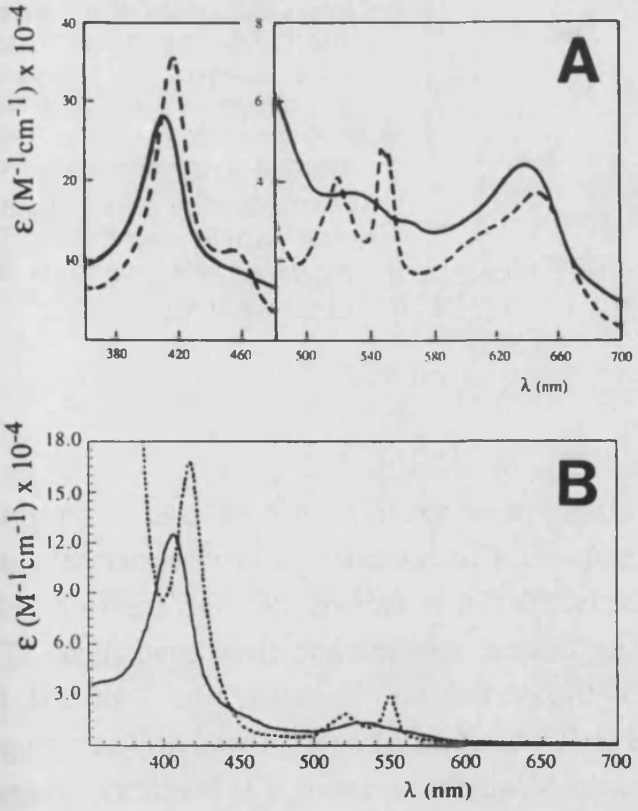

Fig. 2:1. UV-Vis spectra of Pae nitrite reductase (A) and cytochrome c551 (B) in 10 mM-Tris/HCl buffer, pH 7.5. Both proteins are obtained together with azurin using the purification procedure described in the text. The spectra drawn in broken lines correspond to the reduced proteins, and have been recorded in presence of sodium dithionite.

pooled together and the pH was lowered down to 4.0 by adding 1M acetic acid. Then this solution was applied to a CM-Sephadex column (2.5 cm x 30 cm) equilibrated with 50 mM-ammonium acetate buffer, pH 4.0, and a thin intense

6 Silvestrini, M.C., Colosimo, A., Brunori, M., Walsh, T.A., Barber, D. & Greenwood, C. (1979) *Biochem. J. 183*, 701.

7 Ambler, R.P. (1963) *Biochem. J. 89*, 341.

blue band appeared on top of the column. It was washed with the same buffer at pH 4.5 until a weak orange band eluted from the column. Meanwhile, the blue band spread and migrated slowly down. It was finally eluted with 50 mM-ammonium acetate buffer at pH 4.7 as a diluted pale-blue solution. It normally contained pure Cu(II)-azurin which migrated as a single band in SDS PAGE. The UV-Vis spectrum of this sample (Fig. 2:2) displayed only the bands corresponding to azurin with a spectral ratio A_{625}/A_{280}=0.54–0.56. About 0.5 mg of pure azurin per gram of *Pae* cell paste were obtained using this procedure.

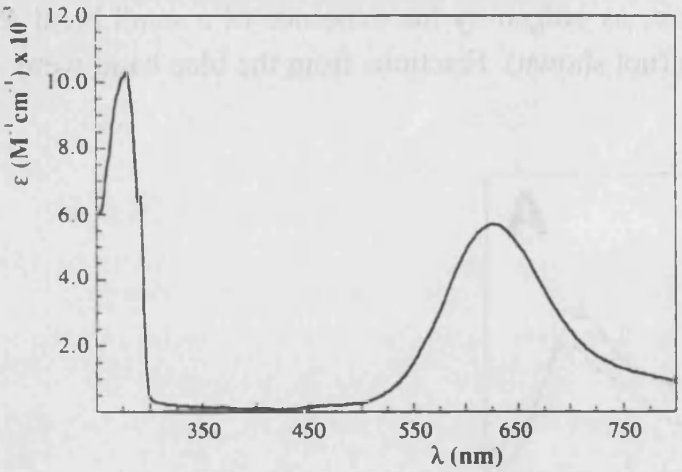

Fig. 2:2. UV-Vis spectrum of oxidized pure *Pae* azurin. No absorption is observed at 414 nm corresponding to the soret band of cytochrome c_{551}, the most common contaminant in *Pae* azurin samples. The A_{625}/A_{280} ratio found in this case was 0.55.

Alcaligenes denitrificans azurin.

Wild-type *Ade* azurin was purified from the *E. coli* cell past as reported previously with minor modifications[2]. The bacterial paste was defrozen and resuspended in 700 ml of sucrose buffer (20 % sucrose, 30 mM Tris/HCl and 1 mM EDTA, pH 8.0), stirred for fifteen minutes and then centrifuged. The supernatant, containing most of the periplasmic proteins, was kept and the precipitate was osmotic shocked with 2 L of cool water. It was also centrifuged and the supernatant was added to the former supernatant. The pH of the obtained solution was lowered down to 6.0 with 1 M acetic acid, and $CuSO_4$ and $K_3Fe(CN)_6$ were added up to 1 mM and 0.1 mM concentrations, respectively. Subsequently, acetic acid was slowly added again until the azurin-containing solution reached a pH of 4.5. This caused a greyish precipitate to appear, which was eliminated by centrifugation. The clear green supernatant was diluted with an equal volume of distilled water and applied to a CM-Sepharose column (2.5cm x 30cm) equilibrated with 50 mM ammonium acetate buffer, pH 4.5. Azurin bound to the top of the column as an intense blue band. This was eluted

by using a linear gradient of 50 mM acetate buffer from pH 4.5 to 6.0 and blue colored fractions were pooled. In this blue solution most of the protein seems to be azurin as judged by PAGE, but part of it is not reducible by ascorbic acid or sodium dithionite as it can be checked by iso-electric focusing, IEF. This has been interpreted as being due to the presence of a significant amount of colorless zinc-azurin together with the copper-azurin[8]. Separation of both metalloderivatives is an important step in the purification process and it was performed by anion-exchange chromatography under reducing conditions as reported previously[8a]. The buffer of the Zn(II)-azurin/Cu(II)-azurin solution was changed to 5 mM Tris/HCl, pH 9.1 by ultrafiltration and sodium dithionite was added until the blue color disappeared completely. The reduced solution was applied to a DEAE-Sepharose column (2.5cm x 30cm) equilibrated with the same buffer and the column was developed by a linear pH gradient from 9.1 to 8.3 (5 mM Tris/HCl buffer). Copper-azurin fractions, that can be identified after oxidation by $K_3Fe(CN_6)$, eluted as a single band fairly separated from the zinc-azurin fractions. Cu(II)-azurin was pure at this stage, as judged by the ratio $A_{619}/A_{280}=0.30\pm0.02$.

The purification of the M121Q azurin was performed by using the published procedure[3b] with some modifications for the separation of the contaminant zinc-azurin. The first steps of this purification process were identical to the procedure described above for the wt-azurin up to the DEAE chromatography. This chromatography was performed in the same way but without the addition of any reducing agent to the protein solution. The azurin sample obtained was pure, but consisted on a mixture of copper and zinc-protein pure as judged by IEF. It was dialyzed against 0.5 M KCN in 0.1 M phosphate buffer at pH 8.5 and room temperature for 1 hour[9]. With this process, we can only demetallate the copper-azurin while the zinc-azurin remains intact. Any attempt made to extract the Zn(II) using different chelating agents (EDTA, 2,6–pyridinedicarboxylic acid and 1,10–phenenthroline) at different pH conditions failed. It seems that the only way to extract this metal ion is to unfold and refold the protein in presence of EDTA and an excess of copper, with this procedure an important amount of the protein becomes denatured[2,3b].The mixture of apo- and zinc-M121Q azurin was separated in a 2.5cm x 10cm CM-Sepharose column (Pharmacia) equilibrated with 25 mM ammonium acetate buffer, pH 5, containing 0.5 mM EDTA, by elution with a 0 to 200 mM sodium chloride

8 a) van de Kamp, M., Hali, F.C., Rosato, N., Finazzi-Agró, A. & Canters, G.W. (1990) *Biochim. Biophys. Acta 1019*, 283. **b)** Nar, H., Huber, R., Messerschmidt, A., Filippou, A.C., Barth, M., Jaquinod, M., van de Kamp, M. & Canters, G.W. (1992) *Eur. J. Biochem. 205*, 1123.

gradient. The apo-M121Q azurin can be reconstituted by the addition of $CuSO_4$ obtaining an A_{610}/A_{280}=0.31 spectral ratio.

c) Metal replacement and preparation of samples.

Apo-azurin, either from *Pae* or *Ade*, was obtained by dialyzing the native oxidized azurin (0.05 mM) against 0.5 M KCN in 0.1 M sodium phosphate pH 8.5 at room temperature[9,10] . The apo-M121Q azurin was taken directly from the last step of the purification process. The Co(II) or Ni(II) metallo-derivatives of wt or M121Q-azurins were prepared by the addition of 5 mol $CoSO_4$ or $NiSO_4$ per mol apoprotein at room temperature. The metal uptake was followed by UV-Vis spectroscopy (Fig. 2:3). It is very slow and pH dependent in the case of the wt azurins, taking at least 48 hours for the total formation of the Co(II) and Ni(II) metallo-derivatives. In contrast, the corresponding metalloderivatives of the M121Q azurin are formed in a few minutes. Both *Pae* and *Ade* wt Ni(II)-azurins lose metal at pH lower than 6.0. All other metalloderivatives are stable at any pH value between 4.5 and 9. The samples were concentrated by either ultrafiltration or centrifuge concentrators up to 1–8 mM. Concentration was measured spectrophotometrically by using the absorption coefficients listed in Table 2:1. Concentrated samples can be stored at -20 °C for various months without a significant change in their spectroscopic properties.

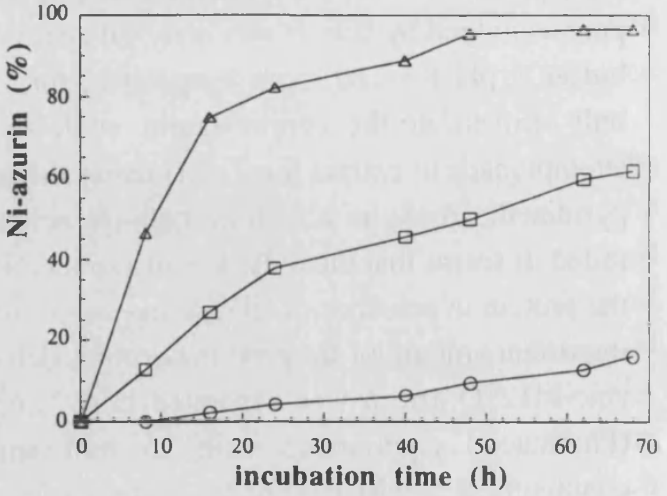

Fig. 2:3 Graphical representation of the Ni(II) uptake by wt-*Pae*-azurin at different pH conditions (△ 8.5, □ 7.5, and ○ 6.5). Apo-azurin samples of 0.05 mM concentration were incubated at room temperature in presence of $NiSO_4$ (0.25 mM). Metal uptake was followed by measuring the absorbance at 354 nm.

[9]Hutnik, C.M. & Szabo, A.G. (1989) *Biochemistry 28*, 3923.

[10] Salgado, J., Jiménez H.R., Donaire, A. & Moratal, J.M. (1995) *Eur. J. Biochem. 231*, 358.

Table 2:1. UV-Vis absorption bands and molar extinction coefficients of the different metalloprotein samples used in this work.

protein	λ (nm)	ε ($M^{-1}cm^{-1}$)
Co(II)-*Pae*-azurin	330	4000[a]
Co(II)-*Ade*-azurin	330	3000[b]
Co(II)-M121Q-azurin	359	1450[b]
Ni(II)-*Pae*-azurin	354	3300[a]
Ni(II)-*Ade*-azurin	354	2900[b]
Ni(II)-M121Q-azurin	320	2400[b]

[a] from reference 11

[b] relative to an ε_{280}=17,000 $M^{-1}cm^{-1}$ [2]

[11] Tennent, D.T. & Mc Millin, D.R. (1979) *J. Am. Chem. Soc. 101*, 2307.

II. NMR spectroscopy: measurements and calculations.

a) Performing the spectra.

NMR spectra were recorded on Varian Unity spectrometers operating at 300 or 400 MHz for ^1H, or on Bruker spectrometers (AC 200 MHz, WM 300 MHz and DMX 600 MHz).

1D spectra were performed by either the one-pulse sequence (*d*1—90°—*Acq*) with presaturation of the H_2O or HDO signal during part of the relaxation delay, or the super-WEFT (water-eliminated Fourier transformation) sequence (*d*1—180°—τ—90°—*Acq*)[12]. The first one was used to observe paramagnetic signals in combination with slow relaxing signals. Acquisition times of 100–200 ms, relaxation delay times of 100–500 ms and presaturation times of 100–500 ms were used in this case. The super-WEFT sequence was used to observe selectively fast relaxing signals. It allows the detection of resonances with short relaxation times within the protein envelope and reduces considerably the H_2O or HDO line. In this case, the values of the τ and recycle (*d*1+*Acq*) times were chosen according to the relaxation times of the signals of interest. Values of τ between 1 and 3 times the T_1 of the less paramagnetic signal among those of interest, and (*d*1+*Acq*)≈ τ gave the best results.

1D spectra were processed using exponential line-broadening (*lb*) weighting functions with values of 10–100 depending on the line-width of the signals of interest. The best *lb* values were found to be 10 % of the line-width at half height ($\Delta\nu_{1/2}$). In most cases a base line straightening was also necessary. It was performed by using a backward linear prediction of the 1–5 first points of the FID and/or a standard base line correction.

Saturation-transfer and steady-state 1D NOE (nuclear Overhauser effect) measurements were made using the super-WEFT pulse sequence, irradiating the resonance of interest during the relaxation delay τ (20–100 ms) with a selective decoupler pulse. Spectra were acquired by interleaving blocks of 32 scans alternating on-resonance and off-resonance saturation.

2D COSY (correlated spectroscopy) spectra were the conventional n-type (MCOSY)[13] . Phase sensitive TOCSY (total correlation spectroscopy) spectra[14],

---

[12] Inubushi, T. & Becker, E.D. (1983) *J. Magn. Reson. 51*, 128.

[13] Bax, A. (1982) *Two-dimensional NMR in liquids*, Reidel Publishing Co., Dordrecht, The Netherlands.

[14] Bax, A. & Davis, D.G.J. (1985) *J. Magn. Reson. 65*, 355.

recorded using the MELV-17 pulse train, were of the "clean" type[15]. NOESY (nuclear Overhauser effect spectroscopy) experiments were performed either in the hypercomplex (States-Haberkorn)[16] or the TPPI (time proportional phase increment)[17] mode. To obtain NOESY correlations between paramagnetic signals in the diamagnetic region the WEFT-NOESY sequence[18] was used. Since the resonance conditions (specially the relaxation times) were extremely diverse among the analyzed signals, 2D NMR spectra were performed using a wide range of conditions. Recycle times for NOESY, COSY and TOCSY ranged over 20–300 ms, and mixing times over 2–200 ms (NOESY) or 15–70 ms (TOCSY). The number of scans, the spectral width, the number of points in the t_2 dimension, and the number of t_1 increments recorded, also varied considerably (64–2048 scans, 10–190 kHz spectral width, 512–2048 t_2 points and 128 to 512 t_1 increments). Additionally, different processing conditions were also used. NOESY and TOCSY spectra were Fourier-transformed using squared sine-bell weighting functions shifted 45º, 60º or 80º, depending on the paramagnetic character of the observed signals. The number of points used for processing was 256, 512, 1024 or 2048 in both dimensions, zero-filling the t_1 dimension when necessary. COSY spectra were transformed using unshifted sine-squared window functions and zero-filled to 1K x 1K points. Both NOESY and TOCSY spectra were base line straightened by backward linear prediction and base line correction.

Finally, for spectra recorded in H_2O, a time domain digital filtering[19] was used in many cases to subtract the solvent line.

b) Determining relaxation times.

Data for non-selective longitudinal relaxation times were determined using the inversion-recovery (inv-rec) pulse sequence ($d1$—180º—τ—90º—Acq)[20]. Various experiments were necessary for every sample, in which the time parameters of the sequence were chosen according to the expected relaxation times of the signals. Thus, $d1+Acq$ values were at least 5 times the longest

---

[15] Griesinger, C., Otting, G., Wüthrich, K. & Ernst, R.R.J. (1988) *J. Am. Chem. Soc. 110*, 7870.

[16] States, D.J., Haberkorn, R.A. & Ruben, D.J. (1982) *J. Magn. Reson. 48*, 286.

[17] Marion, D. & Wütrich, K. (1983) *Biochem. Biophys. Res. Commun. 113*, 967.

[18] Chen, Z., de Ropp, J.S., Hernández, G. & La Mar, G.N. (1994) *J. Am. Chem. Soc. 116*, 8772.

[19] Smallcombe, S.H. (1993) *J. Am. Chem. Soc. 115*, 4776.

[20] Derome, A.E. (1987) *Modern NMR Techniques for Chemistry Research*, Pergamon Press, Oxford.

expected T_1, but no more than 20 times the shorter T_1 among the signals of interest. Analogously, for every experiment, τ was made to change in small steps between 1/5 times the shortest T_1 and 5 times the longest one. To avoid a loss of pulse effectiveness over the signals spread in large spectral windows, the carrier frequency was moved in some cases close to the signals of interest.

T_1 values were calculated by a modified version of the inversion-recovery equation. This is normally written as:

$$M_\tau = M_0(1 - 2e^{-\tau / T_1}) \qquad \text{Eq 2:1}$$

where M_τ is the z-magnetization at a time τ after the 180° pulse, M_0 is the equilibrium z-magnetization and $1/T_1$ is the relaxation rate of the recovery of the z-magnetization to equilibrium. The signal amplitude, I_τ, detected in the *xy* plane after the 90° pulse, similarly follows an exponential recovery from $-I_0$ to I_0:

$$I_\tau = I_0(1 - 2e^{-\tau / T_1}) \qquad \text{Eq 2:2}$$

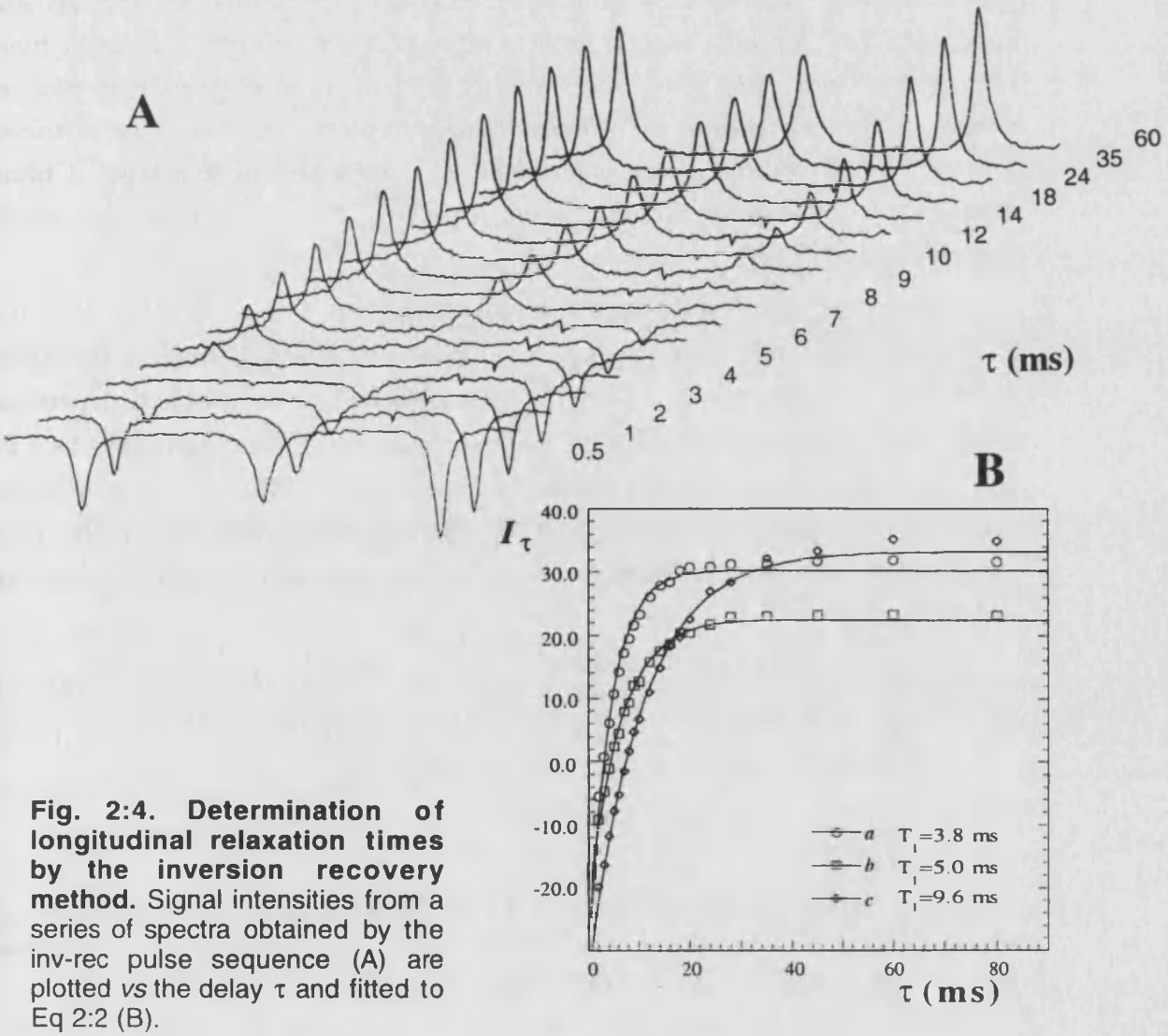

Fig. 2:4. Determination of longitudinal relaxation times by the inversion recovery method. Signal intensities from a series of spectra obtained by the inv-rec pulse sequence (A) are plotted *vs* the delay τ and fitted to Eq 2:2 (B).

The usual way to determine the T_1 is to fit the plot of the signal intensities of an inv-rec experiment *vs* the τ values to the exponential recovery curve (Fig. 2:4). Alternatively, the plot of $\ln(I_0\text{-}I_\tau)$ *vs* τ should give a straight-line with a $-1/T_1$ slope. Although this is a frequently reported method even for paramagnetic macromolecules, it results in a poor fitting, specially for the experimental points at longer τ values (Fig. 2:4). The reason is that the recovery of the z-magnetization in these systems is under no circumstances a single exponential process, because the spin under consideration is not isolated but interacting with other spins in the surroundings[21,22]. The effect of cross-relaxation on the determination of individual relaxation rates is complicated and depends on the experimental method used (selective *vs* non selective T_1 determinations), the size of the molecule and the strength of the cross-relaxation itself [22,23]. For the paramagnetic systems, the relationships between the diamagnetic and paramagnetic contributions to the total relaxation rates under different circumstances have to be also considered[22b]. La Mar and de Ropp[22], based on a previous study published by Granot[21], analyzed the various possibilities and concluded that "*for most cases a reliable estimate of meaningful relaxation times can be obtained only from the initial slope of a semilogarithmic plot of magnetization versus time, for which the measurement time τ must be restricted to a very small fraction of the determined T_1*". In a plot of this type, a linear relationship is found for the first points, from which the relaxation time can be calculated (Fig. 2:5A).

However, this method has the disadvantage that: i) a good value of I_0 has to be determined, which is not easy in all cases due to oscillations in the signal amplitude at long τ values, ii) significant variations can be obtained depending on the number of initial points used for the calculation of the initial slope, and iii) for very fast relaxing signals, the initial points have normally a large inherent error, because they correspond to very short τ values and due to the poor signal/noise ratio of these broad resonances. As an alternative, we have used the following equation:

$$I_\tau = I_0(1 - 2e^{-\tau / T_1}) + I' e^{-\tau / T_1} \qquad \text{Eq 2:3}$$

---

[21] Granot, J. (1982) *J. Magn. Reson. 49*, 257.

[22] a) Sette, M., de Ropp, J.S., Hernández, G. & La Mar, G.N. (1993) *J. Am. Chem. Soc. 115*, 5237. b) La Mar, G.N. & de Ropp, J.S. (1993) in *NMR of paramagnetic molecules* (Berliner L.J. & Reuben , J., ed.) vol. 12 p 1, Plenum Press Dir Plenum Publishing Corp. New York.

[23] Banci, L., Bertini, I. & Luchinat, C. (1991) *Nuclear and Electron Relaxation*, VCH: Weinheim.

which introduces a correction term, $I^* e^{-\tau/T_1}$ to Eq 2:2, meaning the contribution of all the cross-relaxation effects to the recovery of the z-magnetization in the inv-rec experiment. This exponential equation can be used to reproduce the experimental data giving results in very good agreement with those obtained from the initial slope of semilogarithmic plots, but without the drawbacks of this method (Fig. 2:5B).

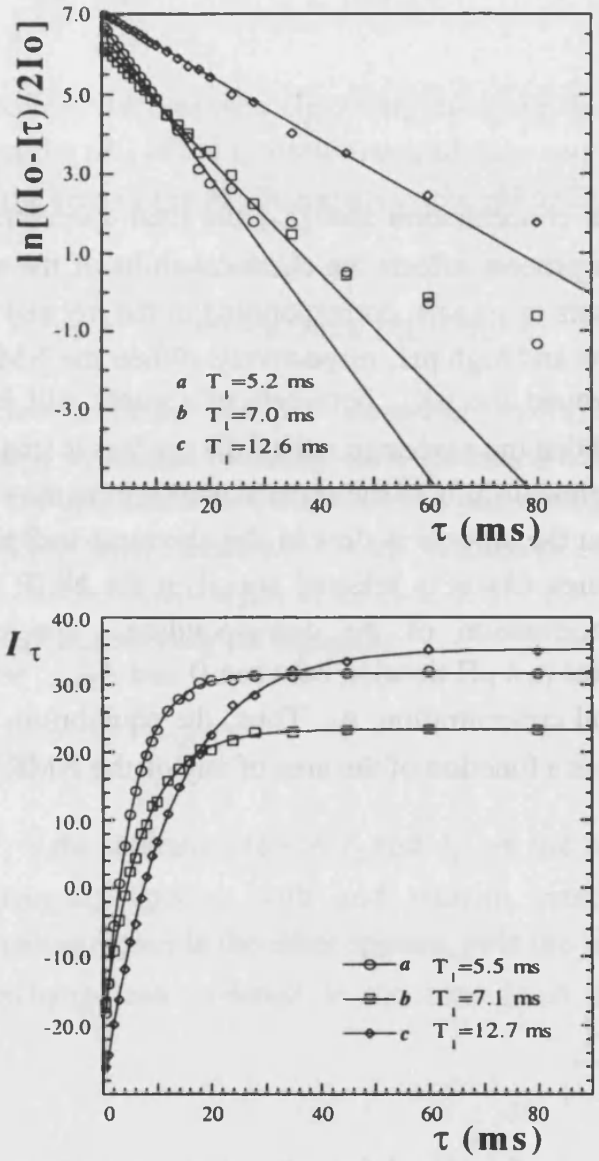

Fig. 2:5. Two ways of considering the deviations from a single exponential of the inv-rec signal intensity data. T_1 relaxation times can be calculated from the initial slope of semilogarithmic plots, since deviationes from the single exponential behaviour are not signifficant at very low τ values (A). Alternatively, Eq 2:3 can be used to fit a normal I_τ *vs* τ plot (B). The data have been taken from the same inv-rec experiment as in Fig. 2:4.

c) Analyzing pH dependent effects.

pH titrations: determining the pK_a.

For the acid-base equilibrium $AH \xleftrightarrow{K_a} A^- + H^+$, the following expressions can be written relating the equilibrium constant (K_a) and the concentration of the protonated and deprotonated species ([AH] and [A^-]):

$$K_a = \frac{[A^-][H^+]}{[AH]} \qquad \text{Eq 2:4}$$

$$[A_t] = [AH] + [A^-] \qquad \text{Eq 2:5}$$

where [H^+] is the proton concentration and [A_t] the total concentration of the titrating molecule. If this process affects the chemical-shifts of the nuclei in the molecule, two different sets of signals, corresponding to the AH and A^- species, should be observed at low and high pH, respectively. When the NMR spectrum is performed at a pH around the pK_a, both sets of signals will be observed simultaneously, provided that the exchange rate of the process is small compared with the difference of chemical shifts of the signals arising from the two species. In this cases, it is said that the process is slow in the chemical-shift time scale[24]. At a particular pH, the area (A) of a selected signal in the NMR spectrum is proportional to the concentration of the corresponding species in those conditions. This area varies in a pH titration between 0 and A_{max}, which in turn is proportional to the total concentration, A_t. Thus, the equilibrium constant of Eq 2:4 can be expressed as a function of the area of any of the NMR signals and the proton concentration:

$$K_a = \frac{A[H^+]}{(A_{max} - A)} \qquad \text{Eq 2:6}$$

$$K_a = \frac{(A_{max} - A')[H^+]}{A'} \qquad \text{Eq 2:7}$$

Here A represents the area of a signal from the deprotonated species and A' stands for the area of a signal from the protonated one. This equations can be rearranged in the form:

---

[24]Sandström, J. (1982) *Dynamic NMR spectroscopy*, Academic Press, New York.

$$A = \frac{A_{max}}{\left(\frac{[H]}{K_a} + 1\right)} = \frac{A_{max}}{\left[10^{(pK_a - pH)} + 1\right]} \qquad \text{Eq 2:8}$$

$$A' = \frac{A_{max}}{\left(\frac{K_a}{[H]} + 1\right)} = \frac{A_{max}}{\left[10^{(pH - pK_a)} + 1\right]} \qquad \text{Eq 2:9}$$

which express the area of a signal increasing or decreasing as a function of the pH. Thus, the pK_a of the ionization equilibrium can be easily obtained fitting the plots of the area of the NMR signals *vs* the pH to Eq 2:8 or Eq 2:9.

Exchange rates of conformational transitions.

The exchange rate of the pH dependent conformational equilibrium can be investigated by means of steady-state saturation transfer experiments[24] at a pH equal to the pK_a of the process. We have performed such experiments using the super-WEFT pulse sequence[12] with irradiation of the exchanging resonance during the relaxation delay as in the case of the 1D NOE experiments. Exchange data are calculated using the equation:

$$F_i = \frac{I_i}{I_i^0} = \frac{\rho_i}{\rho_i + k} \qquad \text{Eq 2:10}$$

where F_i is the saturation factor, I_i and I_i^0 are the intensity of signal i in one of the exchanging species with and without saturation, respectively, of the corresponding signal in the other species, ρ_i is the relaxation rate of signal i and k the exchange rate constant in the considered direction of the equilibrium process.

d) Proton exchange analysis.

The so called labile protons, which in proteins come mainly from NH and OH groups, exchange with protons of the bulk water-solvent in a process that we shall simplify here as the following two-site single equilibrium:

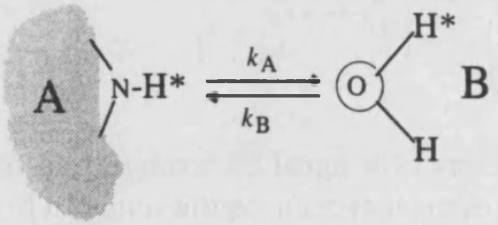

where A and B represent the two sites among which the proton is exchanging, i.e. the protein and the bulk water, being k_A and k_B the rate constants of the exchange equilibrium. The process can be slow, fast or intermediate with regard to the NMR time scale. In principle, for every of these situations, different methods based on the T_1 relaxation times, the bandwidths or the peak separation could be employed to investigate the exchange rate. However, the huge concentration of the bulk water compared to the normal protein concentration in an NMR tube limits the possibilities to obtain quantitative information in most cases.

At the coalescence temperature, the exchange-rate equations simplify to the following very popular expression, provided that the peak separation, $\Delta\nu=\nu_A-\nu_B$ (in Hz), and the exchange rate are much larger than the bandwidth[24]:

$$k = \frac{\pi \Delta\nu}{\sqrt{2}} \qquad \text{Eq 2:11}$$

Although for paramagnetic proteins this condition is normally fulfilled, this equation is only valid for equally populated two-site cases and the errors increase with the deviation from equal population. For cases where the populations of the two exchanging sites are very different, the following expression has been derived[24,25]:

$$P_A - P_B = \Delta P = \left(\frac{X^2 - 2}{3}\right)^{3/2} \frac{1}{X} \qquad \text{Eq 2:12}$$

$$X = 2\pi \tau_{cc} \Delta\nu$$

[25]Shanan-Atidi, H. & Bar-Eli, K.H. (1970) *J. Phys. Chem. 74*, 961.

where P_A and P_B are the molar fractions of the sites A and B (the protein and the solvent water) and τ_{cc} is the life-time τ at the coatescence temperature, being defined as:

$$\tau = \left(k_A + k_B\right)^{-1} = \frac{P_A}{k_B} = \frac{P_B}{k_A} \qquad \text{Eq 2:13}$$

As it is shown in Fig. 2:6, the function expressed by Eq 2:12 have a very defined domain, since $0 \leq \Delta P \leq 1$. So X ranges from $\sqrt{2}$ to $2\sqrt{2}$, and τ_{cc} ranges from $\sqrt{2} / 2\pi\Delta\nu$ to $\sqrt{2} / \pi\Delta\nu$.

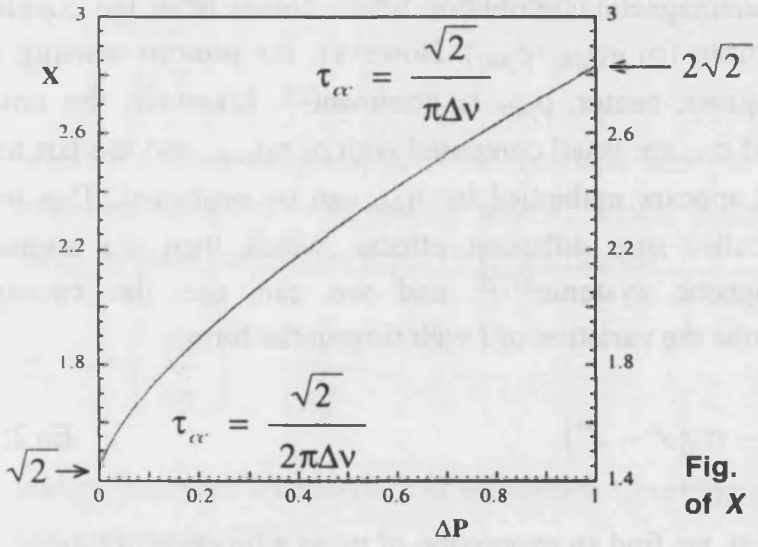

Fig. 2:6. Calculated values of *X vs* ΔP using Eq 2:12 [25].

e) Determining inter-proton distances from 1D NOE data.

The nuclear Overhauser effect (NOE), represented by η_{ij}, is defined as the fractional variation of the integrated intensity I of an NMR signal i upon saturation of another signal j dipolarly coupled to it[26]:

$$\eta_{ij} = \frac{(I - I^0)}{I^0} \qquad \text{Eq 2:14}$$

where I^0 is the equilibrium intensity of signal i. When signal j is saturated in a multispin system, the rate of change of I depends on the relaxation rate of this proton, ρ_i, the cross-relaxation rate between the dipolarly coupled protons i and

[26] a) Noggle, J.H. & Schirmer, R.E. (1971) *The Nuclear Overhauser Effect*, Academic Press, New York. b) Neuhaus, D. & Williamson, M. (1989) *The Nuclear Overhauser Effect in Structural and Conformational Analysis*, VCH Publ., New York.

j, σ_{ij}, as well as the cross-relaxation rate between i and other nuclei k to which it is dipolarly coupled, σ_{ik}, and which can also experience NOE, η_{kj}, as a consequence of the saturation of j [26b]:

$$\frac{d I}{d t} = -\rho_i\left(I - I^0\right) - \sigma_{ij}\left(J - J^0\right) - \sum_k \sigma_{ik}\eta_{ij}\left(K - K^0\right) \qquad \text{Eq 2:15}$$

ρ_i is the selective relaxation rate $1/T_1$. In paramagnetic systems, selective and non-selective relaxation times are often equal[21,23], so relaxation times calculated by the inversion-recovery method (see above) are normally used here. On the other hand, the relaxation rate is the sum of the dipolar proton-proton contribution and the paramagnetic contribution which comes from the coupling with the unpaired electrons ($\rho_i = \rho_{dia} + \rho_{par}$). However, for protons sensing the influence of a paramagnetic center, ρ_{par} is dominant[23]. Likewise, the cross-relaxation rates, σ_{ij} and σ_{ik}, are small compared with $\rho_i \approx \rho_{par}$, and the last term in Eq 2:15, where σ_{ik} appears multiplied by η_{kj}, can be neglected. This term accounts for the so called spin diffusion effects, which then are normally negligible in paramagnetic systems[27,28] and we can use the two-spin approximation to describe the variation of I with time in the form:

$$\frac{d I}{d t} = -\rho_i\left(I - I^0\right) - \sigma_{ij}\left(J - J^0\right) \qquad \text{Eq 2:16}$$

Integrating this equation, we find an expression of η_{ij} as a function of time:

$$\eta_{ij}(t) = \frac{\sigma_{ij}}{\rho_{ij}}\left(1 - e^{-\rho t}\right) \qquad \text{Eq 2:17}$$

and, when the irradiation time t is long with respect to ρ_i^{-1}, it simplifies to:

$$\eta_{ij}(t) = \frac{\sigma_{ij}}{\rho_{ij}} \qquad \text{Eq 2:18}$$

This is the equation for the steady-state NOE experiment, in which the NOE is time independent[26].

---

[27] Banci, L., Bertini, I., Lucinat, C. & Piccioli, M. (1991) in *NMR and biomolecular structure* (Bertini, I., Molinari, H. & Niccolai, N., eds.) p. 31, VCH: Weeinheim.

[28] a) Banci, L., Bertini, I., Luchinat, C. & Piccioli, M. (1990) *FEBS Lett. 272*, 175. b) Thanabal, V., de Ropp, J.S. & La Mar, G.N. (1987) *J. Am. Chem. Soc. 109*, 265.

The cross-relaxation rate σ_{ij} betweeen two protons (homonuclear case) dipolarly coupled is given by[23,28]:

$$\sigma_{ij} = \left(\frac{\mu_0}{4\pi}\right)^2 \frac{\hbar^2\gamma_H^4}{10r_{ij}^6}\left[\tau_c - \frac{6\tau_c}{1 + 4(\omega_H\tau_c)^2}\right] \qquad \text{Eq 2:19}$$

where ω_H is the proton Larmor frequency and τ_c is the correlation time of the reorientation of the spins *i* and *j*. The last parameter is normally dominated by the molecular tumbling rate, τ_r^{-1} ($\tau_c \approx \tau_r$), which can be estimated by the Stokes-Einstein equation:

$$\tau_r = \frac{4\pi\zeta a^3}{3k\,T} \qquad \text{Eq 2:20}$$

where *a* is the average radius of the molecule and ζ is the solvent viscosity. For macromolecules $\tau_r^{-1} \ll \omega_H$ and so $\omega\tau_c \gg 1$, which is known as the slow-motion limit. In these conditions Eq 2:19 simplifies to:

$$\sigma_{ij} = -\left(\frac{\mu_0}{4\pi}\right)^2 \frac{\hbar^2\gamma_H^4\tau_c}{10r_{ij}^6} \qquad \text{Eq 2:21}$$

and σ_{ij} becomes independent of frequency. Combining Eq 2:18 and Eq 2:21, we can express the NOE as:

$$\eta_{ij} = -\left(\frac{\mu_0}{4\pi}\right)^2 \frac{\hbar^2\gamma_H^4\tau_c}{10r_{ij}^6\rho_i} \qquad \text{Eq 2:22}$$

This equation, together with Eq 2:14, means that, from the measurement of an NOE between two paramagnetic proton signals, the distance between the corresponding protons can be calculated if the relaxation time of at least one of them is known. For long correlation times (viscous solutions and large molecules, according to Eq 2:20), larger NOEs can be obtained. These NOEs will be smaller, and more difficult to be detected, in the case of fast relaxing signals (large ρ_i), as those normally found in paramagnetic systems. However, as we have discussed above, in such fast relaxing conditions the effect of spin diffusion, which is an important drawback for the use of steady-state NOE in diamagnetic systems, can be neglected.

f) Analyzing temperature dependence of the isotropic shifts.

The ^1H NMR isotropic shifts from Co(II) and Ni(II) paramagnetic proteins invariably decrease with increasing temperature (Curie-like behavior) and they should extrapolate to zero at infinite temperature[29]. But due to the complexity of the mechanisms which determine these shifts, the temperature dependence is rarely predictable, and the analysis made on this basis are merely qualitative and approximate. Whenever there is spin-orbit coupling, that result in differently populated zero field splitting levels, upon variation of temperature T^{-1} and T^{-2} dependence is expected for both the contact and the dipolar shifts, as it can be seen in the following equations[29b,30]:

$$\left(\frac{\Delta\nu}{\nu_0}\right)^{con} = \left(\frac{A_i}{\hbar}\right)\frac{35\bar{g}\mu_B}{12\gamma_N k\,T}\left[1 - \frac{32(g_\parallel - g_\perp)D}{45\bar{g}k\,T}\right] \qquad \text{Eq 2:23}$$

$$\left(\frac{\Delta\nu}{\nu_0}\right)^{pcm} = \frac{\mu_0}{4\pi}\frac{35\mu_B^2(g_\parallel^2 - g_\perp^2)}{36k\,T}\frac{3\cos^2\theta - 1}{r^3}\cdot \left[1 - \frac{32(g_\parallel^2 + 1/2\,g_\perp^2)D}{15(g_\parallel^2 - g_\perp^2)k\,T}\right] \qquad \text{Eq 2:24}$$

The T^{-2} term is usually larger for the dipolar shifts than for the contact shifts. Additionally, for the later, the T^{-2} contribution can be neglected when the molecular g values are close to the free electron value and D is relatively small. In these cases, a T^{-2} dependence of the isotropic shifts is mostly originated from the dipolar term[29b,30]. Due to the limitations imposed by the protein stability and the physical properties of the solvent, the temperature range which can be investigated is very reduced (usually between 2 and 50 °C). Thus, plots of the isotropic shifts (δ) *vs* T^{-1} appear always linear and deviations due to a small T^{-2} component can not be detected. However, if there is only a T^{-1} dependence, plots of δ *vs* T^{-1}, fitted to a straight line, should extrapolate to zero. Important deviations from the zero extrapolation mean that a T^{-2} dependence can be present and there is possibly sizable dipolar contribution to the isotropic shifts.

[29a] La Mar, G.N., Horrocks, W.D. & Holm, R.H. (1973) *NMR of Paramagnetic Molecules*, Academic Press, New York. b) Bertini, I. & Luchinat, C. (1986) *NMR of Paramagnetic Molecules in Biological Systems*, The Benjamin/Cummings Publishing Company, Menlo Park.

[30] Kurland, R.J. & McGarvey, B.R. (1970) *J. Magn. Reson.* 2, 286.

g) Assigning paramagnetic NMR signals.

The presence of a paramagnetic center conditions the assignment strategy of the NMR signals. We have used the methodology developed by the pioneering groups in the field of paramagnetic NMR[18,22,29,31,32]. The very shifted signals are considered to be due to contact interaction with the paramagnetic metal ion, and thus they are in principle assigned as protons from coordinated residues. The finding of correlations between them, especially through 1D NOE and 2D NOESY, allows a more detailed assignment of the signals. Obtaining contact correlations between these signals, through COSY and TOCSY experiments, is usually prevented by the large shifts and short relaxation times[22b]. Additionally, the broadening of the signals can be the origin of important artifacts, since cross-correlation effects between interproton dipolar coupling and Curie relaxation can induce relaxation-allowed coherence transfer and "false" (non-scalar) couplings in the ^{1}H COSY spectrum[33]. 1D NOE/NOESY correlations between contact-shifted signals and signals near or under the diamagnetic envelope permit the assignment of other protons close to the coordinated residues. At this point, the availability of detailed structural information from a closely analogous protein is of crucial help since it will be used to discriminate which protons are likely to be dipolarly connected with previously assigned protons. We have used the structures of the Ni(II)[34] and Zn(II)[35] azurins, as well as the wild-type Cu(II) protein at low and high pH[36] during the assignment process. The analysis of NOESY, COSY and TOCSY correlations between protons from the second coordination sphere is performed in a more conventional way[37] and permits finding and specifically assigning spin systems which can be in turn dipolarly connected with previously assigned hyperfine-shifted signals. This allows contrasting the assignments in a feed-back way.

---

[31]Bertini, I., Turano, P. & Vila, A. (1993) *Chem. Rev. 93*, 2833.

[32]Banci, L., Bertini, I. & Luchinat, C. (1994) *Methods Enzymol. 239*, 485.

[33]Bertini, I., Luchinat, C. & Tarchi, D. (1993) *Chem. Phys. Lett. 203*, 445.

[34]Moratal, J.M., Romero, A., Salgado, J., Perales-Alarcón, A. & Jiménez, H.R. (1995) *Eur. J. Biochem. 228*, 653.

[35]Nar, H., Huber, R., Messerschmidt, A., Filippou, A.C., Barth, M., Jaquinod, M., van de Kamp, M. & Canters, G.W. (1992) *Eur. J. Biochem. 205*, 1123.

[36]Nar, H., Messerchmidt, A., Huber, R., van de Kamp, M. & Canters, G.W. (1991) *J. Mol. Biol. 221*, 765.

[37]Wüthrich, K. (1986) *NMR of proteins and nucleic acids*, John Wiley & Sons, New York.

III.Other techniques.

a) Electronic spectroscopy.

UV-Vis spectra were recorded at room temperature by any of the following spectrophotometers: Cary 1 (Varian, CA, USA), Lambda 9 (Perkin Elmer) Shimadzu UV-2101PC (Shimadzu, Japan). Semimicro quartz cells of 1 cm path-length were used.

b) EPR spectroscopy.

EPR spectra were recorded with a Bruker ER-200D spectrometer, operating at the X-band frequency of 9.43 GHz and provided with a helium continuous-flow cryostat (Oxford Instruments). Microwave power was 10 dB and modulation amplitude 4 G. Water glass samples were mounted in standard 4-mm quartz EPR tubes.

c) Magnetic measurements.

Variable temperature magnetization measurements were made on a SQUID magnetometer, at a magnetic field of 0.1 Tesla, within the temperature range 120-5 K. Concentrations of the studied solutions (3.6 mM) were determined as described above. Experimental magnetization values were converted to molar susceptibilities. Glycerol was added to the samples (10 %) as a cryoprotectant. All the solutions were carefully degassed using the freeze-pump thaw procedure in order to remove dissolved molecular oxygen, that is especially important when the expected spin state of the protein sample is $S=1$[38]. They were transferred to quartz holders especially designed for SQUID measurements, and kept under argon for storage prior to measurement or use. Separate measurements under identical conditions were made on the buffer solution containing the apoprotein at the same conditions, in order to substract the large diamagnetic correction from the overall signal. Proton buffer was used since it has been checked, in the case of nickel urease, that the possible magnetic noise due to the slowly relaxing $I=1/2$ nuclei of water is within experimental error[39].

---

38 Day, E.P. (1993) *Meth. Enzymol. 227*, 437.

39 Clark, P.A. & Wilcox, D.E. (1989) *Inorg. Chem. 28*, 1326.

d) X-ray diffraction analysis.

Nickel-azurin was crystallized by the hanging drop vapour diffusion method, using a procedure similar to that described for the native copper-azurin[36].

X-ray intensity data was collected with a Hendrix/Lantfer X-ray imaging plate system (Mar Research, Hamburg) with a crystal-to-detector distance of 90 mm. X-rays (Ni-filtered CuK_α radiation) were generated by a rotating anode X-ray source operating at 4.0 kW (Enraf-Nonius, Netherlands). A complete native data set to 2.05 Å resolution was obtained by rotating the crystal 114° with an oscillation range between images of 1.5°. Diffraction images were processed using the program MOSFLM[40]. From a total of 129,132 measured reflections to 2.05 Å resolution, 32,694 unique reflections were obtained with a merging R value of 0.06. Model co-ordinates of copper-azurin from *Pseudomonas aeruginosa* [36] were taken from the Brookhaven Protein Data Base. Structure factors and electron density maps for nickel-azurin were calculated with phases from the copper-azurin model omitting solvent atoms, followed by inspection and manual correction on the graphics display (Evans & Sutherland) using the program FRODO[41]. Crystallographic refinement was carried out with energy restraints using XPLOR[42]. However, the nickel sites were refined with no energy restraints.

---

[40]Leslie, A.G.W. (1990) MOSFLM Program. Abstract of the *Crystallographic Computing School.* Bischenberg.

[41]Jones, T.A. (1978) *J. Appl. Crystallogr. 15*, 24.

[42]Brünger, A.T. (1990) X-PLOR (version 2.1), Manual Yale University, New Haven, CT.

Chapter **3**

Pseudomonas aeruginosa Ni(II)-azurin: a nickel substituted blue copper protein[1].

Summary.

A thorough study of the paramagnetic metalloderivative Ni(II)-azurin by means of NMR, magnetic susceptibility measurements and X-ray diffraction is presented here. The principal ^1H NMR isotropically shifted resonances of Ni(II)-azurin are assigned to five metal coordinated residues: Cys112, His46, His117, Gly45 and Met121. The structure determined by X-ray crystallography shows a metal center intermediate between those of the copper and zinc azurins, that can be described as distorted tetrahedral. Nickel clearly coordinates to the carbonyl oxygen of Gly45 while its distance to the Met121 Sδ enlarges up to 3.30 Å. However, the existence of contact interaction between Met121 and the nickel ion can be still admitted (at least in solution) as it is shown by the NMR properties of the Met121 protons. Temperature dependence of the magnetic susceptibility is in agreement with a distorted tetrahedral metal site that we define here as "pseudo-pentacoordinated".

Being metal centers a fundamental element of the metalloproteins, metal substitution is commonly used in inorganic biochemistry to investigate their structural and functional properties. When the exogenous metal brings along a chromophore with peculiar spectroscopic characteristics, this substitution is used to probe the metal site[2]. Replacement of copper by nickel in blue copper proteins

[1] Partially based on Moratal, J.M., Salgado, J., Donaire, A., Jiménez, H.R. & Castells, J. (1993) *J. Chem. Soc., Chem. Commun.*, 110; Moratal, J.M., Salgado, J., Donaire, A., Jiménez, H.R., Castells, J. & Martínez-Ferrer, M.J. (1993) *Magn. Reson. Chem. 31*, 541; Moratal, J.M., Romero, A., Salgado, J., Perales-Alarcón, A. & Jiménez, H.R. (1995) *Eur. J. Biochem. 228*, 653 and Jiménez, H.R., Salgado, J., Moratal, J.M. & Morgenstern-Badarau, I. (1995) *Inorg. Chem.*, submitted..

[2] a) Bertini, I & Luchinat, C. (1986) in *Zinc Enzymes* (I. Bertini, C. Luchinat, W. Maret, M. Zeppezauer, eds.) p. 27, Birkhäuser, Boston. **b)** See Chapter 1, section IV and references therein.

has been used to study the type 1 metal sites by electronic spectroscopy[3]. Here we study the resulting nickel-metalloderivative by paramagnetic-NMR[4,5], a common strategy in the case of the zinc proteins which use for the blue-copper proteins had been in the pass very limited[6]. The short electronic relaxation time of the paramagnetic Ni(II) ion (10^{-10}-10^{-12} sec) permits the selective observation of relatively narrow isotropically shifted signals corresponding to protons close to the metal ion. Azurin was chosen for us to test this approach. This protein represents a very good example among the blue-copper proteins because of its great stability and the vast structural and functional knowledge which has been accumulated about it in the last years[7,8]. To gain a more complete understanding of this metal site, magnetic studies on Ni(II)-azurin were performed. Additionally, this protein was crystallized and its structure solved by X-ray diffraction. The structural characteristics of the Ni(II)-azurin metal site are discussed herein by using both the spectroscopic (NMR) data in solution and the crystallographic data.

---

3 Tennent, D.L. & McMillin, D.R. (1979) *J. Am. Chem. Soc. 101*, 2307.

4 a) La Mar, G.N., Horrocks, W.D. & Holm, R.H. (1973) *NMR of Paramagnetic Molecules*, Academic Press, New York. b) Bertini, I. Luchinat, C. (1986) *NMR of Paramagnetic Molecules in Biological Systems*, Benjamin Cummings, Menlo Park, CA. c) La Mar, G.N. & de Ropp, J.S. (1993) in *NMR of paramagnetic molecules* (Berliner L.J. & Reuben, J., ed.) vol. 12, p. 1, Plenum Press Dir Plenum Publishing Corp., New York. d) Bertini, I., Turano, P. & Vila, A. (1993) *Chem. Rev. 93*, 2833.

5 See Chapter 1, section V and Chapter 2, section II.

6 Blaszak, J.A., Ulrich, E.L., Markley, J.L. & McMillin, D. R. (1982) *Biochemistry 21*, 6253.

7 a) Adman, E.T. (1985) *Top. Mol. Struct. Biol. 6*, 1. b) Chapman, S.K. (1991) in *Perspectives on Bioinorganic Chemistry* (Hay, R.W., Dilworth, J.R. & Nolan, K.B., eds.)vol. 1, p. 95, Jai Press Ltd, London.

8 See Chapter 1, section II.

I. Characterization of nickel azurin by paramagnetic NMR.

RESULTS.

a) The ^1H NMR spectrum.

The ^1H NMR spectrum of Ni(II)-azurin at pH 4.7 displays, in the downfield region, seven well resolved isotropically shifted signals (a-g) and three other signals (h, i, i') upfield shifted (Fig. 3:1A, Table 3:1). Signal g, which integrates three protons, has been assigned to the methyl group of Met121[6]. When the spectrum of Ni(II)-azurin is registered in D_2O solvent, signals e and f disappear completely. Thus, they can be assigned to the exchangeable $N_{\varepsilon 2}H$ protons of the two coordinated histidines (His46 and His117). Additionally, there are four characteristic broad signals (j-m), two of them (j,k) very shifted up to 232.6 ppm and 187.3 ppm (Fig. 3:1C). Near the diamagnetic region we can observe several other signals that could belong to residues not directly coordinated to the metal ion but close enough to experience dipolar interactions with the unpaired electrons and then some dipolar shift (Fig. 3:1D).

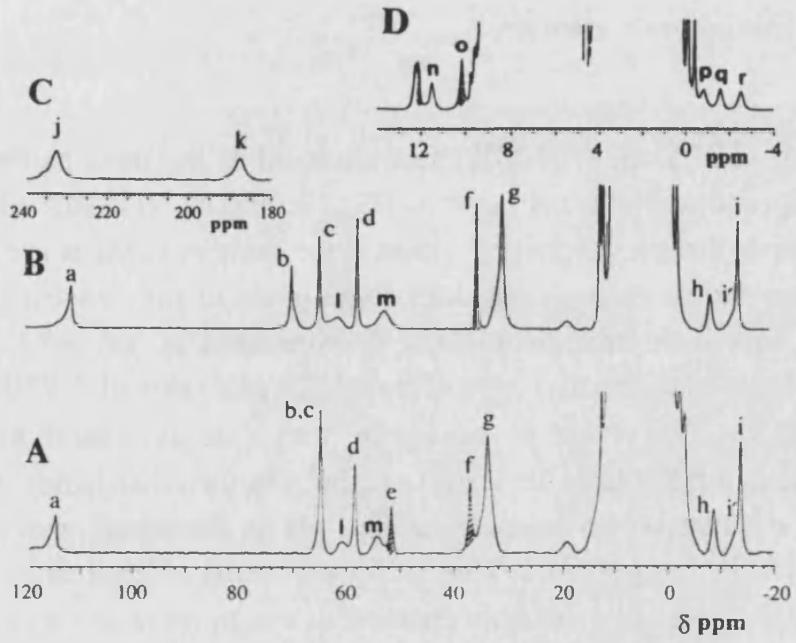

Fig. 3:1. 400 MHz ^1H NMR spectra of 7-8 mM *P. aeruginosa* nickel(II)-azurin. Samples are in H_2O solvent at 45 °C and pH 4.7 (A) or pH 7.6 (B). C shows the most downfield shifted signals of the spectrum B, and D shows an expanded view of the 14/-4 ppm region of the same spectrum. Shaded signals correspond to protons that are exchangeable in a D_2O solution.

Table 3:1. Isotropically shifted resonances of the ^{1}H NMR spectrum (400 MHz) of Nickel(II)-azurin from *P. aeruginosa* at 45 °C. δ and Δν values correspond to pH 7.5.

Signal	δ(ppm)	T_1 (ms)		$\Delta\nu_{1/2}$ (Hz)
		pH 7.5	pH 5	
a	111.3	2.7	2.8	210
b	69.5	7.5	8.1	135
c	64.3	11.6	12.3	120
d	57.2	7.9	8.5	100
e	51.5[a,b]	—	9.2	—
f	35.0[a]	10.6	11.8	80
g	30.3	3.8	3.4	260
h	-8.8	3.5	3.4	335
i	-14.1	9.6	10.2	130
j	232.6	0.7	0.7	1015
k	187.3	0.7	0.7	1000
l	61.2	0.8	0.8	850
m	52.6	1.0	1.0	720
n	11.5	14.0	13.8	66
o	10.1[a]	13.0	13.0	59
p	-0.8	8.6	8.8	100
q	-1.6	8.6	9.2	73
r	-2.5	8.6	9.2	85

[a] solvent exchangeable.

[b] only detected at low pH.

At pH 7.5, the ^{1}H NMR spectrum exhibits the same pattern, but only one exchangeable signal (f) is detected (Fig. 3:1B). A ^{1}H NMR pH titration (Fig. 3:2) shows that only signal c remains at the same position as the pH is increased. All other signals change their shifts some ppms in slow exchange regime on the NMR time scale and the process is completed at pH ~7.5. From the pH dependence of the relative area of signal b, a pK_a value of 5.9±0.1 was obtained (Fig. 3:3). This value is consistent with that associated to the ionization equilibrium of His35 in the Cu(II)-azurin[9]. On the other hand, the exchangeable signal e decreases in intensity as the pH is increased and finally becomes undetectable for pH≥7.5. This behavior clearly differentiates the two $N_{\varepsilon 2}H$ signals and gives us a valuable criterion to assign them. As it can be seen in the

[9] a) Corin, A.F., Bersohn, R. & Cole, P.E. (1983) *Biochemistry 22*, 2032. b) van de Kamp, M., Canters, G.W., Andrew, C.R., Sanders-Loehr, J., Bender, C.J. & Peisach, J. (1993) *Eur. J. Biochem. 218*, 229.

azurin crystal structure[10], His46 is buried inside the protein molecule whereas His117 is allocated in the center of the so-called hydrophobic patch somewhat exposed to the solvent. Moreover, the $N_{\varepsilon 2}H$ proton of His117 forms a hydrogen bond with a water molecule, while His46 $N_{\varepsilon 2}H$ is hydrogen bonded to the Asn10 oxygen under the protein surface[10]. Therefore, considering that signal e is clearly more labile than signal f, the former one is assigned to the $N_{\varepsilon 2}H$ proton of His117, and then signal f is assigned to the $N_{\varepsilon 2}H$ proton of His46.

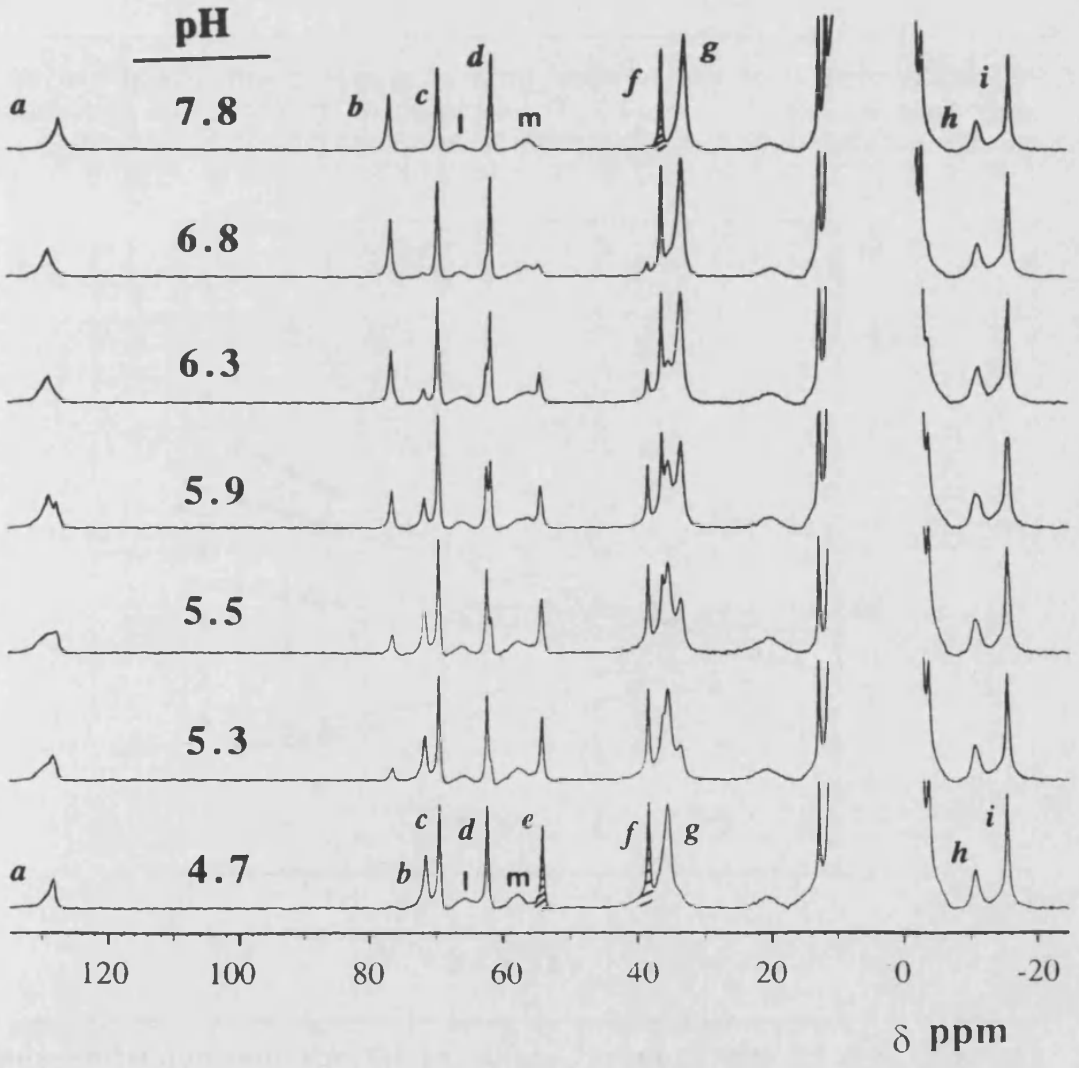

Fig. 3:2. pH dependence of the ^{1}H NMR spectra (300 MHz) of 1.5 mM Ni(II)-azurin at 25 °C. Shaded signals disappear in D_2O.

[10]Nar, H., Messerchmidt, A., Huber, R., van de Kamp, M. & Canters, G.W. (1991) *J. Mol. Biol.* *221*, 765.

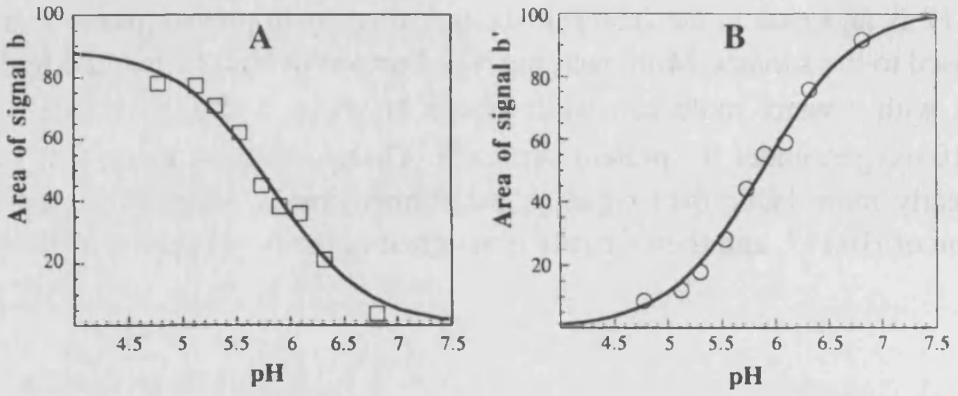

Fig. 3:3. Variation of the relative area of signal b with the pH at 25 °C. Data have been taken from Fig. 3:2. The evolution of signal b in both protonated (A) and deprotonated (B) Ni(II)-azurin species is shown with the best fitting curve.

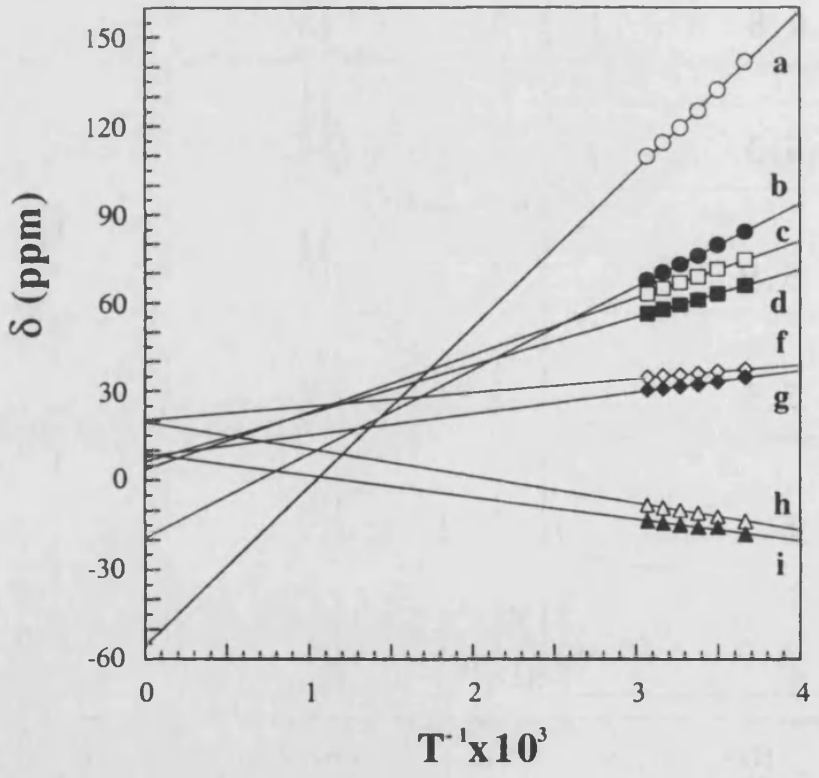

Fig. 3:4. Plot of the chemical shifts *vs* 1/T for the hyperfine-shifted proton resonances of nickel(II)-azurin at pH 7.6.

Variable-temperature ^{1}H NMR spectra of the Ni(II)-azurin at pH 7.6 were registered from 0 °C to 53 °C. The isotropically shifted signals are very temperature-dependent and follow a Curie-like behavior, i.e. their isotropic shifts decrease with increasing temperature. In addition, the line widths become

slightly narrower. In Fig. 3:4, the observed isotropic shifts are plotted against T^{-1} and a linear relationship is found. The intercept values at infinite temperature for signals c, d, g and i are within or close to the diamagnetic region, so indicating little dipolar contribution to the isotropic shifts[4a,b;11]. However, the intercepts for the other shifted signals indicate a sizable dipolar contribution to the isotropic shifts, specially in the case of signal a.

b) Assignment of the isotropically-shifted signals.

The isotropically shifted signals have been assigned on the basis of 1D and 2D NOE experiments, complemented with COSY and TOCSY spectra over the 15 to -5 ppm spectral region. Fig. 3:5 shows the NOESY spectrum of Ni(II)-azurin at pH 7.6 and 45 °C. This spectrum permits to pair the His46 $N_{\varepsilon 2}H$ proton (signal f) with its corresponding $C_{\delta 2}H$ vicinal proton in the same imidazole ring (signal d). To find the His117 imidazole signals a similar experiment has to be run at low pH, where signal e is observed. However, the Ni(II)-azurin loses metal at pH lower than 5 and is not stable for the time needed to obtain a 2D spectrum. So 1D NOE experiments were performed in this case. The corresponding difference spectra (Fig. 3:6B) permits to assign signal c to the His117 $C_{\delta 2}H$ proton. On the other hand, this signal c shows a NOESY cross peak with the exchangeable signal o (Fig. 3:5D). We assign this signal as the backbone amide proton of His117, since it is the only labile proton close to the His117 $C_{\delta 2}H$, apart from the already assigned His117 $N_{\varepsilon 2}H$ proton not observed at this pH conditions.

The NOESY map also displays a remarkably intense cross peak between signals b and i (Fig. 3:5A, see also the NOE difference traces in Fig. 3:7B,C), suggesting that they correspond to CH_2 protons of a coordinated residue. In addition, both signals b and i exhibit a dipolar connectivity with a signal at 2.6 ppms (Fig. 3:5D, E) and signal i presents a NOESY cross-peak with a signal at 7.9 ppm (Fig. 3:5E). These cross peaks disappear in D_2O solvent indicating that they are due to exchangeable protons. According to the azurin crystal structure, the only CH_2 group in the coordination sphere placed near two labile protons is the Gly45 $C_\alpha H_2$, which is close to the amide groups of both Gly45 and His46. Therefore, signals b and i are assigned to the α protons of Gly45. It follows that signal at 2.6 ppm, close to both Gly45 α protons, is assigned to the His46 NH, and signal at 7.9 ppm is assigned to the Gly45 NH. Using the same criterion, we can assign signals b and i stereospecifically, being the α1 and α2 protons of Gly45, respectively.

[11] See Chapter 2, section II.f.

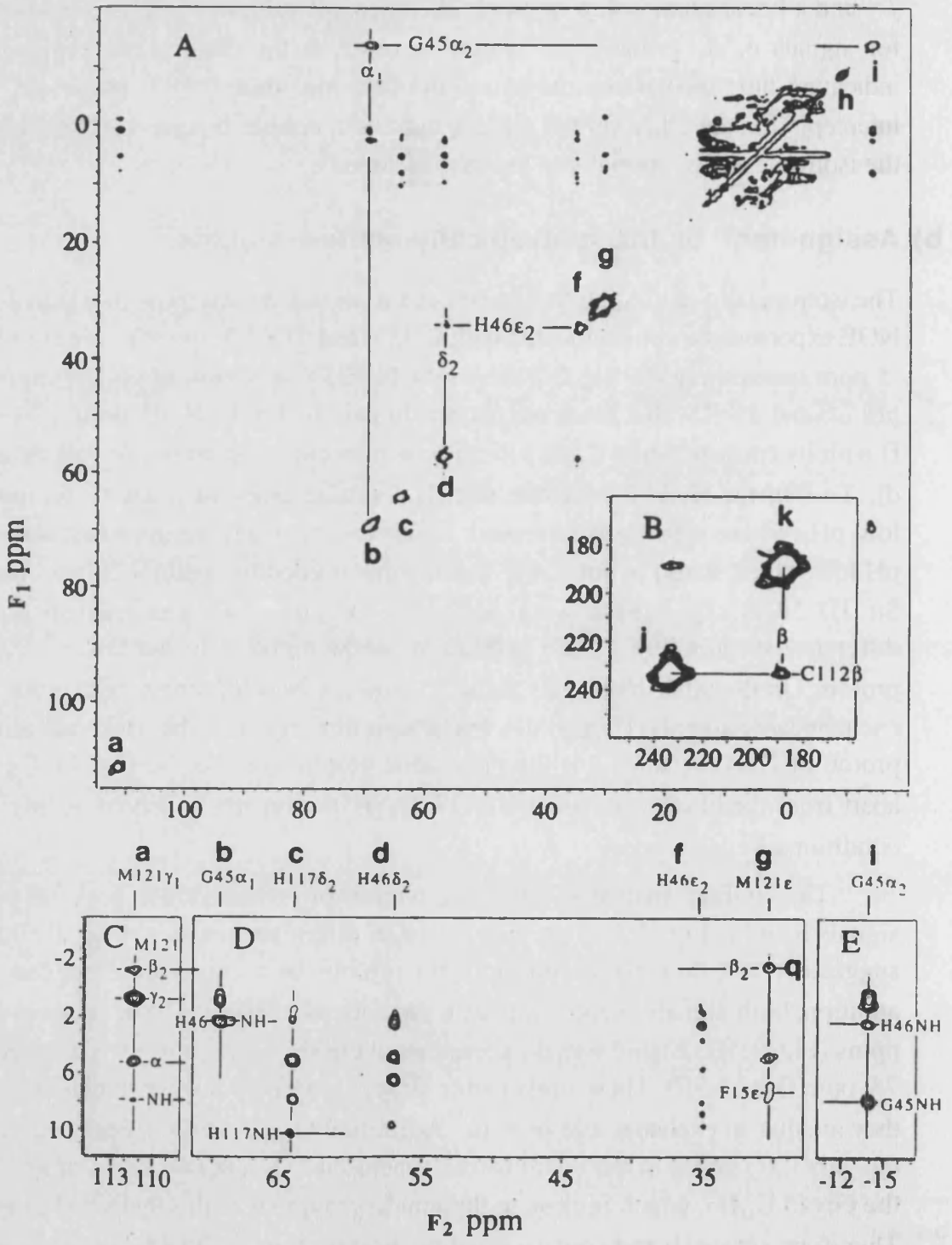

Fig. 3:5. 400 MHz ^{1}H NMR NOESY (phase sensitive, TPPI) spectra of 8 mM Ni(II)-azurin. Map A corresponds to a water sample at pH=7.6 and 45 °C. This spectrum was recorded with 10 ms mixing time and a repetition rate of 8 sec^{-1} over a 100 kHz band width. Inset B shows the downfield portion of a 1 ms mixing time NOESY spectrum of the same sample, collected by setting the carrier frequency at 210 ppm (100 kHz band width, 48 sec^{-1} repetition rate). Maps C, D and E are expanded regions of the NOESY spectrum shown in A.

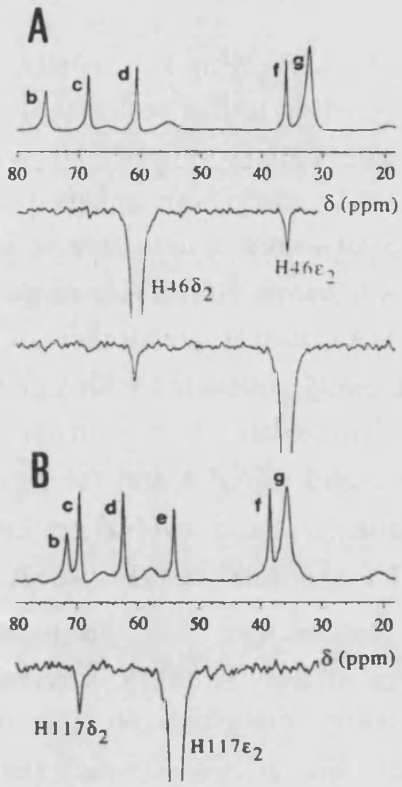

Fig. 3:6. 200 MHz reference and difference ^{1}H NMR spectra from steady-state 1D NOE experiments on Ni(II)-azurin. Samples were 3.0 mM concentration in H_2O solvent at 25 °C and pH 8 (A) or pH 5 (B).

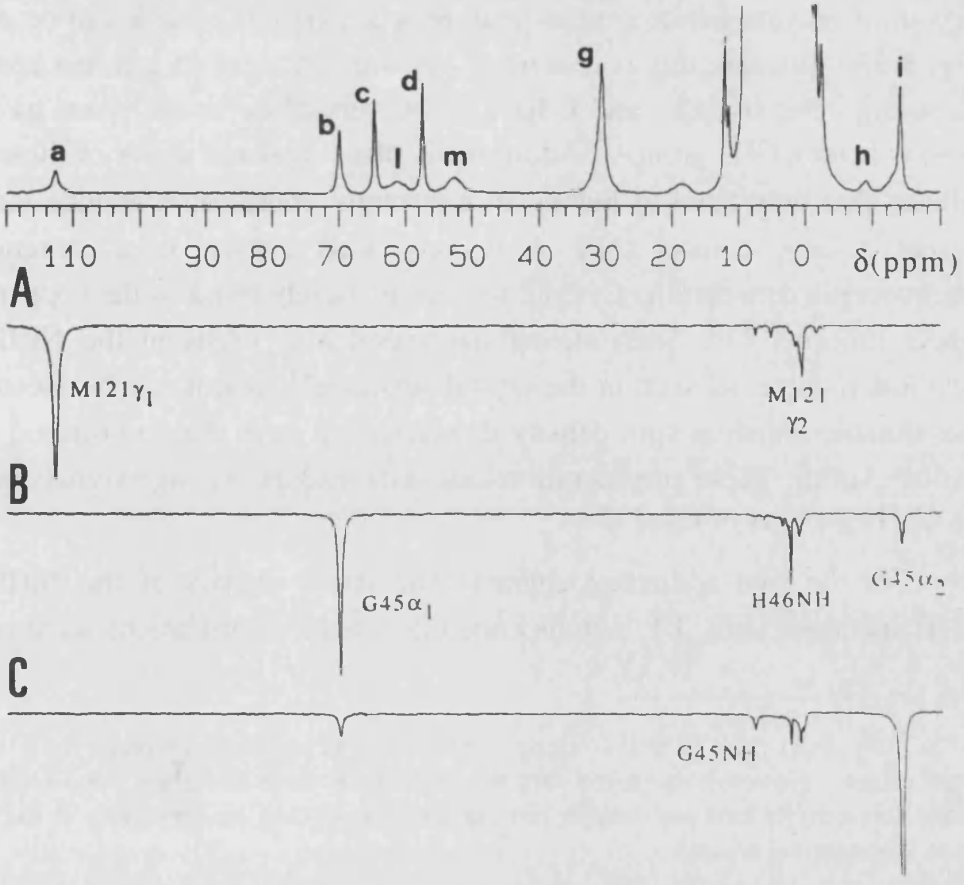

Fig. 3:7. 300 MHz 1D NOE NMR spectra of Ni(II)-azurin obtained upon irradiation of signals a (A), b (B) and i (C). Conditions are 3 mM Ni(II)-azurin, D_2O solvent, pH 7.5 and 45 °C.

The Met121 methyl signal (g) is the key starting point to assign the signals corresponding to this residue. Signal g is connected through a NOESY cross-peak with signal r (Fig. 3:5D), which in turn is contact coupled with signal q (Fig. 3:8A). Since both signals q and r are also connected through a strong NOE (Fig. 3:8B), they have to correspond to a CH_2 group. On the other hand, signal a gives a strong NOESY cross-peak with a signal at 0.6 ppm (Fig. 3:5C and Fig. 3:7A), indicating that they are a couple of geminal protons, and both signals are dipolarly connected with signals q and r, respectively (Fig. 3:5C and Fig. 3:8B). These data are in good agreement with signals q and r being the Met121 β protons and signal a and the signal at 0.6 ppm being the Met121 γ protons. Additionally, the α and NH protons of this residue are found through COSY and NOESY connectivities (Fig. 3:8A and Fig. 3:5C).

Due to their large chemical shifts, signals j and k are a characteristic element in the ^1H NMR spectrum of Ni(II)-azurin, and their assignment is particularly interesting. In spite of the very short T_1 and T_2 values of these signals, dipolar connectivities were obtained between them. In a 1-ms mixing time NOESY experiment optimized for very rapidly relaxing resonances (using a very short recycle time), a cross-peak between signals j and k can be observed (Fig. 3:5B). Because this connectivity has been obtained in extreme conditions, we assume that signals j and k have to be very close in the space as the two protons from a CH_2 group[12]. Additionally, the very large shifts of these signals indicate that they have to belong to a strongly coordinated residue since they present a large contact shift. It is very well known from structural and spectroscopic data that the Cys112 residue is closely bond to the copper in blue copper proteins[10,13]. Such strong interaction also exists in the Ni(II)-azurin metalloderivative, as seen in the crystal structure[14], and it can be the origin of considerable unpaired spin density delocalization over the coordinated Cys112 thyolate sulfur. These considerations and data lead us to assign signals j and k to the $C_\beta H_2$ protons of Cys112.

For the two additional characteristic broad signals of the Ni(II)-azurin NMR spectrum (Fig. 3:1, signals l and m), no NOE correlations were obtained.

---

[12]This NOESY cross-peak is not a strong connectivity as normally observed for a couple of geminal protons. However, due to the very short relaxation times of signals j and k, obtaining a NOESY connectivity between them is not expected unless they are very close in the space, as close as two geminal protons.

[13]a) Gewirth, A.A. & Solomon, E.I. (1988) *J. Am. Chem. Soc. 110*, 3811. **b)** Solomon, E.I. & Lowery, M.D. (1993) *Science 259*, 1575.

[14]Moratal, J.M., Romero, A., Salgado, J., Perales-Alarcón, A. & Jiménez, H.R. (1995) *Eur. J. Biochem., 228*, 653.

However, these signals present the shifts and relaxation times typical of the $C_{\varepsilon 1}H$ protons of histidines coordinated to Ni(II) by the $N_{\delta 1}$ imidazole nitrogen[4d], so we can tentatively assign them as the $C_{\varepsilon 1}H$ protons of the two coordinated histidines, His46 and His117.

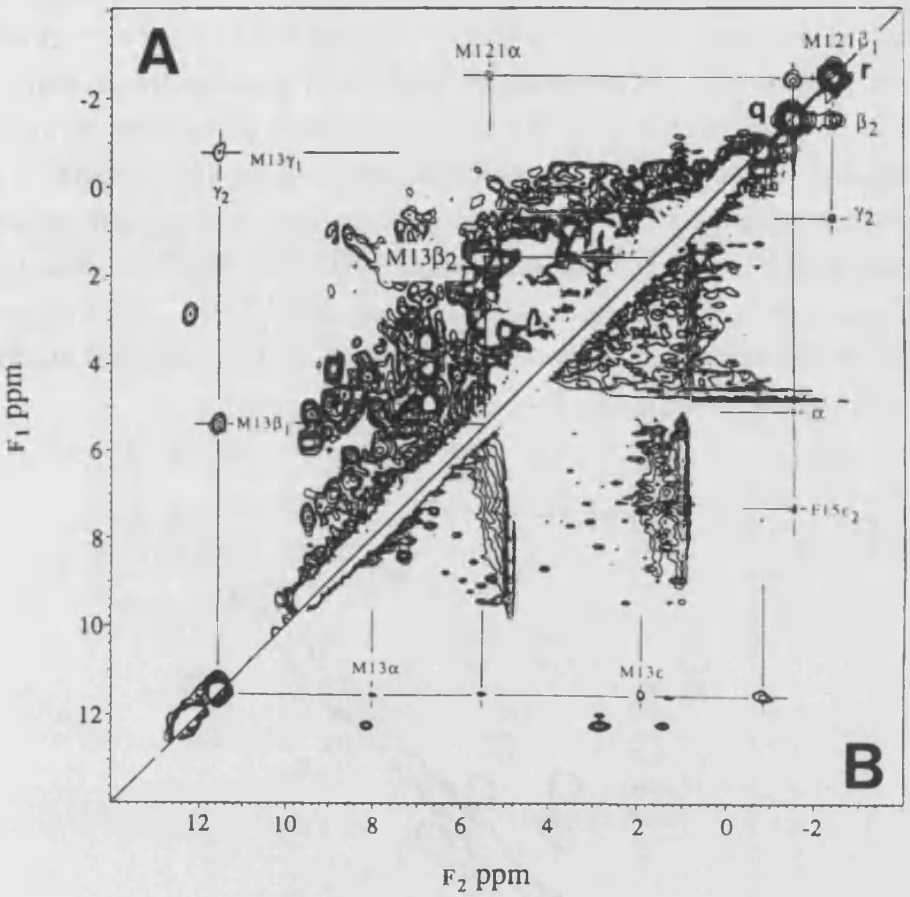

Fig. 3:8. 400 MHz ^{1}H magnitude COSY (A) and phase-sensitive TPPI NOESY (B) spectra of Ni(II)-azurin in D_2O at pH 7.5 and 45 °C. The NOESY has been recorded using a 10 ms mixing time.

Finally, among the principal signals of the NMR spectrum, signal h remains to be assigned. The relaxation time and isotropic shift of this signal (see Table 3:1), indicate that it corresponds to a coordinated residue. However, it does not show any cross peak that permits its assignment. From a cautious use of the Solomon equation[15], its distance from the metal ion can be estimated as 4-5 Å. According to the X-ray data[10], the possible candidates for this signal are the β2 proton of His46 and the α proton of Cys112.

[15]The T_1 values can be interpreted in terms of proton-paramagnetic center distances according to the Solomon equation (Solomon, I. (1955) *Phys. Rev. 99*, 559).

c) Other assignments.

The inspection of the aromatic region of the NMR spectrum (Fig. 3:9) leads to the immediate assignment of the aromatic protons of Trp48, Phe110, Phe111, Phe29, Phe97 and Tyr72. These protons do not exhibit isotropic shifts because they are far from the paramagnetic center. Thus, their specific assignment can be made just by comparison with the spectrum of the diamagnetic Cu(I)-azurin[16]. Conversely, Phe15 and Phe114 are very close to the metal and their proton signals can present some pseudocontact shift. These signals have to present also fast relaxation rates, which make them more difficult to be detected in the TOCSY experiment. Because of this reason, we have tentatively assigned the Phe114 aromatic protons to a spin system giving very weak cross-peaks in the TOCSY map (Fig. 3:9). The Phe15 is observed in a TOCSY spectrum with a shorter relaxation time (Fig. 3:10). This assignment is supported by the existence of two dipolar connectivities between the Phe15 ε signals and signals g and q (see Fig. 3:5D and Fig. 3:8B).

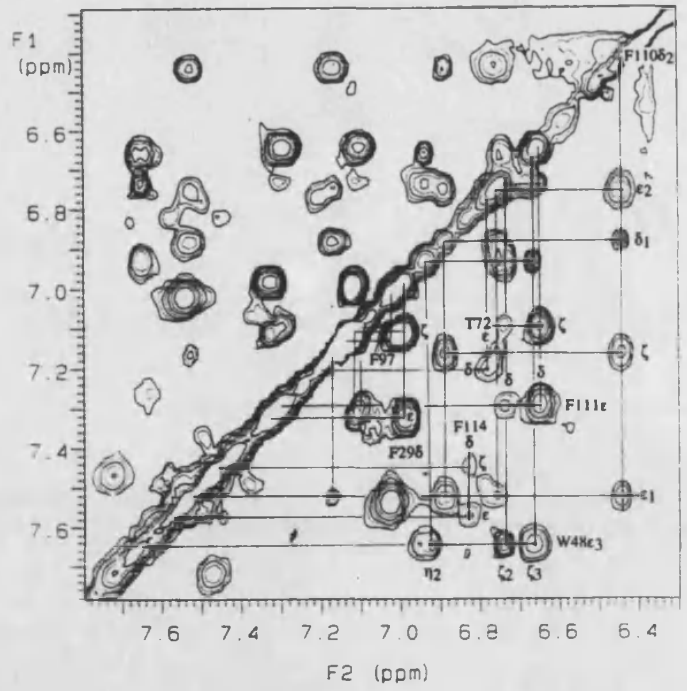

Fig. 3:9. Aromatic region of a ^{1}H phase-sensitive TPPI TOCSY map of Ni(II)-azurin in D_2O, pH 7.5 and 45 °C. 512 fids were recorded over a 10 KHz spectral width with a 70 ms mixing time, and Fourier transformed using shifted squared-sine-bell weighting functions.

---

[16] a) Canters, G.W., Hill, H.A.O., Kitchen, N.A. & Adman, E.T. (1984) *Eur. J. Biochem. 138*, 141. b) van de Kamp, M., Canters, G.W., Wymenga, S.S., Lommen, C.W., Hilbers, H., Nar, A., Messerschmidt, A. & Huber, R. (1992) *Biochemistry 31*, 10194.

Finally, signals n and p, together with other signals under the diamagnetic envelope, are cross-correlated through COSY and NOESY connectivities (Fig. 3:8). This group of signals seems to belong to a methionine-like spin system, that according to the relaxation times of signals n and p (14 ms and 8.6 ms, respectively), has to be at 5-6 Å from the metal site. From the X-ray structural data[10,14], the Met13 γ protons are the best candidates for the assignment of signals n and p, although in the absence of additional connectivities between these signals and other assigned residues, this assignment is only tentative.

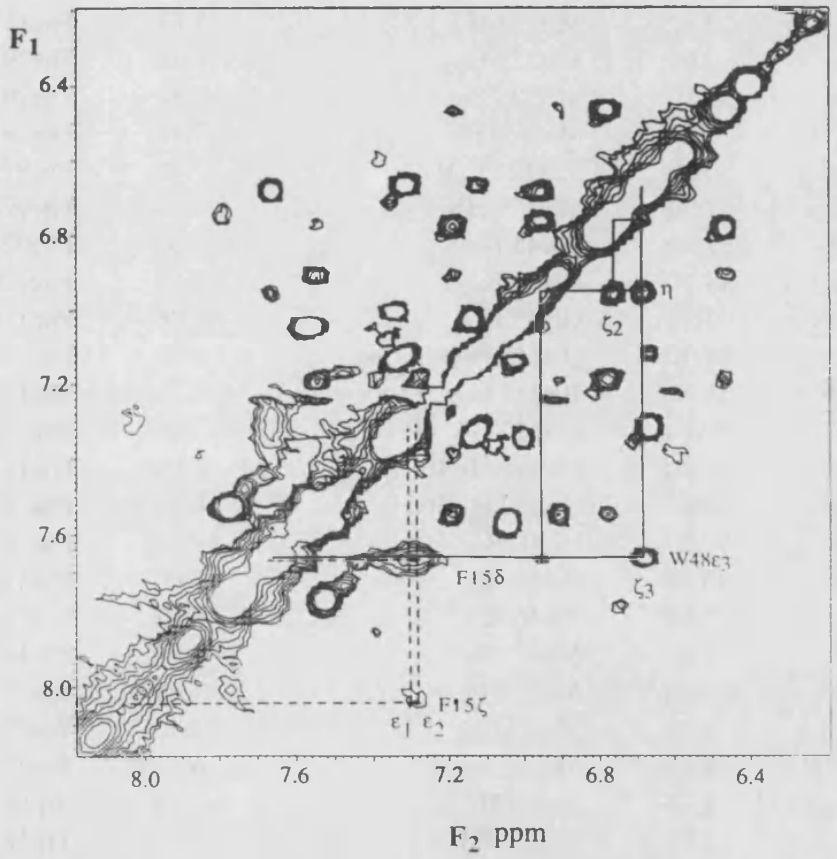

Fig. 3:10. Portion of a TOCSY spectrum of Ni(II)-azurin (D_2O, pH 7.5, 45 °C) performed as in Fig. 3:9 but using a 20 ms mixing time.

Table 3:2. Assignment of the ^{1}H NMR resonances in nickel(II)-azurin from *P. aeruginosa* at pH 7.5 and 45 °C.

signal	δ(ppm)	Assignment	δ(ppm)	Assignment
j	232.50	Cys112 H_β	7.29	Phe15 $H_{\varepsilon 1}$
k	187.30	Cys112 H_β	7.32	Phe15 $H_{\varepsilon 2}$
a	111.30	Met121 $H_{\gamma 1}$	7.66	Phe15 H_δ
	0.62	Met121 $H_{\gamma 2}$	8.02	Phe15 H_ζ
q	-1.60	Met121 $H_{\beta 2}$	6.98	Phe29 H_δ
r	-2.50	Met121 $H_{\beta 1}$	7.32	Phe29 H_ε
	5.20	Met121 $H\alpha$	7.11	Phe29 H_ζ
g	30.30	Met121 $C_\varepsilon H_3$	7.10	Phe97 H_δ
	7.90	Met121 HN	7.14	Phe97 H_ε
b	69.50	Gly45 $H_{\alpha 1}$	7.02	Phe97 H_ζ
i	-14.10	Gly45 $H_{\alpha 2}$	7.52	Phe110 $H_{\varepsilon 1}$
	7.90	Gly45 HN	6.76	Phe110 $H_{\varepsilon 2}$
c	64.30	His117 $H_{\delta 2}$	6.88	Phe110 $H_{\delta 1}$
e[a]	51.50	His117 $H_{\varepsilon 2}$	6.44	Phe110 $H_{\varepsilon 2}$
o	10.10	His117 HN	7.16	Phe110 H_ζ
l	61.20	His117/His46 $H_{\varepsilon 1}$	6.64	Phe111 H_δ
m	52.60	His117/His46 $H_{\varepsilon 1}$	6.73	Phe111 H_δ
d	57.20	His46 $H_{\delta 2}$	7.29	Phe111 H_ε
f	35.00	His46 $H_{\varepsilon 2}$	7.09	Phe111 H_ζ
	2.60	His46 HN	6.82	Phe114 H_δ
n	11.50	Met13 $H_{\gamma 1}$	7.57	Phe114 H_ε
o	-0.80	Met13 $H_{\gamma 2}$	7.44	Phe114 H_ζ
	5.40	Met13 $H_{\beta 1}$	7.20	Tyr72 H_δ
	1.55	Met13 $H_{\beta 2}$	6.77	Tyr72 H_ε
	8.24	Met13 H_α	7.64	Trp48 $H_{\varepsilon 3}$
	1.97	Met13 $C_\varepsilon H_3$	6.92	Trp48 $H_{\eta 2}$
			6.73	Trp48 $H_{\zeta 2}$
			6.66	Trp48 $H_{\zeta 3}$

[a] not observed at pH higher than 7.

DISCUSSION.

a) The analysis of the NMR spectra.

Assigning signals is a crucial step in any NMR investigation aimed to the understanding of either the structural or the dynamic properties of the system. For biological macromolecules (proteins and DNA), powerful strategies based on the application of diverse two-dimensional pulse sequences have been developed in the pass[17], converting the assignment process into an almost automatic (although tedious) task. These techniques have suffered an important development with the access to isotopically enriched (in ^{15}N or/and ^{13}C) molecules, which opened the possibly to perform multinuclear-multidimensional NMR spectra.

The NMR spectra of paramagnetic metalloproteins contain important structurally-related information which can be extracted from the analysis of the isotropic shifts and the relaxation properties of paramagnetic resonances[4]. But first these resonances have to be assigned, and the same properties which make paramagnetic NMR an interesting technique hinder the assignment process[18]. The use of the conventional NMR methodology in these cases meets important limitations, so special strategies for paramagnetic systems have been developed in the last few years[4c,d]. They include the use of normal two-dimensional pulse sequences, sometimes with some modifications. However, these 2D NMR techniques have been applied almost exclusively to the study of iron proteins and mainly to low-spin iron(III) heme proteins. The large electron relaxation rates, and therefore the relatively small nuclear relaxation rates that characterize these proteins, make relatively easy the detection of two-dimensional connectivities[4d]. The work presented here has been one of the first examples on the application of 2D NMR to a non-iron paramagnetic protein[19].

Because of the impossibility to obtain contact couplings among most of the isotropically shifted signals, their assignment has been made mainly on the basis of dipolar (1D or 2D NOE) correlations. In the case of the 1D NOEs, interproton distances are calculated using the NOE intensities and the relaxation times of the

---

[17] Wütrich, K. (1986) *NMR of proteins and Nucleic acids*, John Wiley & Sons, New York.

[18] See Chapter 1, section V.

[19] a) Moratal, J.M., Salgado, J., Donaire, A., Jiménez, H.R. & Castells, J. (1993) *J. Chem. Soc., Chem. Commun.*, 110. b) Moratal, J.M., Salgado, J., Donaire, A., Jiménez, H.R., Castells, J. & Martínez-Ferrer, M.J. (1993) *Magn. Reson. Chem. 31*, 541.

signals[20]. Using this approach, independent conclusions can be reached in two cases: for couples of geminal protons and for protons from imidazole rings. In both cases we rely on standard interproton distances which are compared with the calculated values. For the specific assignment of these CH_2 or imidazole protons, their singular NMR characteristics are used. Thus, although there are four histidines in the azurin sequence, it is reasonable to think that signals c & e and d & f belong to the coordinated ones: His117 and His46. Analogously, among the CH_2 groups around the metal site, the Cys112 $C\beta H_2$ group is assigned to signals j and k because of their very large shifts and short relaxation times. A similar pair of signals are also found in the NMR spectrum of the cobalt(II)-azurin and they have been unequivocally assigned to the Cys112 β protons from the study of the Co(II) derivative of the Cys112Asp-azurin mutant[21]. This is also in agreement with earlier investigations of the nickel(II) and cobalt(II) derivatives of rubredoxin[22] and liver alcohol dehydrogenase[23], where the most downfield shifted proton resonances were tentatively assigned to the $C\beta H_2$ protons of the bound cysteines, only on the basis of their large chemical shifts.

The rest of the assignments cannot be performed independently, and the interpretation of the NMR data needs to be assisted by structural information available from other sources, like X-ray crystallography. Thus, we have used previous structural information for the assignments made on the basis of some special characteristics of the signals, like the differences in the exchange rate of the labile signals e and f, which permits to assign every of them specifically to a particular coordinated histidine (see above). The crystallographic structural information is also used to interpret many of the NOESY connectivities. Examples of this type are the assignment of signals b and i to the Gly45 α protons because of their dipolar connectivities with two exchangeable protons, or the assignment of the Met121 γ and β protons because of their NOESY connectivities between them and with signal g, the Met121 methyl signal. Additionally, proton-metal distances taken from the crystallographic structure are used to assign signals like h, taking into account the relaxation time data and the Solomon equation[15]. However, this is an approximate method (assignments

[20]See Chapter 2, section II.e.

[21]Piccioli, M., Luchinat, C., Mizoguchi, T.J., Ramírez, B.E., Gray, H.B. & Richards, J.H. (1995), *Inorg. Chem. 34*, 737.

[22]Moura, I., Teixeira, M., LeGall, J. & Moura, J.J.G. (1991) *J. Inorg. Biochem. 44*, 127.

[23]Bertini, I., Gerber, M., Lanini, G., Luchinat, C., Maret, W., Rawer, S. & Zeppezauer, M. (1984) *J. Am. Chem. Soc. 106*, 1826.

made on this basis are considered as "tentative") due to the so called ligand-centered dipolar effects[24], the intrinsic problems in determining the T_1 values[4c,25], and the approximate value of the correlation time used in the Solomon equation. The first operates when there is delocalization of unpaired spin density over the coordinated ligands. The uncertainty of the relaxation times comes from the difficulties to fit the z-magnetization recovery processes as a single exponential[4c,25,26]. With regard to the correlation time, for metalloproteins it is normally assumed to be equal to the electronic correlation time of the paramagnetic metal ion, τ_s [27]. This is in the range of 10^{-10}-10^{-12} sec for Ni(II) complexes[28], and the exact value needs to be experimentally determined for every case. We have taken an approximated value of $5x10^{-12}$ sec, estimated from the Met121 methyl signal (g) with a T_1= 3.8 ms, assuming a proton-metal distance of 4.2 Å as determined by X-ray crystallography[14]. Another source of error when assignments are made based calculated proton-metal distances comes from the use of an inadequate structure as a reference. In a previous report[19a], the geminal protons b & i, assigned here as the Gly45 α protons, were tentatively assigned to a CH_2 group of Met121. This assignment was based on the comparison of the proton-metal distances calculated by the Solomon equation with proton-metal distances from the Cu(II)-azurin crystal structure[10], since the structure of the Ni(II)-azurin was not yet available. A comparison of the NMR data with the structure of the Zn(II)-azurin[29], which as we know now is more similar to the structure of the Ni(II)-azurin[14], would have given a better result.

[24a] Banci, L., Bertini, I., C., Luchinat, C. & Scozzafava, A. (1987) *J. Am. Chem. Soc. 109*, 2328. **b)** Banci, L., Bertini, I., Luchinat, C., Monnanni, R. & Moratal, J.M. (1989) *Gazz. Chim. Ital. 119*, 23.

[25]See Chapter 2, section II.b.

[26]Granot, J. (1982) *J. Magn. Reson. 49*, 257.

[27]The correlation rate τ_c^{-1} for the dipolar coupling is given by $\tau_c^{-1} = \tau_s^{-1}+\tau_r^{-1}+\tau_M^{-1}$ (τ_s^{-1}, τ_r^{-1} and τ_M^{-1} are the electronic, rotational and exchange correlation rates, respectively). The fastest of the three determines the correlation rate. τ_M^{-1} does not apply in the absence of exchange and τ_r^{-1} amounts 10^6-10^5 sec^{-1} for proteins, so τ_s^{-1}, in the range of 10^8-10^{12}, is dominant. See the next reference for more details.

[28a] Banci. L., Bertini, I. & Luchinat, C. (1991) *Nuclear and Electron Relaxation*, VCH, Weinheim. **b)** Bertini, I., Luchinat, C. & Messori, L. (1987) in *Metal Ions in Biological Systems* (Sigel, H., ed.), vol. 21, p. 47, Marcell Dekker, New York.

[29]Nar, H., Huber, R., Messerschmidt, A., Filippou, A.C., Barth, M., Jaquinod, M., van de Kamp, M. & Canters, G.W. (1992) *Eur. J. Biochem. 205*, 1123.

b) The nickel-azurin metal site.

The most isotropically shifted signals of the ^{1}H NMR spectrum of Ni(II)-azurin belong to five different residues (Table 3:2). The magnitude of these isotropic shifts makes us thinking that they have a contact contribution and, consequently, these five residues are coordinated to the Ni(II). Considering the structure of the native Cu(II)-azurin[10], a penta-coordinated metal site is not surprising if we admit an approach of the Gly45 ligand to the metal ion, since no significant orbital overlap can be expected for a 2.97 Å metal-O_{Gly45} distance[10]. But the crystal structures of both the Ni(II)[14] and the Zn(II)-azurin[29] metalloderivatives tell us that this approach does not happen without a simultaneous enlargement of the metal-S^{δ}_{Met121} bound, placed in the opposite axial position. It seems that the azurin metal site is designed to avoid a simultaneous coordination of both axial ligands and it would be also an expression of the rack-induced bonding suggested by Malmström[30]. But the NMR data, which suggest the participation of both the Gly45 O and the Met121 S_{δ} in a penta-coordinated metal site, seem to disagree with this idea.

The isotropic shifts of the Gly45 α protons indicate the existence of contact contribution and a clear metal-O_{Gly45} bond in the Ni(II)-azurin. On the other hand, the short relaxation times observed for these protons (see Table 3:1) is not in agreement with the structure of the metal site in the native Cu(II)-azurin[10] and can be better explained as a result of a shorter distance to the paramagnetic center and unpaired spin density delocalization on the ligand nuclei. With regard to the Met121 residue, its proton resonances have been clearly identified above and the assignments have been verified by comparison with the ^{1}H NMR spectra of the Ni(II)-Met121Gln azurin mutant[31]. It is worth noting that the γ_1 proton of Met121 is one of the most downfield shifted resonances of the ^{1}H NMR spectrum of Ni(II)-azurin (Fig. 3:1, signal a).

The analysis of the temperature dependence of the isotropic shifts can be used to estimate the extent of the pseudocontact contribution to these shifts[4a,b]. A T^{-2} dependence of the isotropic shifts is ascribed principally to the pseudocontact term[32]. At the small temperature range normally investigated (due to the limitations imposed by the solvent and the stability of the protein) the shifts are usually inversely proportional to temperature, and the normal procedure to check over a non-T^{-1} dependence is to extrapolate the plot of δ *vs*

[30] Malmström, B.G. (1994) *Eur. J. Biochem. 223*, 711.

[31] Salgado, J. Jiménez H.R., Moratal, J.M., Kroes, S., Warmerdam, G & Canters, G.W. (1995) , *Biochemistry*, in press. See Chapter 5.

[32] See Chapter 2, section II.f.

T^{-1} at infinite temperature. Extrapolated values which fall far from the shifts expected in the absence of paramagnetic effect are an indication of pseudocontact contribution to the isotropic shifts. The Met121 γ1 and Gly45 α1 proton signals extrapolate far from the diamagnetic region (Fig. 3:4, signals a and b). The former one shows a particularly large deviation (more than 50 ppm), indicating the existence of important pseudocontact shift in this signal. However, this isotropic shift is too large (111 ppm at 45 °C) to be only of dipolar origin, suggesting also the existence of contact contribution. Likewise, we have to assume that there is contact contribution to the isotropic shift of the Met121 methyl signal (signal g), because although it is considerably shifted (30.3 ppm), the pseudocontact term seems to be negligible according to the very small deviation from the expected diamagnetic position showed by the extrapolation of this δ at T^{-1}=0 (Fig. 3:4). Therefore, we conclude that, at least in solution, the Met121 residue is at some extent coordinated to the nickel(II) ion. However, a more complete analysis of the isotropic shift data, which includes the separation of pseudocontact and Fermi-contact contributions, is needed to confirm this conclusion. To perform this factorization, the knowledge of the orientation and components of the magnetic susceptibility tensor is necessary. Such information is normally extracted from single crystal magnetic susceptibility measurements, but they are not yet available for metalloproteins. A second possibility is to use pure pseudocontact shifts measured in the NMR spectra to extract the magnetic susceptibility components of the metal site, as it has been done for some low-spin Fe(III)-hemoproteins[33] and cobalt substituted carbonic anhydrase[34].

c) pH dependent structural variations.

The pH dependent behavior of *Pseudomonas aeruginosa* azurin is well documented in the literature and has been characterized at a molecular level by X-ray crystallography. NMR studies on Cu(I)-azurin ligated the observed pH induced changes with the ionization of the His35 residue[35]. The possible functional significance attributed this titration appeared related with the pH dependence of the midpoint potential (a 60 mV E_m decrease from pH 5 to 8)[9b,36], and the observation of a slow reaction coupled with a fast one in the electron

[33]La Mar, G.N., Chen, Z. & de Ropp, J. (1995) in *Nuclear Magnetic Resonance of Paramagnetic Macromolecules, seriesC: Mathematical and Physicals Sciences* (La Mar, G.N., ed.), vol. 457, p. 55, Kluwer Accademic Publishers, Dordrecht.

[34]Banci, L., Dugad, L.B., La Mar, G.N., Keating, K.A., Luchinat, C. & Pieratelli, R. (1992) *Biophys. J. 63*, 530.

[35]Adman, E.T., Canters, G.W., Hill, H.A.O. & Kitchen, N.A. (1982) *FEBS Lett. 143*, 287.

[36]Strong, C., Ellis, W.R. & Gray, H.B. (1992) *Inorg. Chim. Acta 191*, 149.

transfer kinetics between azurin and cytochrome c_{551}[9a,37]. On the other hand, electron transfer experiments using Cr-labeled azurin made some authors thinking on the possible existence of two distinct electron transfer docking patches: the His35 patch, for the reaction with cytochrome c_{551}, and the hydrophobic patch around the His117 metal ligand, responsible for the reaction of azurin with nitrite reductase[38].

More recently, a deep structural study by X-ray diffraction at different pH conditions was in agreement with the existence and origin of the pH induced structural change. However, it showed that its effects are limited to a local zone close to the His35 residue, while the metal center structure remains unaffected or suffers small changes below the 0.1 Å resolution limit[10]. Additionally, replacement of His35 by means of site directed mutagenesis definitively demonstrated that this residue is not functionally essential neither for the reaction of azurin with cytochrome c_{551} nor for its reaction with nitrite reductase[39]. Conversely, replacement of Met44 in the hydrophobic patch, demonstrates that this is the relevant surface zone for the reaction of azurin with its redox partners, putting finally an end to the existence of a second docking patch in azurin[39b].

Our investigation on Ni(II)-azurin permits the observation of a pH-linked transition affecting most of the isotropically shifted resonances. The pK_a value associated with it, 5.9, is the same as that obtained for the Co(II)-azurin[40]. For a long time, this value was assumed as the pK_a corresponding to the Cu(II)-azurin because of the difficulties in determining it by NMR[41]. More recent investigations report pK_a values of 6.26 and 6.5 for the Cu(II)-azurin, derived

---

[37a] Rosen, P. & Pecht, I. (1976) *Biochemistry 15*, 775. **b)** Silvestrini, M.C., Brunori, M., Wilson, M.T. & Darley-Usmar, V. (1981) *J. Inorg. Biochem. 14*, 327.

[38a] Farver, O. & Pecht, I. (1981) *Israel J. Chem. 21*, 13. **b)** Farver, O., Blatt, Y. & Petch, I. (1982) *Biochemistry 21*, 3556.

[39a] van de Kamp, M., Floris, R., Hali, F.C. & Canters, G.W. (1990) *J. Am. Chem. Soc. 112*, 907. **b)** van de Kamp, M., Silvestrini, M.C., Brunori, M., van Beeumen, J., Hali, F.C. & Canters, G.W. (1990) *Eur. J. Biochem. 194*, 109.

However, these site-directed mutagenesis experiments also demonstrated that His35 is responsable for the slow relaxation phase observed in the reaction between azurin and cytochrome c_{551}, as well as for the pH dependent effects observed in the NMR spectra[9b].

[40a] Hill, H.A.O., Smith, B.E., Storm, B.C. & Ambler, R.P. (1976) *Biochem. Biophys. Res. Comm. 70*, 783. **b)** Moratal, J.M., Salgado, J., Donaire, A., Jiménez, H.R. & Castells, J. (1993) *Inorg. Chem. 32*, 3587.

[41] The NMR signals of the His35 residue are broadened beyond detection in the spectrum of Cu(II)-azurin[16]. However, the His35 pK_a can be determined indirectly from the pH dependence of the Val31 γ resonances, which are less broadened and sensitive to the state of protonation of His35[9b].

from spectroelectrochemistry[36] and NMR experiments[9b], respectively. These values are significantly larger than the one reported here. To explain this apparent discrepancy, we must consider the origin of the influence of the metal ion in the titration of an acid group placed close to it. The difference in the His35 pK_a between the reduced and oxidized azurins is attributed to electrostatic effects[9b], i.e. to the existence of a larger repulsion of the titrating $N_{\delta 1}H$ proton by the metal in the Cu(II)-azurin than in the Cu(I)-azurin. Such electrostatic effect depends on the metal-$N_{\delta 1}H_{His35}$ distance[9b]. Examining this distance in the crystal structures of Cu(II)[10] and Ni(II)-azurin[14], we find that it is 0.25 Å shorter in the Ni(II) derivative, which can explain the smaller pK_a value obtained in this case.

Almost all the isotropically shifted signals belonging to coordinated residues change their position as a consequence of the His35 titration. This effect is also observed in the spectrum of Co(II)-azurin[40] and in some resonances from coordinated residues in the spectrum of Cu(I)-azurin[16]. The observed changes could be probing the existence of a structural effect of the His35 titration over the metal site geometry. We have tried to address this possibility by using the relaxation times of the paramagnetic signals at pH 5 and 7.5 (Table 3:1) as an indication of the proton-metal distances according to the Solomon equation[15]. As we have explained above, the application of this method lead to significant errors due to the uncertainty of some of the parameters needed in the equation. However, we use this approach to compare proton-metal distances at different conditions, calculated from the corresponding T_1 values, when we can assume that the correlation times remain the same as those conditions. Keeping constant all the parameters in the Solomon equation except the proton-metal distance r and the relaxation time ($T_{1M}^{-1}=Kxr^{-6}$), we find that a 12 % variation in the T_1 value corresponds to a 2% change in the proton-metal distance, which means a 0.1 Å change for a proton placed 5 Å from the metal. Variations of the relaxation times of the hyperfine shifted signals are less than 12 % (Table 3:3) and they are even less significant if we consider an estimated 5% error in the T_1 values. This indicates that the possible pH-induced structural changes in the metal site are not significant, in good agreement with X-ray structures of Cu(II)-azurin at pH 5 and pH 9[10] (Table 3:3).

Additionally, signal e, corresponding to the $N_{\varepsilon 2}H$ proton of His117, decreases in intensity when the pH is increased (Fig. 3:2). Curiously, from the pH dependence of the relative area of this signal we obtain the same pK_a value as for the slow exchange transition affecting the rest of the paramagnetic signals (Fig. 3:11).

Table 3:3. Comparison of the structure of the azurin metal site at low and high pH. r_1 and r_2 values are proton-Cu(II) distances at pH 5 and pH 9, respectively, taken from the crystal structure[10].

	Ni(II)-azurin[b]		Cu(II)-azurin[c]		
proton[a]	signal (δ, ppm)	ΔT_1 (%)[d]	r_1	r_2	Δr (%)[d]
Cys112 β	j (232.60)	0.0	3.55	3.56	+0.3
Cys112 β	k (187.30)	0.0	3.42	3.43	+0.3
Met121 γ1	a (111.30)	-3.7	5.48	5.52	+0.7
Met121 β2	q (-1.60)	-7.0	4.99	4.94	-1.0
Met121 β1	r (-2.50)	-7.0	4.66	4.61	-1.1
Met121 ε(CH_3)	g (30.30)	+10.5	4.16	4.32	+4.0
Gly45 α1	b (69.50)	-8.0	5.86	5.82	-0.7
Gly45 α2	i (-14.10)	-6.2	5.79	5.73	-1.0
His117 δ2	c (64.30)	-6.0	5.29	5.23	-1.1
His117 ε2	e (51.50)	—	5.04	5.00	-0.8
His117 HN	o (10.10)	0.0	5.49	5.49	0.0
His46 δ2	d (57.20)	-7.5	5.21	5.19	-0.4
His46 ε2	f (35.00)	-11.3	4.95	4.92	-0.6

[a] assignments as in Table 3:2.

[b] data from the ^{1}H NMR spectrum of Ni(II)-azurin at pH 5 and 7.5 presented in Table 3:1.

[c] data from reference 10.

[d] a positive sign means an increase in the value from low to high pH.

Because this value is too low to reflect the deprotonation of a coordinated histidine, the behavior of signal e can be better explained by assuming that at high pH the His117 $N_{\varepsilon 2}H$ proton exchanges fast with bulk water on the NMR time-scale. A possible reason for this phenomenon is that, as a consequence of the pH induced conformational change, the His117 $N_{\varepsilon 2}H$ becomes more exposed to solvent, enters fast exchange, and becomes undetectable. The $N_{\varepsilon 2}H$ imidazole edge of the His117 lays in a shallow depression in the center of the hydrophobic patch (Fig. 3:12)[10,42]. This group could become more exposed to the solvent by either a movement of the His117 imidazole ring or a reorganization of the hydrophobic patch. However, none of these possibilities is very likely, since they would mean that the effects of the pH dependent structural change extend much more than showed by the X-ray structural data[10]. A second, less conflicting, possibility is that the exchange rate of the His117 $N_{\varepsilon 2}H$ proton with solvent H_2O increases at high pH just because of a general

[42]Nar, H., Messerschmidt, A., Huber, R., van de Kamp, M. & Canters, G.W. (1991) *J.Mol. Biol. 218*, 427.

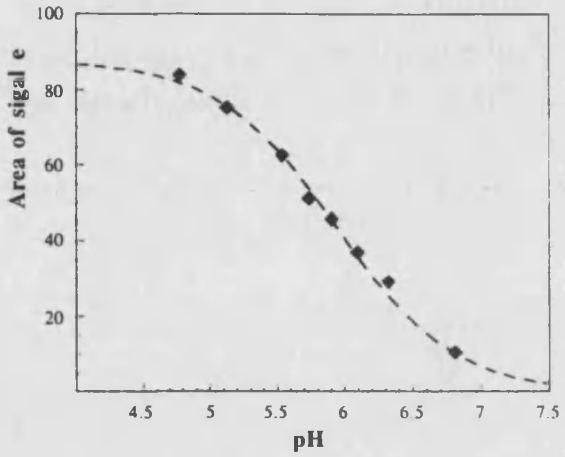

Fig. 3:11. Variation of the relative area of signal e with the pH at 25 °C. These data, taken from the spectra in Fig. 3:2, can be fitted to a theoretical curve giving a pK_a = 5.93 ±0.10.

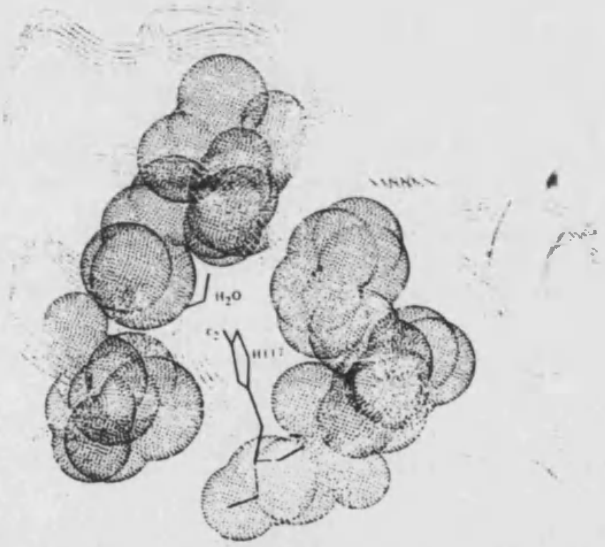

Fig. 3:12. A view of the hydrophobic patch of azurin from the top of the molecule. The His117 metal ligand is placed in a depression in the center of the patch, with the imidazole $N_{\varepsilon 2}H$ group pointing towards the surface of the molecule and interacting with a well defined water molecule. Surrounding this zone, there are various hydrophobic side-chains (represented here by dotted balls) from residues Met13, Met14, Phe114 and Pro115, among others.

base catalysis phenomenon. Although the exchange rate with the bulk water of the so called labile protons can be either acid or base-catalyzed[43], the observation of these protons by NMR appears more frequently influenced by base catalysis because the effect of acid catalysis is normally important only at very low pH[17]. If this is the case here, the disappearance of signal e with increasing pH does not represent a titration process, and the apparent pK_a value obtained from signal e would coincide with the His35 pK_a just by chance. The fact that this behavior is

[43]Eigen, M. (1964) *Angew. Chem. (Intl. Ed.) 3*, 1.

also observed for the equivalent signal in the spectrum of the *A. denitrificans* Ni(II)-azurin, where the His35 residue does not titrate, confirms that there is no connection between the increased exchange of the His117 $N_{\varepsilon 2}H$ proton and the pH induced conformational change in *P. aeruginosa* azurin.

II. The X-ray structure of nickel-azurin.

RESULTS.

Ni(II)-azurin was crystallized by a procedure similar to that for the native copper-azurin[10]. The hanging drop vapor diffusion method was used with droplets containing 15 mg/ml of protein, 1.5 M $(NH_4)_2SO_4$, 0.25 M $LiNO_3$ and 0.1 M CH_3COONa at pH 5.05, which were equilibrated with reservoir buffers containing precipitant increasing concentration. At 3.1 M $(NH_4)_2SO_4$, 0.5M $LiNO_3$, 0.1M CH_3COONa large prisms of a bright yellow color grew within two weeks to a maximum size of 0.8 mm x 0.5 mm x 0.4 mm. These crystals diffracted well up to 2.05 Å resolution. The symmetry of the nickel-azurin crystals and the unit cell parameters, a=57.3 Å, b=80.9 Å and c=110.5 Å, remained essentially the same as for the copper-azurin. Other crystallographic data are summarized in Table 3:4.

Table 3:4. Ni(II)-azurin crystallographic data and refinement results.

Crystallographic data		Refinement results	
Space group	$P2_12_12_1$	Resolution range (Å)	8.00 to 2.05
Unit cell constants (Å)	57.31, 80.86, 110.53	Number of reflections	31,439
		R=Σ(|Fo|–|Fe|)/Σ|Fo| (%)	
Resolution (Å)	2.05	8.00 to 2.05 Å	17.9
Measurements [I>2.5 σ(I)]	129,132	2.15 to 2.05 Å	23.8
Unique reflections	32,694	Number of atoms	
Data completeness (%)		all non-hydrogen atoms	4,179
∞ to 2.05 Å	90	non-hydrogen protein atoms	3,900
2.10 to 2.05 Å	74	solvent	275
Reflections averaging (%)		nitrate ion	1
R_{merge} †	6.0	Total internal energy	
R_{FR} ¥	3.8	(Kcal/mol)	-10,178
		r.m.s. deviation from standard geometries	
		Bonds (Å)	0.012
		Angles (°)	2.76

† $R_{merge}=\Sigma|I(k)-\langle I\rangle|/\Sigma I(k)$, where I(k) and <I> are the intensity values of individual measurements and of the corresponding mean values. The summation is over all measurements.

¥ $R_{FR}=R_{merge}$ after independent averaging of Friedel pairs.

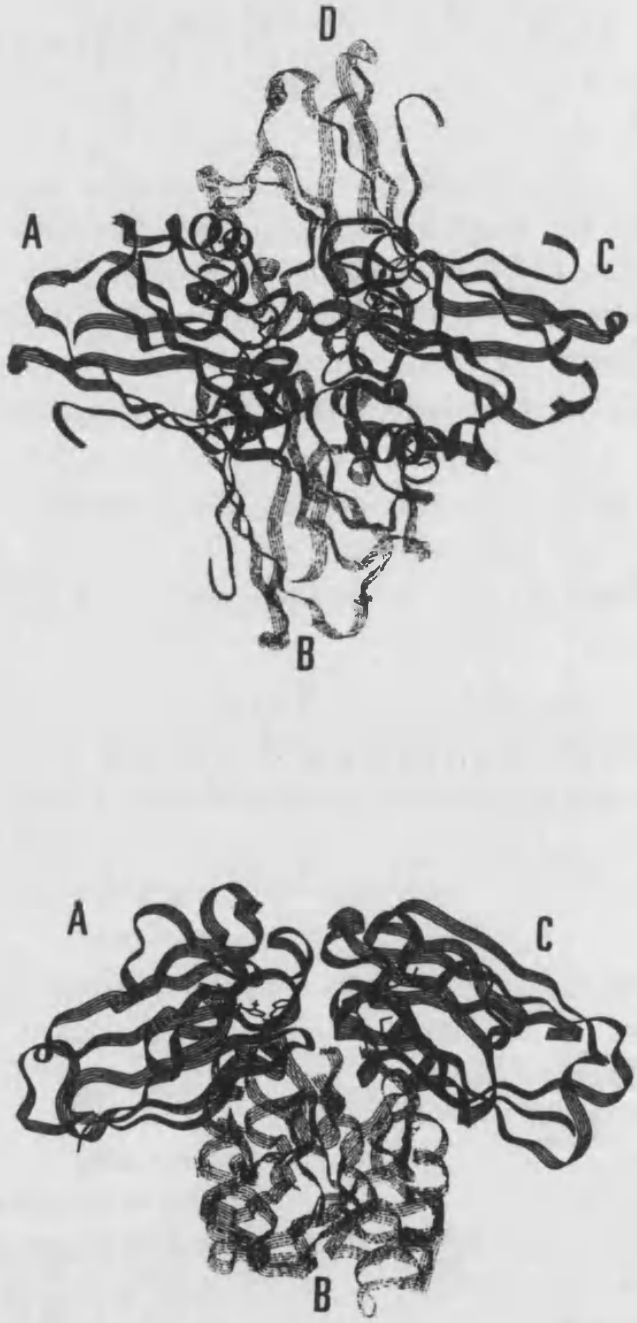

Fig. 3:13. Two views (ribbon drawings) of the four crystallographically independent molecules of Ni(II)-azurin. The tetramer assembly can be described as having *C*2 symmetry and being a dimer of dimers. The AB dimer can be transformed into the DC dimer by a local symmetry axis (perpendicular to the plane of the paper in the figure of the top). Monomers A and C (B and D) interact through the residues Met13, Leu39, Asn42, Val43, Met44, Tyr72, Phe114, Pro115 and Gly116, that constitute the hydrophobic patch. Residues 53 to 57 and 107 to 109 are in the interface between monomers A and B (C and D), and residues 10 to 18 and 123 to 124 participate in the contact between monomers A and D (B and C). This molecular packing is essentially the same as found in other wt and mutant azurin structures[10,42].

The crystallographic analysis of Ni(II)-azurin at 2.05 Å resolution reveal that the overall structure of the protein is not perturbed by the metal exchange. As in the case of *Pae* Cu(II)-azurin[10,42], there are four crystallographically independent molecules per asymmetric unit. The four monomers are organized as a dimer of dimers (Fig. 3:13) and the contacts between every azurin monomer with neighboring molecules are essentially the same as in other *Pseudomonas aeruginosa* azurin structures[10,42]. Superposition of the main chain (Cα, N, C, O) coordinates of the Ni(II) and Cu(II)-azurin gave a root-mean-square (r.m.s.) deviation of 0.16 Å. The final R value for 31,439 reflections between 8.0 and 2.05 Å resolution was 0.179. In the final model, r.m.s. deviations from standard geometry were 0.012 Å for bond lengths and 2.7° for bond angles.

A difference Fourier map computed with coefficients ($|F_{obs}|-|F_{calc}|$) and phases derived from the Cu(II)-azurin[10] shows clearly that the major changes occur near the metal binding site. Part of this electron density map in the metal binding region is shown in Fig. 3:14. Two lobes of positive and negative density (12σ) are seen above and below the plane defined by the ligand atoms N^{δ}_{His46}, N^{δ}_{His117}, S^{γ}_{Cys112} and the metal ion, similar to that encountered in the Zn(II)-azurin structure[29].

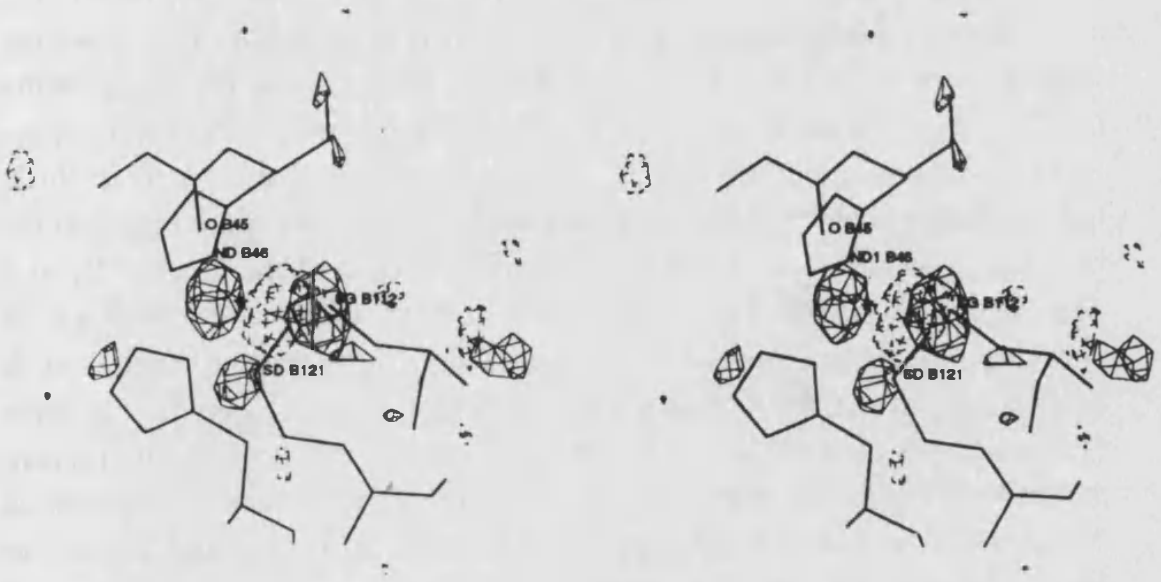

Fig. 3:14. Stereo plot of the difference Fourier map computed with coefficients $|F_{obs}|-|F_{calc}|$ and phases derived from the Cu(II)-azurin[10] in the metal binding region. Positive difference density (solid lines) and negative difference density (dashed lines).

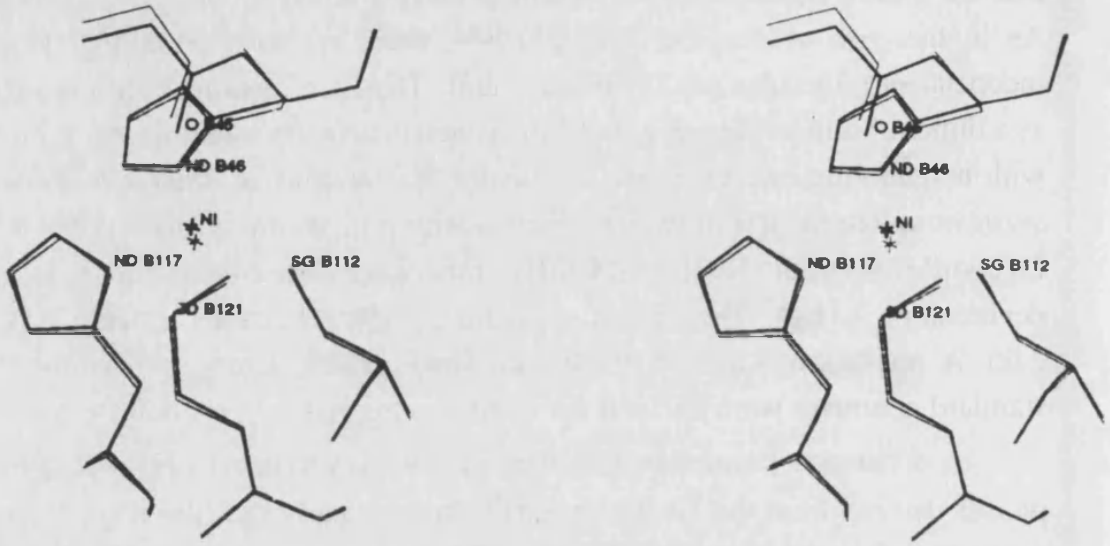

Fig. 3:15. Superimposition of the metal binding sites in Ni(II)-azurin (heavy lines) and Cu(II)-azurin (light lines). The major differences are the position of Ni(II) ion with regard to the N_2S trigonal plane (0.18 Å above this plane in Ni(II)-azurin and 0.05 Å underneath it in Cu(II)-azurin), and a 0.26 Å shift of the Gly45 O towards the Ni(II). These changes are accompanied with minor reorganizations in the rest of the ligands.

The movement of the nickel ion away from the S^{δ}_{Met121} towards the O_{Gly45} by 0.25 Å produces a rearrangement in the geometry of the nickel site. These changes are shown in Fig. 3:15. Nickel(II) is located 0.18 Å above the trigonal plane defined by the S^{γ}_{Cys112}–N^{δ}_{His46}–N^{δ}_{His117}, and the O_{Gly45} shifts 0.26 Å towards the metal ion. Such rearrangements produce a shortening in the Ni-O_{Gly45} distance to 2.46 Å (2.97 Å in Cu(II)-azurin). The other three Ni(II) ligands change relatively little: the His46 and His117 N_{δ} atoms are ligated to the nickel at distances of 2.23 and 2.22 Å, respectively and the Cys112 S_{γ} at a distance of 2.39 Å (Fig. 3:16). The S^{δ}_{Met121} to Ni(II) distance of 3.30 Å is 0.15 Å longer than the corresponding distance in the Cu(II)-protein[10] but 0.10 Å shorter than in the Zn(II)-azurin[29]. These shifts are just close to the error estimated from a Luzzati plot (0.2 Å). However, in the metal coordination sphere the errors in bonds and angle dimensions can be estimated from the differences between the four crystallographically independent molecules and amount to about 0.08 Å and 3°. So the structural differences between Cu(II)-azurin and Ni(II)-azurin are significant, but the observed changes in the metal-S^{δ}_{Met121} contact distances, relative to the Zn(II)-azurin, are not significant. Some relevant parameters for the nickel site geometry are listed in Table 3:5.

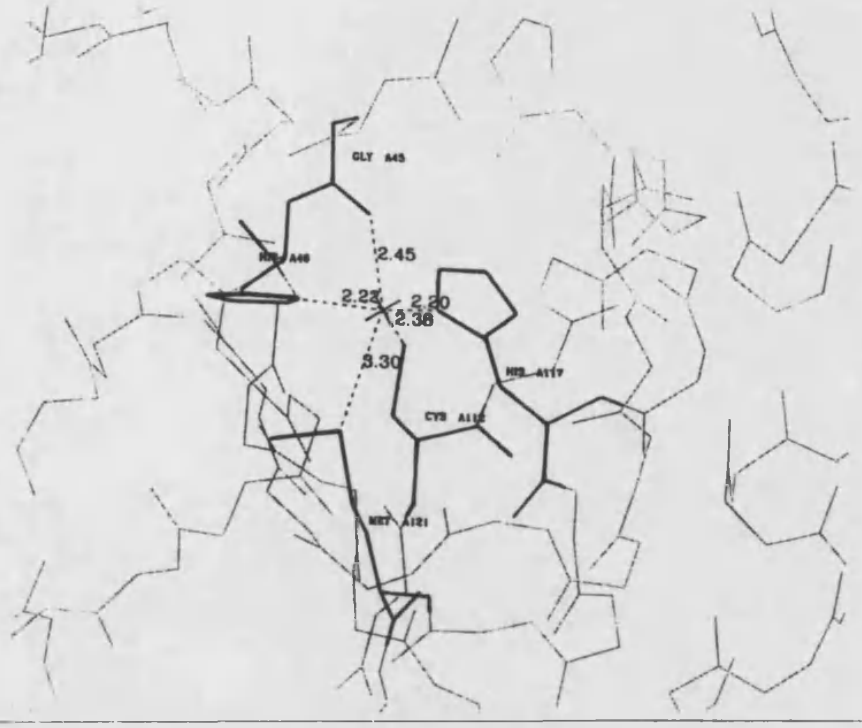

Fig. 3:16. The metal site geometry in Ni(II)-azurin. Ni(II) lays slightly above (0.18 Å) the trigonal plane defined by the S^{γ}_{Cys112}, the $N^{\delta 1}_{His46}$ and the $N^{\delta 1}_{His117}$. A close contact with the O_{Gly45} gives a coordination site which is best described as distorted tetrahedral.

Table 3:5. Structural data of the Ni(II)-azurin metal site. Deviations from the mean are in parenthesis.

Bond angles (°)		Ni(II)–ligand bond lengths (Å)	
Sγ112–Ni–Nδ46	127 (5)	Ni–Sγ112	2.39 (7)
Sγ112–Ni–Nδ117	123 (5)	Ni–Sδ121	3.30 (5)
Sγ112–Ni–Sδ121	100 (3)	Ni–Nδ46	2.23 (9)
Nδ46–Ni–Sδ121	69 (1)	Ni–Nδ117	2.22 (12)
Nδ46–Ni–Nδ117	108 (1)	Ni–O45	2.46 (6)
Sδ121–Ni–Nδ117	85 (1)		
O45–Ni–Sγ112	99 (1)		
O45–Ni–Sδ121	154 (1)		
O45–Ni–Nδ46	86 (1)		
O45–Ni–Nδ117	97 (4)		

DISCUSSION.

a) The structure of the Ni(II)–azurin metal site.

Comparison of the X-ray data for both Ni(II) and Cu(II) azurins (Table 3:6), reveals that the arrangement of ligands around the metal is more tetrahedral in the Ni(II) derivative than in the Cu(II)-azurin, as it had been proposed from a resonance Raman study[44]. The metal-O_{Gly45} distance in the Ni(II)-azurin (2.46 Å) is substantially shorter than in the Cu(II)-azurin (2.97 Å)[10], in agreement with the ^1H NMR data presented above, which indicate the existence of a metal-O_{Gly45} bond in the Ni(II)-protein[45]. The distance between the nickel ion and the Gly45 α protons (5.4 Å) is also shorter than in the native protein (5.8 Å)[10], explaining the short relaxation times observed for these protons (see Table 3:1). So, in the Ni(II)-azurin, the carbonyl oxygen of Gly45 forms a relatively strong bond with the nickel atom, in contrast to Cu(II)-azurin, where this axial interaction is very weak[10,46].

The metal coordination polyhedron in the Zn(II)-azurin has been described as distorted tetrahedral, since the Met121 S_δ to Zn(II) distance (3.40 Å) is too long for a covalent bond[29]. In the case of the Ni(II)-azurin this distance displays an intermediate value (3.30 Å) between those of Zn(II)-azurin and Cu(II)-azurin (3.15 Å). From electronic structure calculations it was found that the methionine sulfur atom binds covalently to the copper(II) ion with ~30% the strength of a standard ligand-copper bond[46]. Additionally, from the analysis of the hyperfine splitting constants of the axial methionine protons in Cu(II)-azurin and amicyanin, it is concluded that the unpaired electron density on this ligand is very low (1% on Met99 in Cu(II)-amicyanin)[47]. Thus, if any covalent interaction between the Ni(II) and Met121 S_δ is to be present it would be very weak. According to this, the metal site of Ni(II)-azurin would be better described as distorted tetrahedral, instead of trigonal bipyramidal. However, the results of the ^1H NMR study of Ni(II)-azurin would disagree with this conclusion, and we have to admit either a different structure of the metal site in solution or the existence of some orbital overlap between the metal and the ligand Met121 S_δ even at a 3.3 Å distance.

---

[44]Ferris, N.S., Woodruff, W.H., Tennet, D.L. & McMillin, D.R. (1979) *Biochem. Biophys. Res. Comm. 88*, 288.

[45]See section I of this chapter.

[46]Lowery, M.D. & Solomon, E.I. (1992) *Inorg. Chim. Acta 198-200*, 233.

[47]Kalverda, A.P., Salgado, J., Dennison, C. & Canters, G.W. (1995) *Biochemistry*, submitted.

b) Binding of different metals to azurin.

It is generally accepted that blue copper proteins in general, and azurin in particular, have a very rigid metal site which constrains the metal to adopt a particular coordination structure. This strained coordination has been explained by Malmström with an extension of the concept of the "rack mechanism"[48]: "the rack-induced bonding"[49]. The validity of this idea was proved when no significant structural differences were found in the metal site structure of oxidized and reduced native copper-azurin[10,50], and even in the apo-azurin[51]. It seems that the protein keeps the metal site frozen in a structure which is a compromise between those preferred by Cu(II) and Cu(I). Thus, a rapid electron transfer is favored because changes in the oxidation state of the copper are not charged with a large reorganization energy[49,50].

It is interesting to compare the binding of different metals to azurin in order to analyze to what extent this protein-controlled coordination is kept. First, we should notice that the protein exhibits a natural preference for copper as compared to other transition metals. Thus, the rate of metal uptake is much slower in the case of nickel (this is true also for cobalt)[52] than in the case of copper. However, it has been found that significant amounts of zinc-azurin are produced in the heterologous expression of azurin[53,29], and it seems to be necessary a homeostatic control, or the involvement of metal-specific carrier proteins, which mediate the correct metal uptake *in vivo*. Results presented here, as other from the literature[29,54], demonstrate that azurin can bind different metals without drastic conformational changes with regard to the native copper-protein. But the above discussed rigidity of the azurin metal site cannot prevent slight

---

[48]a) Lumry, R. & Eyring, H. (1954) *J. Phys. Chem. 58*, 110. b) Eyring, H., Lumry, R. & Spikes, J.D. (1954) in *The mechanism of enzyme action* (McElroy, W.D. & Glass, B., eds) p. 123, The Johns Hopkins Press, Baltimore.

[49]a) Malmström, B.G. (1965) in *Oxidases and related redox systems* (King, T.E., Mason, H.S. & Morrison, M., eds) vol. 1, p. 207, Wiley, New York. b) Gray, H.B. & Malmström, B.G. (1983) *Comments Inorg. Chem. 2*, 203. c) Malmstrom, B.G. (1994) *Eur. J. Biochem. 223*, 711.

[50]a) Baker, E.N. (1988) *J. Mol. Biol. 203*, 1071. b) Shepard, W.E.B., Anderson, B.F., Lewandoski, D.A., Norris, G.E. & Baker, E.N. (1990) *J. Am. Chem. Soc. 112*, 7817.

[51]a) Shepard, W.E.B., Kingston, R.L., Anderson, B.F. & Baker, E.N. (1993) *Acta Crystallogr. D49*, 331. b) Nar, H., Messerschmidt, A., Huber, R., van de Kamp, M. & Canters, G.W. (1992) *FEBS Lett. 306*, 119.

[52]See Chapter 2, section I.c.

[53]van de Kamp, Hali, F.C., Rosato, N., Finazzi-Agro, A. & Canters, G.W. (1990) *Biochim. Biophys. Acta 1019*, 283.

[54]Blackwell, K.A., Anderson, B.F. & Baker, E.N. (1994) *Acta Crystaallogr. D50*, 263.

reorganizations, including some distortions at the polipeptide backbone and side-chain atoms in the proximity of the coordination center, when a non-native metal is replacing the copper (see Table 3:6 and Fig. 3:15). The rack-induced bonding can guarantee a particular strained-coordination structure for the binding of the metal for which the protein is designed, but it seems to fail in doing it for the non-native metals, although they are forced to adopt a coordination very similar to that of the native one.

Table 3:6. Comparison of different azurin metal sites.

	Ni(II)-azurin	Zn(II)-azurin[a]	Cd(II)-azurin[b]	Cu(II)-azurin[c]
Bond lengths (Å)				
M-Sγ112	2.39	2.30	2.39	2.25
M-Sδ121	3.30	3.40	3.23	3.15
M-Nδ46	2.23	2.01	2.25	2.11
M-Nδ117	2.22	2.07	2.21	2.03
M-O45	2.46	2.32	2.76	2.97
Bond angles (°)				
Sγ112–M–Nδ46	127	128	132	133
Sγ112–M–Nδ117	123	121	121	123
Sγ112–M–Sδ121	100		102	110
Nδ46–M–Sδ121	69		73	78
Nδ46–M–Nδ117	108	110	106	103
Sδ121–M–Nδ117	85		90	87
O45–M–Sγ112	99	101	105	98
O45–M–Sδ121	154		150	149
O45–M–Nδ46	86	84	80	73
O45–M–Nδ117	97	98	86	89
Other distances (Å)				
O45···Sδ121	5.65	5.35	5.78	5.80
M···N_2S plane[d]	0.18	0.15	0.05	-0.05
O45···N_2S plane[d]	2.58	2.32	2.71	2.71
Sδ121···N_2S plane[d]	3.03	2.99	-3.06	3.07
N47···Sγ112	3.59	3.55	3.45	3.61
N114···Sγ112	3.49	3.46	3.45	3.44

[a] data from ref. 29.

[b] *Alcaligenes denitrificans* Cd(II)-azurin, data from ref. 54a.

[c] data from ref. 10.

[d] the sign indicates the relative position of the metal with regard to the N_2S plane: (+) means above the plane (towards the Gly45 residue) and (–) means below the plain (towards the Met121 residue).

We can try to rationalize the binding modes of different metal ions by considering their particular characteristics. For the Cd(II)-azurin, the slight approach of the metal to the Gly45 carbonyl, and its subsequent withdrawal from the Met121 S_δ, have been interpreted as being due to the preference of Cd(II) for oxygen rather than sulfur[54]. Additionally, the less tetrahedral character of the Cd(II)-azurin with regard to the Zn(II)-azurin is attributable to the larger size of Cd(II)[54]. Cu(II), Ni(II) and Zn(II) have the same charge and a very similar size, so it should be their different stereochemical preferences and their Lewis acidity which could explain a different (although slightly different) way of binding. Following this reasoning, it is not surprising that the main variations affect the axial ligands, considering the different donor properties between a harder oxygen and a softer sulfur. Being them in opposite axial positions, the metals will choose according to their preferences, having to deal at the same time with the structural restrictions imposed by the protein which are designed for a trigonal bipyramidal copper site. This may be the reason why, in the case of plastocyanin, the Cu(II) by Hg(II) substitution cause hardly any change[55]. In contrast to azurin, the equivalent Gly45 carbonyl O in plastocyanin is placed too far from the metal (0.5 Å further away than in copper-azurin) to be taken into consideration as a possible ligand[56,50a]. So plastocyanin has only a possible axial ligand and the normal Cu(II) coordination in the native protein coincide with the structural preferences of Hg(II) (tetrahedral). It seems that the Gly45 carbonyl axial ligand of azurin, although only coulombically interacting with the copper, may have more than a superfluous role, and this can make an important difference with regard to the rest of the blue copper proteins. The Gly45 axial ligand can be seen as an extra possibility for the geometrical flexibility of azurin, since the metal can find potential ligands on either side of the N_2S plane. This idea emphasizes also the role of the Met121 axial ligand in azurin as a sticking point placed opposite to Gly45. Both axial ligands could play an important role in the rack mechanism modulating the distortion of the metal site by keeping the metal more or less out of the N_2S plane, depending on the coordination preferences of the metal. As it has been suggested elsewhere[57], the position of the metal in a direction perpendicular to the plane defined by the three strong equatorial ligands depends on a subtle balance between its interaction with

---

[55]Church, W.B., Guss, J.M., Potter, J.J. & Freeman, H.C. (1986) *J.Biol. Chem. 261*, 234.

[56]Colman, P.M., Freeman, H.C., Guss, J.M., Murata, M., Norris, V.A., Ramshaw, J.A.M. & Venkatappa, M.P. (1978) *Nature* 272, 319.

[57]Canters, G.W., Kalverda, A.P. & Hoitink, C.W.G. (1993) in *Proc. Internatl. Confer. on the Chemistry of the Copper and Zinc Triads* (Welch, A.J. & Chapman, S.K. eds) p. 30, The Royal Society of Chemistry, Cambridge.

the weaker axial ligands. In the case of the copper protein, this can help to buffer the effects derived from a change in the oxidation state, making the metal site insensitive to the redox state of the copper.

III. Magnetic susceptibility of Ni(II)-azurin.

RESULTS AND DISCUSSION.

Fig. 3:17 displays the temperature dependence of the molar paramagnetic susceptibility χ_M and the effective magnetic moment μ_{eff} (inset) of *Pae* Ni(II)-azurin. A Curie law behavior is observed in the 120 K–30 K temperature range, leading to a constant μ_{eff} value of around 2.8 μ_B, in agreement with a S=1 as the ground state. Below 30 K, the deviation from the Curie law behavior indicates that the zero field splitting of the triplet state is operative. The effective magnetic moment decreases and reaches the value of 1.8 μ_B at 5 K. In an earlier investigation of Ni(II)-azurin at room temperature, a higher value for the effective magnetic moment was found. On these basis, it was proposed a distorted tetrahedral coordination[6]. However, the magnitude of the effective magnetic moment at room temperature does not always provide a reliable method for distinguishing between tetracoordinate and pentacoordinate Ni(II) geometries.

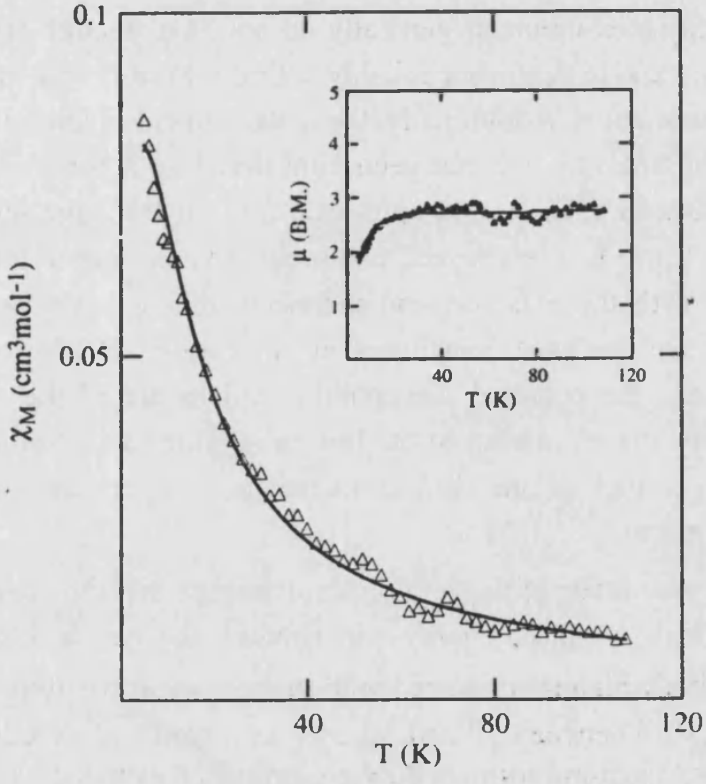

Fig. 3:17. Temperature dependence of the magnetic susceptibility for Ni(II)-azurin between 120 and 5 K. The inset shows the plot of magnetic moment *versus* temperature. Solid lines represent the best fitting of the data. Conditions are H_2O solvent, 3.6 mM protein, 20 mM CH_3COONH_4 and pH 7.5.

In order to analyze this magnetic behavior, the following spin hamiltonian is considered:

$$\aleph = D_S\left(\mathbf{S}_Z^2 - \frac{1}{3}\mathbf{S}^2\right) + \beta g_S \sum_{i=x,y,z}(\mathrm{H}_i\,\mathbf{S}_i) \qquad \text{Eq 3:1}$$

with D_S and g_S being the axial zero field splitting parameter and the isotropic g factor, respectively, associated with the spin state S. In the case of a triplet $S=1$ ground state, the molar susceptibility is derived according to the equation:

$$\chi_M = \left(\frac{2\,\mathrm{N}\beta^2}{3k\,\mathrm{T}}\right) g_S^2 \frac{e^{-D_S/k\mathrm{T}} + k\,\mathrm{T}/\mathrm{D_s}\left(1 - e^{-D_S/k\mathrm{T}}\right)}{1 + 2\,e^{-D_S/k\mathrm{T}}} \qquad \text{Eq 3:2}$$

The best fitting of the data to this theoretical curve gives the following values for the parameters defined above:

$$g_S = 1.98(0.1)$$

$$D_S = 17.7(1)\ \mathrm{cm}^{-1}$$

(the sign of D_S cannot be deduced from these magnetic measurements).

We have restricted the set of parameters to be fitted since magnetization or susceptibility measurements generally do not have enough resolution to provide g anisotropy and to determine reliably both the axial D and rhombic E zero field splitting parameters. Additionally, the metal content of the solution, known from independent analysis, has not been considered as a parameter, in order not to scale the data to the expected spin state $S=1$ in the large temperature range in which the Curie law is obeyed. Consequently, the metal concentration is only correlated with the g factor, and therefore, this g factor is the only variable parameter that we have considered in this region. On the other hand, at high temperatures, the obtained susceptibility values are of the order magnitude of experimental errors, owing to the low metal content of the samples and to the substantial scatter of the data at increasing temperature, when paramagnetic signal decrease.

The magnitude of the zero field splitting of distorted tetrahedral complexes depends strongly on the energy gap between the two levels of the $^3T_1$ parent ground state, which is connected with the spin-orbit coupling. It has been shown that D can vary between 30 and 50 cm^{-1} in a series of pseudo-tetrahedral nickel complexes of general formula NiN_2S_2, proposed as models for N–S coordinated

nickel enzymes and nickel substituted proteins[58]. Similar values of D have been reported from Ni(II) substituted rubredoxin with distorted tetrahedral centers[59]. In the case of distorted octahedral Ni(II) complexes, D is much smaller (D=5 cm^{-1} in the case of trans $Ni(py)_4Cl_2$).

In our study, it is evident that the observed magnetic behavior corresponds to the temperature dependence expected for an orbitally non degenerate ground state that implies low electronic symmetry. The D value that we propose lies between those corresponding to distorted tetrahedral and octahedral symmetry. Although a reduced magnetic moment or zero field splitting (due to second order spin-orbit coupling), compared to the expected ones in tetrahedral symmetry, can be also the result of ligand effects, that could give lower spin-orbit coupling constants[60], these results suggest that five-coordination is probably achieved in frozen Ni(II)-azurin solutions. The possibility of five-coordination in Ni(II)-azurin implies that Met121 can be a metal ligand, since the coordination of the Gly45 in this metalloderivative is clear from the X-ray structure and NMR data. However, as it is shown above, the Ni(II)–S^{δ}_{Met121} interaction must be very weak (see the previous sections).

[58]Frydendahl, H., Toftlund, H., Becher, J., Dutton, J.C., Murray, K.S., Taylor, L.F., Anderson, O.P. & Tieking, E.R.T. (1995) *Inorg. Chem. 34*, 4467, and references within.

[59]Kowal, A.T., Zambrano, I.C., Moura, I., Moura, J.J.G., LeGall, J. & Johnson, M.K. (1988) *Inorg. Chem.*, *27*, 1162.

[60]Gerloch, M. (1983) *Magnetism and ligand field analysis*, Cambridge University Press, Cambridge.

IV. Concluding remarks.

Ni(II) has proved to be a good probe to study blue copper sites by paramagnetic NMR. The corresponding spectra show relatively sharp signals which can be assigned and studied. A rough structural interpretation of the NMR data indicates that the metal center is very similar to the one present in Cu(II)-azurin since signals from the five possible metal ligands have been found to experience significant isotropic shifts. However, a detailed description of the metal site meet apparent contradictions, since the NMR data suggest a pentacoordinate metal site while the crystal structure demonstrates that the distance from the metal to one of the supposed ligands (Met121) is probably too large for a coordination bond.

The interpretation of the temperature dependence of the magnetic susceptibility seems to support a possible five-coordination. This apparent contradictions between the structural and the spectroscopic data are a demonstration that the structure alone is not enough to describe very distorted metal sites. Thus, from a pure structural point of view, the Ni(II)-azurin metal site can be described as tetrahedral, but this site exhibit also some spectroscopic characteristics of pentacoordination. An intermediate geometry between tetra and five-coordinate, such as a trigonal bipyramid with one axial ligand (Met121), moving away may reconcile apparent contradictory results. Since a metal site like this would preserve only a partial pentacoordinate character, manifested in some of its spectroscopic properties, we can define it as pseudo-pentacoordinate.

The results presented here, as well as other from the literature[29,54], demonstrates that, although the structural rigidity of azurin basically imposes the coordination, slight movements of the polipeptide structure surrounding the metal site are still possible. The existence of two axial ligands with very different donor properties also contributes to facilitate some adjustment of the metal binding site to the particular coordination preferences of the metal ion.

Chapter **4**

Characterization of Co(II)-azurin from *P. aeruginosa*[1].

Summary.

Substitution of copper by cobalt in blue copper proteins gives a paramagnetic metalloderivative suitable for paramagnetic NMR studies. A thorough analysis of the ^1H NMR spectrum of *Pseudomonas aeruginosa* Co(II)-azurin is presented here. Contact-shifted signals and other paramagnetic signals from protons placed up to about 10 Å around the metal center have been assigned. The results obtained permit the study of important dynamic processes, like the structural variations originated by the His35 ionization and the His117 $N_{\varepsilon 2}H$ proton exchange, and allow us to draw a feasible picture of the metal coordination site. Contact-shifted signals correspond to the same five residues which are found in the coordination sphere of the native Cu(II)-azurin, i.e. His46, His117, Cys112, Met121 and Gly45. The very weak copper ligand, Gly45, appears here as clearly coordinated to cobalt. In contrast, the Met121 signals indicate a weak, but still existent, contact interaction with the metal center. The EPR spectrum of Co(II)-azurin is also analyzed, and the results are consistent with a distorted tetrahedral metal site with the cobalt deviated from the N_2S plane towards the Gly45 O axial position and weakly interacting with the Met121 sulfur.

Because of its electronic properties, cobalt(II) is, together with nickel(II), one of the preferred metal ions to monitor the structure and reactivity of several metalloproteins. Cobalt is normally used as a substitute of zinc in Zn-metalloproteins[2], and also has been chosen to replace copper in blue copper

[1] Based on Moratal, J.M., Salgado, J., Donaire, A., Jiménez, H.R. & Castells, J. (1993) *Inorg. Chem. 32*, 3587; Salgado, J., Jiménez, H.R., Donaire, & Moratal, J.M. (1995) *Eur. J. Biochem. 231*, 358; and Jiménez, H.R., Salgado, J., Moratal, J.M. & Morgenstern-Badarau, I. (1995) *Inorg. Chem.*, submitted.

[2] a) Bertini, I & Luchinat, C. (1986) in *Zinc Enzymes* (I. Bertini, C. Luchinat, W. Maret, M. Zeppezauer, eds.) p. 27, Birkhäuser, Boston. b) Bertini, I. & Luchinat, C. (1984) in *Advances in Inorganic Biochemistry* (G.L. Eichorn & L.G. Marzilli, eds) p. 71, Elsevier, New York.

proteins, being of considerable utility to interpret their optical spectra[3]. However, few examples on the application of NMR to the study of Co(II)-substituted blue copper proteins can be found in the literature[1,4]. The present chapter is mainly devoted to these studies. The NMR characterization of Co(II)-azurin was performed in parallel with the study of Ni(II)-azurin[5], in an attempt to set the basis to extract structural information about the type 1 metal sites through these paramagnetic metalloderivatives. The spectroscopic data presented here are discussed in relation to the structural data available from different azurin metalloderivatives[5c,6].

---

c) Donaire, A., Salgado, J., Jiménez, H.R. & J.M. Moratal (1995) in *Nuclear Magnetic Resonance of Paramagnetic Macromolecules. C-Mathematical and Physicals Sciences series* (La Mar, G.N., ed.) vol. 457, p. 213, Kluwer Academic Publishers, Dordrecht.

3 a) McMillin, D.R., Rosemberg, R.C. & Gray, H.B. (1974) *Proc. Natl. Acad. Sci. USA 71*, 4760. b) Tennent, D.L. & McMillin, D.R. (1979) *J. Am. Chem. Soc. 101*, 2307.

4 a) Hill, H.A.O., Smith, B.E. & Storm, C.B. (1976) *Biochem. Biophys. Res. Commun. 70*, 783. b) Dahlin, S., Reinhammar, B. & Ångström, J. (1989) *Biochemistry 28*, 7224. c) Piccioli, M., Luchinat, C., Mizoguchi, T.J., Ramírez, B.E., Gray, H.B. & Richards, J.H. (1995) *Inorg. Chem. 34*, 737. d) Vila, A.J. (1994) *FEBS Letters* 355, 15.

5 a) Moratal, J.M., Salgado, J., Donaire, A., Jiménez, H.R. & Castells, J. (1993) *J. Chem. Soc., Chem. Commun.*, 110. b) Moratal, J.M., Salgado, J., Donaire, A., Jiménez, H.R., Castells, J. & Martínez-Ferrer, M.J. (1993) *Magn. Reson. Chem. 31*, 541. c) Moratal, J.M., Romero, A., Salgado, J., Perales-Alarcón, A. & Jiménez, H.R. (1995) *Eur. J. Biochem. 228*, 653. d) See Chapter 3.

6 a) Nar, H., Huber, R., Messerschmidt, A., Filippou, A.C., Barth, M., Jaquinod, M., van de Kamp, M. & Canters, G.W. (1992) *Eur. J. Biochem. 205*, 1123. b) Blackwell, K.A., Anderson, B.F. & Baker, E.N. (1994) *Acta Crystaallogr. D50*, 263.

I. Paramagnetic-NMR study.

RESULTS.

a) The ^1H NMR spectrum of Co(II)-azurin.

The ^1H NMR spectrum of Co(II)-azurin is shown in Fig. 4:1. It consists on 11 well resolved signals spread from 80 to -40 ppm (a-g, m-p), two of which are solvent exchangeable (a,b). Four additional very broad signals (around 2000 Hz), shifted downfield up till near 300 ppm, are also found (signals A-D, see Fig. 4:1 and Table 4:1 for details). Longitudinal relaxation times range from less than 0.2 ms in the case of signals C and D to 13.3 ms for signal c (Table 4:1). The temperature dependence of the paramagnetic shifts is shown in Fig. 4:2. All signals follow the Curie-like behavior. Extrapolated values at infinite temperature[7] (Fig. 4:2) indicate the existence of some dipolar contribution to the isotropic shifts, which is moderate for signals f and p but sizable for signals A and B.

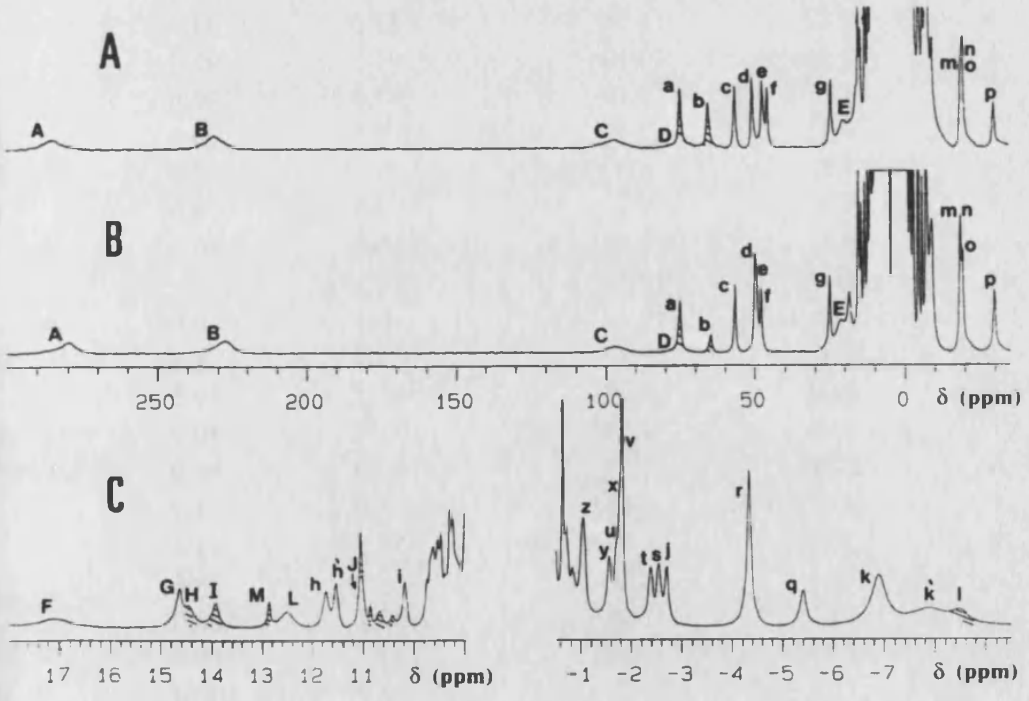

Fig. 4:1. 1D ^1H NMR spectra of 4 mM Co(II)-azurin. 300 MHz spectra at 37 °C and pH 4.5 (A) or pH 7.5 (B). Expansion of a 400 MHz spectrum (pH 7.5, 50 °C) to observe paramagnetic signals close to the diamagnetic region (C). Samples were H_2O unbuffered solution (A) or 20 mM NaH_2PO_4 (B, C). Shaded signals disappear in D_2O.

[7] See Chapter 2, section II.f.

Table 4:1. Characteristics of the principal signals of the ^{1}H NMR spectrum of Co(II)-azurin. Chemical shift data (δ) correspond to 37 °C. Longitudinal relaxation time (T_1) and line broadening ($\Delta\nu_{1/2}$) data were measured at 50 °C, because signals overlap less at these conditions. Data marked * are measured at pH 7.5.

	δ (ppm)		T_1 (ms)		
signal	pH 4.5	pH 7.5	pH 4.5	pH 7.5	$\Delta\nu_{1/2}$ (Hz)
A	285	280	0.6	0.6	2100
B	232	228	0.5	0.5	2100
C	97	97	< 0.2	< 0.2	2400
D	75	75	< 0.2	<0.2	2600
E	20.3	21.0	1.0	1.2	560
a	74.9	74.6	5.8	5.4	215
b	65.8	64.9	7.1	—	245
c	56.4	56.7	13.3	13.1	160
d	50.6	50.3	10.1	8.4	195
e	47.8	49.8	4.6	4.8	225
f	45.3	48.6	5.7	5.4	195
g	24.5	24.4	7.5	7.2	170
h	12.01	11.88	39.7	40.0	65 *
h'	11.82	11.94	32.0	33.9	40 *
i	10.51	10.19	91.2	92.0	40
j	-3.17	-3.10	41.0	40.6	35
k	-7.5	-7.3	5.5	5.5	170
k'	-7.3	-8.5		2.5	335 *
l	-9.1	-9.2	4.5	4.3	170
m	-18.5	-18.4	6.5	6.2	
n	-18.9	-18.4	6.1		
o	-19.1	-19.1	6.1	6.0	
p	-29.4	-29.4	4.7	4.4	210
q	-6.02	-5.78	21.1	19.6	70
r	-4.76	-4.58	31.6	30.7	40
s	-2.81	-2.73	85.0	85.0	35
t	-2.45	-2.63	78.0	73.7	30
u	-2.10	-2.07	53.5	54.2	
v	-2.04	-1.86		66	
x	-2.02	-1.98	132.1	128.0	
y	-1.83	-1.70	107.3	110.0	
z	-1.28	-1.19	98.2	100.4	
F	16.0	17.8	5.1	4.5	260 *
G	15.36	15.11	34.2	36.2	65
H	14.6	14.7	15.1	14.2	127
I		14.19		15.8	76 *
J	13.06	11.20	54.9	83.0	45
L	12.70	12.90	12.9	13.4	110
M	12.11	12.97	165.1	167.0	25 *

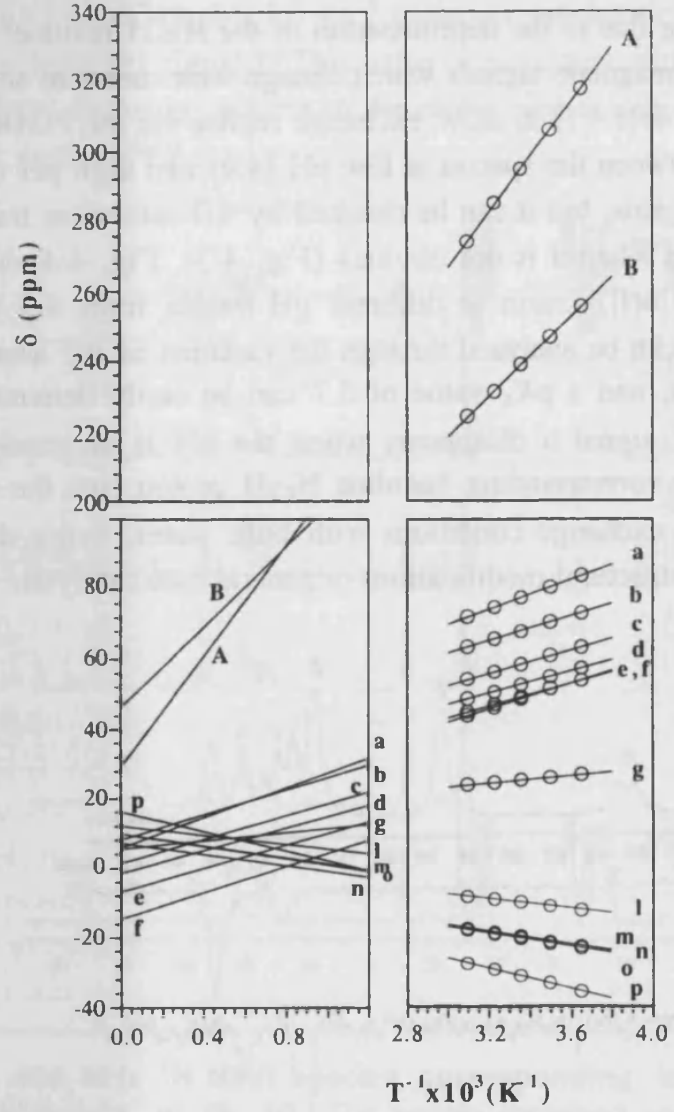

Fig. 4:2. Temperature dependence of the ^{1}H NMR hyperfine-shifted resonances of Co(II)-azurin at pH 4.5.

Close to the diamagnetic region, there is a significant number of paramagnetic signals whose T_1 values are longer in general, although some of them are still very fast relaxing (Fig. 4:1C). Among them, two methyl signals, k and k', are particularly characteristic, and the faster relaxing one (k') could correspond to the Met121 $C_\varepsilon H_3$ group. Looking under the diamagnetic envelope, with the help of the super-WEFT sequence[8], more paramagnetic signals can be observed (see the upper traces in Fig. 4:8D-H) whose relaxation times cannot be easily determined due to the overlaps.

8 Inubushi, T. & Becker, E.D. (1983) *J. Magn. Reson. 51*, 128.

As occurs in the case of the native protein, cobalt(II)-azurin undergoes a pH induced conformational transition. This exchange process has been interpreted as being due to the deprotonation of the His35 residue[9], and affects almost all the paramagnetic signals which change their chemical shifts by even some ppms (see Table 4:1) in slow exchange regime on the NMR time scale. The correlation between the spectra at low pH (4.4) and high pH (7.0) is clear for most of the signals, but it can be checked by 1D saturation transfer or 2D EXSY experiments when it is not obvious (Fig. 4:3). Fig. 4:4 shows the ^{1}H NMR spectra of Co(II)-azurin at different pH values from 4.5 to 7.5. The exchange process can be analyzed through the variation of the area of the less overlapped signals, and a pK_a value of 5.7 can be easily determined[10] (Fig. 4:5). Furthermore, signal b disappears when the pH is increased (Fig. 4:4) suggesting that the corresponding histidine $N_{\varepsilon 2}H$ proton (see the assignments below) enters fast exchange conditions with bulk water, being due to either slight pH induced structural modifications or general base catalysis.

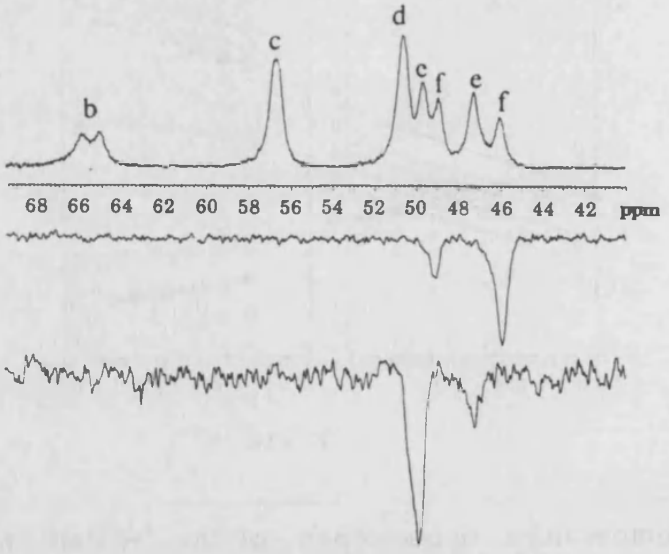

Fig. 4:3. 1D saturation-transfer difference spectra showing the correlation between signals e and f in the low and high-pH species of Co(II)-azurin. The experiments were performed at 50 °C and pH=5.7.

The exchange rate of the conformational equilibrium was calculated from steady-state saturation transfer experiments[10,11]. Irradiation of the low pH signal

[9] a) Farver, O., Blatt, Y. & Petch, I. (1982) *Biochemistry 21*, 3556. b) Corin, A.F., Bersohn, R. & Cole, P.E. (1983) *Biochemistry 22*, 2032. c) Adman, E.T., Canters, G.W., Hill, H.A.O. & Kitchen, N.A. (1982) *FEBS Lett. 143*, 287.

[10] See Chapter 2, section II.c.

[11] Sandström, J. (1982) *Dynamic NMR spectroscopy*, Academic Press, New York.

J at pH=pK_a (5.7) and 50 °C produces an 80% saturation of the high pH signal J (Fig. 4:8A), from which a 3.0 sec^{-1} exchange rate is calculated using a T_1 = 83 ms for the high pH signal J. This value is consistent with the rate constant for the acid-base exchange process of the native copper-azurin estimated by means of kinetic methods[9a,b].

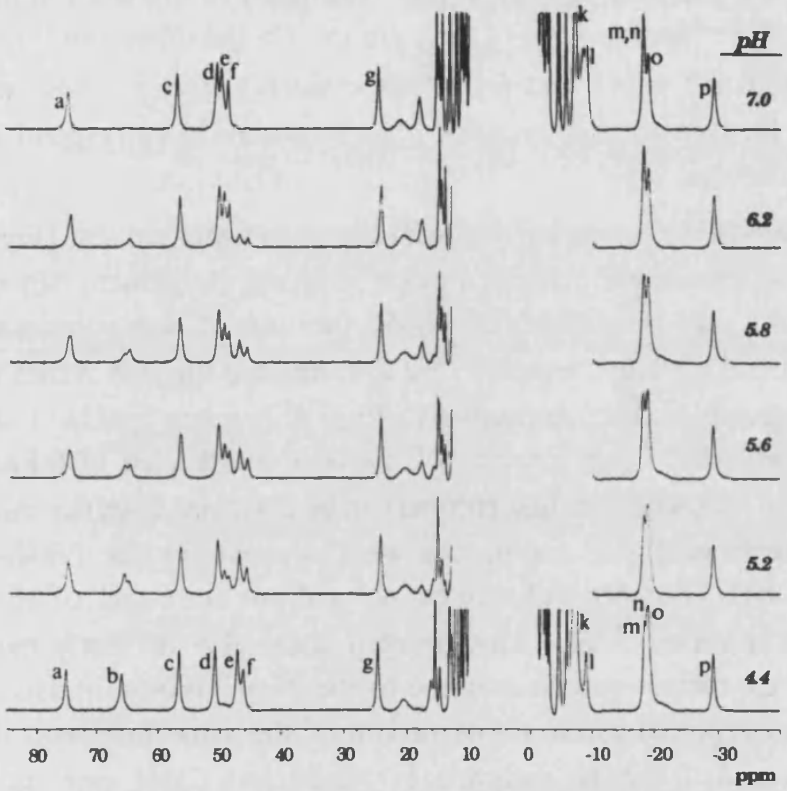

Fig. 4:4. 400 MHz ^{1}H NMR spectra corresponding to a pH titration of 2 mM Co(II)-azurin at 45 °C. The sample contained no-buffer to facilitate pH adjustments with minimum additions of base or acid (0.1 M NaOH or HCl, respectively). pH values were checked before and after recording every NMR spectrum.

Fig. 4:5. Variation of the relative area of signals from the NMR spectrum of Co(II)-azurin with the pH at 45 °C. Data from the same experiment as in Fig. 4:4. The overlapped signals e and f were taken together. The data can be fitted to a theoretical curve (Eq 2:9) giving a pK_a value of 5.7±0.1. The same result is obtained from the variation of signal J (not shown), correspon-ding to the His35 residue (see below the assignments of the signals).

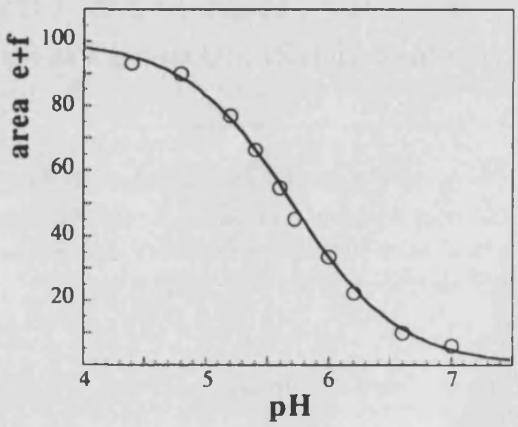

b) Assignment of the ^{1}H NMR signals.

Most of the hyperfine-shifted resonances can be assigned with the help of 2D NMR experiments. Fig. 4:6 represents the 400 MHz COSY spectrum of Co(II)-azurin in D_2O solvent. Five scalar connectivities numbered 1-5 allow us to distinguish three sets of signals: e,p (giving cross peak 1); f,n,o,j (2, 3); and g,h' and a signal at 9.28 ppm (4, 5). The pairs of signals e-p and f-o can be assigned as geminal protons of CH_2 groups. On the other hand, relaxation times of signals j and n (41 and 6 ms, respectively), giving cross peak 3, are too different for two geminal protons[12], so they should correspond to protons on adjacent carbons.

The NOESY spectrum of Co(II)-azurin in water solvent (Fig. 4:7) give us valuable information to achieve a more complete assignment, since we can now observe the two exchangeable $N_{\varepsilon 2}H$ protons of the coordinated histidines (signals a and b). Thus, signals c and d, connected through NOESY cross peaks with signals b and a, respectively (Fig. 4:7, cross peaks 1 and 2), must correspond to the $C_{\delta 2}H$ protons of the two coordinated histidines. A specific assignment of these histidine protons can be achieved from the inspection of the X-ray structure of *Pae* azurin. As we discussed for the Ni(II)-azurin[13], the $N_{\varepsilon 2}H$ of His117 is accessible to the solvent but the $N_{\varepsilon 2}H$ of His46 is hidden inside the molecule[14]. So, considering that signal b is clearly more labile than signal a, the former one is assigned to the $N_{\varepsilon 2}H$ proton of His117, and then signal c is assigned to the $C_{\delta 2}H$ proton of the same histidine. It follows that signals a and d can be assigned as $N_{\varepsilon 2}H$ and $C_{\delta 2}H$ protons of the other coordinated histidine, His46.

In agreement with the COSY experiment, the two pairs of protons, f-o and e-p, exhibit strong NOESY cross peaks as expected for geminal protons (Fig. 4:7, cross signals 3 and 4). We can also observe dipolar connectivities between signals n-j (5), f-j (6), and f-n (3'). This pattern suggests that signals f, j, n, and o belong to the same residue, and Met121 is the most reliable possibility. Consequently, considering the COSY data, signal j can be assigned as the α proton of Met121 and signal n as one of its β protons. It follows that the pair of

---

[12]The T_1 values can be interpreted in terms of ^{1}H-paramagnetic center distances according to the Solomon equation (Solomon, I. (1955) *Phys. Rev. 99*, 559). If these protons are on the same carbon, their distance to the metal ion can not be so different as to explain such a difference in their relaxation times.

[13]See Chapter 3, section I.

[14]Nar, H., Messerschmidt, A., Huber, R., van de Kamp, M. & Canters, G.W. (1991) *J. Mol. Biol. 221*, 765.

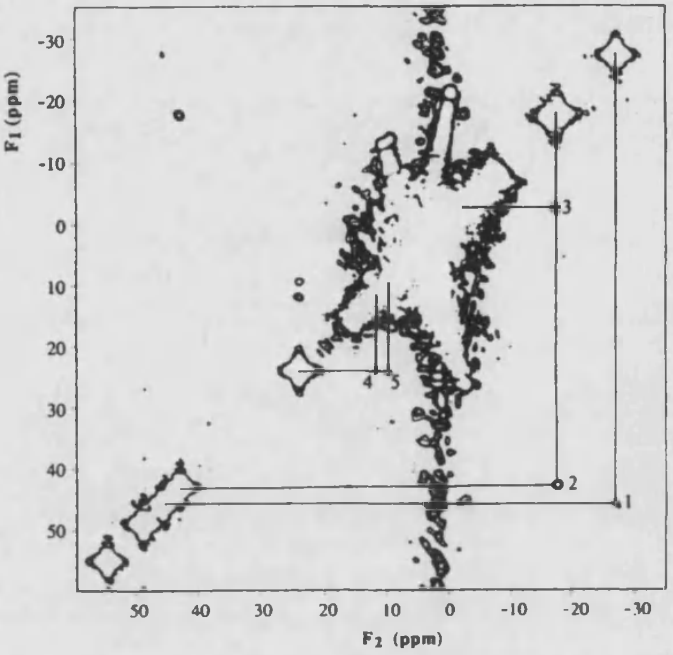

Fig. 4:6. 400 MHz magnitude COSY map of 8 mM Co(II)-azurin in D_2O (pH 4.5, 50 °C). 256 experiments, 8192 scans each, were recorded using a 70-kHz bandwidth in the *F*1 dimension over 1 K data points in the *F*2 dimension. Data were processed in each dimension using a 0°-shifted sine-bell-squared function.

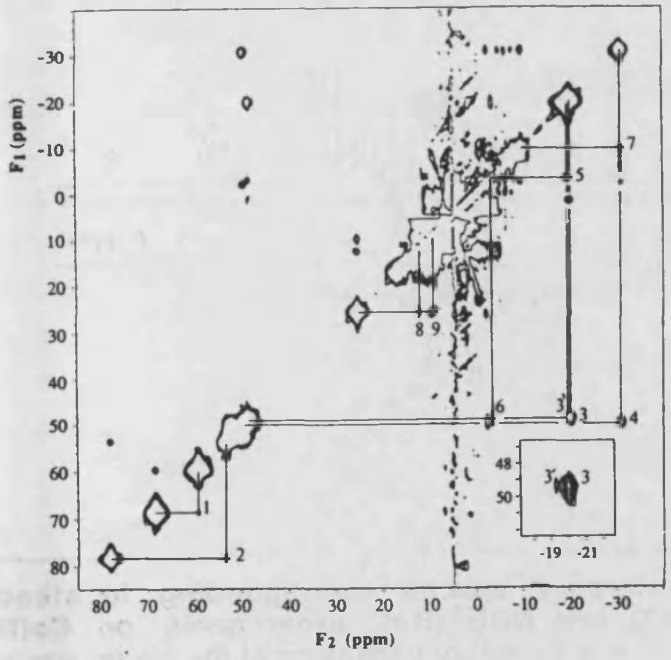

Fig. 4:7. Phase sensitive (TPPI) ^1H NOESY spectrum obtained at 400 MHz on a 4 mM sample of Co(II)-azurin in water (pH 4.5, 25 °C). This map was collected with a 6-ms mixing time, 256 *t*1 values (4096 scans each) over a 70-kHz bandwidth using 1 K data points in the *F*2 dimension. A 80°-shifted sine-bell-squared weighting function was applied in both dimensions. The inset shows cross peaks 3 and 3' of the same spectra processed to find more resolution.

signals f-o corresponds to the $C\gamma H_2$ protons of the same residue. The other β proton could correspond to signal m, but signals n and m are not resolved enough to allow the detection of any connectivity.

On the other hand, signal p gives a NOE connectivity with signal l (Fig. 4:7, cross peak 7). This later signal disappears in D_2O after several weeks, showing the characteristic behavior of an internal labile amide proton. This

pattern fits well with the assumption of signal l being the backbone amide proton of Gly-45 and so the pair of signals e-p being the two α protons of this coordinated residue.

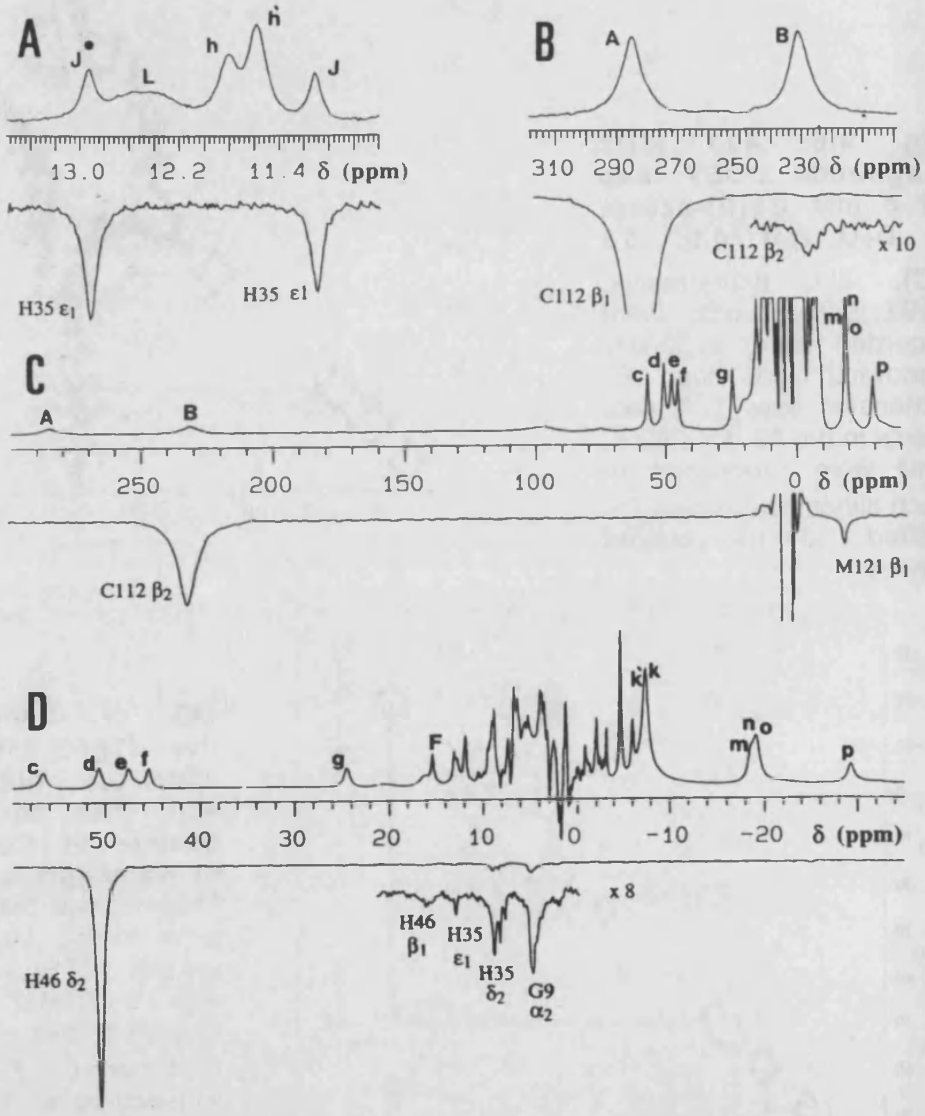

Fig. 4:8. Difference and reference spectra corresponding to steady state saturation transfer (A) and NOE (B-H) experiments on Co(II)-azurin. A) Difference trace spectrum obtained upon saturation of the low pH species signal J (marked *) at pH 5.7 and 50 °C. B) 300 MHz NOE difference spectrum obtained upon saturation of signal A (pH 4.5, 37 °C). To optimize the observation conditions a 40 kHz spectral width was used, centered between both signals A and B. The spectrum is the result of $1x10^6$ scans obtained at a repetition rate of 30 s^{-1}. C) 300 MHz NOE difference spectrum (pH 4.5, 37 °C) obtained from the irradiation of signal B. $3x10^5$ scans were acquired placing the carrier frequency in the center of the spectrum to have a better pulse effectiveness over all signals. D, H) 400 MHz NOE difference trace spectra obtained upon irradiation of signals d and g (pH 4.5, 37 °C). E-G) 400 MHz NOE experiments performed saturating signals F, k' and L (pH 7.5, 50 °C).

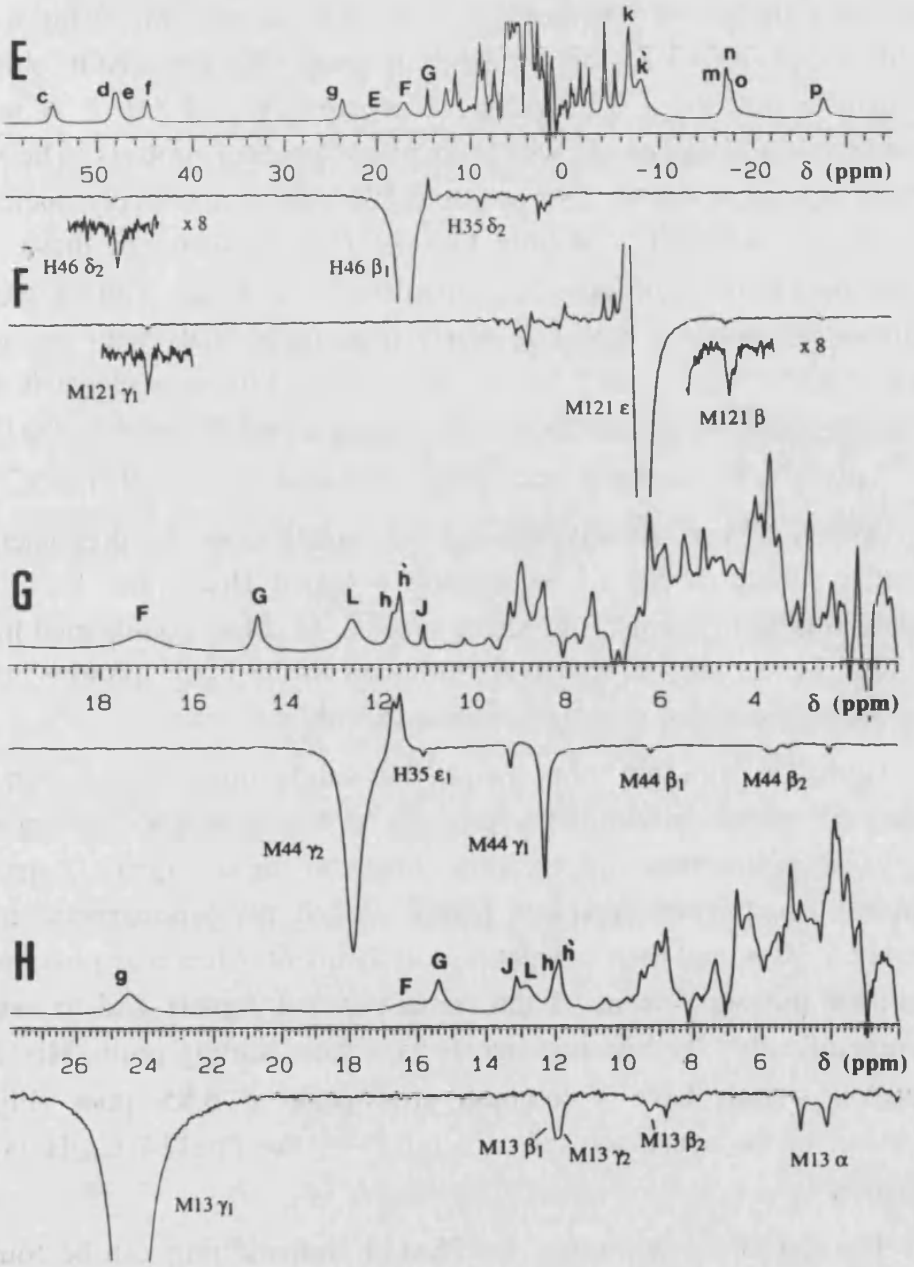

The broad signals A-E have to be protons very close to the metal center. According to the azurin crystal structure[5c,6a,14], protons in a 3.4-3.8 Å distance to the metal ion capable of presenting contact contribution to the isotropic shifts (that is, belonging to coordinated residues) are the two Cys112 β protons, the imidazole $C_{\varepsilon 1}H$ protons of the two coordinated histidines, the two β protons of His117 and the β_2 proton of His 46 (the His46 β_1 proton is around 4.6 Å from the metal and the signal corresponding to it should be sharper than signals A-E). Despite the very large relaxation rates of signals A and B, NOEs can be detected

from them. Signals A and B are connected to each other as viewed by 1D NOE experiments (Fig. 4:8B) performed in conditions optimized for their observation, i.e. placing the carrier frequency between both signals and using a very fast repetition rate and a very large number of scans. The small NOE obtained (0.7 %) corresponds, for a 0.5 ms relaxation time, to a 1.8±0.1 Å inter-proton distance, in good agreement with a couple of geminal protons. The very large shifts of signals A and B, 285 ppm and 232 ppm, respectively, indicate a very important contact shift, and only Cys112 $C_\beta H_2$ protons fit these conditions among the initial set of possible candidates. As already shown elsewhere[4c], irradiation of signal B gives a clearly observable NOE with the overlapped signals n and o (Fig. 4:8C). Since such a NOE difference signal is not found irradiating signal A, we can specifically assign signals B and A to the Cys112 β2 and β1 protons, respectively, according to the azurin crystal structure[5c,6a].

Although no NOE was obtained for signals C and D, their chemical shift pattern is similar to that of the already assigned His46 and His117 protons (signals a-d) and typical of imidazole protons of cobalt-coordinated histidines[2]. So these signals can be tentatively assigned to the $C_{\varepsilon 1}H$ protons of the two coordinated histidines, as suggested elsewhere[4c].

Going on from this point, we can find neighboring protons even under the diamagnetic envelope with the help of 1D NOE and NOESY spectra and using the available structural information. Most of these signals correspond to additional paramagnetic residues placed around the paramagnetic metal in a radius of 5-10 Å, and their independent assignment, when it is possible, is used to confirm the assignment of the contact-shifted signals and to assign them stereospecifically. The histidine signals are a clear starting point. His117 δ_2 and ε_2 proton signals have a common cross-peak at 6.85 ppm (Fig. 4:9A). According to the azurin crystal structure[5c,6a], the Phe114 $C_{\delta 2}H$ is the only possibility.

The rest of the protons of the Phe114 aromatic ring can be found in the aromatic part of a TOCSY spectrum (Fig. 4:13B). Additionally, His117 $C_{\delta 2}H$ gives NOESY cross-peaks with the exchangeable signal H and with a signal at 5.53 ppm (Fig. 4:9A), which can only be assigned to the NH and $C_\alpha H$ protons of His117. Signal H is in turn connected with an NH proton whose TOCSY pattern corresponds to a glycine spin system (Fig. 4:10C,E) and gives a strong NOESY connectivity with the α proton of a proline residue. These two residues have to be Gly116 and Pro115, respectively.

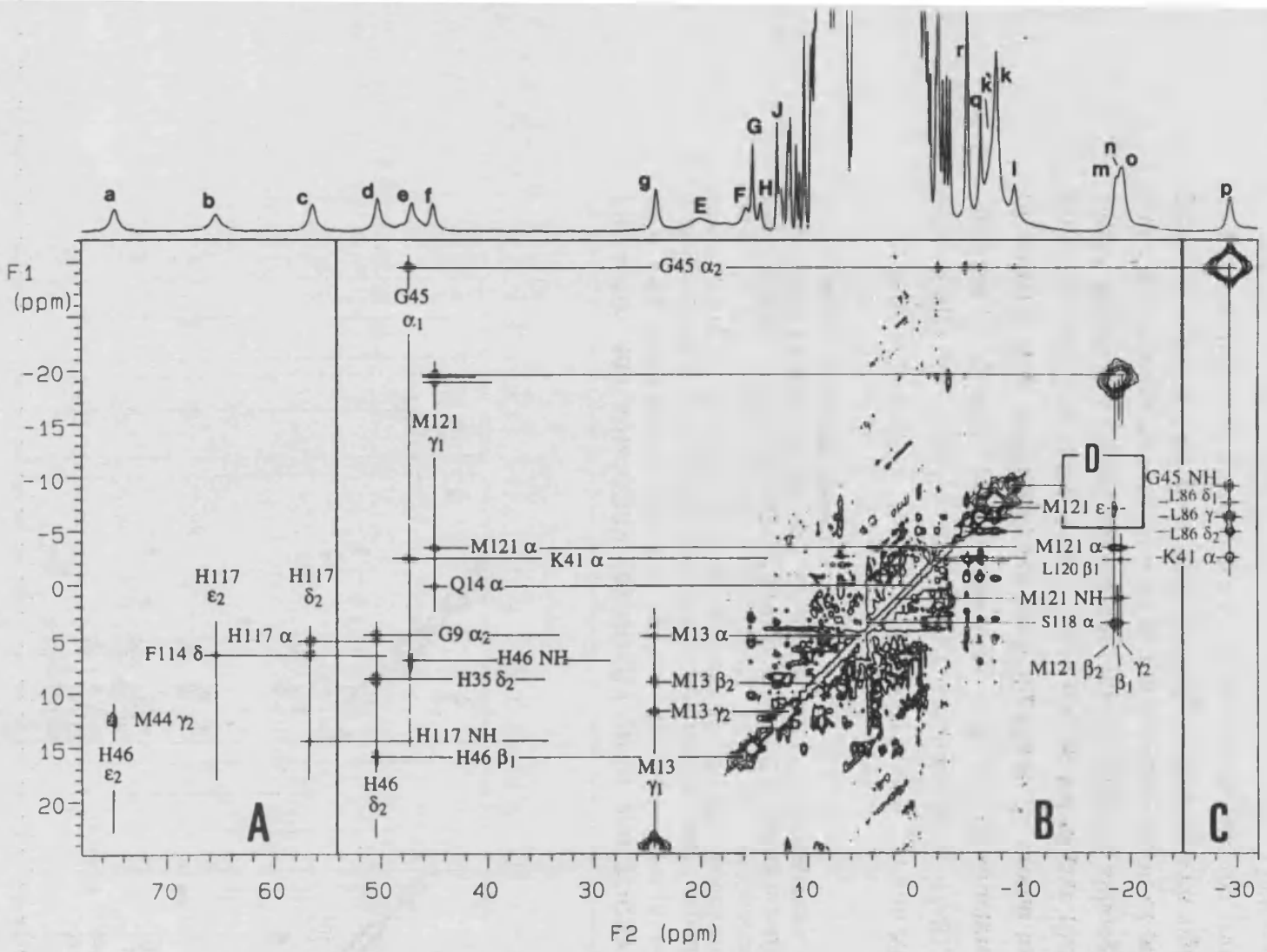

Fig. 4:9. 400 MHz NOESY spectra of 8 mM Co(II)-azurin at pH 4.5 and 37 °C in H_2O (A, C) or D_2O solvent (B, D). Panels A and B are 10 ms mixing time and 10 sec^{-1} repetition rate NOESY spectra (512 increments 2048 data points and 512 scans each). Panel C corresponds to a 6 ms mixing time and 20 sec^{-1} repetition rate NOESY spectrum (512 increments 1024 data points and 1024 scans each). Panel D is part of a 4 ms mixing time and 50 s^{-1} repetition rate NOESY where 256 t1 points, 4096 scans each, were acquired.

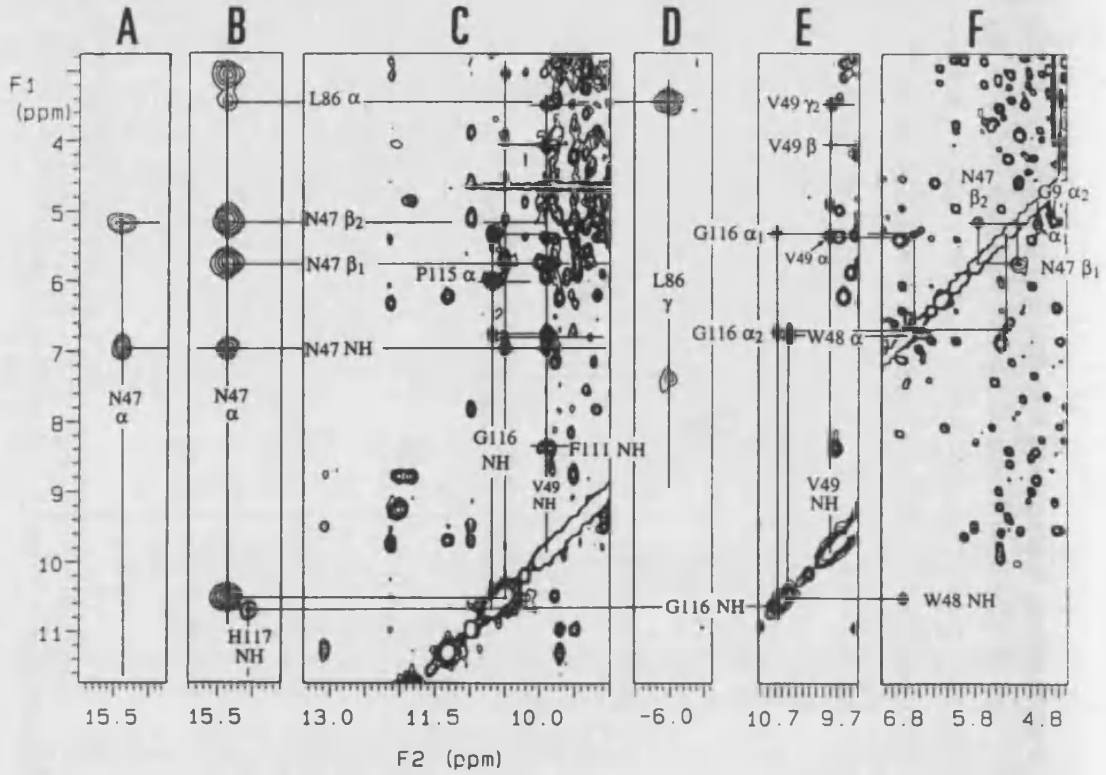

Fig. 4:10. 400 MHz COSY (A) NOESY (B-D) and TOCSY (E-F) spectra of 4 mM Co(II)-azurin (pH 4.5, 37 °C). The COSY map (A) was obtained upon transformation of a 300 x 200 data point matrix from a 5 sec^{-1} repetition rate MCOSY. Panels B and C are portions of a 10 ms mixing time NOESY spectrum (12 kHz spectral width, 512 increments 1024 points each). Panel D corresponds to the Fourier transformation of a 30 ms mixing time NOESY. TOCSY spectra are 40 (E) and 20 (F) ms mixing time. Marked are the N47, G116, G9 and V49 spin systems and some of their connectivities with other residues.

With regard to the His46 residue, its δ_2 proton gives an NOE with signal F (Fig. 4:8D) also found in the NOESY spectrum (Fig. 4:9B). We assign this signal as the His46 β_1 proton, according to the crystal structure[5c,6a]. Irradiation of signal F (Fig. 4:8E) does not allow the His46 β2 proton to be found. This proton is very close to the metal[5c,6a] and is expected to give rise to a very broad signal. Signal E is a good candidate for this assignment, although both signals E and F are too close to each other to permit the observation of any NOE between them. A signal at 4.96 ppm, also dipolarly connected with signal d (Fig. 4:8D and Fig. 4:9B), is assigned to the Gly9 α_2 proton, and the corresponding Gly9 α_1 proton is found in a TOCSY spectrum (Fig. 4:10F). On the other hand, from the His46 ε_2 proton (signal a), we find the Met44 residue. The observed NOE between signals a and L (Fig. 4:9A) permits the assignment of signal L to the Met44 γ_2 proton according to the crystal structure[5c,6a]. The Met44 $C_{\gamma 1}H$ signal

is found through a COSY cross-peak with signal L (Fig. 4:11A) confirmed with a strong NOE (Fig. 4:8G and Fig. 4:11B,C). This last signal is in turn dipolarly connected with signals at 6.78 and 3.82 ppm (Fig. 4:11B,C). Although no other contact connectivity is found affecting these signals, we assign them to the Met44 β protons, since they are also connected with the His35 signals (Fig. 4:11B,C ; see below).

Signal p, one of the two Gly45 α protons, gives clear NOESY cross-peaks with signals l, k, q and r (Fig. 4:9C). Signal l has been assigned above to the amide proton of Gly45. Signals k and r are two methyl signals, and they are dipolarly connected to each other and with signal q (Fig. 4:12C). A TOCSY spectrum allows the complete spin system of a leucine to be observed (Fig. 4:12D,G). Only Leu86 is close enough to the metal center to have a paramagnetic methyl signal[5c,6a] and this permits the assignment of signal k to the Leu86 $C_{\delta 1}H_3$ methyl group, and consequently, the rest of the Leu86 signals in agreement with a similar interpretation[4c] (Fig. 4:12, Table 4:2).

Signals k and k' overlap, but they are clearly resolved as two methyl signals at pH 7.5 and 50 °C (Fig. 4:1C). Methyl signal k' is much broader and its T_1 shorter than signal k, which means that the k' methyl group is closer to the metal than the k methyl group (Leu86 $C_{\delta 1}H_3$). Only the Met121 $C_{\varepsilon}H_3$ group meets this condition. This assumption is confirmed through the irradiation of signal k', which gives an NOE with signal f and the overlapped signals m and n (Fig. 4:8F) previously assigned to the β protons of Met121. A weak NOESY cross-peak between signals m and k' is also observed (Fig. 4:9D). Additionally, signal j, assigned above to the Met121 α proton of this residue, gives a TOCSY cross-peak with a signal at 1.7 ppm (Fig. 4:12F), which can only correspond to the amide NH proton of the same residue, and is also connected through NOE with the signals n and o (Fig. 4:9B). Although signals m, n and o always overlap, we can try to assign them stereospecifically. As shown above, signal m is contact coupled with the Met121 α signal (signal j) and is assigned to one of the Met121 β protons. Analogously, signals f and o were connected through a COSY cross-peak being assigned to the couple of Met121 γ protons. As it is shown in Fig. 4:9 and Fig. 4:8F, signal k' gives a stronger NOE with signals f and m than with signals o and n. On the other hand, the Met121 NH signal gives NOESY cross-peaks only with signals n and o. This scheme is compatible with the assignment of signals f, o, n and m to the γ_1, γ_2, β_1 and β_2 Met121 protons, respectively, considering the azurin structure[5c,6a].

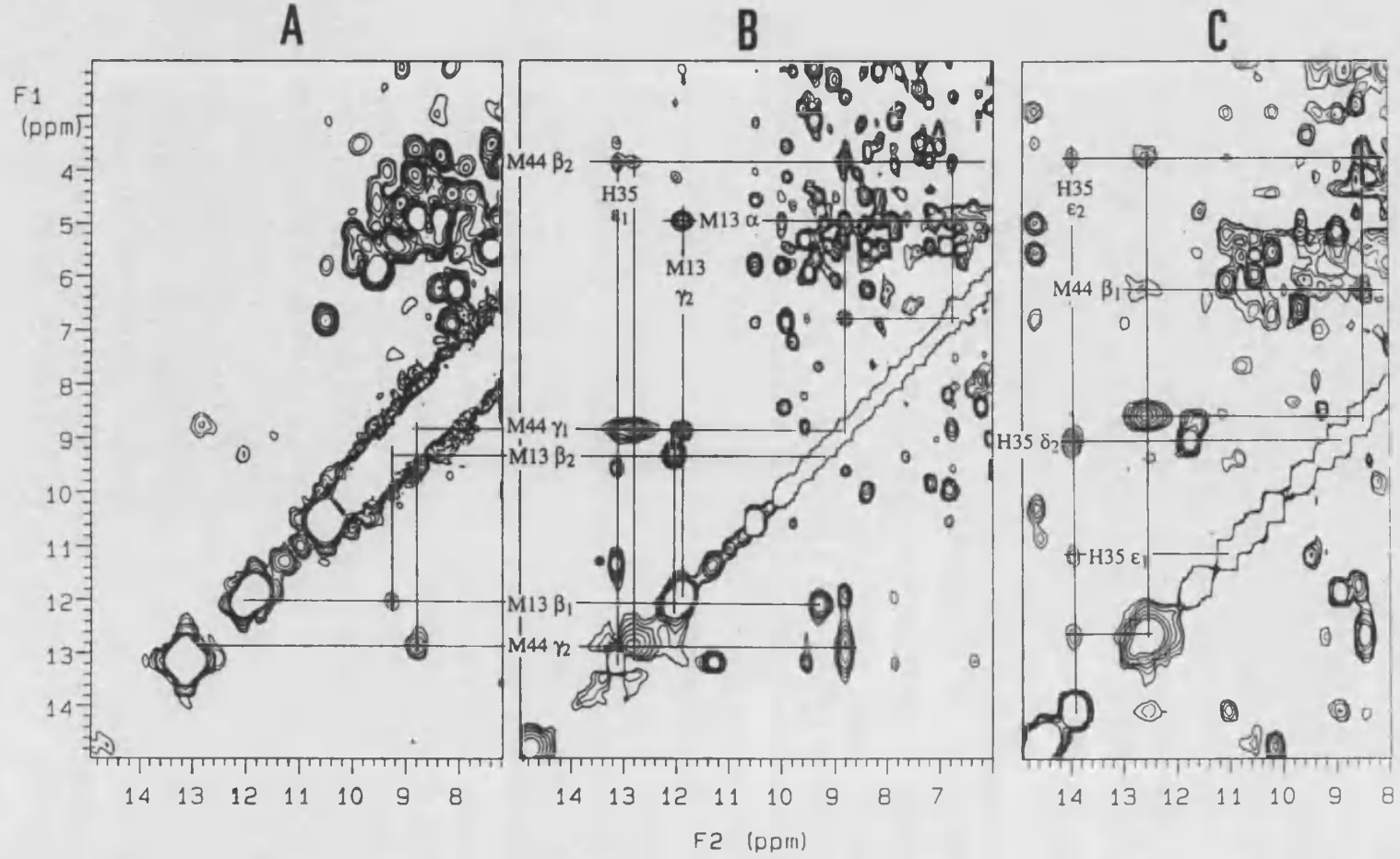

Fig. 4:11. COSY (A) and NOESY (B, C) maps obtained at 400 MHz from Co(II)-azurin in D_2O solvent, pH 4.5 at 37 °C (A, B) or pH 7.8, H_2O solvent at 50 °C (C). Spectra show Met13 and Met44 signals and some connectivities between the Met44 and His35 residues. Panel A is part of the same COSY spectrum as panel A in Fig. 4:10. Both NOESY spectra are 10 ms mixing time and they were acquired and processed as in Fig. 4:10 B and C. Cross-signal marked * is an exchange signal correlating the two pH dependent positions of the His35 ε_1 proton, due to the presence of residual deprotonated species at pH 4.5.

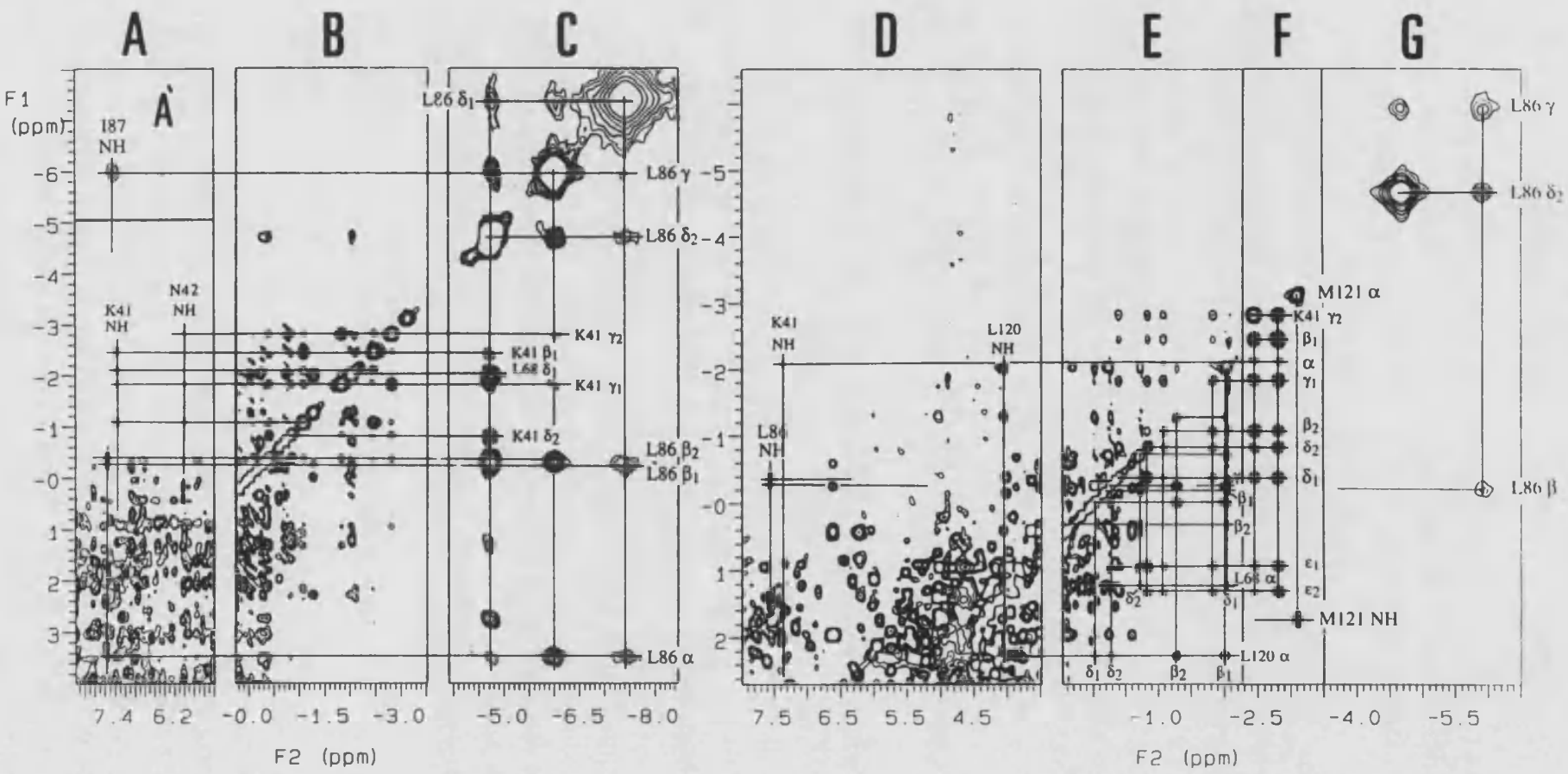

Fig. 4:12. Portions of NOESY (A-C, A') and TOCSY (D-G) spectra from Co(II)-azurin at pH 4.5, H_2O solvent and 37 °C. The spin systems corresponding to leucines 86, 68 and 120, Lys 41 and part of Met121 are observed in 20 ms (G), 40 ms (D, F) and 70 ms (E) mixing time TOCSY maps. Dipolar connectivities between some of these residues are detected in 10 ms (C and A') and 30 ms (A, B) mixing time NOESY spectra.

Finally, as mentioned above, signal g is contact coupled with signal h' and a signal at 9.28 ppm (Fig. 4:6). In Fig. 4:11A, a COSY cross-peak between the last signal and signal h is shown, and a dipolar connection between signal g and both signals h and h' is found in Fig. 4:8H. Additionally, signal g has a short relaxation time which corresponds to a distance of around 5 Å from the metal center, and signal at 9.28 ppm is also broad as judged from its NOESY cross-signal with signal h. In contrast, signals h and h' are considerably sharper. The Met13 is the only residue around the metal site compatible with this scheme apart from the already assigned Met44.

c) Additional assignments.

Examining Table 4:1, we find that signal J considerably change its relaxation time and chemical shift with the pH. This signal is dipolarly connected with the exchangeable signal I (Fig. 4:11C), which is only present at pH higher than 6 indicating that the corresponding proton is in fast exchange regime at low pH. On the other hand, signal I gives a NOESY cross-peak with signal at 8.98 ppm (Fig. 4:11C), which in turn is connected with the His46 δ_2 and β_1 proton signals (Fig. 4:9B and Fig. 4:8E). Since the δ_2 protons of both His35 and His46 are very close to each other[5c,6a], we assign signals J, I and the signal at 8.98 ppm to the His35 ε_1, ε_2 and δ_2 imidazole protons, respectively. The assignment of the His35 proton signals nicely agrees with the assignment of the Met44 residue since protons from both residues are dipolarly connected (Fig. 4:11B,C) as expected from the crystal structure[5c,6a].

In the TOCSY spectra of Fig. 4:12, two Leu and a Lys spin systems involving signals s-z can be drawn. Some signals of the Lys spin system are dipolarly connected with Leu86 and Gly45 signals (Fig. 4:12C and Fig. 4:9C), so, according to the azurin structure[5c,6a], it can be assigned to the Lys41 residue, as already reported elsewhere[4c]. The assignment of Leu86 and Lys41 gives additional support to the previous assignment of the Gly45 signals and allows the specific assignment of signals e and p to the $\alpha 1$ and $\alpha 2$ protons of this residue. The Gly45 NH proton is close to both Gly45 α protons while the His46 NH proton is only close to the Gly45 $\alpha 1$ proton[5c,6a]. Thus, a slowly exchangeable signal at 6.84 ppm, which gives a NOESY cross-peak with signal e (Fig. 4:9B) is assigned to the His46 NH proton.

On the other hand, the existence of NOESY connectivities between signal v and the Leu86 $C_{\delta 2}H3$ signal (Fig. 4:12C), and between signal x and the Met121 γ_2 signal (Fig. 4:9B), permits assigning the Leu68 and Leu120 residues.

Further analysis of the NMR spectra permit the assignment of other residues like Ile87 (Table 4:2).

In the aromatic zone of the spectrum we can clearly localize Trp48, the only tryptophan residue in the *P. aeruginosa* azurin sequence (Fig. 4:13). The rest of the aromatic spin systems can also be found (Fig. 4:13, Table 4:2). Those which are far from the metal center, like Phe97, Phe29 and Tyr108, present

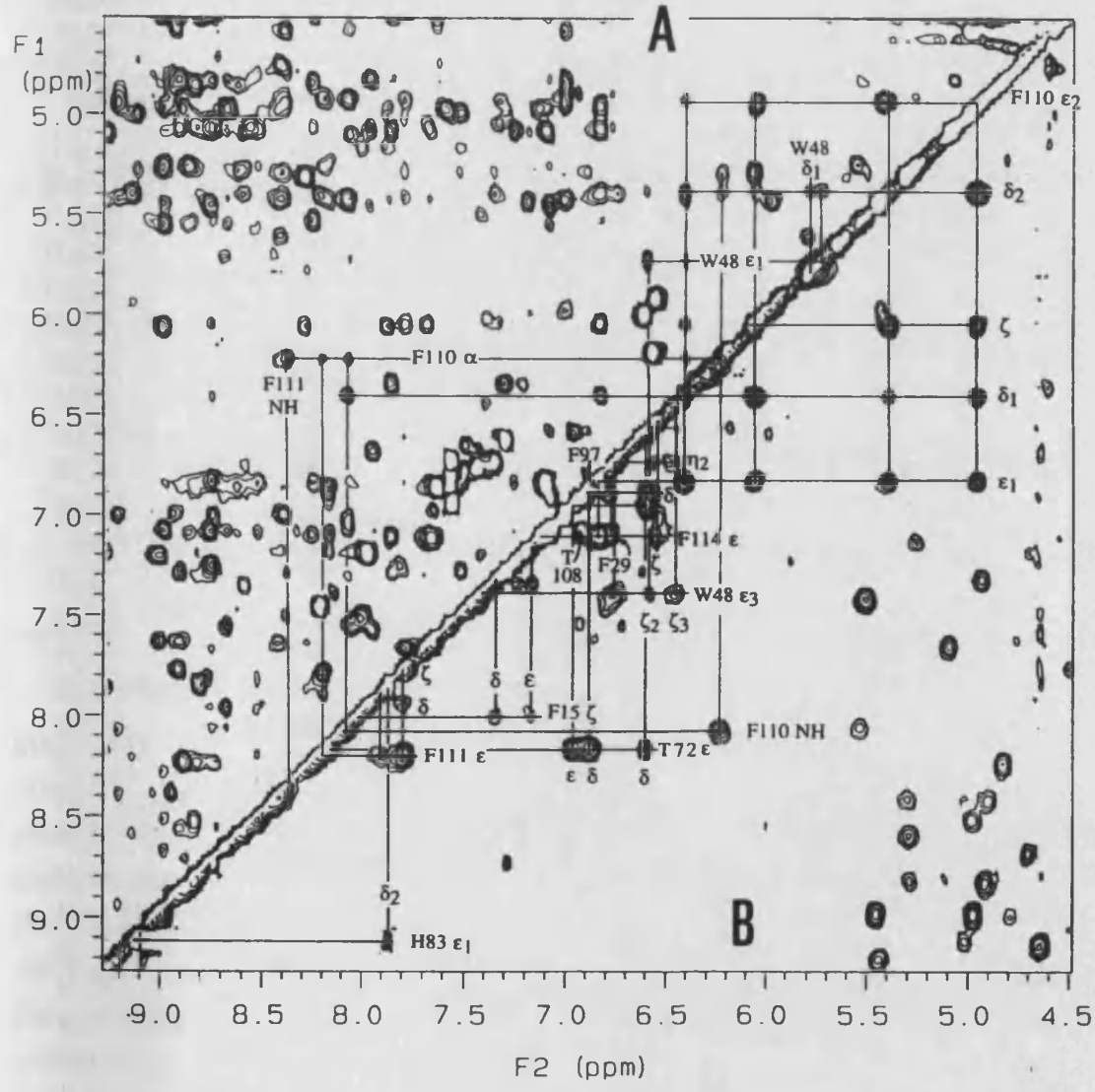

Fig. 4:13. Aromatic zone of the 400 MHz ^{1}H NMR spectrum of 4 mM Co(II)-azurin at pH 4.5 and 37 °C. The upper part (A) corresponding to a 200 ms mixing time NOESY map, shows the connectivities between the Phe110, Phe111 and Trp48 residues. A 50 ms spin lock TOCSY of the same region of the spectrum is shown down the diagonal (B). Marked are all the aromatic spin systems.

Table 4:2. Assignments of signals from the ^{1}H NMR spectrum of Co(II)-azurin at pH 4.5 and 37 °C. In the left are residues presenting all or some signals clearly resolved out of the protein envelope. These signals are named with letters as in Fig. 4:1 and Table 4:1. Signal marked * corresponds to pH 7.5.

signal	δ (ppm)	assignment	δ (ppm)	assignment
A	285	Cys112 $C_{\beta 1}H$	10.69	Gly116 NH
B	232	$C_{\beta 2}H$	5.35	$C_{\alpha 1}H$
	6.8	His46 NH	6.78	$C_{\alpha 2}H$
a	74.9	$N_{\varepsilon 2}H$	6.03	Pro115 $C_\alpha H$
d	50.6	$C_{\delta 2}H$	2.25	$C_\beta H$
F	16.0	$C_{\beta 1}H$	1.34	$C_\gamma H$
E	20.3	$C_{\beta 2}H$	2.79	$C_\delta H$
C	97	His46/117 $C_{\varepsilon 1}H$	8.04	Phe110 NH
D	75	His117/46 $C_{\varepsilon 1}H$	6.20	$C_\alpha H$
H	14.6	His117 NH	1.38	$C_{\beta 1}H$
	5.5	$C_\alpha H$	1.84	$C_{\beta 2}H$
b	65.8	$N_{\varepsilon 2}H$	6.38	$C_{\delta 1}H$
c	56.4	$C_{\delta 2}H$	5.35	$C_{\delta 2}H$
l	-9.1	Gly45 NH	6.80	$C_{\varepsilon 1}H$
e	47.8	$C_{\alpha 1}H$	4.92	$C_{\varepsilon 2}H$
p	-29.4	$C_{\alpha 2}H$	6.02	$C_\zeta H$
	1.7	Met121 NH	6.85	Phe114 $C_\delta H$
j	-3.2	$C_\alpha H$	7.07	$C_\varepsilon H$
m	-18.5	$C_{\beta 2}H$	6.51	$C_\zeta H$
n	-18.9	$C_{\beta 1}H$	8.36	Phe111 NH
f	45.3	$C_{\gamma 1}H$	7.89	$C_\delta H$
o	-19.1	$C_{\gamma 2}H$	8.17	$C_\varepsilon H$
k'	-7.3	$C_\varepsilon H_3$	7.77	$C_\zeta H$
	4.9	Met13 $C_\alpha H$	6.85	Phe97 $C_\delta H$
h	12.0	$C_{\beta 1}H$	6.87	$C_\varepsilon H$
	9.3	$C_{\beta 2}H$	6.76	$C_\zeta H$
g	24.5	$C_{\gamma 1}H$	6.74	Phe29 $C_\delta H$
h'	11.8	$C_{\gamma 2}H$	7.07	$C_\varepsilon H$
J	13.06	His35 $C_{\varepsilon 1}H$	6.88	$C_\zeta H$
I	14.19	$N_{\varepsilon 2}H$*	7.30	Phe15 $C_\delta H$
	8.90	$C_{\delta 2}H$	7.13	$C_\varepsilon H$
L	12.70	Met44 $C_{\gamma 2}H$	7.98	$C_\zeta H$
	8.79	$C_{\gamma 1}H$	6.85	Tyr72 $C_\delta H$
	6.72	$C_{\beta 1}H$	6.93	$C_\delta H$
	3.72	$C_{\beta 2}H$	6.57	$C_\varepsilon H$
	6.98	Asn47 NH	8.14	$C\varepsilon H$
G	15.36	$C_\alpha H$	7.05	Tyr108 $C_\delta H$
	5.72	$C_{\beta 1}H$	6.90	$C_\varepsilon H$
	5.16	$C_{\beta 2}H$	10.52	Trp48 NH
	7.57	Leu86 NH	6.83	$C_\alpha H$
	3.45	$C_\alpha H$	4.55	$C_{\beta 1}H$

	-0.27		$C_{\beta 1}H$	3.94	$C_{\beta 2}H$
	-0.37		$C_{\beta 2}H$	5.76	$C_{\delta 1}H$
q	-6.02		$C_{\gamma}H$	5.70	$C_{\varepsilon 1}H$
k	-7.50		$C_{\delta 1}H_3$	7.36	$C_{\varepsilon 3}H$
r	-4.76		$C_{\delta 2}H_3$	6.71	$C_{\eta 2}H$
	7.36	Lys41	NH	6.52	$C_{\zeta 2}H$
u	-2.10		$C_{\alpha}H$	6.41	$C_{\zeta 3}H$
t	-2.45		$C_{\beta 1}H$	9.90	Val49 NH
	-1.10		$C_{\beta 2}H$	5.41	$C_{\alpha}H$
s	-1.83		$C_{\gamma 1}H$	4.10	$C_{\beta}H$
y	-2.81		$C_{\gamma 2}H$	2.09	$C_{\gamma 1}H_3$
	-0.39		$C_{\delta 1}H$	3.51	$C_{\gamma 2}H_3$
	-0.86		$C_{\delta 2}H$	7.38	Ile87 NH
	0.93		$C_{\varepsilon 1}H$	0.61	$C_{\gamma 2}H_3$
	1.32		$C_{\varepsilon 2}H$	2.46	$C_{\gamma 11}H$
	1.22	Leu68	$C_{\alpha}H$	2.10	$C_{\gamma 12}H$
	-0.20		$C_{\beta 1}H$	1.65	$C_{\delta 1}H_3$
	0.32		$C_{\beta 2}H$	4.96	Gln9 $C_{\alpha 2}H$
	-0.27		$C_{\gamma}H$	5.18	$C_{\alpha 1}H$
v	-2.04		$C_{\delta 1}H_3$	-0.04	Gln14 $C_{\alpha}H$
	-0.72		$C_{\delta 2}H_3$	6.03	Asn42 NH
	4.04	Leu120	NH	3.83	Ser118 $C_{\alpha}H$
	2.26		$C_{\alpha}H$		
x	-2.02		$C_{\beta 1}H$		
z	-1.28		$C_{\beta 2}H$		
	-0.05		$C_{\gamma}H$		
	-0.02		$C_{\delta 1}H_3$		
	-0.27		$C_{\delta 2}H_3$		

practically identical chemical shifts as they have in the diamagnetic Cu(I)-protein[15]. Other aromatic residues like Tyr72, Phe110 and Phe111 present sizable isotropic shifts, although their protons are between 8-11 Å from the paramagnetic center. And finally, two phenylalanin spin systems, Phe114 and Phe15, present small or non-isotropic shifts despite being between 5-8 Å from the metal ion. The Phe110 aromatic signals are in principle assigned because they are non-degenerated as occurs in the case of the Cu(I)-azurin[15]. This initial assumption is confirmed because of the existence of the expected dipolar connectivities with some of the Trp48 signals (Fig. 4:13A). Additionally, the Phe110 α and NH protons can also be found in the NOESY spectrum and they lead to the Phe111 NH and aromatic signals (Fig. 4:13A) which are very close in the space to the Phe110 residue.

[15]van de Kamp, M., Canters, G.W., Wymenga, S.S., Lommen, C.W., Hilbers, H., Nar, A., Messerschmidt, A. & Huber, R. (1992) *Biochemistry 31*, 10194.

Residues Asn47 and Val49 are also assigned from their NOESY connectivities with Phe111 NH and Trp48 α signals (Fig. 4:10C) all of them are very close in the space[5c,6a]. These assignments are supported by the expected NOESY connectivity between the Asn47 α and Leu86 α protons (Fig. 4:10B), which in turn support the assignments of Leu86 and those residues connected to it. Finally, the Asn42 NH, Gln14 α and Ser118 α signals have been only tentatively assigned from NOESY connectivities with the Lys41 and Met121 protons (Fig. 4:12 and Fig. 4:9).

DISCUSSION.

a) The assignments.

As we have already seen in the previous chapter, assigning paramagnetic signals needs different NMR experiments to be performed in multiple resonance conditions, which frequently are extreme from the NMR point of view[16]. Thus, finding ambiguous situations is more frequent here than in conventional (diamagnetic) NMR studies[17]. But, fortunately, enough information from those resonances belonging to coordinated residues can be obtained in most cases to ensure their assignment.

The assignment of the isotropically shifted signals is supported by intra-residue and inter-residue connectivities which are interpreted in agreement with the available structural information. The assignment of the histidine signals is in principle self-consistent due to the very clear pattern of the imidazole resonances from histidines coordinated to cobalt(II)[2]. Their specific assignment based on the different exchange behavior of signals a and b is confirmed when we find His117 resonances connected with the Gly116 and Phe114 residues, and His46 resonances connected with the His35 and Met44 residues. The assignment of Leu86 and Lys41 residues, which are dipolarly connected with the Gly45 protons, confirms the independent assignment of this residue. The Met121 residue, assigned first on the basis of some dipolar and contact correlations between signals f, j, m, n and o, is then clearly identified through the connection of these signals with the paramagnetic methyl signal k'. Additionally, the ^{1}H NMR spectrum of the cobalt derivative of the Met121Gln *Alcaligenes denitrificans* mutant confirms the above interpretations[18]. The assignment of the Cys112 signals has been clearly stated by comparison between the spectra of the wild-type and Cys112Asp azurin cobalt(II) derivatives[4c]. The distance calculated here from 1D NOE experiments is in agreement with those results. Although the NOE between signals A and B is very small (less than 1%), choosing the appropriate resonance conditions allows it to be observed. Considering the relationship between the NOE, the T_1 and the inter-proton distance[19,20], this

---

[16a] La Mar, G.N. & de Ropp, J.S. (1993) in *NMR of paramagnetic molecules* (Berliner L.J. & Reuben , J. ed.) Vol. 12, p. 1, Plenum Press Dir Plenum Publishing Corp. New York. b) Bertini, I., Turano, P. & Vila, A. (1993) *Chem. Rev. 93*, 2833.

[17] Wüthrich, K. (1986) *NMR of proteins and nucleic acids*, John Wiley & Sons: New York.

[18] Salgado, J., Jiménez, H.R., Moratal, J.M., Kroes, S., Warmerdam, G & Canters, G.W. (1995), *Biochemistry*, in press. See Chapter 5.

[19] Neuhaus, D. & Williamson, M. (1989) *The Nuclear Overhauser Effect in Structural and*

NOE is probably close to the detection limit in paramagnetic systems. On the other hand, the assignments of the Cys112 and Met121 protons support each other through the NOE connection between signals B and n.

The aromatic part of the spectrum is particularly interesting if we compare it with the Cu(I)-azurin[15] and even the Ni(II)-azurin[21] spectra. We distinguish here three types of residues. Those which are far from the metal center, like Phe97, Phe29, Tyr108 and Trp48, present practically identical chemical shifts as they have in the diamagnetic Cu(I)-protein[15]. Other aromatic residues like Tyr72, Phe110 and Phe111 present sizable isotropic shifts although their protons are between 8-11 Å from the paramagnetic center. Finally, two phenylalanine ring protons present small, if any, isotropic shifts despite being between 5-8 Å from the metal ion. Closer distances to the paramagnetic center are not always associated with larger isotropic shifts due to the capital importance of the orientation in the magnitude of the pseudocontact shifts[22,23].

Finally, a critical comment should be added about the use of COSY spectra for some of the assignments. It has been demonstrated that COSY cross-peaks of fast relaxing signals do not represent scalar couplings but relaxation allowed coherence transfer of dipolar origin, due to cross-correlation effects between dipole-dipole coupling and Curie spin relaxation[24]. COSY information of broad signals ($\Delta\nu_{1/2}$>100 Hz) has been used in the of the Gly45, Met121, Met44 and Met13 residues. For the first three cases, the conclusions extracted from the COSY data are supported by abundant NOE (1D and 2D) correlations. Thus, the assignments of geminal protons are confirmed by strong NOEs, and intraresidue connectivities confirm the specific assignments. However, for the Met13 the spin connectivities are principally based on COSY data, and no dipolar connectivities have been found with other assigned residues. So, in this case, the assignments should be considered as tentative.

Conformational Analysis, VCH Publications, New York.

[20]See Chapter 2, section II.e.

[21]See Chapter 3, section I.

[22]Bertini, I. & Luchinat, C. (1986) *NMR of Paramagnetic Molecules in Biological Systems*, The Benjamin/Cummings Publishing Company, Menlo Park.

[23]See Chapter 1, section V.a.

[24]a) Bertini, I., Luchinat, C. & Tarchi, D. (1993) *Chem. Phys. Lett. 203*, 445. b) Qin, J., Delaglio, F., La Mar, G.N. & Bax, A. (1993) *J. Magn. Reson. Ser. B 102*, 332.

b) NMR properties: interpretation and consequences.

Metal coordination.

Once the assignments have been made, some structural conclusions based on the properties of the NMR signals can be drawn. According to the crystal structure of different azurin metalloderivatives, the metal site is defined as a trigonal bipyramid, in the case of the copper protein[14], or a distorted tetrahedron, in the cases of the zinc and nickel derivatives[5c,6a]. The slight differences between them are due to the position of the metal with regard to the N_2S equatorial plane and its distance from the two possible axial ligands (the Gly45 oxygen and Met121 sulfur). Due to the rigidity of the coordination site, the approach of the metal towards one axial position means its withdrawal from the other. Thus, it is considered that the Gly45 ligand interacts only coulombically with the copper in the native azurin[25], while the Met121 is placed out of the coordination sphere in the case of the zinc azurin[6a]. What we observe in the cobalt azurin, is that there are important isotropic shifts for signals from both Met121 and Gly45 residues, which are hard to be explained attending only to a pseudocontact origin. Moreover, the magnitude and pattern of these shifts for the γ Met121 and α Gly45 signals is very similar. So, if the coordination of one of them is accepted, the coordination of the other may also be assumed.

We can use the relaxation times of the paramagnetic protons to obtain structural information about the metal site through the Solomon equation (Eq 1:12)[26]. As we have discussed in the previous chapter, this approach is frequently inaccurate due to the difficulty to have an appropriate τ_c value. Another important source of error is the uncertainty of the relaxation times caused by the existence of unpaired spin density delocalization over the coordinated ligands[27] and intrinsic errors in the determination of such relaxation times[16a,28,29]. The proton-metal distances, taken from the crystal structures of Ni(II), Zn(II) and Cu(II)-azurin[5c,6a,14], for protons corresponding to the paramagnetic NMR signals of Co(II)-azurin, are collected in Table 4:3. Many of

---

[25]Lowery, M.D. & Solomon, E.I. (1992) *Inorg. Chim. Acta 198-200*, 233.

[26]Solomon, I. (1955) *Phys. Rev. 99*, 559.

[27]a) Banci, L., Bertini, I., Luchinat, C. & Scozzafava, A. (1987) *J. Am. Chem. Soc. 109*, 2328. b) Banci, L., Bertini, I., Luchinat, C., Monnanni, R. & Mascarell, J.M. (1989) *Gazz. Chim. Ital. 119*, 23.

[28]Granot, J. (1982) *J. Magn. Reson. 49*, 257.

[29]See the discussion in Chapter 2, section II.b, about the problems related with the determination of relaxation times.

these distances are very similar in the former three azurin metalloderivatives and the larger differences affect to protons from the coordinated residues. It is reasonable to assume that the distances in the Co(II)-azurin have to be also very similar to the former ones, so we can use those distances, together with the relaxation rates of the Co(II)-azurin NMR signals, to estimate a τ_c value from the best fitting of the Solomon equation curve (Fig. 4:14). This gives a τ_c=9.5x10^{-12} sec, from which we can calculate proton-metal distances corresponding to the Co(II)-azurin using the T_1^{-1} values of the paramagnetic signals. These data are summarized in Table 4:3, and a graphical comparison of the metal sites of Ni(II), Zn(II) and Cu(II)-azurin with regard to the Co(II)-azurin is represented in Fig. 4:15.

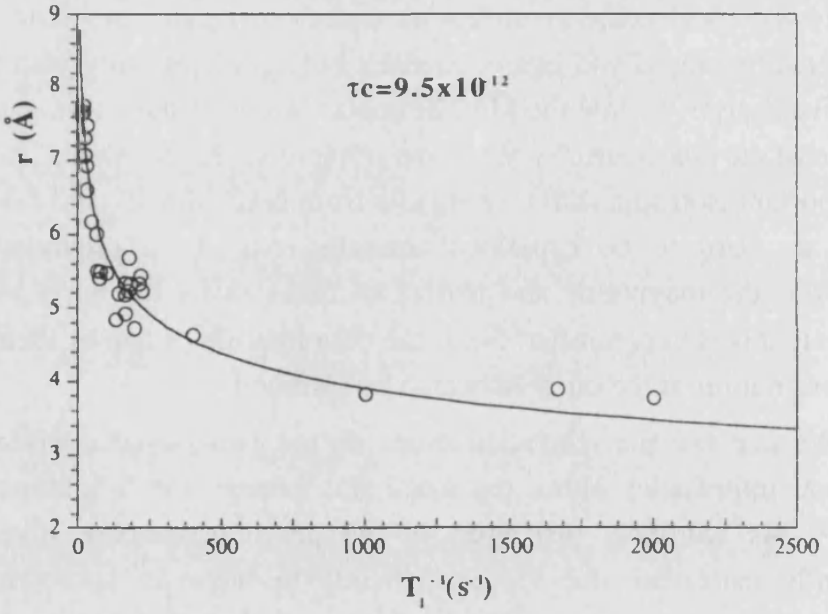

Fig. 4:14. Plot of the relaxation rates of protons in the metal site of Co(II)-azurin *vs* the proton-metal distances taken from the crystal structure of Ni(II)-azurin[5c]. Data are fitted to the Solomon equation (Eq 1:12) theoretical curve[26] obtaining a τ_c=9.5x10^{-12} sec.

As we can observe, the calculated proton-Co(II) distances for the Gly45 α protons are in closer agreement with the distances found in the Zn(II) and Ni(II)-azurins, than in the case of Cu(II)-azurin. The fact that these distances are significantly shorter in the Co(II)-azurin can be due to unpaired spin density delocalization over the ligand Gly45 O. With regard to the Met121 protons, the corresponding ^{1}H-Co(II) distances are also in better agreement with the structures of the Ni(II) and Zn(II)-azurins than with the Cu(II)-azurin (except the Met121 $C_{\gamma 1}H$), while for protons from other residues there is not a clear

correlation. This indicates that at least the mode of axial coordination is very similar in the cobalt, zinc and nickel metalloderivatives. However, because of the considerations expressed above, it also would mean that we have to admit contact interaction between the metal and the Met121 sulfur despite the fact that they are 3.30-3.40 Å apart[5c].

Table 4:3. Proton-metal distances (*r*) in Co(II), Ni(II), Zn(II) and Cu(II) azurins. For the Co(II)-azurin, the distances have been calculated by using the Solomon equation (Eq 1:12)[26], taking a $\tau_C=9.5\times10^{-12}$ sec (see the text). The distances corresponding to the Ni(II), Zn(II) and Cu(II)-azurins have been taken from the X-ray crystal structure of these metalloderivatives[5c,6a,14].

			r (Å)			
signal	T_1^{-1} (sec^{-1})	proton	Co^{II}-azu	Ni^{II}-azu	Zn^{II}-azu	Cu^{II}-azu
A	1666.7	Cys112 $C_{b1}H$	3.58	3.90	3.58	3.55
B	2000.0	$C_{\beta2}H$	3.48	3.78	3.57	3.42
a	172.4	His46 $N_{\varepsilon2}H$	5.23	5.24	4.99	4.95
d	99.0	$C_{\delta2}H$	5.74	5.48	5.19	5.21
F	196.1	$C_{\beta1}H$	5.12	4.73	4.47	4.58
E	1000.0	$C_{\beta2}H$	3.90	3.82	3.58	3.58
C	[a] 5000.0	His46/117 $C_{\varepsilon1}H$	3.00	3.40	3.20	3.1/3.3
D	[a] 5000.0	His46/117 $C_{\varepsilon1}H$	3.00	3.40	3.20	3.1/3.3
H	66.2	His117 NH	6.14	5.51	5.52	5.49
b	140.8	$N_{\varepsilon2}H$	5.41	5.20	4.98	5.04
c	75.2	$C_{\delta2}H$	6.01	5.41	5.25	5.29
l	222.2	Gly45 NH	5.01	5.24	5.44	5.97
e	217.4	$C_{\alpha1}H$	5.03	5.44	5.29	5.86
p	212.8	$C_{\alpha2}H$	5.05	5.33	5.10	5.79
j	24.4	Met121 $C_{\alpha}H$	7.25	7.31	7.23	7.02
m	[b] 163.9	$C_{\beta2}H$	5.28	5.34	5.17	4.99
n	[b] 163.9	$C_{\beta1}H$	5.28	4.93	4.94	4.66
f	175.4	$C_{\gamma1}H$	5.22	5.69	5.65	5.48
o	[b] 163.9	$C_{\gamma2}H$	5.28	5.18	5.07	4.95
k'	[c] 400.0	$C_{\varepsilon}H_3$	4.55	4.64	4.56	4.17
h	25.2	Met13 $C_{\beta1}H$	7.21	7.08	7.05	7.02
g	133.3	$C_{\gamma1}H$	5.46	4.85	5.19	4.82
h'	31.2	$C_{\gamma2}H$	6.96	6.60	6.90	6.59
J	18.2	His35 $C_{\varepsilon1}H$	7.61	7.76	7.82	7.96
I	[c] 63.3	$N_{\varepsilon2}H$	6.18	6.01	6.09	6.19
L	77.5	Met44 $C_{\gamma2}H$	5.98	5.50	5.62	5.73
G	29.2	Asn47 $C_{\alpha}H$	7.03	6.94	6.71	6.79
q	47.4	Leu86 $C_{\gamma}H$	6.49	6.17	6.29	6.47
k	181.8	$C_{\delta1}H_3$	5.19	5.33	5.23	5.47
r	31.6	$C_{\delta2}H_3$	6.95	7.49	7.60	7.74
u	18.7	Lys41 $C_{\alpha}H$	7.58	7.67	7.65	8.15
y	9.3	$C_{\gamma2}H$	8.51	8.82	8.50	8.67

[a] approximated value.

[b] value corresponding to the group of overlapped signals m, n and o.

[c] value corresponding to pH 7.5.

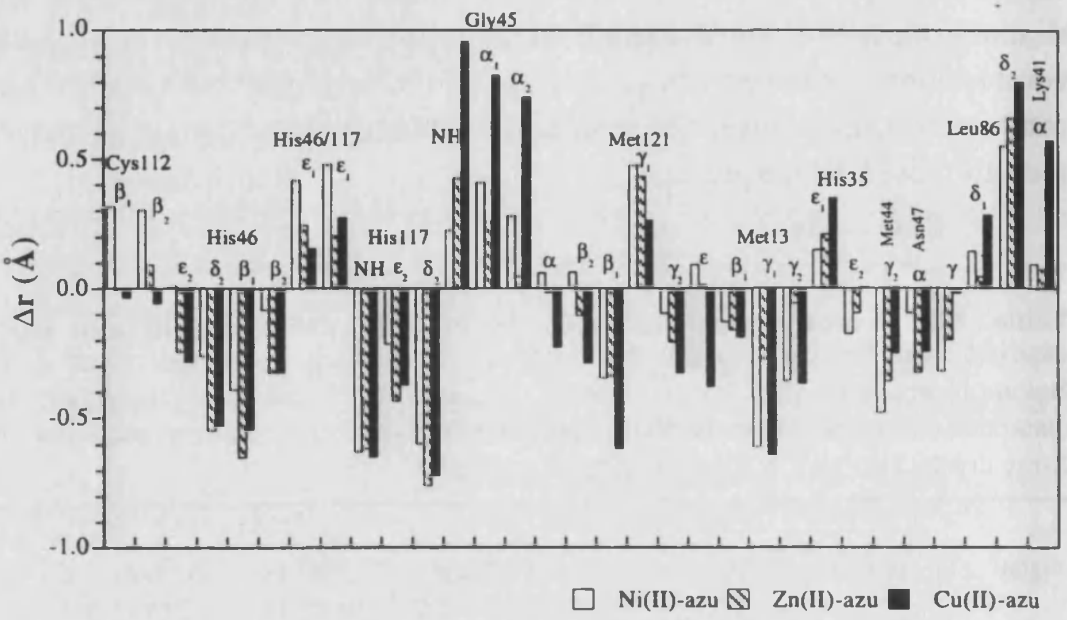

Fig. 4:15. A graphical comparison of the metal sites in Ni(II), Zn(II), Cu(II) and Co(II)-azurin. The horizontal line at r=0 represents proton-metal distances for Co(II)-azurin calculated by the Solomon equation (Eq 1:12). Δr represents the difference between those distances and the corresponding proton-metal distances in the Ni(II), Zn(II) or Cu(II)-azurin (values taken from Table 4:3).

Discriminating between the contact and pseudocontact contributions to the isotropic shifts in Co(II)-azurin is crucial for obtaining a realistic idea about the possible existence of this axial coordination. As already showed in the case of the Ni(II)-azurin, one possible approach to address this problem is to analyze the temperature dependence of the isotropic shifts[7,22,30]. Extrapolated values in the plot of δ *vs.* T^{-1} falling clearly out of the position expected for the corresponding protons in diamagnetic conditions, indicate the existence of dipolar contribution to the isotropic shifts. In the present case (Fig. 4:2), only the Cys112 β signals (signals A and B) present significantly large δ values at T^{-1}=0 (between 30-45 ppm), and the relatively low intercept values corresponding to the Met121 and Gly45 proton signals (~10 ppm) indicate that the dipolar contribution to their hyperfine shifts is only moderate. Knowing the magnetic anisotropy tensor could give the necessary information to allow the evaluation of the contact and dipolar contributions to the isotropic shifts[16b,22,3031]. This can be performed

[30]La Mar, G.N., Horrocks, W.D. & Holm, R.H. (1973) *NMR of Paramagnetic Molecules*, Academic Press, New York.

[31]See Chapter 2, section V.a.

using a sufficient number of pure pseudocontact shifts, like those reported here, and the appropriate structural information, available in this case from different sources[5c,6,14]. In the absence of a detailed knowledge of the g tensor, the coordination of the Met121 ligand is additionally supported in the fact that no other residue, apart from the coordinated ones, have isotropic shifts comparable with those of the Met121 signals. On the other hand, the very weak character of the Co(II)-S^{δ}_{Met121} interaction is clearly appreciable when we compare the Met121 resonances (their isotropic shifts and relaxation times) with the signals of Cys112, which is strongly ligated to cobalt by its S^{γ}.

His35 and the effect of pH in the azurin structure.

The effect of the His35 deprotonation on the redox and structural properties of the metal site had been studied in solution by NMR on the reduced Cu(I)-azurin, predicting substantial changes in the position of the His35 imidazole ring which, however, do not affect the electron self-exchange rate[9c,32]. Later on, the X-ray crystal structure of the oxidized Cu(II)-azurin at pH 5 and 9 revealed that the pH dependent changes are only local, while metal-ligand distances remain unchanged or change less than the 0.1 Å crystallographic detection limit[14]. Since the oxidation state of the metal and the His35 deprotonation process affect each other (the azurin redox potential decreases 70 mV from pH 5 to 9 and the His35 pK_a is larger by 1 in the reduced copper protein)[4a,9], it is interesting to compare the crystal structural data of Cu(II)-azurin with the present NMR results on Co(II)-azurin (formally an analog of the Cu(II)-azurin). Although most of the isotropically shifted signals change their chemical shift, the relaxation times, which can be more directly translated in terms of distance because they are strongly dependent on the distance to the paramagnetic center, are essentially the same with the exception of signal J (see Table 4:1). We then conclude that, for these residues at least, the cobalt-proton distances remain unchanged in the two pH dependent species, in agreement with the mentioned crystallographic data[14].

Variations in the isotropic shifts of paramagnetic signals are due to their increased sensitivity towards subtle changes in the surroundings. Thus, the less shifted a signal is, the more significant the variations in its position. Signal J, assigned here to the ε_1 proton of His35, is moderately shifted (as compared to the corresponding signal in the diamagnetic Cu(I) protein[15]) and changes almost 2 ppm from pH 4.5 to 7.5. Additionally its relaxation time is about 50 % larger at high pH, which according to the Solomon equation[26] corresponds to an increase of 0.5 Å in its distance from the cobalt (II) ion. This result is only

[32]Groeneveld, C.M. & Canters, G.W. (1988) *J. Biol. Chem. 263*, 167.

partially in agreement with the X-ray structural data which showed only a 0.2 Å shift of the His35 imidazole ring as a consequence of the deprotonation of the His35 $N_{\delta 1}$ [14].

On the other hand, the His35 ε2 signal is also affected by the pH transition, since its exchange rate with the solvent H_2O slows down as the pH increases allowing its observation at high pH. This may be the reason why this proton was not observed in the NMR study of the Cu(I)-azurin at pH 5.5 [15]. Although the exchange rate with the bulk water of the imidazole labile protons can be acid-catalyzed, this effect is normally important only at very low pH values[17,33]. Thus, we interpret this behavior as being due to an increased protection of the His35 ε_2 proton from the solvent, originated by the structural reorganization near the His35 residue observed in the X-ray structural study at different pH values[14]. According to it, the His35 $N_{\varepsilon 2}H$ is hydrogen bonded to the O44 at low pH and this interaction is conserved at high pH (Fig. 4:16)[14]. Admitting a similar situation in the case of Co(II)-azurin in solution, we can conclude that the His35 $N_{\varepsilon 2}H$-O44 hydrogen bond is stronger at high pH, which would explain the reduction of the exchange rate of this proton.

Exchange of the His117 $N_{\varepsilon 2}H$ proton.

As we have seen in the case of the Ni(II)-azurin[34], the $N_{\varepsilon 2}H$ proton of the coordinated residue His117 is in fast exchange with bulk water at high pH. Although the disappearance of the corresponding ^1H NMR signal seems to be parallel to the general slow exchange transition affecting the rest of the signals, we concluded that it is due to base-catalysis which increases the exchange of this proton with the solvent[34,5b]. In the NMR spectrum of the Co(II)-azurin, we observe the same behavior affecting signal b (Fig. 4:4). However, in this case "two signals b" can be observed, corresponding to the protonated and deprotonated species of azurin. They follow the slow exchange transition with the pH as the rest of the NMR signals, but they both vanish at high pH, indicating that the increase of the exchange rate is due to the increase of the pH through base-catalysis but not to a structural change. Moreover, the same increase of the exchange rate of the His117 $N_{\varepsilon 2}H$ proton is also observed for the Co(II)-azurin from *A. denitrificans*, where His35 does not titrate[18]. This demonstrates that it is actually not connected with the His35-dependent transition in *P. aeruginosa* azurin, and supports the base-catalysis explanation for both *P. aeruginosa* and *A. denitrificans* azurins.

---

[33]Eigen, M. (1964) *Angew. Chem. (Intl. Ed.) 3*, 1.

[34]See Chapter 3, section I.

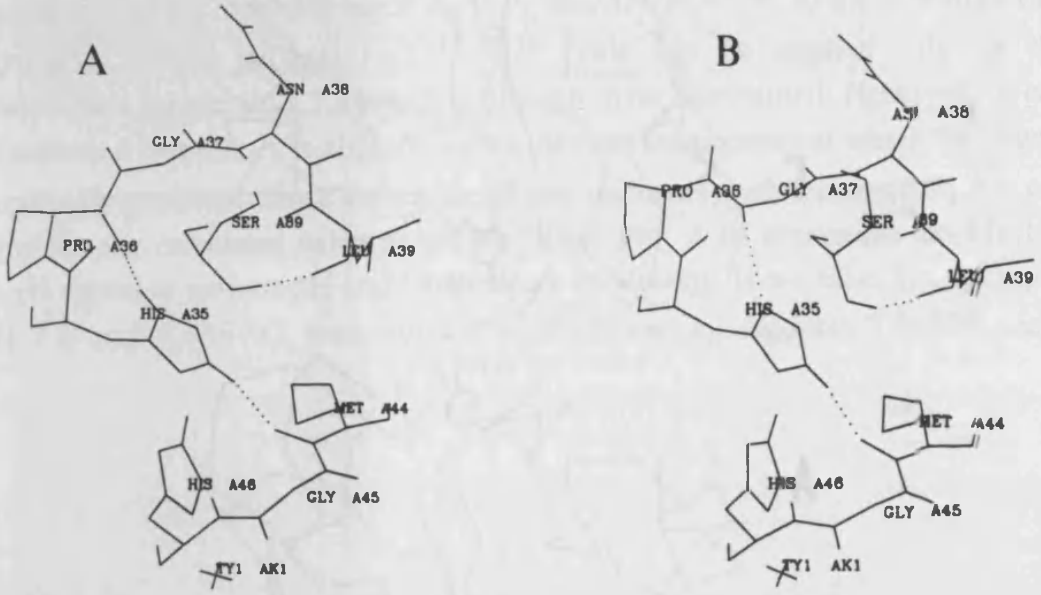

Fig. 4:16. The His35 residue as seen in the X-ray crystal structure of Cu(II)-azurin at pH 5.5 (A) and 9 (B)[14]. At low pH (A), both His35 imidazole NH groups are hydrogen-bonded: the $N_{\delta 1}H$ with O36 and the $N_{\varepsilon 2}H$ with O44. At high pH (B), the $N_{\delta 1}$ is deprotonated and makes a weak contact wit the Gly37 NH, facilitated by a peptide flip of the Pro36-Gly37. The $N_{\varepsilon 2}H$--O44 interaction is still conserved despite the His35 imidazole ring has shifted by 0.2 Å.

Since it was demonstrated that the hydrophobic patch is the relevant surface zone for the electron transfer between azurin and its redox partners and for the electron self-exchange reaction[35], a crucial functional role for the His117 was postulated. Additionally, the crystal structure of azurin shows a dimeric association. In it, two azurin molecules interact by their hydrophobic patches (see Fig. 3:13), and their His117 $N_{\varepsilon 2}H$ groups are hydrogen bonded with two well defined H_2O molecules, which in turn are hydrogen bonded to each other[36] (Fig. 4:17). It was then suggested that the His117 $N_{\varepsilon 2}H$--H_2O network would be an entrance/exit pathway for the electrons traveling to or from the copper. This idea provides an interesting through H-bonds mechanism for the azurin-azurin electron self-exchange reactions, where electrons would move in a continuous electron density bridge between the two coppers[36,37].

[35]a) van de Kamp, M., Floris, R., Hali, F.C. & Canters, G.W. (1990) *J. Am. Chem. Soc. 112*, 907. b) van de Kamp, Silvestrini, M.C., Brunori, M., van Beeumen, J., Hali, F.C.. & Canters, G.W. (1990) *Eur. J. Biochem. 194*, 109.

[36]Nar, H., Messerschmidt, A., Huber, R., van de Kamp, M. & Canters, G.W. (1991) *J. Mol. Biol. 218*, 427.

[37]Canters, G.W. & van de Kamp, M. (1992) *Curr. Opin. Struct. Biol. 2*, 859.

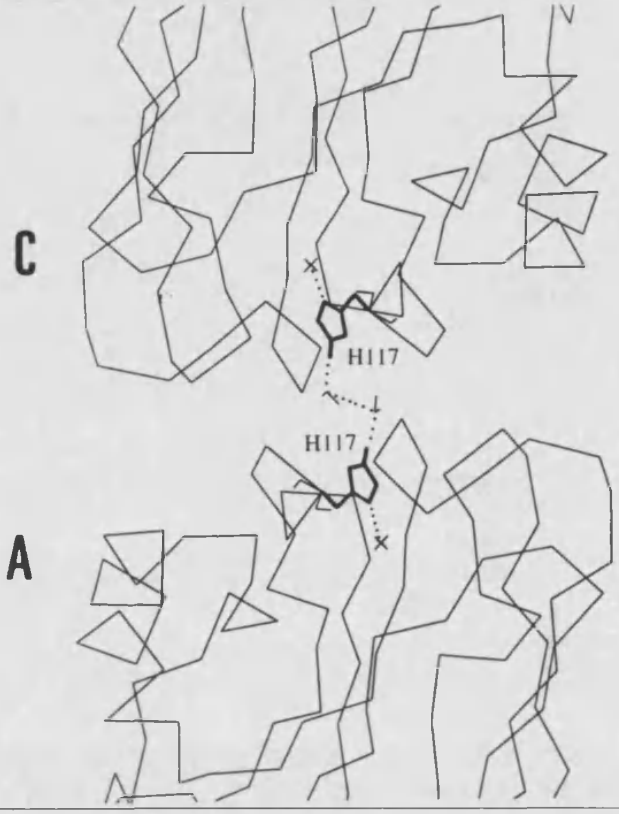

Fig. 4:17. Representation of the A-C dimer contact (see Fig. 3:13) in *P. aeruginosa* wild-type Cu(II)-azurin. The picture shows both azurin monomers interacting by their hydrophobic patches and the His117 residues connected through a proton-bridge network via two water molecules. The coordinates have been taken from the crystal structure of *Pae* Cu(II)-azurin[14].

In the case of the Co(II)-azurin studied here, we observe that the His117 ε_2 proton can exchange fast with the solvent at high pH. Depending on the value of this exchange rate, it could affect the His117 $N_{\varepsilon 2}H$--H_2O network and so the proposed electron transfer mechanism. To calculate this rate, methods based on peak separation, $\Delta\nu$, provide good results when the $\Delta\nu$ value and the exchange rate are much larger than the bandwidth[11,38]. For cases where the populations of the two exchanging sites (here the bulk water and the protein) are very different[39], a lifetime τ is defined from $1/\tau=(1/\tau_A)+(1/\tau_B)$, where τ_A and τ_B are the live times of species A and B. At the coalescence temperature, $\tau \equiv \tau_{cc}$ ranges from $\sqrt{2}\ /\ 2\pi\Delta\nu$ to $\sqrt{2}\ /\ \pi\Delta\nu$, for values of $\Delta P=P_B-P_A$ between 0 and 1, respectively (see Fig. 2:6)[38,39], being P_B and P_A, the molar fractions of the protons in the water-molecule site and the protein site, respectively. The present

[38]See Chapter 2, section II.d.

[39]Shanan-Atidi, H. & Bar-Eli, K.H. (1970) *J. Phys. Chem.* *74*, 961.

case is one of the extremes since $P_B >> P_A$ and $\Delta P \approx P_B \approx 1$ [40], so the exchange rate $k_A = P_B/\tau_{cc}$ would be $\pi\Delta\nu / \sqrt{2}$ [11,38,39]. This can be applied only at the coalescence temperature T_c, which is difficult to be determined. However, it can be assumed that this T_c is slightly higher than the temperature at which the signal eventually vanished. Since the exchange rate increases with temperature, we can consider the calculated value as a lower limit. Fig. 4:18 represents the His117 $N_{\varepsilon 2}H$ signal at various pH and temperature conditions. If we take, for example, pH 7.0 and T_c=35 °C, then $\Delta\nu$=2.37x10^4 Hz and k_B amounts 5.3x10^4 sec^{-1}.

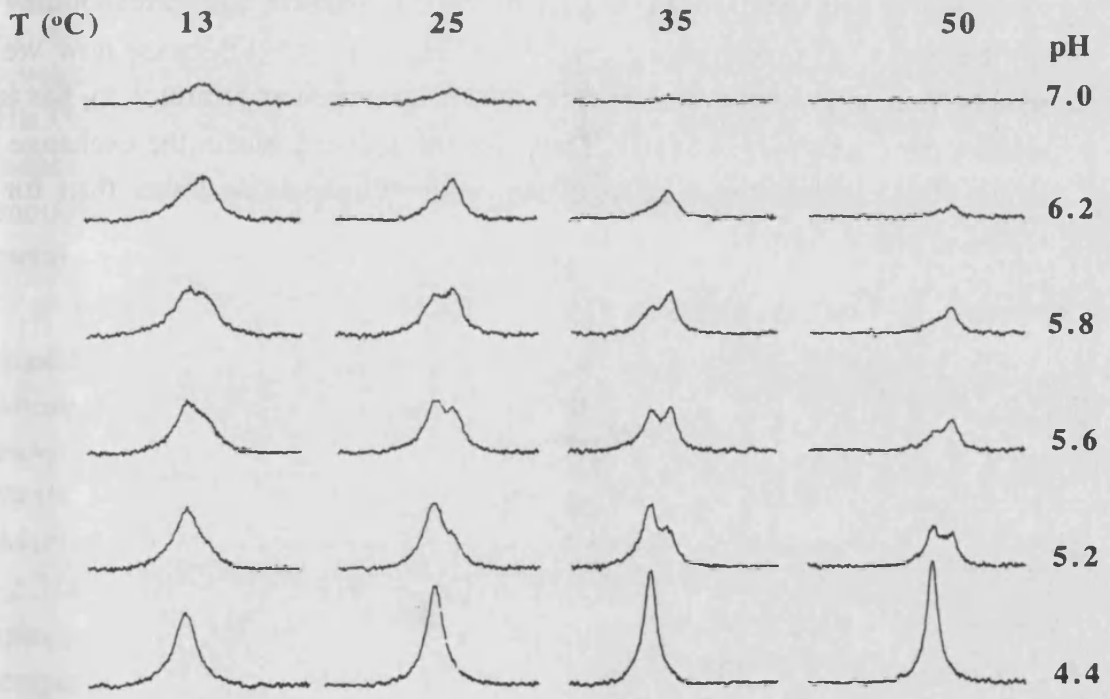

Fig. 4:18. The His117 $N_{\varepsilon 2}H$ signal at different pH and temperature conditions. At intermediate pH values, the signal displays two different position corresponding to the low-pH and high-pH species of the His35 slow ionization equilibrium. At high temperature and high pH conditions this signal enters fast exchange with bulk H_2O and disappears.

[40] The concentration of the protein in these experiments was around 3x10^{-3} M, which is very low compared with 111, the "molarity" of the water protons.

Although this is a large value, it is still two orders of magnitude lower than the azurin electron self-exchange rate[41]. It has been proposed that the exchange of this proton is hindered by its interaction with a defined H_2O molecule in the protein surface[15]. If this is the case, we can assume that this exchange rate is an upper limit for the exchange of that H_2O molecule. So the lifetime of the His117 $N_{\varepsilon 2}H$--H_2O bridge would be long enough to be used as traveling path for very fast moving electrons.

In the NMR spectrum of Cu(I)-azurin, the His117 $N_{\varepsilon 2}H$ proton is present even at high pH (7.7)[42]. Admitting that the solvent exposition of the His117 $N_{\varepsilon 2}H$ is similar in both the Cu(I) and Co(II)-azurins, it can be assumed that the difference in the exchange rate of the His117 imidazole proton is due to the a difference in charge between the two metal ions. Indeed, only one isotropically shifted exchangeable signal is observed in the NMR spectrum of Cu(II)-azurin at pH 7.0[43], in agreement with a fast exchange affecting the His117 ε_2 proton also in this protein. It means that the exchange rate of this proton becomes faster when azurin gets oxidized. In the case of the Cu(I)-azurin, the corresponding $\Delta\nu$ for the His117 ε_2 proton signal is 2.77×10^3 Hz at 40 °C[15]. Because now we are in slow exchange conditions (far from the coalescence temperature), k_B has to be smaller than $\pi\Delta\nu / \sqrt{2} = 6 \times 10^3$. Thus, for the reduced azurin the exchange rate of the His117 ε_2 proton is at least one order of magnitude lower than for the oxidized one.

---

[41] Groeneveld, C.M. & Canters, G.W. (1985) *Eur. J. Biochem. 153*, 559.

[42] Kalverda, A.P., personal communication.

[43] Kalverda, A.P., Salgado, J., Dennison, C. & Canters, G.W. (1995) *Biochemistry*, submitted.

II. EPR spectroscopy of Co(II)-azurin.

RESULTS AND DISCUSSION.

The EPR spectra of Co(II)-azurin at 5 K (Fig. 4:19) display a typical distorted axial pattern for high-spin Co(II) with three resonances, the perpendicular signal being split in two components due to rhombic distortion. The effective g values at two different pH conditions are 5.91 (g_y), 3.77 (g_x) and 2.01 (g_z) at pH=7.5 and 5.20 (g_y), 3.85 (g_x) and 2.0 (g_z) at pH=4.5. The differences in the two components of the perpendicular signal can be related with a pH-induced conformational change originated by the titration of the His35 residue in the native protein[9c,14,44], which has been also observed for the Ni(II) an Co(II) metalloderivatives[5b,45]. The comparison of the g values suggest that the rhombicity at pH=7.5 is slightly higher than at pH=4.5, indicating that the conformational change implies some structural rearrangements in the metal binding site. However, the X-ray structure of Cu(II)-azurin at pH 5 and pH 9[14], as well as NMR studies at various pH values on Co(II)-azurin (see above), revealed that the conformational transition affects mainly the surroundings of His35, while the structural changes in the metal coordination site are probably meaningless (≤0.1 Å)[14]. It seems that these changes, although small, are large enough to produce significant variations in some spectroscopic properties of the metal site, as it can be observed by EPR[44] and NMR[4a,5a,9c].

On the other hand, in the EPR spectra there is no evidence of resolved hyperfine structure from the ^{59}Co nuclear spin momentum, except at lower field, where the absorption-shaped component indicates possible ill-defined hyperfine transitions (Fig. 4:19). These spectra are consistent with those expected for S=3/2 molecules subject to zero-field splitting where only the (±1/2) Kramers' doublet, identified from the effective g values, is resonant. A mean g value of ~2.3 is calculated from the effective g factors, in agreement with second order spin-orbit coupling and an orbitally non degenerate ground state. When the temperature is increased from 5 K to 20 K, a maximum of intensity is found at 10 K. The same intensity variation is observed for the three resonances, confirming that they arise from rhombic anisotropy of the single doublet (±1/2). The intensity maximum shows that this doublet is the excited one and therefore, the predominant axial zero field splitting D is negative. At temperatures higher

---

[44]Groeneveld, C.M., Aasa, R., Reinhammar, B. & Canters, G.W. (1987) *J. Inorg. Biochem. 32*, 143.

[45]See above and Chapter 3, section I.

than 10 K, the intensity decreases according to the Curie law behavior. When the temperature further increases, the signals vanish. The resonances are so extremely fast relaxing, that they are only clearly visible below 20 K.

The value of the zero field splitting parameter D can be evaluated from the intensity dependence of the transitions, according to the Boltzmann distribution of the two Kramers' levels, (±1/2) and (±3/2) associated with the ground spin state S=3/2. They follow the approximate expression:

$$F = \frac{1}{T\left(1 + e^{2D/kT}\right)} \qquad \text{Eq 4:1}$$

where $2D$ is the energy gap between the two Kramers' levels, and the rhombic parameter E is supposed be E=0. From this treatment, it is found that D=-3.5 cm^{-1}, as it is shown in the following scheme:

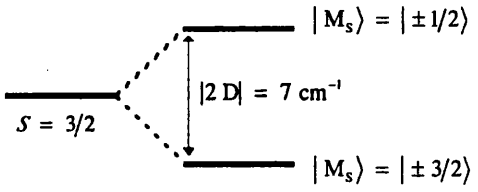

In structurally defined Co(II) complexes, ranges of values of the splitting between the two doublets have been established from -36 to +13 cm^{-1} for tetracoordinate sites, from +20 to +50 cm^{-1} in pentacoordinate sites and ≥50 cm^{-1} in hexacoordinate sites[46]. Although these ranges are probably not appropriate for highly distorted tetracoordinate Co(II) species[47], it seems that a negative D value is only possible for tetracoordinate Co(II). On the other hand, possible distortions from trigonal bipyramidal coordination that preserve the trigonal symmetry are described as the so-called tetrahedral distortion[48]. Thus, we interpret our results of the cobalt(II)-azurin active site on this line, i.e. the electronic structure probes a highly distorted tetrahedral geometry that preserves a trigonal coordination, with one of the axial ligands moving away from the cobalt center. The g values presented above, which indicate the existence of a

[46]Makinen, M.W., Kuo, L.C., Yim, M.B., Wells, G.B., Fukuyama, J.M. & Kim, J.E. (1985) *J. Am. Chem. Soc. 107*, 5245.

[47]Werth, M.T., Tang, S.F., Formicka, G., Zeppezauer, M. & Johnson, M.K. (1995) *Inorg. Chem. 34*, 218.

[48]Banci, L., Bencini, A., Benelli, C., Gattesci, D. & Zanchini, C. (1982) *Structure and Bonding 52*, 37.

rhombic field and a low symmetry distortion, would be in agreement with this conclusion.

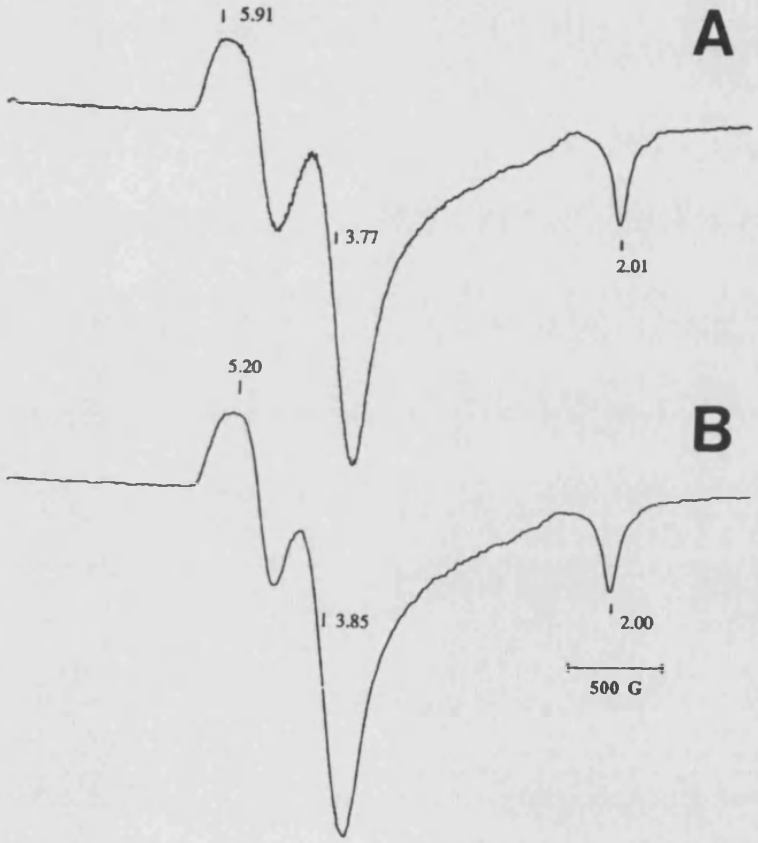

Fig. 4:19. Electron paramagnetic resonance spectra (X-Band) of Co(II)-azurin in H_2O solvent at 5 K (2 mM protein, 20 mM CH_3COONH_4): (A) pH 7.5, (B) pH 4.5.

III.Concluding remarks.

The NMR study of cobalt(II) azurin has led to find and assign five residues whose proton resonances witness that they are coordinated to the metal. Among them, Cys112 is strongly ligated to cobalt and the large isotropic shifts of its proton signals probe the existence of important unpaired spin delocalization over this residue. In contrast, Met121 proton shifts are moderate, but still too large to be only of pseudocontact origin, indicating that this residue is weakly ligated. Histidines 46 and 117 and Gly45 behave as residues normally coordinated to cobalt. These results, and the study of the electronic structure of cobalt-substituted azurin by EPR, suggest a tetrahedral metal site which could be consistent with a distorted five-coordinate trigonal geometry where one axial ligand (Met121) has moved away. These conclusions are in agreement with a parallel study of Ni(II)-azurin[5] and suggest that the metal site is very similar in both cases. An analysis of the magnetic anisotropy tensor would be of help to discriminate the pseudocontact and contact contributions to the isotropic shifts in the coordinated residues, allowing the evaluation of the strength of the Met121 coordination.

Many of the residues up till 11 Å around the metal have been also assigned. They present only small pseudocontact shifts, except in the case of Met13 γ1 proton, and correspond to the two functionally important parts of the protein: the hydrophobic patch and the His35 zone. The analysis of the pH effects on the NMR spectra is consistent with the crystallographic study of Cu(II)-azurin.

Finally, the exchange rate of the His117 $N_{\varepsilon 2}H$ proton is dependent on the pH and oxidation state of the metal. Thus, it is faster for the Co(II) and Cu(II)-azurins than for the Cu(I)-azurin, and increases with the pH. However, it is much slower than the electron self-exchange rate, and so it is consistent with the a proposed mechanism for the azurin electron self-exchange reaction, in which two solvent molecules participate in a proton-bridge network linking the His117 coordinated residues of two azurin molecules[36,37].

Chapter **5**

Alcaligenes denitrificans azurin and its M121Q mutant:

A ^{1}H NMR Study of the cobalt and nickel derivatives[1].

Summary.

Using cobalt or nickel to replace copper in native azurin allows one to fingerprint the metal coordination site of the protein. The metal sites of wild-type *Alcaligenes denitrificans* azurin and its M121Q mutant are clearly distinguishable through the paramagnetic ^{1}H NMR spectra of the Ni(II) and Co(II) derivatives. In the wild-type azurin, Gly45 coordinates to nickel or cobalt, while Met121 appears as a weak metal ligand. Conversely, in the M121Q azurin mutant, the metal exhibits a clear preference for the Gln121, which coordinates by the side-chain carbonyl oxygen, and Gly45 is not a ligand. Changes in the isotropic shifts and relaxation properties of signals from the Cys112, His46 and His117 metal ligands suggest a movement of the metal ion out of the equatorial plane, indicating that the metal site is tetrahedral. These effects are less pronounced in the Ni(II)-M121Q azurin than in the Co(II) metalloderivative. The similarity between the NMR spectra of the Co(II) derivatives of stellacyanin and the M121Q azurin is in agreement with a very similar metal site in both proteins and supports the existence of a coordinated Gln in stellacyanin.

Many of the site-directed mutagenesis studies in azurin have been directed to the Met121 axial ligand, whose role is not completely understood. It is has been proposed that it is responsible for the particularly high redox potential characteristic of blue-copper proteins[2], and for tuning this potential through slightly different ways of interaction with the metal ion[3]. Thus, the copper-

[1] Based on Salgado, J., Jiménez H.R., Moratal, J.M., Kroes, S., Warmerdam, G & Canters, G.W. (1995), *Biochemistry*, in press.

[2] Guckert, J.A., Lowery, M.D. & Solomon, E.I. (1995) *J. Am. Chem. Soc. 117*, 2817.

[3] Gray, H.B. & Malmström, B.G. (1983) *Comments Inorg. Chem. 2*, 203.

S^{δ}_{Met121} coordination is weaker in azurins, which are also unique in having a carbonyl glycine as a second axial ligand[4]. Other blue copper proteins, like stellacyanin, cucumber peelings cupredoxin and umecyanin, seem to present an oxygen from a glutamine side chain in the axial position, instead of the methionine sulfur which is common to the rest of the type 1 copper proteins[5] .

The M121Q azurin mutant is of great interest because it is supposed to be a good model for stellacyanin[6], a protein which lacks methionine and whose structure is still unknown[7]. The UV-Vis and EPR spectra of the Cu(II)-M121Q azurin nicely resemble those of stellacyanin. However, while the second presents the lower redox potential in the blue copper proteins family (184 mV), the corresponding potential in the M121Q azurin is 263 mV, only 25 mV lower than the wt azurin potential[6]. The structure of the copper-M121Q azurin in the oxidized and reduced states is known from X-ray diffraction studies[6]. The Cu(II)-M121Q azurin is described as a distorted tetrahedron where the metal is coordinated to the Gln121 O^{ε} but not to the Gly45 backbone carbonyl, which is now placed too far from the copper (Fig. 5:1C)[8].

Here we present the results of the study of the cobalt(II) and nickel(II) derivatives of *Alcaligenes denitrificans* (*Ade*) M121Q azurin by ^{1}H NMR. We study also the corresponding metalloderivatives of the wild-type (wt) *Ade* azurin in order to compare them with the Co(II) and Ni(II)-wt azurin from *Pseudomonas aeruginosa* (*Pae*)[9]. The present work can form the basis to characterize a paramagnetic metallosubstituted type 1 copper site with Gln in the axial position, which then can help to understand the stellacyanin and stellacyanin-like metal sites through the study of their cobalt(II) and nickel(II) metalloderivatives.

---

4 Baker, E.N. (1988) *J. Mol. Biol. 203*, 1071.

5 van Driessche, G., Dennison, C., Sykes, A.G. & van Beeumen, J. (1995) *Protein Science 4*, 209.

6 Romero, A., Hoitink, C.W.G., Nar, H., Huber, R., Messerschmidt, A. & Canters, G.W. (1993) *J. Mol. Biol. 229*, 1007.

7 a) Fields, B.A., Guss, J.M. & Freeman, H.C. (1991) *J. Mol. Biol. 222*, 1053. b) Thomann, H., Bernardo, M., Baldwin, M.J., Lowey, M.D. & Solomon, E.I. (1991) *J. Am. Chem. Soc. 113*, 5911.

8 See Chapter 1, section IIc, for more comments on the structure of this metal site.

9 a) Moratal, J.M., Salgado, J., Donaire, A., Jiménez, H.R., Castells, J. & Martínez-Ferrer, M^a.J. (1993) *Magn. Reson. Chem. 31*, 541. b) Piccioli, M., Luchinat, C., Mizoguchi, T.J., Ramírez, B.E., Gray, H.B. & Richards, J.H. (1995) Inorg. Chem. 34, 737. c) Salgado, J., Jiménez H.R., Donaire, A. & Moratal, J.M. (1995) *Eur. J. Biochem 231*, 358.

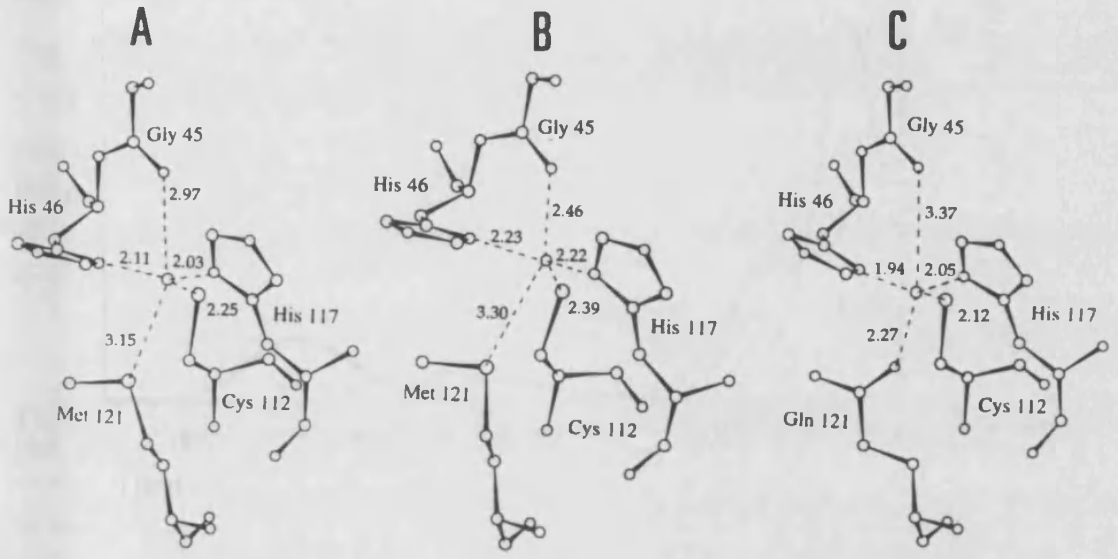

Cu(II)-wt azurin *Ni(II)-wt azurin* *Cu(II)-M121Q azurin*

Fig. 5:1. Schematic representation of the structure of different azurin metal sites as determined by x-ray crystallography. Data from references 10 (A), 11 (B) and 6 (C).

---

[10]Nar, H., Messerchmidt, A., Huber, R., van de Kamp, M. & Canters, G.W. (1991) *J. Mol. Biol. 221*, 765.

[11]Moratal, J.M., Romero, A., Salgado, J., Perales-Alarcón, A. & Jiménez, H.R. (1995) *Eur. J. Biochem. 228*, 653.

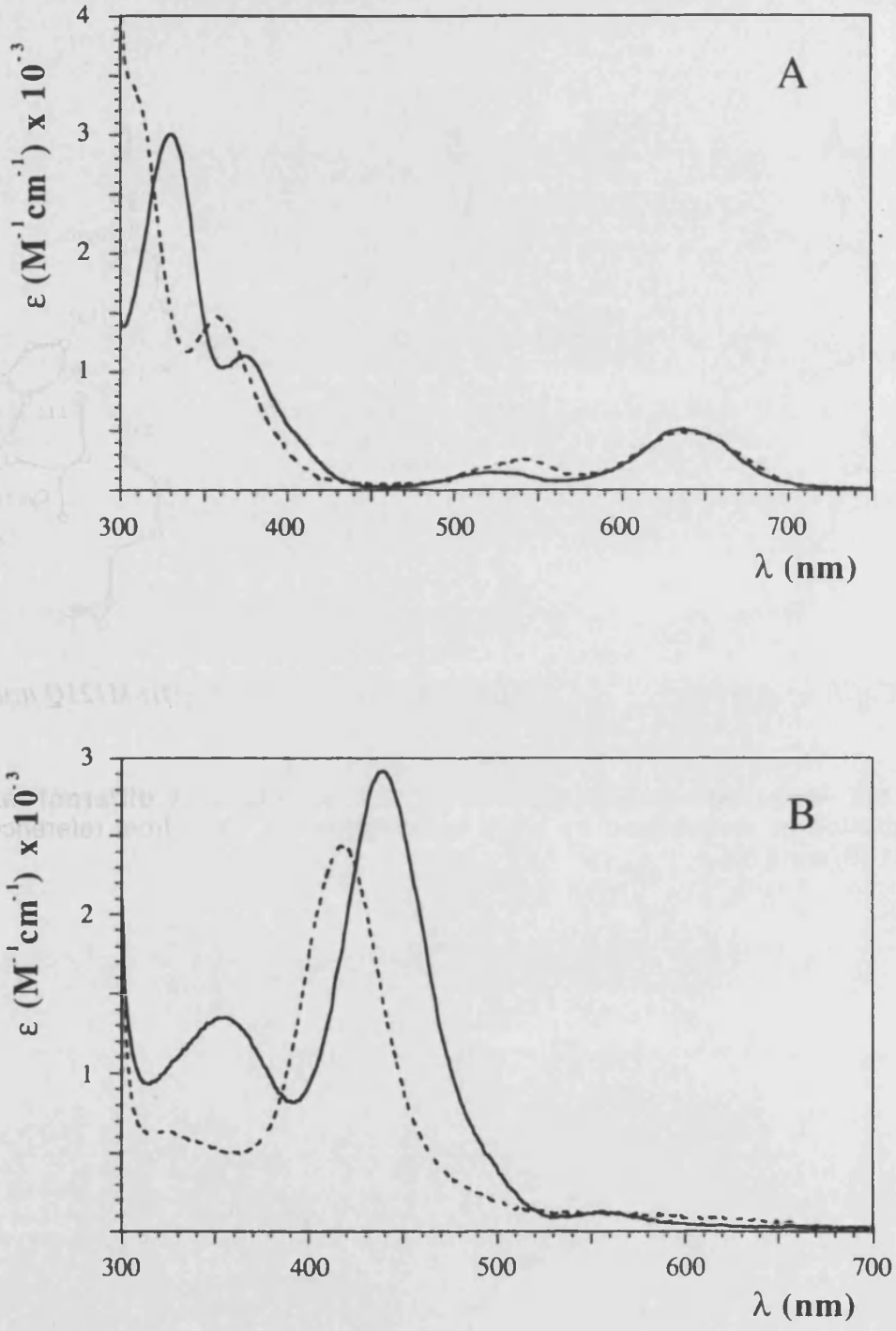

Fig. 5:2. Uv-vis Absorption spectra of cobalt (A) and nickel (B) derivatives of wild type (—) and M121Q (- - -) *A. denitrificans* azurins (pH 7.0, 25 °C).

RESULTS.

a) UV-Vis spectra of Co(II) and Ni(II) derivatives of wild type and M121Q azurins.

The UV-Vis spectrum of the Co(II)-wt *Alcaligenes denitrificans* azurin (Fig. 5:2A, Table 5:1) is essentially the same as that of the Co(II) derivative of *Pae* azurin, whose bands have been already assigned[12] . It consists of two intense ligand-to-metal charge transfer transitions (LMCT) and various ligand-field (LF) or d-d transitions. The spectrum of the Ni(II)-wt *Ade* azurin (Fig. 5:2B, Table 5:2) is also very similar to the corresponding spectrum of *Pae* azurin[12b].

Table 5:1, UV-Vis bands (λ, nm) for Co(II) substituted wild-type azurin (wt azu), azurin mutants and stellacyanin (stc).

wt azu[a]	stc[b]	M121Q azu[a]	M121G azu[c]	M121D azu[c]	M121E azu[c]	assignment[d]
330	310 (sh)	308 (sh)	305	303 (sh)	290 (sh)	LMCT
375 (sh)	365 (sh)	359	358	341	328	LMCT
403 (sh)		~392 (sh)				
520		517 (sh)				LF
531	540	543	535	564	564	LF
635	625 (sh)	634	620 (sh)	625 (sh)	603 (sh)	LF
651 (sh)	655	~648 (sh)	640	645	620	LF

[a] *Alcaligenes denitrificans* azurin (this work).

[b] Data from reference 12a.

[c] *Pseudomonas aeruginosa* azurin mutants. Data from reference 12c.

[d] Assignments as in reference 12c.

The spectra of the Co(II) and Ni(II)-M121Q proteins (Fig. 5:2, Table 5:1 and Table 5:2) are similar to those of the wild type metallo-derivatives but present some significant differences. The LMCT bands are 10-30 nm blue shifted, being in very nice agreement with the Co(II) and Ni(II)-stellacyanin spectra[12a,13]. A similar result is obtained from the UV-Vis spectrum of the

[12a] McMillin, D.R., Rosenberg, R.C. & Gray, H.B. (1974) *Proc. Natl. Acad. Sci. USA 71*, 4760. b) Tennent, D.L. & McMillin, D.R. (1979) *J. Am. Chem. Soc. 101*, 2307. c) Di Bilio, A.J., Chang, T.K., Malmström, B.G., Gray, H.B., Karlsson, B.G., Nordling, M., Pascher, T. & Lundberg, L.G. (1992) *Inorg. Chim. Acta 198-200*, 145.

[13] Lum, V & Gray, H.B. (1981) *Isr. J. Chem. 21*, 23.

Cu(II)-M121Q protein, in agreement with a similar coordination environment in both stellacyanin and the M121Q azurin[6].

Table 5:2. UV-Vis bands (λ, nm) of Ni(II) substituted wild-type azurin (wt azu), azurin mutants and stellacyanin (stc).

wt azu[a]	stc[b]	M121Q azu[a]	M121G azu[c]	M121D azu[c]	M121E azu[c]	assignment[d]
354	335	320	~356	~346	320	LMCT
440	410	416	418	414	392	LMCT
490 (sh)	470 (sh)	480 (sh)				
560	550	550	~530		499	LF
	590	620	~620		546	LF

[a] *Alcaligenes denitrificans* azurin (this work).
[b] Data from reference 13.
[c] *Pseudomonas aeruginosa* azurin mutants. Data from reference 12c.
[d] Assignments as in reference 12c.

b) ^{1}H NMR spectra of the Ni(II) metalloderivatives.

Wild-type nickel azurin.

The 1D ^{1}H NMR spectrum of the Ni(II)-wt azurin from *Alcaligenes denitrificans* (at pH 7.0) is shown in Fig. 5:3B. The paramagnetic zone of the spectrum shows the same pattern of hyperfine shifted signals as the spectrum of the Ni(II) derivative of *Pae* azurin (Fig. 5:3A), and a similarity between them can be easily drawn. In contrast to the *Pae* azurin, the NMR spectrum of the Ni(II)-wt azurin from *Alcaligenes denitrificans* does not depend on the pH in the range of 4.5 to 8.0. The only pH dependent effect is the increase of the exchange rate of signal h, whose intensity decreases at high pH as also observed in the case of the *Pae* Ni(II)-azurin[14]. This fact is used also here to assign h as the His117 Nε_2H signal[14,15]. The assignment of the rest of paramagnetic signals by means of NOESY spectra is in close agreement with the reported ^{1}H NMR study of the Ni(II) *Pae* azurin[9a,15]. Thus, the far downfield shifted signals, a and b, are connected through NOESY cross-peaks (Fig. 5:4A), and they are assigned to the Cys112 β protons. The stereoespecific assignment of these signals is performed

[14] Moratal, J.M., Salgado, J., Donaire, A., Jiménez, H.R. & Castells, J. (1993) *J. Chem. Soc. Chem. Commun.*, 110.

[15] See Chapter 3, section I.

by analogy with the corresponding signals of the Ni(II)-M121Q azurin, where 1D NOE connectivities with other protons are observed (see below). Additionally, the His117 and His46 imidazole $C_{\delta 2}H$ protons, signals d and f, are found through NOESY connectivities with their vicinal $N_{\varepsilon 2}H$ protons, signals h and j, respectively (Fig. 5:4B). As in the case of *Pae*-wt-Ni(II)-azurin, the two intense cross-peaks connecting signal c and a signal at 7.7 ppm, as well as signals e and l, correspond to the dipolar coupling of the Met121 $C_{\gamma}H_2$ and Gly45 $C_{\alpha}H_2$ protons, respectively (Fig. 5:4B). The Met121 $C_{\beta}H_2$ protons give also a strong NOESY crosspeak and are dipolarly coupled with the Met121 γ_1 proton (Fig. 5:4C). As a difference with regard to the *Pae*-Ni(II)-azurin, no NOE connectivities were found between the three-protons signal i, assigned to the Met121 methyl group, and other Met121 signals. However, the assignment of all the Met121 signals is proved to be correct by comparison of the spectra of the wt and M121Q azurins (Fig. 5:3, see below).

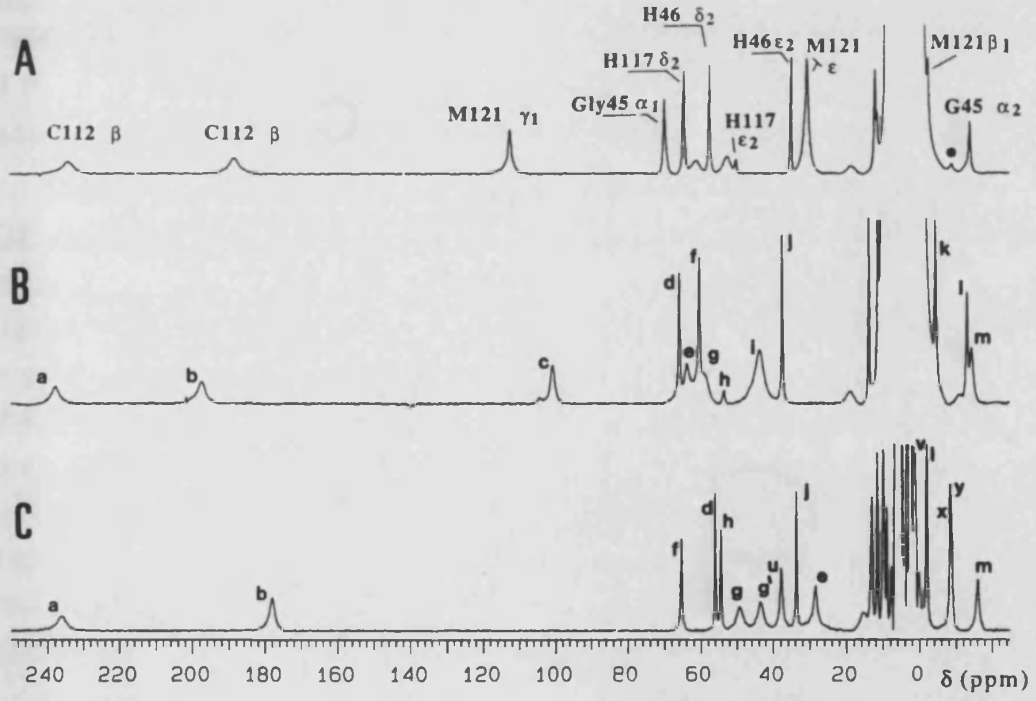

Fig. 5:3. Comparison between the 300 MHz ^{1}H NMR spectra of *P. aeruginosa* Ni(II)-wt azurin (A), *A. denitrificans* Ni(II)-wt azurin (B) and *A. denitrificans* Ni(II)-M121Q azurin (C). Conditions are H_2O solvent, 30 °C, NaH_2PO_4 20 mM, pH 7.0 (A, B) or pH 5.2 (C). The assignment of the signals of the spectrum A are taken from reference 9a. Signals mentioned in the text are labeled with letters.

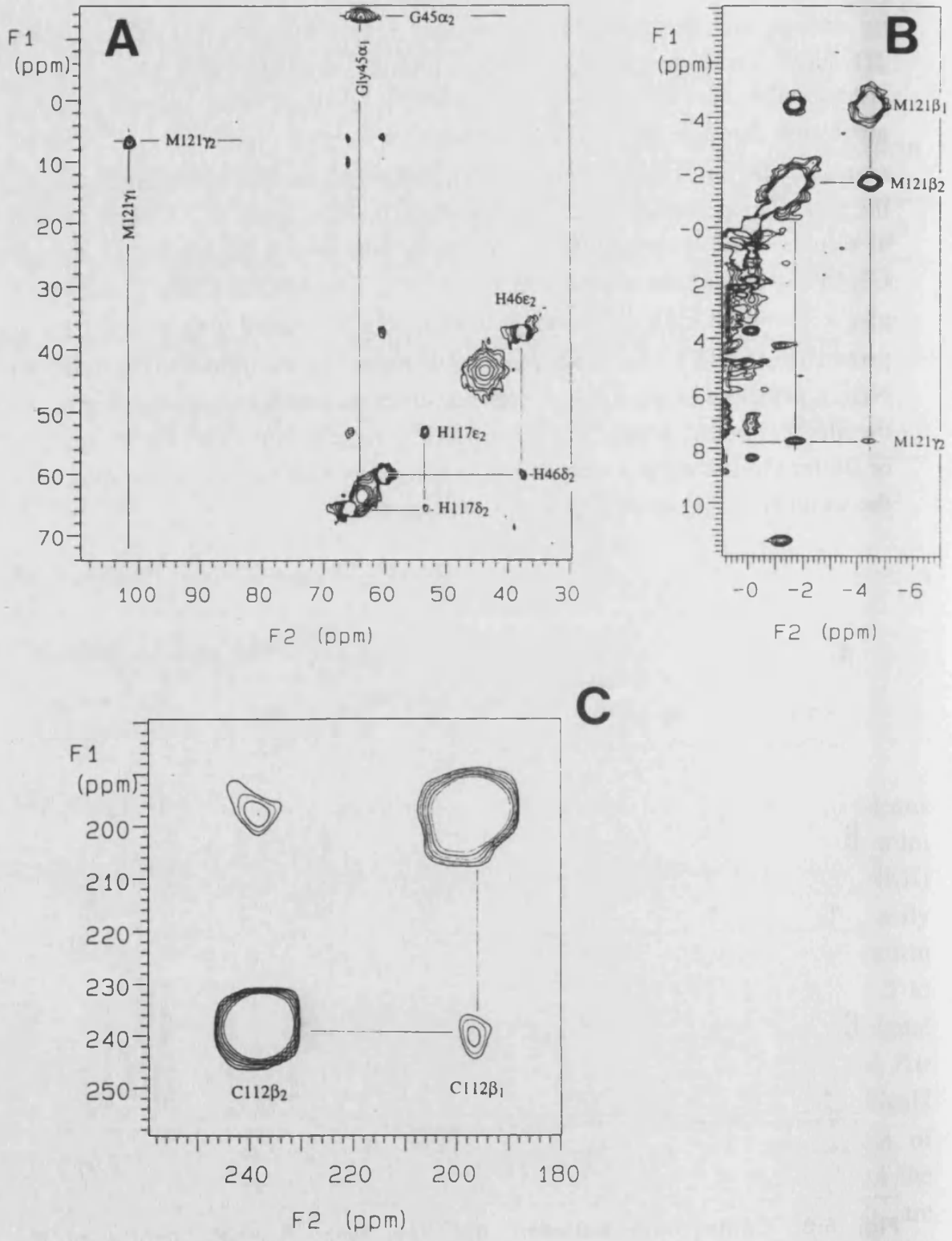

Fig. 5:4. WEFT-NOESY spectra of Ni(II)-wt-azurin (400 MHz, pH 6.0, 30 °C). A is part of a 5 ms mixing time WEFT-NOESY map recorded over a 100 kHz spectral window. Spectrum represented in B has been obtained using a 10 ms mixing time and a 20 kHz spectral window. In C the carrier frequency has been set between the two observed signals and the spectrum has been recorded with a 2 ms mixing time and a 20 ms recycle time. The solvent was H_2O for A, and D_2O for B and C.

M121Q nickel azurin.

The spectrum corresponding to the Ni(II)-M121Q azurin mutant is shown in Fig. 5:3C. The absence of the wt signals i, c and k, confirm their assignment to the Met121. Additionally, a similar pattern is found for the resonances of the three equatorial ligands: Cys112, His117 and His46 (signals a, b, d-h, j in Fig. 5:3B,C). Thus, the two far downfield shifted signals would correspond to the Cys112 beta protons, and this is confirmed by the clear 1D NOE difference signals which are observed upon irradiation of both of them (Fig. 5:5A and B). On the other hand, the two labile proton signals, corresponding to the imidazole $N_{\varepsilon 2}H$ of the two coordinated histidines (signals h and j) can be also paired with their vicinal imidazole $C_{\delta 2}H$ protons (signals d and f, respectively) by means of 1D NOE (Fig. 5:5C,D). The specific assignment of these signals is made according to the same criteria as in the case of the wt azurin spectra[14,15], i.e. taking into account the expected different exchange behavior of the two histidine $N_{\varepsilon 2}H$ signals, due to their different exposition to the solvent in the M121Q-azurin crystal structure[6]. So, since signal h enters fast exchange conditions as the pH is increased (not shown), the pair of signals d,h are assigned to the $C_{\delta 2}H$ and $N_{\varepsilon 2}H$ protons of His 117 and signals f,j to the corresponding protons of His46.

The very broad signals g and g' are also present in the spectra of the wt Ni(II)-azurins. A similar pair of signals can be found in the spectra of the Co(II) derivatives of azurin and stellacyanin[9b,c;16], where they have been tentatively assigned to the imidazole $C_{\varepsilon 1}H$ protons of the coordinated histidines. Irradiation of signal g' (Fig. 5:5E) confirms this assumption through a clear NOE difference signal corresponding to the His46 $N_{\varepsilon 2}H$ proton (signal j). Although irradiation of signal g does not give NOE with signal h, we assign signal g to the His117 $C_{\varepsilon 1}H$ proton due to their close similarity with signal g'. Since signals h and g are quite close, and a strong decoupling have to be used in order to saturate the broad signal g, the absence of an NOE between both signals can be due to a cancellation effect produced during the off-resonance irradiation.

In the azurin structure, the Cys112 beta protons are very close to the Met121 gamma and beta protons, and this is also the case when the Met121 is replaced by a glutamine[6]. Irradiation of signal a gives very weak NOEs with both signals u and x (Fig. 5:5A), but irradiation of signal b gives a clear NOE with signal u (Fig. 5:5B). On the other hand, signals u and x are connected by a strong NOE, as expected for a pair of geminal protons (Fig. 5:5F).

---

[16]Vila, A.J. (1994) *FEBS Lett. 355*, 15.

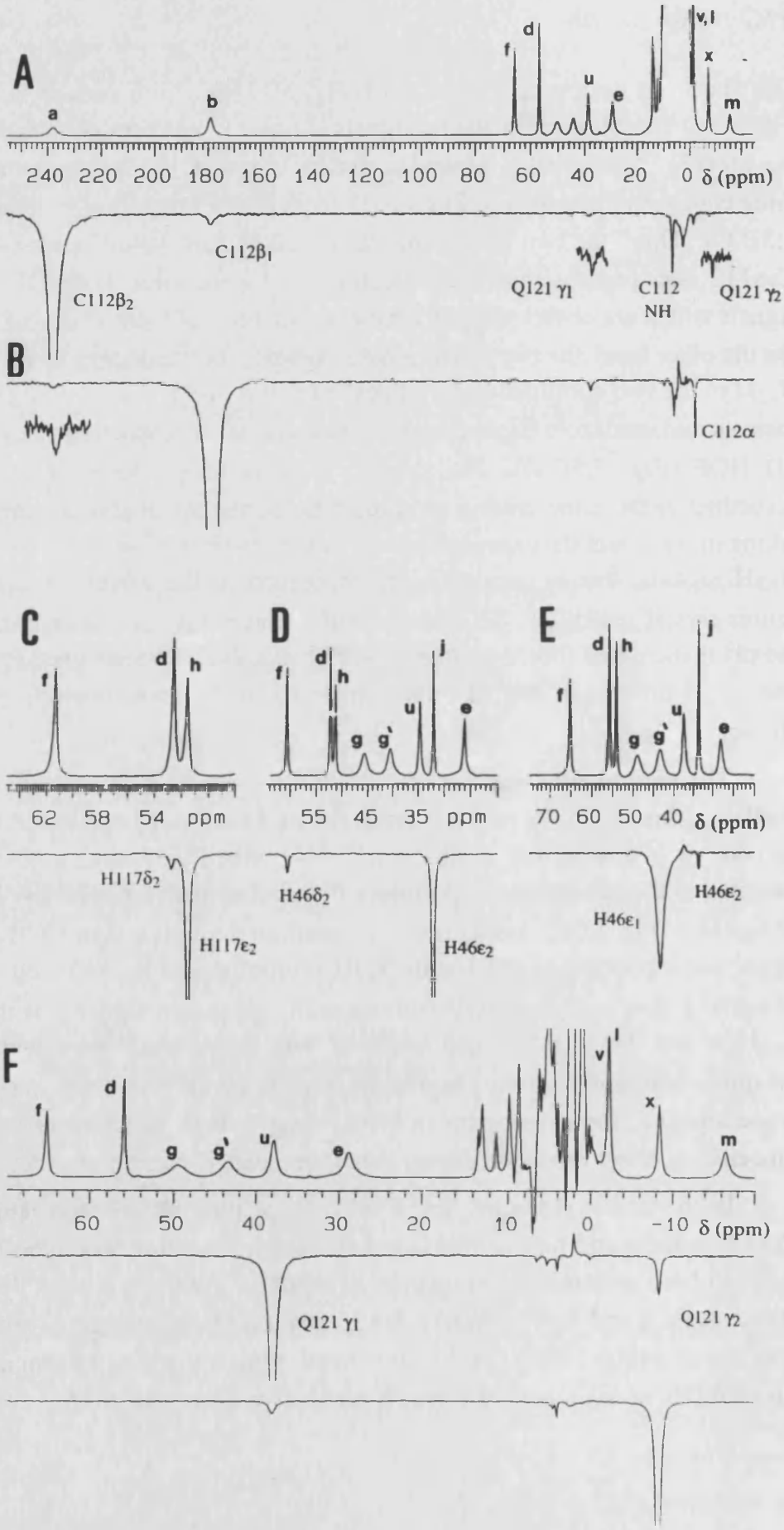
A
a
b
f
d
u
e
v,l
x
m
240 220 200 180 160 140 120 100 80 60 40 20 0 δ (ppm)
C112β1
C112β2
Q121 γ1
C112 NH
Q121 γ2
B
C112α
C
f
d
h
62 58 54 ppm
H117δ2
H117ε2
D
f
d
h
g
g`
u
j
e
55 45 35 ppm
H46δ2
H46ε2
E
f
d
h
g
g`
u
j
e
70 60 50 40 δ (ppm)
H46ε1
H46ε2
F
f
d
g
g`
u
e
v
l
x
m
60 50 40 30 20 10 0 -10 δ (ppm)
Q121 γ1
Q121 γ2

Fig. 5:5. Difference and reference spectra from steady NOE experiments on Ni(II)-M121Q azurin. Conditions are D_2O solvent, pH 5.2, 30 °C (A, B, F) or H_2O solvent, pH 5.2, 50 °C (C-E). Please, notice that signals h, j and y have disappeared in A and F because of exchange with D_2O, and signal positions in C-E do not correspond with the values in Table 5:3 because of the different temperature.

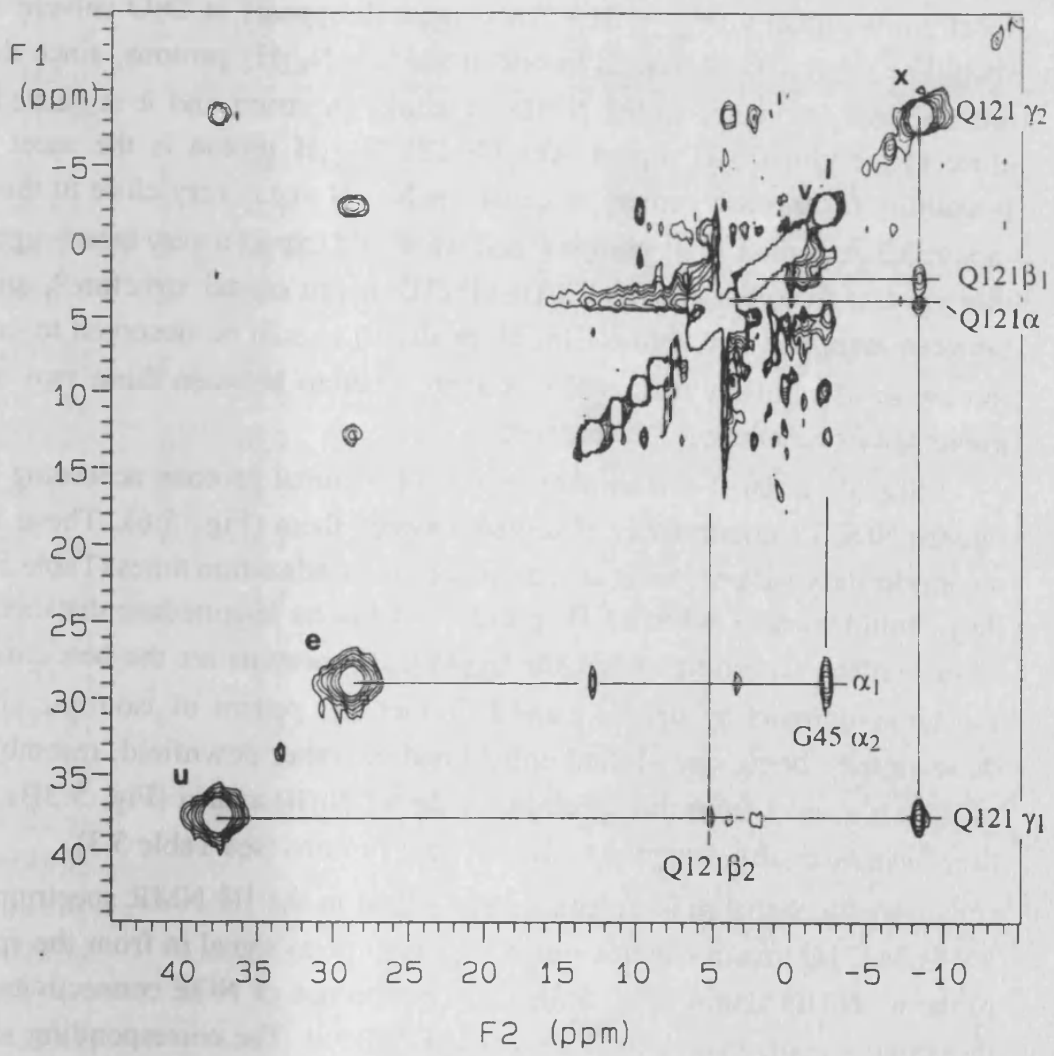

Fig. 5:6. 400 MHz Phase-sensitive ^1H NMR WEFT-NOESY spectrum of Ni(II)-M121Q azurin (4 mM protein concentration, D_2O solvent, pH 5.2, 30 °C). The spectrum was obtained with a 6-ms mixing time, 512 t1 values (1024 scans each) over a 56 kHz bandwidth.

This pattern is compatible with signals u and x being the Gln γ1 and γ2 protons, respectively, and signals a and b the Cys112 β2 and β1 protons. Additionally, these 1D NOE spectra allowed us to find the Cys112 $C_\alpha H$ and NH protons (Fig. 5:5A, B). As it was shown in a complete ^1H NMR study of the wt *Alcaligenes denitrificans* Cu(I)-azurin, the amide proton of Cys112 is in slow exchange with the solvent and it can be observed even in D_2O[17]. No other signal shifted out of the protein envelope is dipolarly connected with signals u and x, so the rest of the Gln121 signals must be buried in the diamagnetic region of the spectrum. A WEFT-NOESY spectrum (Fig. 5:6) interpreted according to the M121Q azurin crystal structure allows us to find the Gln121 β and α protons.

A particularly characteristic resonance in the Ni(II)-M121Q azurin spectrum is signal y (Fig. 5:3C). This signal disappears in D_2O solvent and it should be in principle assigned to one of the Gln $N_{\varepsilon 2}H_2$ protons, since there is not a similar resonance in the Ni(II)-wt azurin spectrum and it is shifted very close to the Gln $C_{\gamma 2}H$ signal. The Gln121 $N_{\varepsilon 21}H$ proton is the most likely possibility for this assignment, because the $N_{\varepsilon 22}H$ one is very close to the metal (about 3.3 Å in the Cu(II) protein)[6] and we would expect a very broad signal for this proton. According to the Cu(II)-M121Q azurin crystal structure[6], an NOE between signals y and x (the Gln121 γ_2 signal) should be observed to confirm the above assignment of signal y, but the overlap between these two signals prevents this coupling to be observed.

Signals e and l are another couple of geminal protons according to the intense NOESY connectivity observed between them (Fig. 5:6). These signals are moderately paramagnetic as indicated by their relaxation times (Table 5:3), so they should correspond to a CH_2 group placed at an intermediate distance to the metal center. According to this, the Gly45 $C_\alpha H_2$ protons are the best candidates for the assignment of signals e and l. In fact, the pattern of isotropic shifts of these signals, being one shifted upfield and the other downfield, resembles that of signals e and l from the spectrum of the wt Ni(II)-azurin (Fig. 5:3B), where they have been also assigned to the Gly45 α protons (see Table 5:3).

Finally, signal m is a characteristic signal in the ^1H NMR spectrum of the Ni(II)-M121Q azurin which seems to be the same as signal m from the spectrum of the wt Ni(II)-azurin (Fig. 5:3B,C). The absence of NOE connectivities from these two signals makes their assignment difficult. The corresponding signal in the spectrum of Ni(II)-wt-azurin from *P. aeruginosa* (signal labeled * in Fig. 5:3A) was tentatively assigned to the Cys112 α or the His46 β1 proton[9a].

[17]Hoitink, C.W.G., Driscoll, P.C., Hill, H.A.O. & Canters (1994) *Biochemistry 33*, 3560.

Table 5:3. Paramagnetic ^1H NMR resonances of *Alcaligenes denitrificans* Ni(II)-wild type azurin and its M121Q mutant. Data from the Ni(II)-M121Q azurin correspond to pH 5.5 (unbuffered sample) and 30 °C. Data from the Ni(II)-wt azurin have been obtained at 30 °C and pH 7 (20 mM phosphate buffer) because the Ni(II) metal complex is not stable at low pH. No effects of the pH and buffer in the NMR spectra (δ and relaxation times) are observed for both wt and M121Q azurin Ni(II) metalloderivatives.

	Ni(II)-wt azurin				Ni(II)-M121Q azurin			
assigned proton	signal	δ (ppm)	T_1 (ms)	$\Delta\nu_{1/2}$ (Hz)	signal	δ (ppm)	T_1 (ms)	$\Delta\nu_{1/2}$ (Hz)
Cys112 β_2	a	238	1.1	800	a	237	0.8	860
Cys112 β_1	b	197	1.4	750	b	178	1.6	470
Cys112 α					v	-2.1	17.6	[a]
Cys112NH						6.2	[b]	[b]
His46 ε_1	g	59	[a]	[a]	g'	43.5	1.5	450
His46 ε_2	j	37.5	14.0	78	j	33.5	17.5	62
His46 δ_2	f	60.3	10.3	160	f	65.1	12.5	68
His46 β_1[d]	m	-14.4	4.0	326	m	-16.3	3.0	300
His117 ε_1	g	59	[a]	[a]	g	49.0	1.6	560
His117 ε_2	h	53.4	[c]	150	h	54.1	12.2	72
His117 δ_2	d	65.7	14.2	120	d	55.7	12.5	100
Gly45 α_1	e	63.7	8.2	330	e	28.9	17.4	325
Gly45 α_2	l	-13.2	10.6	140	l	-2.3	19.4	[a]
Met121 ε	i	43.7	4.9	900				
Met121 γ_1	c	101.1	5.4	390				
Met121 γ_2		7.7	[b]	[b]				
Met121 β_1	k	-4.4	12.9	115				
Met121 β_2		-1.6	16.7	[a]				
Gln121 γ_1					u	37.7	10.1	225
Gln121 γ_2					x	-8.6	11.5	120
Gln121 β_1						2.4	[b]	[b]
Gln121 β_2						5.2	[b]	[b]
Gln121 α						3.9	[b]	[b]
Gln121 ε_{21}					y	-8.9	8.2	[a]

[a] Overlap prevents measuring this value.

[b] Signal buried in the diamagnetic region of the spectrum.

[c] Signal is in partial exchange with the solvent.

[d] Tentative assignment.

These two candidates were chosen as the most probable according to their distance to the metal center (4-5 Å)[10] and the relaxation time of the signal. The Cys112 α proton has been assigned above in the case of the Ni(II)-M121Q azurin to signal v, so signal m can be tentatively assigned as the His46 β1 proton.

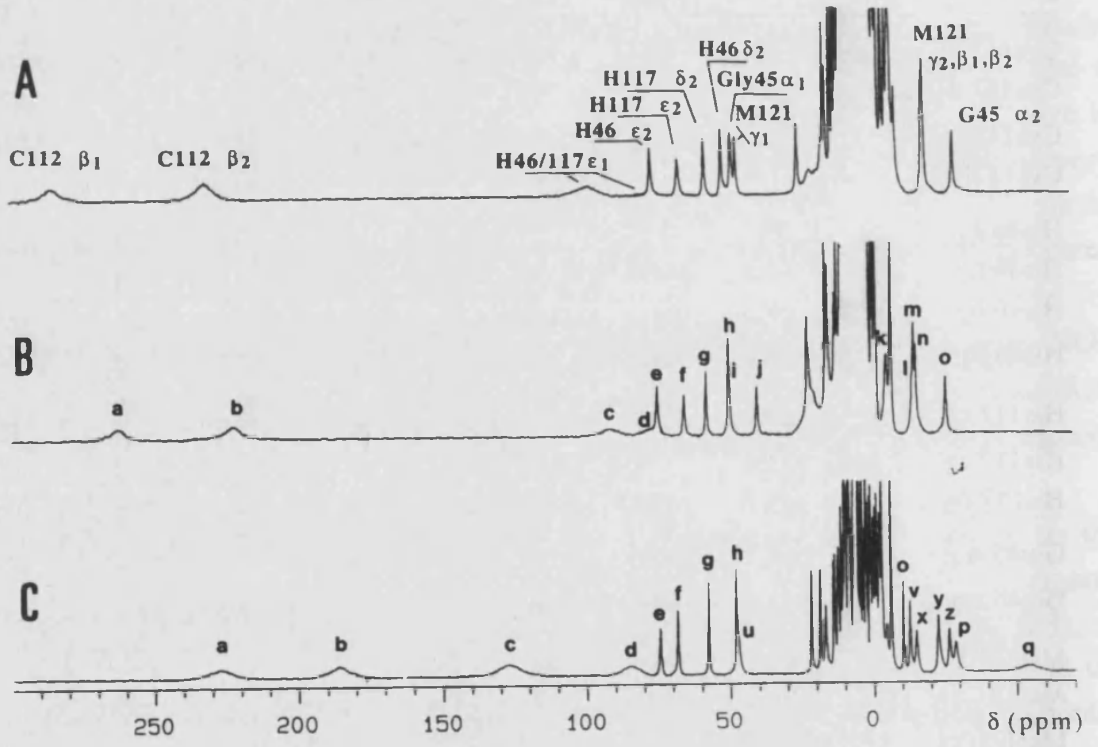

Fig. 5:7. 300 MHz ^{1}H NMR spectra of *P. aeruginosa* Co(II)-wt azurin (A), *A. denitrificans* Co(II)-wt azurin (B) and *A. denitrificans* Co(II)-M121Q azurin (C). Conditions are H_2O solvent, 37 °C, unbuffered solutions at pH 4.5. Assignment of the signals of the spectrum A according to reference 9a. Only those signals mentioned in the text are labeled.

c) ^{1}H NMR spectra of the Co(II) metalloderivatives.

wild-type cobalt azurin.

The ^{1}H NMR spectrum of the *Ade* Co(II)-wt azurin is also very similar to the spectrum of the corresponding *Pae* azurin metalloderivative, and most of their signals are practically in the same position (Fig. 5:7A and B). As in the case of the Ni(II) derivative, the Co(II)-*Ade*-azurin signals can be assigned in agreement with the reported studies of the Co(II)-*Pae*-azurin[9b,c,18]. Thus, the correlations corresponding to the M121 and Gly45 protons can be found in a NOESY map (Fig. 5:8A). As a difference with regard to the *Pae* Co(II)-azurin, the Gly45 amide signal is not clearly observed out of the protein envelope. Although this signal is important for the assignment of the Gly45 α protons[18], here this assignment is supported on their clear dipolar connection with the Val86 $C_{\gamma 1}H_3$ signal (Fig. 5:8A and Fig. 5:9), also observed in the *Pae* Co(II)-azurin derivative[9b,c;19].

The imidazole signals of the coordinated histidines are also paired through NOESY connectivities (Fig. 5:8B), and the specific assignment of the histidines is made following the same reasoning as in the case of wt azurin metalloderivative[18]. However, no clear correlations are found for signals a-d. Signals a and b have been safely assigned to the beta protons of the coordinated Cys112 residue in Co(II)-*Pae*-azurin by site-directed mutagenesis. Additionally, in this protein, 1D NOE correlations are found between both signals a and b, and between signal b and the Met121 $C_{\beta 1}H$ signal[9b]. Although such correlations have not been obtained here[20], the very large shifts of these signal are a distinctive characteristic which permits to assign them by comparison with the analogous signals of the *Pae*-Co(II)-azurin[9b]. With regard to signals c and d, they are tentatively assigned to the imidazole $C_{\varepsilon 1}H$ protons of the coordinated histidines[9b,c]. All these assignments are summarized in Table 5:4.

---

[18]Moratal, J.M., Salgado, J., Donaire, A., Jiménez, H.R. & Castells, J. (1993) *Inorg. Chem. 32*, 3587.

[19]See Chapter 4, section I.

[20]In *Pae* azurin, these NOE correlations were obtained in extreme conditions, due to the broadening of the signals, their large isotropic shifts and their short relaxation times. The slightly shorter longitudinal relaxation times found in this case may impair obtaining NOEs.

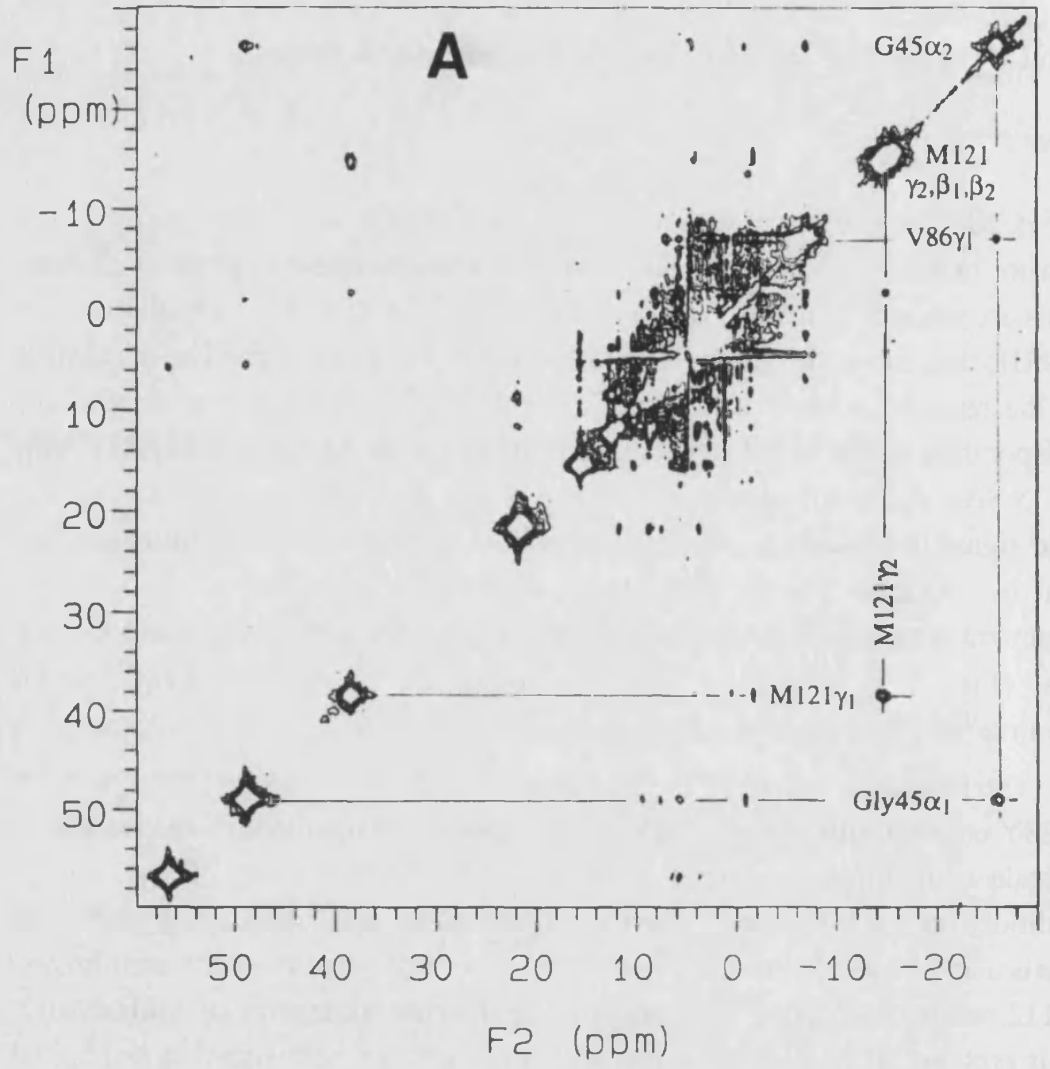

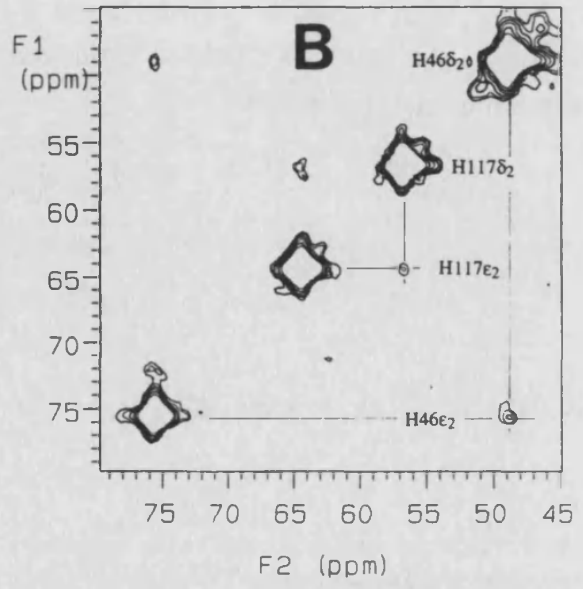

Fig. 5:8. 400 MHz phase sensitive WEFT-NOESY maps of wt-Co(II)-azurin (pH 4.5, 37 °C). Spectrum A was obtained using D_2O as solvent, but it was exchanged to H_2O in B in order to observe the labile imidazole protons of the two coordinated histidines. In both cases 512 FIDs were recorded, 1024 scans each, using a 5 ms mixing time and a 49 ms time between the 90 and 180 pulses of the WEFT pre-sequence, being the acquisition time 20 ms and the relaxation delay, d1, 30 ms.

The overlap of signals corresponding to the Met121 γ_2, β_1 and β_2 protons can not be resolved at any temperature or pH conditions, as it was also observed in the Co(II)-azurin from *P. aeruginosa* (see Fig. 4:7 and Fig. 4:9).

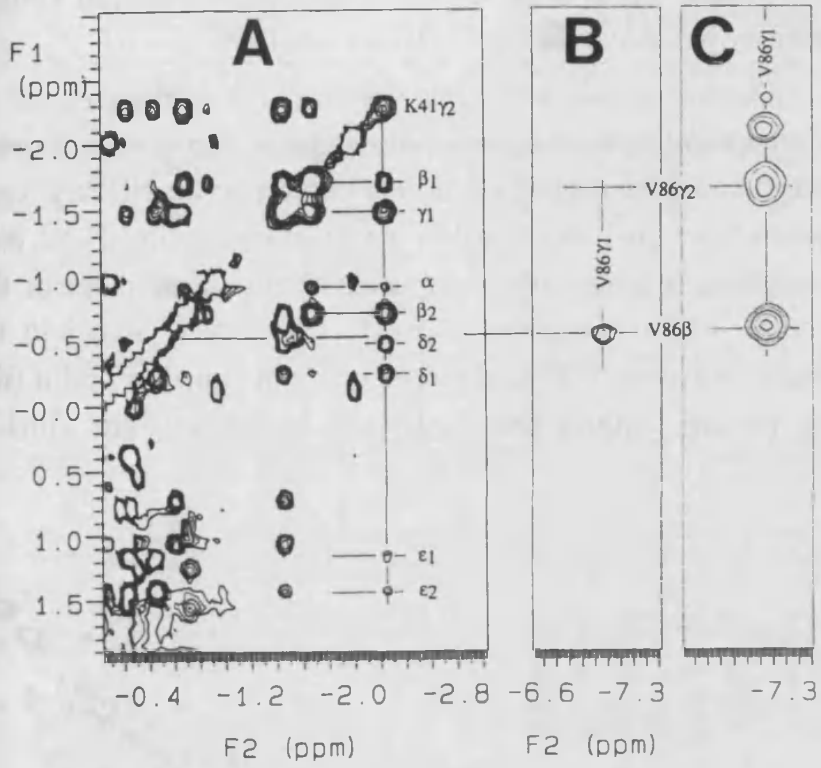

Fig. 5:9. Parts of TOCSY (A, B) and NOESY (C) maps showing some of the correlations of Val86 and Lys41. The spectra are 30 ms (A) and 20 ms (B) spin-lock and 25 ms (C) mixing time.

M121Q cobalt azurin.

Fig. 5:7C shows the spectrum of the Co(II)-M121Q azurin. The two far downfield shifted signals a and b can be assigned to the Cys112 beta protons as in the Co(II) and the Ni(II) derivatives of the wt azurin (see above). Signals corresponding to the two coordinated histidines are also assigned by means of NOESY correlations between the imidazole $C_{\delta 2}H$ and $N_{\varepsilon 2}H$ protons (Fig. 5:10)[18] (see above and Table 5:4).

On the other hand, when we compare the spectra of the Co(II)-wt and Co(II)-M121Q azurins, very clear differences are found in the signals corresponding to the two potential axial ligands. As shown in Fig. 5:10, only a couple of well shifted protons, one placed upfield and the other downfield, exhibit a strong NOESY connectivity (signals u and v). These can be assigned to a CH_2 group and they are dipolarly connected with signals x and y, which in turn present a strong NOESY cross-signal between them. This pattern fits well with signals u, v, x and y being the γ and β protons of the Gln121 residue. The

Gly45 α signals can be found again through their NOESY connectivities with the Val86 γ1 methyl signal (Fig. 5:10, see also the Val86 spin system in Fig. 5:11), as it is shown above for the Co(II)-wt azurin.

It is important to notice that, as we observed in the case of the nickel derivative, an upfield shifted exchangeable signal is also observed in the Co(II)-M121Q azurin spectrum (signal z). In this case, a weak NOESY crosspeak is found between this signal and signal v, assigned to the Gln121 γ2 proton (Fig. 5:10). This crosspeak leads to the assignment of this signal to one of the Gln121 $N_{\varepsilon 2}H_2$ protons as it is suggested above for the similar signal in the Ni(II)-M121Q azurin. Since no NOE is observed between signals z and u (the Gln121 γ1 proton), we can confirm that signal z is most likely the Gln121 $N_{\varepsilon 21}H$ proton.

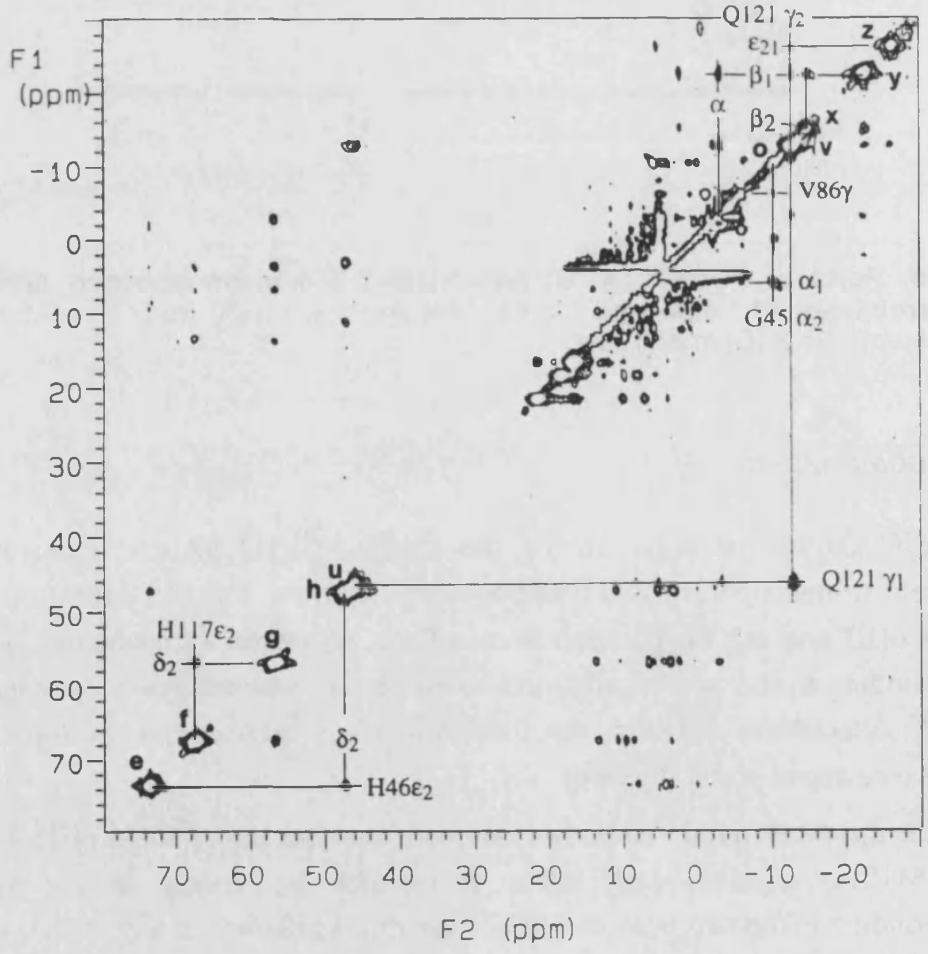

Fig. 5:10. 400 MHz Phase-sensitive ^{1}H NMR WEFT-NOESY spectrum of Co(II)-M121Q azurin (6 mM protein concentration, H_2O solvent, pH 4.7, 37 °C). The map was collected using a 10-ms mixing time and 512 t1 values (2024 scans each) over a 70 kHz bandwidth.

Finally, among the principal signals of the NMR spectrum, signals p and q remain to be assigned. Signal q is even broader than signals a-d and must correspond to a proton very close to the metal (around 3 Å). The His117 β protons and the His46 α and β2 protons fit this condition according to the Cu(II)-M121Q azurin structure[6]. With regard to signal p, no NOE with the rest of isotropically shifted signals was obtained. Again in this case, as we suggested for signal m from the Ni(II)-M121Q azurin spectrum, the His46 β1 proton seems to be the best possibility.

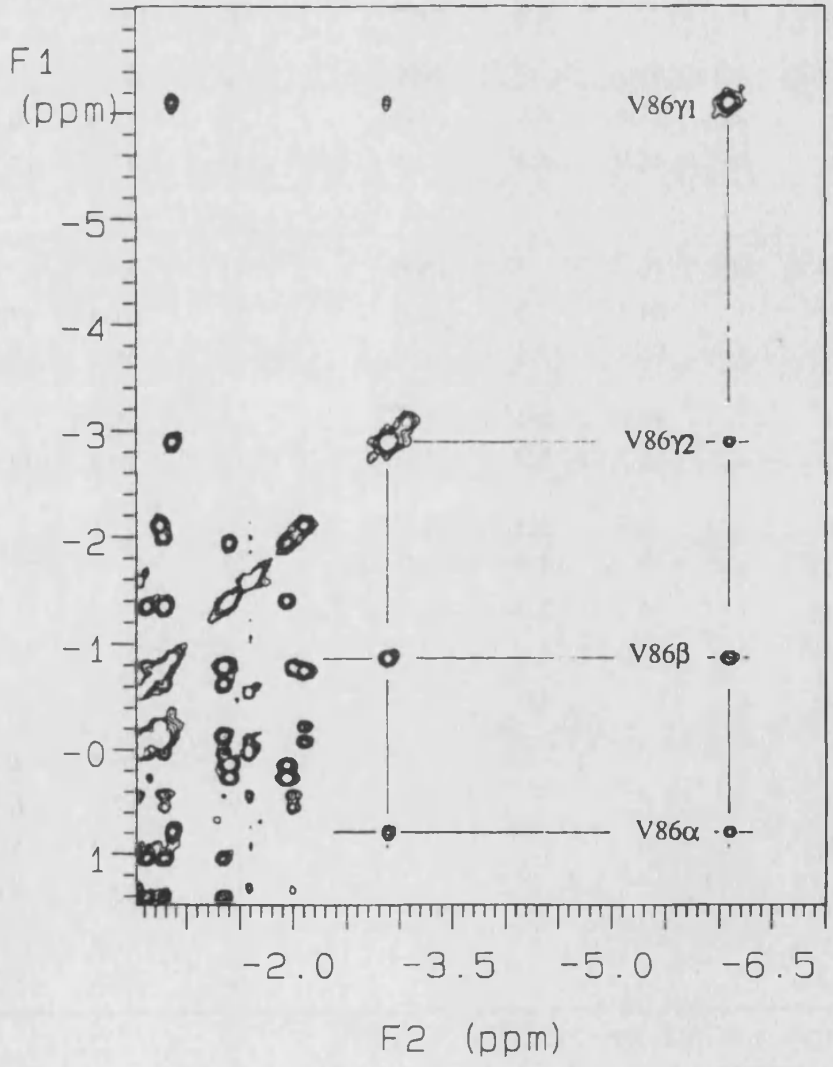

Fig. 5:11. Assignment of the Val86 proton signals in Co(II)-M121Q azurin. The map shows the TOCSY pattern typical of a valine spin system whose protons are moderately paramagnetic. Val86 is the only valine which fits these conditions, according to the *Ade* azurin crystal structure[4,6].

Table 5:4. Paramagnetic ^{1}H NMR resonances of *Alcaligenes denitrificans* Co(II)-wild type azurin and its M121Q mutant. Data correspond to pH 4.5 (unbuffered solutions) and 37 °C in both cases.

	Co(II)-wt azurin				Co(II)-M121Q azurin			
assigned proton	signal	δ (ppm)	T_1 (ms)	$\Delta\nu_{1/2}$ (Hz)	signal	δ (ppm)	T_1 (ms)	$\Delta\nu_{1/2}$ (Hz)
Cys112 β	a	262	0.5	1700	a	224	*c*	2100
Cys112 β	b	222	0.4	1900	b	183	*c*	2600
His46/117 ε_1	c	90	*c*	2000	c	125	*c*	2000
His46 ε_2	e	75.6	4.9	240	e	73.4	6.1	167
His46 δ_2	h	48.9	6.4	*a*	h	47.2	12.7	140
His46 β_1 *d*					p	-28.6	2.2	430
His117/46 ε_1	d	76	*c*	1800	d	83	*c*	2600
His117 ε_2	f	64.4	7.3	230	f	67.4	7.8	138
His117 δ_2	g	56.7	12.4	180	g	56.8	15.0	100
Gly45 α_1	i	49.0	6.4	*a*		5.9	*b*	*b*
Gly45 α_2	o	-26.3	3.5	241	o	-10.5	22.5	77
Met121 ε	k	-5.7	2.5	439				
Met121 γ_1	j	39.2	4.8	245				
Met121 γ_2	l	-14.7	5.3	*a*				
Met121 β_1	m	-15.0	6.4	*a*				
Met121 β_2	n	-15.7	5.0	*a*				
Gln121 γ_1					u	46.4	4.2	320
Gln121 γ_2					v	-12.8	6.8	140
Gln121 β_2					x	-15.0	3.2	280
Gln121 β_1					y	-22.7	4.0	250
Gln121 α						-3.2	*a*	*a*
Gln121 ε_{21}					z	-26.4	3.2	260

a Overlap prevents measuring this value.

b Signal buried in the diamagnetic region of the spectrum.

c $T_1 \leq 0.2$ ms.

d Tentative assignment.

DISCUSSION.

a) Absorption spectra.

Studying the electronic spectra in Co(II) and Ni(II) azurins is a frequently used approach to discuss the electronic and structural properties of the type 1 metal site, since LMCT and LF absorption systems are normally well separated in these metallosubstituted proteins[12a,b]. In the case of the LF bands of the Co(II)-azurins, the magnitude of the extinction coefficients can be related with the coordination geometry of the metal center. For both wt and M121Q Co(II) derivatives the intensity of these bands is very similar and it is clearly in the range typical for distorted tetrahedral Co(II) complexes (ε_{max} > 250 M^{-1} cm^{-1})[21,22]. This interpretation agrees with the crystal structures of the Zn(II)-wt-azurin[11], the Ni(II)-wt-azurin[23] and the Cu(II)-M121Q azurin[6].

With regard to the LMCT transitions, their characteristics have been recently studied in detail by H.B. Gray and coworkers for various Met121 *Pae* azurin mutants, and they have found that the position of these bands depends on the nature of the 121 residue[12c]. Thus, the blue shifts of the LMCT bands are interpreted as due to an inner-sphere carboxylate interaction in the case of the M121E mutant, or an outer-sphere interaction of the polar carboxylate group in the case of the M121D mutant[12c]. For the M121Q azurin metalloderivatives studied here, LMCT bands are also blue shifted with regard to the wt azurin metalloderivatives (Fig. 5:2). In the case of the Ni(II)-M121Q azurin the main LMCT band is placed almost in the same position as the corresponding band in the Ni(II)-M121D azurin, while the second LMCT band is at 320 nm as the corresponding band in the Ni(II)-M121E azurin (Table 5:2). The Co(II)-M121Q azurin bands are less shifted than those from the Co(II) derivatives of both the M121D and M121E azurin mutants, and their position is very similar to the bands of the Co(II)-M121G azurin (Table 5:1).

These results are in agreement with the presence of an oxygen from the carbonyl of the Gln121 side chain in the metal coordination sphere, which would be the main cause for the blue shifts of the absorption bands[12c]. The fact that

---

[21]Rosenberg, R.C., Root, C.A., Wang, R.-H., Cerdonio, M. & Gray, H.B. (1973) *Proc. Natl. Acad. Sci. U.S.A. 70,* 161.

[22]Bertini, I. & Luchinat, C. (1984) in *Advances in Inorganic Biochemistry* (G.L. Eichorn & L.G. Marzilli, eds) p. 71, Elsevier, New York.

[23]Nar, H., Huber, R., Messerschmidt, A., Filippou, A.C., Barth, M., Jaquinod, M., van de Kamp, M. & Canters, G.W. (1992) *Eur. J. Biochem. 205,* 1123.

these shifts are less dramatic than those observed for the M121E mutant, where oxygen is most probably also coordinated[12c], can be due to the lower polar character of the glutamine carbonyl oxygen with regard to a glutamate carboxylic oxygen. On the other hand, the similarity between the Co(II)-M121Q and Co(II)-M121G azurin bands is compatible with the presence of an oxygen from a water molecule coordinated to the metal in the case of the second protein, as already suggested[12c].

b) ^{1}H NMR spectra of wt and M121Q azurin metalloderivatives.

As discussed in the literature[24,25], the NMR spectra of paramagnetic metalloproteins contain important structural information which can be extracted from an analysis of the isotropic shifts and the relaxation properties of previously assigned resonances. The ^{1}H NMR spectra of Ni(II) and Co(II) derivatives of azurins from two different bacterial sources (*Pseudomonas aeruginosa* and *Alcaligenes denitrificans*) are very similar. In other words, signals corresponding to analogous protons in the structure of the two molecules display almost the same isotropic shifts and relaxation times and, as in the case of the His117 Nε_2H signals, show also the same behavior, like the variations in the exchange rate with the solvent due to changes in the solution conditions. The structure of the metal site in both azurins is practically identical, and the close similarity between the paramagnetic-NMR spectra is just an expression of such structural resemblance. The slight differences observed can be due to small variations in the first coordination sphere or in some aminoacid positions in the second coordination sphere. So, the same conclusions derived from the studies of the cobalt and nickel derivatives of *Pae* azurin[9] can be stated here. Mainly, the existence of paramagnetic signals presenting large isotropic shifts and corresponding to the five possible coordinating residues leads to the conclusion that all of them exhibit contact interaction with the paramagnetic center.

This interpretation can be safely accepted in the case of the three equatorial ligands, due to the dramatic shifts of the Cys112 β protons, and the pattern observed for the histidine signals which is typical of coordination to the paramagnetic center. However, evaluating the evidence for coordination of Met121 or Gly45 is more problematic also because there seems to be disagreement with other spectroscopic data (as the intensity of the d-d

---

[24]a) Bertini, I. & Luchinat, C. (1986) *NMR of Paramagnetic Molecules in Biological Systems*, The Benjamin/Cummings Publishing Company, Menlo Park. b) La Mar, G.N., Horrocks, W.D. & Holm, R.H. (1973) *NMR of Paramagnetic Molecules*, Academic Press, New York.

[25]Bertini, I., Turano, P. & Vila, A. (1993) *Chem. Rev. 93*, 2833.

transitions) and the available structural information (which describes a tetrahedral metal site with the methionine sulfur placed 3.3 Å away from the metal)[23,11]. The structural rigidity in the metal site would prevent the simultaneous approach of both axial ligands. Coordination by the Gly45 carbonyl oxygen is more probable according to the crystal structure. There are not examples in the literature of ^{1}H NMR spectra of Co(II) or Ni(II) complexes with a sulfur methionine as a ligand, but comparison of the Met121 signals with those from the strongly coordinated Cys112 permit to conclude that the coordination of the Met121, if present, has to be very weak. The observed shifts for some of the Met121 signals (the γ1 proton signal in both Co(II) and Ni(II) derivatives and the methyl signal in the Ni(II)-azurin) are ascribed primarily to the pseudocontact contribution, as expected for tetrahedral Co(II) and Ni(II) complexes (it should be larger for the Ni(II) ones).

In the case of the M121Q azurin metalloderivatives, we have quite a different scenery. First, we notice that the observed NMR results are only compatible with the coordination of the metal through the Gln121 side chain $O^{\varepsilon 1}$, since the $N_{\varepsilon 2}H$ signal should be broadened beyond detection in case of coordination by the amide Gln121 $N^{\varepsilon 2}$. So, the two alternative axial ligands (the carbonyl oxygens of Gly45 and Gln121) are now chemically similar and the choice for one of them must be dictated by the structural restrictions of the metal site and the geometrical preferences of the metal. If we look at the isotropic shifts of the Gln121 signals, we find that they are slightly larger than the Met121 signals of the wt protein in the case of the Co(II) metalloderivatives. But, conversely, the Met121 signals are significantly more shifted than the Gln121 signals in the case of the Ni(II)-substituted proteins. The γ and β protons from a methionine and a glutamine side chain which coordinate through their S^{δ} and O^{ε} atoms, respectively, are not exactly equivalent in terms of their contact interaction with the metal center, since the glutamine protons are separated from the metal by an additional (double) bond. Thus, supposing we have the same pseudocontact contributions in both cases, the isotropic shifts should be larger in the case of the Met121 signals of the wt protein than in the case of the Gln121 signals of the M121Q protein. This could explain why the Gln121 signals are less shifted than the Met121 ones in the Ni(II) derivatives. Analogously, in the case of the cobalt-derivatives, we can conclude that the Gln121 residue interacts more strongly with the Co(II) ion than the Met121 does.

Considering the Gly45 resonances, we find that for both Ni(II) and Co(II) derivatives of the M121Q azurin they are significantly less shifted than in the corresponding wt metalloderivatives. Moreover, their relaxation times are also larger, indicating a weaker interaction with the paramagnetic metal center in both

cases. Various different NMR patterns of protons from possible axial ligands in cobalt-substituted blue-copper proteins are represented in Fig. 5:12. As it can be seen, the Met121 signals in the wt-Co(II)-azurins are shifted at intermediate positions between those corresponding to a non coordination, as in the *Pae* Co(II)-C112D azurin[9b], and a close coordination, as the Met99 in the Co(II)-amicyanin[26]. On the other hand, the Gln121 and Gly45 residues, which interact with the metal through their side-chain and back-bone carbonyl oxygens, respectively, display similar isotropic shifts for their $C_\gamma H_2$ and $C_\alpha H_2$ protons when they are coordinated.

Although the pattern of the signals from the equatorial ligands is similar in the wt and M121Q mutant metalloderivatives, some important differences can be observed. Signals from the two Cys112 β protons are less shifted in the Co(II)-M121Q azurin than in the corresponding wt metalloderivative. Since the contact contribution to the isotropic shifts of these protons have to be clearly dominant, we conclude that the unpaired spin delocalization over the Cys112 ligand is smaller in the M121Q azurin. The origin of this effect can be a reduction in the orbital overlap between the cobalt and the cysteine sulfur, due to the movement of the metal out of the equatorial plane because of a stronger axial coordination. Moreover, the relaxation times of these signals decrease significantly indicating that these protons are closer to the paramagnetic center as a consequence the reorganization of the metal site. Additionally, changes are also observed in at least one of the $C_{\varepsilon 1}H$ histidine signals (signal c in the Co(II)-M121Q azurin spectrum), which is now more shifted, although no other histidine signal is significantly displaced with regard to the positions in the spectrum of the wt protein.

For the Ni(II) metalloderivatives, differences in the resonances from the equatorial ligands are less marked. Variations in the isotropic shifts affect only one of the Cys121 β protons, whose relaxation time increases in the case of the Ni(II)-M121Q azurin. With regard to the histidine signals some variations are also observed which indicate that the structure of the metal site has changed, but they are not so significant as in the case of the cobalt derivatives. So one interpretation is that the tetrahedral character of the Ni(II)-M121Q metal site is less pronounced than in the case of the Co(II)-M121Q, being the metal-O^{ε}_{Gln121} bond weaker in the Ni(II) derivative. The fact that the Gly45 α signals are more shifted in the Ni(II)-M121Q azurin would agree with this conclusion.

[26]Salgado, J. & Kalverda, A., unpublished results.

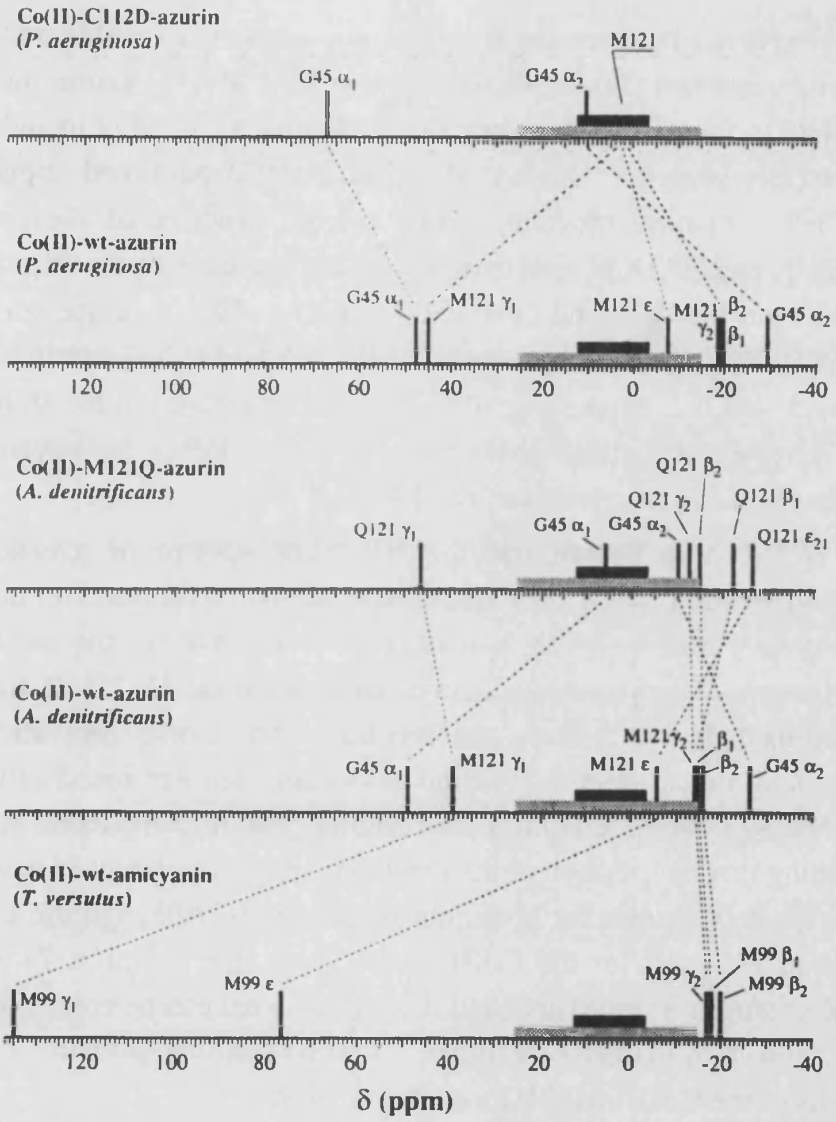

Fig. 5:12. Schematic representation of the hyperfine shifts of protons from the two possible axial ligands in various cobalt-substituted blue-copper sites (black and grey bars represent the diamagnetic and pseudodiamagnetic regions of the spectrum). The Co(II)-amicyanin[26], at the bottom of the figure, represents one extreme case, in which the coordination of methionine is clear. In amicyanin, the carbonyl oxygen equivalent to O45 in azurins, is placed too far from metal to be coordinated, and the metal ion ligates to Met99 adopting a tetrahedral geometry[27]. In the opposite side (top of the figure) is the *Pae* C112D mutant[9b], where the Asp112, replacing the cysteine equatorial ligand, binds bidentate to the metal and takes Met121 out of the coordination sphere. The wt-Co(II)-azurins are intermediate cases which present a weak Met121 ligand. Cases of clear coordination of the Gly45 carbonyl are both wt-Co(II)-azurins, while the Co(II)-M121Q azurin is an example of a non ligated Gly45.

[27]Romero, A., Nar, H., Messerschmidt, A., Kalverda, A., Canters, G.W., Durley, R. & Mathews, F.S. (1994) *J. Mol. Biol. 236*, 1196.

c) The Met121Gln azurin mutant and the stellacyanin metal site.

The coincidence between the spectroscopic properties (visible and EPR spectra) of stellacyanin and the *Alcaligenes denitrificans* M121Q azurin mutant is a solid argument in favor of the presence of a glutamine as the axial ligand in the former blue copper protein[6]. Other studies like ^{111m}Cd perturbed angular correlation (PAC)[28], structural modeling based on the structure of the cucumber basic protein[7a], and ENDOR spectroscopy[7b], also agree with the idea of a Gln side chain as the fourth ligand in stellacyanin. The absorption spectra of the Co(II) and Ni(II) derivatives of both stellacyanin and the M121Q azurin are very similar (tables 1 and 2), supporting the above interpretation of the stellacyanin metal site. A recent crystallographic study of the cucumber stellacyanin-like copper protein (SLCP) confirms these results[29].

It has been shown that the ^{1}H NMR spectra of azurin paramagnetic metalloderivatives are a very informative method to fingerprint the metal site of the protein[9], and we have demonstrated above that for the same coordination environment of the paramagnetic metal a very similar ^{1}H NMR spectrum should be obtained. If we compare the spectra of the Co(II) derivatives of M121Q azurin and stellacyanin[16], we find also many similarities. Resonances of the coordinated cysteine and histidine residues present comparable isotropic shifts, indicating that the position of the metal with regard to the three equatorial ligands has to be very similar for both cobalt derivatives. Although the axial ligand has not been assigned for the Co(II)-stellacyanin, the signal at 71 ppm in its ^{1}H NMR spectrum[16] is a likely candidate. This signal can be cross-correlated by 1D NOE with an upfield shifted signal[30], thus resembling the pair of Gln121 $C_\gamma H_2$ protons of the Co(II)-M121Q azurin spectrum.

Finally, an important difference between the Co(II)-stellacyanin and the Co(II)-M121Q azurin spectra is the upfield shifted exchangeable signal z present in the latter (assigned here as the Gln121 $N_{\varepsilon 21}H$ proton), since no labile proton signal of these characteristics is reported in the NMR spectrum of Co(II)-stellacyanin[16,31]. It has been suggested that the metal center in stellacyanin is more exposed to the solvent than the azurin metal center, on the basis of the

---

[28]Danielsen, E., Bauer, R., Hemmingsen, L., Andersen, M.L., Bjerrum, M.J., Butz, T., Tröger, W., Canters, G.W., Hoitink, C.W.G., Karlsson, G., Hansson, Ö. & Messerschmidt, A. (1995) *J. Biol. Chem. 270*, 573.

[29]Nersissian, A.M., Nalbandyan, R.M., Herrmann, R.G. & Valentine, J.S., unpublished resuts.

[30]Vila, A., unpublished results.

[31]Dahlin, S., Reinhammar, B. & Ångström, J. (1989) *Biochemistry 28*, 7224.

higher exchange rate of the $N_{\varepsilon 2}H$ protons from both coordinated histidines[16]. A fast exchange affecting also the Gln97 $N_{\varepsilon}H_2$ protons could explain the absence of the corresponding signal in the Co(II)-stellacyanin spectrum.

CONCLUDING REMARKS.

The Ni(II) and Co(II)-wt azurin metalloderivatives from both *Pseudomonas aeruginosa* and *Alcaligenes denitrificans* present almost the same ^1H NMR spectrum as expected for a similar coordination environment. Signals from the five possible metal ligands are assigned. Cobalt(II) and nickel(II) are clearly coordinated to the Cys112, His46, His117 and Gly45 side chains. Additionally, some signals from the Met121 residue present large isotropic shifts suggesting also a weak coordination of this residue.

The spectra of Ni(II) and Co(II)-M121Q azurin confirm the assignments of the Met121 signals in the wt metalloderivatives. The characteristics of the assigned resonances indicate that the metal center is tetrahedral for both Ni(II) and Co(II)-M121Q azurins. The metal has moved towards the Gln121 axial position and coordinates to this residue through the side chain carbonyl O, while the Gly45 O is not coordinated. This tetrahedral character seems to be less clear in the case of the Ni(II) derivative than for the Co(II) one.

The spectra from both Co(II)-stellacyanin and Co(II)-M121Q are remarkably similar for those signals corresponding to the cysteine and histidine ligands, and a more complete assignment of the former should be made in order to compare the signals from the fourth ligand. These data represent additional evidence for a glutamine side chain in the axial ligand position of stellacyanin as already suggested in other investigations[6,7], and are in agreement with a recent structural determination of a stellacyanin-like cucumber protein[29].

Chapter 6

Final conclusions.

Cobalt and nickel as NMR-probes for the azurin copper site.

The use of paramagnetic metals to probe the metal site in blue copper proteins, which have been exploited for decades in electronic spectroscopy studies, can be also of great help in NMR as it was anticipated by Hill and coworkers[1]. Being blue copper proteins in general of small size, the complete NMR structural analysis of the diamagnetic species (like the reduced copper protein) can be achieved by the standard methodology. Conversely, the complete analysis of a paramagnetic NMR spectrum cannot be performed in a conventional way and needs help from already existing structural information. Despite these drawbacks, the use of a paramagnetic probe permits selecting and analyzing the metal site signals out of the protein envelope and introduces powerful structural-related parameters like isotropic shifts and paramagnetic relaxation. A study of the contact-shifted signals give important information about the first coordination sphere, like the nature of the ligands, the coordination geometry and the strength of the ligand-metal interaction. Additionally, even subtle structural variations can be detected and studied due to the increased sensitivity of the hyperfine shifted signals. As it is found in the X-ray structures of azurin metalloderivatives[2], apart

---

[1] Hill, H.A.O., Smith, B.E., Storm, B.C. & Ambler, R.P. (1976) *Biochem. Biophys. Res. Comm. 70*, 783-790.

[2] a) Nar, H., Huber, R., Messerschmidt, A., Filippou, A.C., Barth, M., Jaquinod, M., van de Kamp, M. & Canters, G.W. (1992) *Eur. J. Biochem. 205*, 1123. b) Moratal, J.M., Romero, A., Salgado, J., Perales-Alarcón, A. & Jiménez, H.R. (1995) *Eur. J. Biochem. 228*, 653. c) Blackwell, K.A., Anderson, B.F. & Baker, E.N. (1994) *Acta Crystallogr. D50*, 263.

from small variations in the coordination geometry, the overall structure of the protein remains unchanged with regard to the copper protein. Although the cobalt and nickel azurins are obviously not functional, these findings validate their use as substitutes for copper in the structural investigation of type 1 copper proteins.

For similar coordination environments as in *Pseudomonas aeruginosa* and *Alcaligenes denitrificans* wt azurins, the Ni(II) and Co(II) metalloderivatives present almost the same ^{1}H NMR spectrum. This spectrum can be considered as a finger-print of the azurin metal site, in which the more significant features are: i) the large shifts of the Cys112 $C_\beta H_2$ signals, that witness a very efficient orbital overlap between the cysteine S^γ and the metal ion and the existence of important unpaired-spin delocalization over this ligand residue; ii) the pattern of the methylene resonances of the axial ligands (the Gly45 $C_\alpha H_2$ and the Met121 $C_\gamma H_2$), which are shifted in opposite directions (one upfield and the other downfield) probably due to a different sign of the pseudocontact contribution depending on the orientation of these protons with regard to the magnetic axis; iii) and the pattern of the histidine resonances, specially the observation of both $N_{\varepsilon 2}H$ histidine signals at low pH but only the His46 $N_{\varepsilon 2}H$ at high pH.

The Co(II)-stellacyanin[3] and Co(II)-M121Q azurin spectra have also significant similarities, especially for those signals corresponding to the cysteine and histidine ligands. Although a more complete assignment of the former should be made in order to compare the signals from the fourth ligand, the results are in agreement with the presence of a glutamine side chain in the axial position.

The structure of the metal site.

Distorted tetrahedral coordination environments, leading to geometries intermediate between tetra and penta-coordination, are difficult to evaluate and give raise to apparent contradictions. The azurin metal site provides one of these examples. The existence of two possible axial ligands and a set of three closely interacting equatorial ligands conditions the coordination of the metal. Thus, it adopts distorted coordination geometries whose main structural feature is the equatorial trigonal plane. As a consequence, the metal can approach more the Met121 axial ligand, as in the case of the native Cu(II)[4], or the Gly45 axial

---

[3] **a)** Vila, A.J. (1994) *FEBS Lett. 355*, 15. **b)** Dahlin, S., Reinhammar, B. & Ångström, J. (1989) *Biochemistry 28*, 7224.

[4] a) Baker, E.N. (1988) *J. Mol. Biol. 203*, 1071. b) Nar, H., Messerchmidt, A., Huber, R., van de Kamp, M. & Canters, G.W. (1991) *J. Mol. Biol. 221*, 765.

ligand, as in the Zn(II)[2a], Ni(II)[2b], and probably Co(II), but it always stays close to the equatorial plane. In all these situations there is doubt about the existence of interaction with the fifth ligand, and while Gly45 is considered to be only coulombically interacting in the case of Cu(II)-azurin[5], Met121 seems to be out of the coordination sphere in the other metalloderivatives[2].

For the Ni(II)-azurin, the crystallographic distance corresponding to the supposed fifth ligand, the Met121 S^{δ}, is too large for a coordination bond (3.30 Å). However, some spectroscopy properties, specially the magnitude of the isotropic shifts, suggest possible penta-coordination. It has been shown in an NMR study of the Cu(II)-amicyanin that the covalent interaction between the copper and the axial Met99 is very weak, leading to only a 1% unpaired spin density over this ligand[6]. The corresponding interaction between the Cu(II) and Met121 in azurin is even weaker[6], since the ligand-metal distance is larger in this case[4]. In view of these results, even a very weak coordination of the Met121 in Co(II) or Ni(II) is hard to imagine, suggesting that a very large pseudocontact interaction is present in these cases, which could be the origin of the large isotropic shifts of the Met121 signals in the absence of contact interaction. Important pseudocontact contribution is expected for tetrahedral Ni(II) complexes, but even in this case no pseudocontact shifts as large as 100 ppm are reported in the literature[7]. On the other hand, the existence of relatively sharp signals (large relaxation times) in the NMR spectrum of Ni(II)-azurin suggest more a tetrahedral site than a penta-coordinate one, in line with the X-ray structure. For the Co(II)-azurin, however, is difficult to admit that the Met121 isotropic shifts are only due to pseudocontact origin, since it also would mean that the metal site is tetrahedral, for which no significant magnetic anisotropy and pseudocontact shifts are expected[4a]. Is clear that a qualitative analysis of the isotropic shifts is not enough in this case and a separation of the contact and pseudocontact contributions is needed to make a clear conclusion. This could be achieved by single crystal magnetic susceptibility measurements[4a], which are not available for metalloproteins. An analysis of the magnetic anisotropy tensor could be also performed by using pure pseudocontact shifts from non coordinated aminoacid residues[8].

---

5 Lowery, M.D. & Solomon, E.I. (1992) *Inorg. Chim. Acta 198-200*, 233.

6 Kalverda, A.P., Salgado, J., Dennison, C. & Canters, G.W. (1995) *Biochemistry*, submitted.

7 a) Bertini, I. & Luchinat, C. (1986) *NMR of Paramagnetic Molecules in Biological Systems*, The Benjamin/Cummings Publishing Company, Menlo Park. b) Bertini, I., Turano, P. & Vila, A. (1993) *Chem. Rev. 93*, 2833.

8 Banci, L., Dugad, L.B., La Mar, G.N., Keating, K.A., Luchinat, C. & Pieratelli, R. (1992) *Biophys. J. 63*, 530.

From the study of the electronic structures of both cobalt and nickel substituted azurins by EPR and low temperature magnetic measurements, quite similar conclusions can be drawn. Distorted tetrahedral environments of the active sites, such as distorted trigonal bipyramidal geometry, with the Met121 axial ligand moving away, may reconcile apparent contradictory results. Since this metal site would be not five-coordinate from a strict structural point of view, we denominate it "pseudo-pentacoordinate".

With regard to the M121Q metalloderivative, the characteristics of the assigned resonances indicate that the metal center is tetrahedral for both Ni(II) and Co(II)-M121Q azurins. The metal has moved towards the Gln121 axial position and coordinates to this residue through the side chain carbonyl O, while the Gly45 O is not coordinated. The displacement of the metal from the N_2S plane is perceived by the proton signals of the equatorial ligands, and so the metal-S^{δ}_{Cys112} orbital overlap appears less efficient in the mutant.

These results, in line with other from the literature[2], demonstrate that the very rigid azurin metal site permits only slight structural changes when copper is replaced by other metals, and basically imposes the coordination geometry. The small variations observed depend on the existence of two alternative axial ligands with very different donor properties which determine the coordination structure according to the preferences of the metal ion.

Other investigated properties of azurin.

The ^1H NMR spectra of azurin paramagnetic metalloderivatives have proved to be very powerful for the detection of even tiny structural changes, like the effects of the titration of His35 on the metal site. These changes, which are probed by the variations in the chemical shifts of some of the isotropically shifted signals, are not structurally significant in terms of proton-metal distances as indicated by the small variations of the relaxation times. The analysis of this transition permits the determination of the exchange rate constant and the pK_a of the equilibrium. Although the values of pK_a obtained here are significantly smaller than that corresponding to the Cu(II)-azurin[9], they can be explained by a shorter metal-$N^{\delta 1}_{His35}$ distance in the Ni(II) and Co(II) derivatives. Analogously, the similarity of the pK_a values obtained for the Co(II) and Ni(II)-azurins suggests that this distance is very similar in both cases, in line with a similar structure of the metal site.

---

[9] a) van de Kamp, M., Canters, G.W., Andrew, C.R., Sanders-Loehr, J., Bender, C.J. & Peisach, J. (1993) *Eur. J. Biochem. 218*, 229. b) Strong, C., Ellis, W.R. & Gray, H.B. (1992) *Inorg. Chim. Acta 191*, 149.

The exchange rate of the His117 $N_{\varepsilon 2}H$ proton has been also estimated. Is found that it is dependent on the pH and oxidation state of the metal, being faster for the Co(II) and Cu(II)-azurins than for the Cu(I)-azurin, and at high pH. However, it is still two orders of magnitude slower than the electron self-exchange rate. So, the present results are in agreement with the proposed mechanism for the azurin electron self-exchange reaction, in which two solvent molecules participate in a proton-bridge network linking the His117 coordinated residues of two azurin molecules[10].

[10a] Nar, H., Messerchmidt, A., Huber, R., van de Kamp, M. & Canters, G.W. (1991) *J. Mol. Biol. 218*, 427. **b)** Canters, G.W. & van de Kamp, M. (1992) *Curr. Opin. Struct. Biol.* 2, 859.

Sustitución metálica en proteínas azules de cobre:

propiedades químicas y estructurales de las azurinas de níquel y cobalto[1].

Resumen.

El centro metálico de la azurina es caracterizado a través de los derivados de Ni(II) y Co(II). Estos se estudian mediante espectroscopía UV-vis, EPR y a partir de medidas magnéticas, aunque es la resonancia magnética nuclear de paramagnéticos la que proporciona mayor información. Los espectros de RMN de protón de estos derivados metálicos presentan patrones característicos según las propiedades del centro metálico. Así, las azurinas silvestres de Ni(II) y Co(II) de las bacterias *Pseudomonas aeruginosa* y *Alcalígenes denitrificans* dan lugar a espectros muy similares, que son a su vez diferentes de los espectros correspondientes al mutante M121Q. Entre las principales características de estos espectros, son de destacar los grandes desplazamientos isotrópicos de las señales de la cisteina coordinada, los cuales parecen depender de la fuerza del enlace de coordinación al metal de este ligando y por tanto del mayor o menor carácter tetraédrico. La estructura de rayos X de la azurina de Ni(II) muestra un centro metálico tetraédrico en el que la Gly45 aparece claramente coordinada y la Met121 queda posiblemente fuera del entorno de coordinación. Sin embargo, la magnitud de los desplazamientos isotrópicos de las señales de Met121 en las azurinas de Ni(II) y Co(II) permite sugerir la existencia de una débil coordinación para este residuo. El estudio de la estructura electrónica mediante EPR y medidas magnéticas es consistente con la existencia de geometrías distorsionadas que podrían corresponder a situaciones intermedias entre tetracoordinación y bipirámide trigonal. Los espectros de RMN permiten también la observación y el estudio de procesos dinámicos, como son la transición conformacional dependiente de la His35 en la azurina de *Pseudomonas aeruginosa* y el canje del protón $N_{\varepsilon 2}H$ de la His117. Por último, del estudio de la azurina mutada M121Q se deduce que la Gln121 se encuentra coordinada al metal a través del oxígeno carbonílico de la cadena lateral, y la comparación de su espectro de RMN con el de la estelacianina de cobalto permite sugerir una geometría de coordinación similar en esta última proteína.

---

[1] Este trabajo está basado en parte en:

a) Moratal, J.M., Salgado, J., Donaire, A., Jiménez, H.R. & Castells, J. (1993) *J. Chem. Soc. Chem. Commun.*, 110. b) Moratal, J.M., Salgado, J., Donaire, A., Jiménez, H.R., Castells, J. & Martínez-Ferrer, Mª.J. (1993) *Magn. Reson. Chem. 31*, 541. c) Moratal, J.M., Salgado, J., Donaire, A., Jiménez, H.R. & Castells, J. (1993) *Inorg. Chem. 32*, 3587. d) Salgado, J., Jiménez H.R., Donaire, A. & Moratal, J.M. (1995) *Eur. J. Biochem. 231*, 358. e) Moratal, J.M., Romero, A., Salgado, J., Perales-Alarcón, A. & Jiménez, H.R. (1995) *Eur. J. Biochem. 228*, 653. f) Jiménez, H.R., Salgado, J., Moratal, J.M. & Morgenstern-Badarau, I. (1995) *Inorg. Chem.*, submitted. g) Salgado, J. Jiménez H.R., Moratal, J.M., Kroes, S., Warmerdam, G & Canters, G.W. (1995) , *Biochemistry*, in press.

I. Introducción y objetivos

La sustitución metálica en metaloproteínas es una estrategia comúnmente utilizada en Bioquímica Inorgánica[2]. De manera general, puede considerarse una forma directa, normalmente sencilla, de investigar la esencialidad del metal. Así, al sustituir el metal nativo, podemos conocer su papel en el contexto de la función del sistema, ya sea estructural o catalítico. Adicionalmente, la sustitución metálica proporciona información acerca de la selectividad y rigidez del sitio metálico. En todos estos casos, dada la especificidad del cambio introducido, podemos considerarlo al mismo nivel que una mutagénesis dirigida sobre cualquiera de los aminoácidos de la proteína; en realidad la más simple que pueda pensarse en el caso de una metaloproteína.

Cuando el metal exógeno introduce un cromóforo con propiedades espectroscópicas singulares, que puedan ser aprovechadas para la obtención de información estructural o el seguimiento de procesos dinámicos que afecten al centro metálico o sus proximidades, la sustitución metálica es utilizada como sonda del centro metálico[2c]. Ello permite el seguimiento de cambios estructurales, equilibrios ácido base, unión de ligandos, etc., y es especialmente importante cuando el metal nativo no presenta tales propiedades espectroscópicas, como en el caso del cinc en enzimas y proteínas de cinc[2a,c].

Sin embargo, en las proteínas de cobre, entre ellas la azurina, el ion metálico nativo confiere de por sí propiedades espectroscópicas singulares[3]. Así, por ejemplo, las proteínas azules de cobre presentan espectros electrónicos y de EPR muy característicos, cuyo estudio extensivo durante las últimas décadas ha contribuido al conocimiento detallado de estos centros metálicos[3,4]. Pero incluso en este caso, la sustitución metálica se reveló de extraordinaria importancia a la hora de resolver aspectos tan importantes como la asignación de las bandas

---

[2] a) Bertini, I. & Luchinat, C. (1984) in *Advances in Inorganic Biochemistry* (Eichorn, G.L. & Marzilli, L.G. eds.) p. 71, Elsevier, New York. b) Hauenstein, B.L. & McMillin, D.R. (1981) in *Metal ions in biological systems* (Sigel, H., ed.) vol. 13, p. 319, Marcel Dekker, New York. c) Bertini, I & Luchinat, C. (1986) in *Zinc Enzymes* (I. Bertini, C. Luchinat, W. Maret, M. Zeppezauer eds.) p. 27, Birkhäuser, Boston.

[3] a) Gray, H.B. & Solomon, E.I. (1981) in *Copper proteins* (Spiro, T.G., ed) p. 1, Wiley, New York. b) Solomon, E.I. & Lowery, M.D. (1993) *Science 259*, 1575.

[4] a) Adman, E.T. (1985) *Top. Mol. Struct. Biol. 6*, 1. b) Adman, E.T. (1991) *Adv. Protein Chem. 42*, 145. c) Chapman, S.K.(1991) in *Perspectives on Bioinorganic Chemistry* (Hay, R.W., Dilworth, J.R. & Nolan, K.B., eds.) vol 1, p. 95, Jai Press Ltd, London. d) Adman, E.T. & Turley, S. (1993) in *Bioinorganic chemistry of copper.* (Karlin, K.D. & Teyklar, Z., eds.) Chapman & Hall, New Yok.

principales de su espectro visible[5]. Mas recientemente, estudios similares son utilizados para caracterizar proteínas de cobre poco conocidas, ya sea de reciente descubrimiento o generadas mediante mutagénesis[6].

Consideración a parte merece la Resonancia Magnética Nuclear aplicada a sistemas paramagnéticos, pues constituye una potente técnica espectroscópica para la caracterización de metaloproteínas que proporciona información estructural y de procesos dinámicos[7]. Aunque el ion Cu(II) es paramagnético, sus propiedades de relajación electrónica lo hacen poco adecuado para este tipo de estudios[7a]. Por ello, nosotros abordamos la investigación de proteínas azules de cobre mediante RMN de paramagnéticos a través de sus derivados de Ni(II) y Co(II). Ambos iones metálicos han sido ampliamente utilizados con éxito para el estudio de metaloenzimas de cinc[2a,c]. Sin embargo, sólo unos pocos ejemplos de su aplicación en proteínas azules de cobre podían encontrarse en la bibliografía antes de la iniciación de este estudio[2b,8]. Nos planteamos por tanto, como primer objetivo, sentar las bases para el estudio de las proteínas azules de cobre mediante RMN de paramagnéticos de los derivados de Ni(II) y Co(II). Para ello elegimos la azurina, una de las proteínas azules de cobre mejor caracterizadas, tanto a nivel estructural como funcional[3,4]. Paralelamente, prestaremos también atención a aquellos aspectos del sistema elegido que resulten de especial significación, por su importancia para el conocimiento general de la propia azurina, por las controversias que haya podido suscitar su investigación mediante otras técnicas, o por las implicaciones que puedan tener para el entendimiento de otros sistemas relacionados. Así, se estudiará la estructura del centro metálico de la azurina en el contexto de su probada rigidez y del supuesto control que la proteína ejerce sobre la coordinación del metal[9,10]. Para ello contaremos con datos estructurales tanto en disolución como en estado cristalino, que serán analizados además en comparación con la estructura de otros derivados

---

5 a) McMillin, D.R., Rosemberg, R.C. & Gray, H.B. (1974) *Proc. Natl. Acad. Sci. USA 71*, 4760. b) Tennent, D.L. & McMillin, D.R. (1979) *J. Am. Chem. Soc. 101*, 2307.

6 a) Strong, C., Harrison, S.L. & Wesley, Z. (1994) *Inorg. Chem. 33*, 606. b) Mizoguchi, T.J., Di Bilio, A.J., Gray, H.B. & Richards, J.H. (1992) *J. Am. Chem. Soc. 114*, 10076. c) Di Bilio, A.J., Chang, T.K., Malmström, B.G., Gray, H.B., Karlsson, B.G., Nordling, M., Pascher, T. & Lundberg, L.G. (1992) *Inorg. Chim. Acta 198-200*, 145.

7 a) Bertini, I. & Luchinat, C. (1986) *NMR of Paramagnetic Molecules in Biological Systems*. The Benjamin/Cummings Publishing Company, Menlo Park. b) Bertini, I., Turano, P. & Vila, A. (1993) *Chem. Rev. 93*, 2833.

8 a) Hill, H.A.O., Smith, B.E. & Storm, C.B. (1976) *Biochem. Biophys. Res. Commun. 70*, 783. b) Blaszak, J.A., Ulrich, E.L., Markley, J.L. & McMillin, D.R. (1982) *Biochemistry 21*, 6253. c) Dahlin, S., Reinhammar, B. & Ångström, J. (1989) *Biochemistry 28*, 7224.

9 a) Baker, E.N. (1988) *J. Mol. Biol. 203*, 1071. b) Nar, H., Messerchmidt, A., Huber, R., van de Kamp, M. & Canters, G.W. (1991) *J. Mol. Biol. 221*, 765.

10 Gray, H.B. & Malmström, B.G. (1983) *Comments Inorg. Chem. 2*, 203.

metálicos de azurina caracterizados en los últimos años[11]. Adicionalmente, analizaremos aspectos dinámicos de la proteína, como cambios conformacionales, equilibrios ácido-base y canje de protón.

[11] a) Nar, H., Huber, R., Messerschmidt, A., Filippou, A.C., Barth, M., Jaquinod, M., van de Kamp, M. & Canters, G.W. (1992) *Eur. J. Biochem. 205,* 1123. b) Blackwell, K.A., Anderson, B.F. & Baker, E.N. (1994) *Acta Crystallogr. D50,* 263.

II. Breve revisión sobre la azurina.

a) La azurina: una proteína azul de cobre.

El cobre es junto con el hierro y el cinc uno de los metales de mayor importancia en los sistemas biológicos, no sólo por su abundancia, sino también por la relevancia y diversidad de las funciones que desempeña[4d]. Así, las proteínas de cobre aparecen en plantas, animales, bacterias y archaeobacterias y participan en procesos metabólicos importantes, como transporte de oxígeno, catálisis oxidativa y transferencia electrónica[4d]. En cada caso, las propiedades químicas necesarias para el perfecto desarrollo de su función son proporcionadas por entornos y geometrías de coordinación especiales.

Una de las clasificaciones mas extendidas de las proteínas de cobre fue establecida a partir del estudio de los centros metálicos de lacasa y ceruloplasmina[12]. Estos fueron divididos básicamente en tres tipos en atención a sus propiedades espectroscópicas específicas, llamados tipo 1, 2 y 3. Las proteínas azules de cobre responden a las propiedades de los centros de cobre de tipo 1, por lo que son también conocidas como proteínas de cobre de tipo 1. Estas propiedades son, principalmente, la presencia de un centro metálico de cobre susceptible de oxido-reducción y detectable por EPR en su forma oxidada, en el cual se dan una absorción intensa en el espectro electrónico alrededor de 600 nm ($\varepsilon \geq 1500\ M^{-1}cm^{-1}$), y constantes de acoplamiento hiperfino y valores de g en el espectro de EPR que son anormalmente pequeños si se comparan con los obtenidos en complejos "normales" de cobre[4]. Además, las proteínas azules de cobre se caracterizan por ser hidrosolubles y de pequeño tamaño (10-20 kDa), poseer una estructura característica denominada barril-β, y realizar una función de transferencia electrónica. Debido a esta función redox se les ha dado en llamar también cupredoxinas[4].

Las azurinas son, junto con las plastocianinas, las proteínas azules de cobre más conocidas y mejor caracterizadas. Son bacterianas y su función concreta depende del microorganismo del que proceden, aunque en la mayoría de los casos ésta es poco conocida[4]. Otras proteínas azules de cobre importantes son la amicianina, la pseudoazurina o la estelacianina.

---

[12] a) Vänngård, T. (1972) in *Biological Applications of Electron Spin Resonances* (Schwartz, ed.) p. 441, Wiley, New York. b) Fee, J.A. (1975) *Struct Bonding 23*, 2.

b) Estructura de la azurina.

La estructura de la azurina ha sido determinada por difracción de rayos X en sus formas oxidada y reducida, así como en la apoproteína[9,13]. El cobre aparece fuertemente unido a los nitrógenos imidazol δ1 de las histidinas 46 y 117 y al azufre tiolato de la Cys112. Además presenta interacciones débiles con el oxígeno carbonílico de la Gly45 y con el azufre de la Met121 (figura IA). En este entorno de coordinación, el metal se encuentra prácticamente en el plano ecuatorial N_2S, formado por los tres ligandos fuertemente coordinados, y la geometría se define como bipirámide trigonal distorsionada. Esta particular estructura del centro metálico parece ser la responsable de las singulares características espectroscópicas de los centros azules de cobre[3,14], pues posibilita un solapamiento muy eficiente entre el orbital $d_{x^2-y^2}$ del Cu(II) y el orbital $3p\pi$ del S^{γ}_{Cys}, dando lugar a una banda de transferencia de carga intensa en el espectro UV-vis y constantes de acoplamiento muy pequeñas en el espectro de EPR[3b,14].

La zona situada alrededor del sitio metálico es particularmente rígida, debido a la abundancia de puentes de hidrógeno e interacciones de van der Waals[9]. Así, la estructura se mantiene prácticamente inalterada en la azurina reducida[13a], e incluso cuando el metal es extraído[13b,c], lo cual ha sido relacionado con la extraordinaria facilidad con que el metal cambia de estado de oxidación durante el desarrollo de su función redox[9,10]. Se dispone además del conocimiento de la estructura de varios derivados metálicos de azurina, en los cuales se observa que la estructura global de la proteína no varía al reemplazar el metal, siendo las diferencias en el centro metálico de pequeña importancia[11,15]. En las azurinas de cinc y níquel el metal se encuentra ligeramente desplazado hacia el ligando axial O_{Gly45} mientras que se aleja del S^{δ}_{Met121}, de manera que la geometría de coordinación resultante puede describirse como tetraédrica distorsionada (figura IB)[11a,15].

[13a] Shepard, W.E.B., Anderson, B.F., Lewandoski, D.A., Norris, G.E. & Baker, E.N. (1990) *J. Am. Chem. Soc. 112*, 7817. **b)** Shepard, W.E.B., Kingston, R.L., Anderson, B.F. & Baker. E.N. (1993) *Acta Crystallogr. D49*, 331. **c)** Nar, H., Messerschmidt, A., Huber, R., van de Kamp, M. & Canters, G.W. (1992) *FEBS Lett. 306*, 119-124.

[14] Gewirth, A.A. & Solomon, E.I. (1988) *J. Am. Chem. Soc. 110*, 3811.

[15] Moratal, J.M., Romero, A., Salgado, J., Perales-Alarcón, A. & Jiménez, H.R. (1995) *Eur. J. Biochem. 228*, 653.

Diversos mutantes de azurina han sido también caracterizados estructuralmente[16,17]. De entre ellos nos detendremos en la azurina M121Q de *Alcalígenes denitrificans*[17], cuyo estudio se aborda aquí a través de sus derivados de Ni(II) y de Co(II). Este mutante de azurina adquiere una especial importancia por ser además un buen modelo de la estelacianina[17], otra proteína azul de cobre que presumiblemente presenta una glutamina en lugar de metionina como ligando axial. La azurina M121Q de Cu(II) posee un centro metálico claramente tetraédrico, donde el metal aparece unido al oxígeno carbonílico de la cadena lateral de la Gln121 mientras que la Gly45 se encuentra a una distancia excesiva para ser considerada un ligando del metal (figura IC)[17].

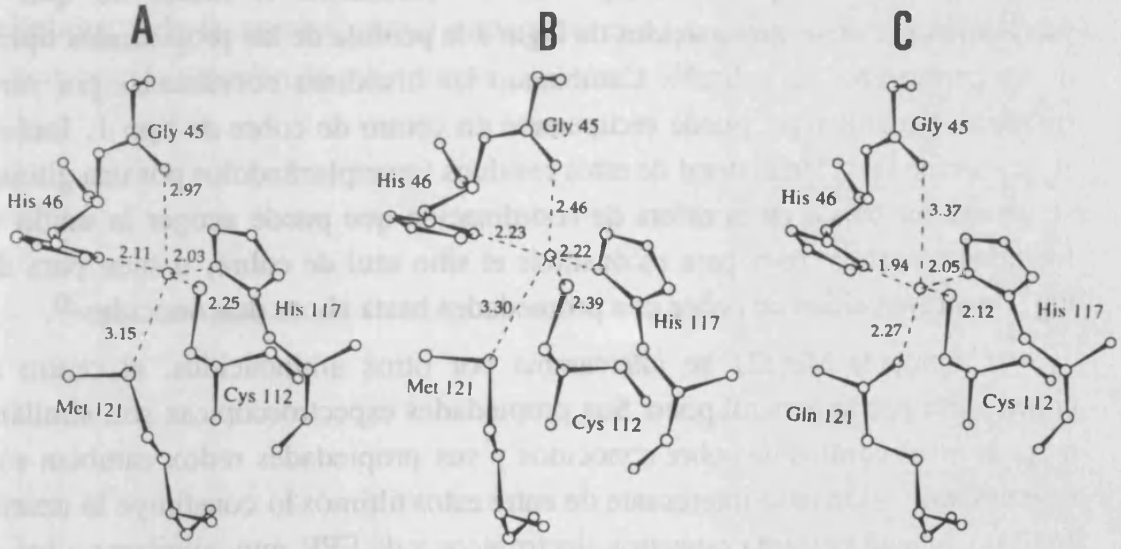

Cu(II)-wt azurin *Ni(II)-wt azurin* *Cu(II)-M121Q azurin*

Figura I. Representación esquemática de la estructura del centro metálico en varias azurinas. Los datos han sido tomados de las referencias 9b (A), 15 (B) y 17 (C).

[16]Nar, H., Messerchmidt, A., Huber, R., van de Kamp, M. & Canters, G.W. (1991) *J. Mol. Biol. 218*, 427.

[17]Romero, A., Hoitink, C.W.G., Nar, H., Huber, R., Messerschmidt, A. & Canters, G.W. (1993) *J. Mol. Biol. 229*, 1007.

c) Relaciones estructura/función en azurina: estudios de mutagénesis dirigida.

La clonación, sobreexpresión y modificación selectiva de varios genes de azurina ha supuesto un hito importante en la investigación de las relaciones estructura-función en esta proteína[18]. Mediante mutagénesis dirigida, se ha estudiado desde la importancia individual de cada uno de los ligandos del metal[6b,c;19,20,21] hasta la localización de las zonas de la superficie que son utilizadas por la azurina para reaccionar con otras proteínas redox[22]. La sustitución mediante mutagénesis dirigida de los aminoácidos que se encuentran coordinados al metal ha llevado a conocer que el plano ecuatorial formado por los tres ligandos fuertes: His46, His117 y Cys112, constituye la entidad estructural básica responsable de las propiedades de los centros azules de cobre. De ellos, la Cys112 es el único cuya presencia resulta imprescindible, como lo demuestra el hecho de que su sustitución por otros aminoácidos da lugar a la pérdida de las propiedades típicas de un centro azul de cobre[6b]. Cambiando las histidinas coordinadas por otros residuos, sin embargo, puede recuperarse un centro de cobre de tipo 1. Incluso si se elimina la cadena lateral de estos residuos (reemplazándolos por una glicina) se genera un hueco en la esfera de coordinación que puede acoger la unión de ligandos externos, bien para reconstituir el sitio azul de cobre, o bien para dar lugar a nuevos sitios de cobre con propiedades hasta ahora desconocidas[20].

Cuando la Met121 se intercambia por otros aminoácidos, el centro de cobre varía por lo general poco. Sus propiedades espectroscópicas son similares a las de otros centros de cobre conocidos y sus propiedades redox cambian sólo ligeramente[21]. Un caso interesante de entre estos últimos lo constituye la azurina M121Q, la cual presenta espectros electrónicos y de EPR muy similares a los de la estelacianina[17].

---

[18]a) Canters, G.W. (1987) *FEBS Lett. 212*, 168. **b)** Arvidsson, R.H.A., Nordling, M. & Lundberg, L. (1989) *Eur. J. Biochem. 179*, 195. **c)** Hoitink, C., Woudt, L.P., Turenhout, J.C.M., van de Kamp, M. & Canters, G.W. (1990) *Gene 90*, 15. **d)** Chang, T.C., Iverson, S.A., Rodrigues, C.G., Kiser, C.N., Lew, A.Y., Germanas, J.P. & Richards, J.H. (1991) *Proc. Natl. Acad. Sci. U.S.A. 88*, 1325.

[19]Germanas, J.P., Di Bilio, A.J., Gray, H.B. & Richards, J.H. (1993) *Biochemistry 32*, 7698.

[20]a) den Blaauwen, T., Hoitink, C.W.G., Canters, G.W., Han, J., Loehr, T.M. & Sanders-Loehr, J. (1993) *Biochemistry 32*, 12455. **b)** den Blaauwen, T. & Canters, G.W. (1993) *J. Am. Chem. Soc. 115*, 1121.

[21]a) Karlsson, B.G., Nordling, M., Pascher, T., Tsai, L.C., Sjölin, L. & Lundberg, L.G. (1991) *Protein Eng. 4*, 343. **b)** Pascher, T., Karlsson, B.G., Nordling, M., Malmtröm, B.G. & Vänngård, T. (1993) *Eur. J. Biochem. 212*, 289.

[22]a) van de Kamp, M., Silvestrini, M.C., Brunori, M., van Beeumen, J., Hali, F.C., Canters, G.W. (1990) *Eur. J. Biochem. 194*, 109. **b)** van de Kamp, M., Floris, R., Hali, F.C. & Canters, G.W. (1990) *J. Am. Chem. Soc. 112*, 907.

Mediante otras sustituciones de aminoácidos importantes se ha podido determinar cuáles son las zonas superficiales, llamadas "patch", que la azurina utiliza en su interacción con otras proteínas. Dos eran tradicionalmente los supuestos *patches* en azurina: el *patch* de la His35 y el *patch* hidrofóbico[23]. El primero aparecía relacionado con la variación del potencial redox al cambiar el pH (una disminución de 60 mV entre pH 5 y 8)[24], así como con las modificaciones estructurales dependientes de la desprotonación de la His35[9b,25] y las características cinéticas de la reacción entre la azurina y el citocromo c_{551}[26]. El segundo *patch* sería utilizado en la reacción entre la azurina y la nitrito reductasa, según parece deducirse a partir de un estudio de azurina modificada con cromo en la superficie[23b]. La sustitución por mutagénesis dirigida de His35 y Met44[27], mostró definitivamente que es el *patch* hidrofóbico, y no la zona entorno a la His35, quien resulta esencial para las reacciones de transferencia electrónica de la azurina con el citocromo c_{551} y con la nitrito reductasa, así como para la reacción de autotransferencia electrónica[22].

[23a] Farver, O. & Pecht, I. (1981) *Israel J. Chem. 21*, 13. **b)** Farver, O., Blatt, Y. & Petch, I. (1982) *Biochemistry 21*, 3556.

[24] Strong, C., Ellis, W.R. & Gray, H.B. (1992) *Inorg. Chim. Acta 191*, 149.

[25] Adman, E.T., Canters, G.W., Hill, H.A.O. & Kitchen, N.A. (1982) *FEBS Lett. 143*, 287.

[26a] Rosen, P. & Pecht, I. (1976) *Biochemistry 15*, 775. **b)** Silvestrini, M.C., Brunori, M., Wilson, M.T. & Darley-Usmar, V. (1981) *J. Inorg. Biochem. 14*, 327. **c)** Corin, A.F., Bersohn, R. & Cole, P.E. (1983) *Biochemistry 22*, 2032.

[27] La Met44 es uno de los restos de aminoácido que constituyen el *patch* hidrofóbico.

III.Experimental.

a) Obtención de azurina y preparación de muestras.

Extracción y purificación de azurina.

La bacteria *Pseudomonas aeruginosa* (*Pae*) (CECT 110) era cultivada en condiciones anaerobias a 35 °C en el medio descrito por Parr, et al[28]. Para ello se utilizaba un fermentador automático de 14 L (New Brunswick). Las células crecidas hasta el final de la fase exponencial se recogían por centrifugación y se guardaban para su posterior utilización a -20 °C.

La azurina de *Pae* se purificó de acuerdo con el procedimiento descrito en la bibliografía[28,29], consistente en una precipitación fraccionada con sulfato amónico seguida de cromatografías de intercambio aniónico en una columna de DEAE-Sephacel (3cm x 50cm), de exclusión molecular en Sephadex G-100 (2.5cm x 90cm) y de intercambio catiónico en CM-Sephadex C-25 (2.5cm x 30cm). La azurina obtenida era pura de acuerdo con la relación A_{625}/A_{280}=0.54-0.56.

Las azurinas de *Alcaligenes denitrificans* (*Ade*), tanto la proteína silvestre (wt) como su mutante M121Q, se obtenían de la expresión heteróloga del gen correspondiente en *E. coli.* (K12, cepa JM101). Los plásmidos de expresión utilizados (pCH5 para la azurina-wt y pCH6 para su mutante M121Q) habían sido construidos por Carla Hoitink[17,30]. Las células de *E. coli* recién transformadas se crecían en medio LB con $CuSO_4$ 0.1 mM, en un fermentador de 30L controlado por ordenador (New Brunswick). 3 horas después de la inducción del cultivo con IPTG (100 μM), las bacterias se recogían por filtración tangencial (Millipore).

La purificación de la azurina-wt de *Ade* y del mutante M121Q se realizó de acuerdo con el procedimiento descrito por otros autores[17,30], con ligeras modificaciones para la separación de la Zn(II)-azurina, que aparece como contaminante en las preparaciones de azurina obtenidas por expresión heteróloga en *E. coli*[11a,31]. Dicha separación es necesaria debido a la imposibilidad de

---

[28]Parr, S.R., Barber, D., Greenwood, C., Phillips, B.W. & Melling, J. (1976) *Biochem. J. 157*, 423.

[29]Ambler, R.P. & Wynn, M. (1973) *Biochem. J. 131*, 485.

[30]a) Hoitink, C., Woudt, L.P., Turenhout, J.C.M., van de Kamp, M. & Canters, G.W. (1990) *Gene 90*, 15. b) Hoitink, C. (1993) PhD Thesis, *Leiden University*, The Netherlands.

[31]van de Kamp, M., Hali, F.C., Rosato, N., Finazzi-Agró, A. & Canters, G.W. (1990) *Biochim. Biophys. Acta 1019*, 283.

extraer el cinc mediante métodos no desnaturalizantes[17]. Así, en el caso de la azurina-wt, el derivado de cinc se separaba de la azurina de cobre mediante cromatografía de intercambio aniónico en DEAE-Sepharose, después de la reducción de la segunda con ditionito de sodio. Sin embargo, en el caso de la azurina mutante M121Q, el derivado de cinc contaminante se separaba en la misma columna anterior previo tratamiento por diálisis de la muestra con KCN 0.5 M a pH 8.5, cuya consecuencia es la desmetalación de la azurina de cobre. La apoazurina así obtenida, podía ser reconstituida mediante la adición de $CuSO_4$, o bien ser utilizada directamente para la preparación de los derivados de Ni(II) y Co(II). Las muestras de Cu(II)-azurina, tanto wt como M121Q, mostraban una sola banda en geles de isoelectroenfoque, y relaciones espectrales de A_{619}/A_{280}=0.3 y A_{610}/A_{280}=0.31, respectivamente

Preparación de los derivados metálicos.

Los derivados de níquel y cobalto de azurina se preparaban por adición de 5 moles de $CoSO_4$ o $NiSO_4$ por mol de apoproteína. La apoazurina se tomaba directamente del último paso de la purificación en el caso del mutante M121Q o se preparaba por diálisis frente a KCN 0.5 M (NaH_2PO_4 0.1 M, pH 8.5) en el caso de las azurinas-wt. La formación de los metaloderivados se seguía a través del espectro UV-vis. Ésta era lenta y dependiente del pH para las azurinas-wt, siendo necesarias al menos 48 horas para la total formación del complejo a pH 8.5 (Fig. 2:3, pág. 52). Sin embargo, las azurinas-M121Q de Ni(II) o Co(II) se metalaban de manera casi instantánea.

Las muestras eran concentradas mediante ultrafiltración o concentradores de centrífuga (amicon) hasta 1-8 mM, según los casos, determinándose las concentraciones a partir de las bandas de absorción y los coeficientes de extinción molar mostrados en la Tabla 2:1 (pág. 53).

b) Métodos físicos.

Espectroscopia UV-vis.

Los espectros electrónicos se registraron a temperatura ambiente en los siguientes espectrofotómetros: Cary 1 (Varian), Lambda 9 (Perkin Elmer) y Shimadzu UV-2101PC (Shimadzu), utilizando celdas semimicro de cuarzo de 1 cm de paso.

Espectros de EPR.

Los espectros EPR se registraron en un espectrómetro Bruker ER-200D, que operaba a la frecuencia de 9.43 GHz de la banda X. La potencia de microondas

fué de 10 dB y la amplitud de modulación de 4 G. Las muestras eran montadas en tubos de EPR de 4 mm.

Medidas magnéticas

Las medidas magnéticas a temperatura variable fueron realizadas en un magnetómetro SQUID a un campo de 0.1 Tesla y en el rango de temperaturas de 120 a 5 K, utilizando glicerol al 10% como crioprotector. La concentración de las muestras estudiadas (3.6 mM) se determinaba de la forma ya descrita. Todas las disoluciones fueron cuidadosamente desgasificadas con objeto de eliminar el oxígeno molecular. Las muestras eran después transferidas a soportes de cuarzo especialmente diseñados para la realización de medidas de SQUID, y mantenidas en atmósfera de argón hasta su uso. Los valores de magnetización experimentales eran convertidos a susceptibilidades magnéticas molares. La corrección diamagnética sustraída de la señal total, se obtenía de la medida de la apoproteína en idénticas condiciones.

Resonancia magnética nuclear.

Los espectros de RMN fueron registrados utilizando espectrómetros Varian Unity que operaban a la frecuencia del protón de 300 o 400 MHz o espectrómetros Bruker AC 200 MHz, WM 300 MHz y DMX 600 MHz.

Los espectros monodimensionales (1D) se registraron utilizando, bien una secuencia de un solo pulso (d_1—90°—*Acq*), con presaturación de la señal del disolvente durante el tiempo de relajación, o bien la secuencia super-WEFT (d_1—180°—τ—90°—*Acq*)[32]. La primera se empleaba para observar simultáneamente señales tanto de relajación lenta como rápida. La secuencia super-WEFT era utilizada para observar las señales de relajación rápida selectivamente, especialmente aquellas que se encuentran bajo la zona diamagnética del espectro.

Los tiempos de relajación longitudinal (no selectivos) fueron determinados a través de la secuencia de inversión-recuperación. Para ello se representaban los valores de intensidad de las señales para distintos walores de τ y se ajustaban a la ecuación 2:3 (pág. 58), o bien se determinaba la pendiente inicial de la representación semilogarítmica de la magnetizaciôm-z frente al tiempo τ[33,34] (ver Fig. 2:5, pág. 59).

---

[32]Inubushi, T. & Becker, E.D. (1983) *J. Magn. Reson. 51*, 128.

[33]Granot, J. (1982) *J. Magn. Reson. 49*, 257.

[34]a) Sette, M., de Ropp, J.S., Hernández, G. & La Mar, G.N. (1993) *J. Am. Chem. Soc. 115*, 5237. b) La Mar, G.N. & de Ropp, J.S. (1993) in *NMR of paramagnetic molecules* (Berliner L.J. & Reuben , J., ed.) vol. 12 p 1, Plenum Press Dir Plenum Publishing Corp. New York.

Las medidas de transferencia de saturación y de efecto NOE (efecto nuclear Overhauser) se realizaron utilizando la secuencia super-WEFT, con irradiación de la señal de interés durante el tiempo τ. Los espectros eran adquiridos en bloques de 32 scans cada uno, alternando la saturación en el centro de la señal con la saturación en posiciones simétricas a ambos lados de ésta. A partir de los valores de efecto NOE obtenidos, se calculaban distancias interprotónicas mediante la ecuación 2:22 (pág. 65).

Los equilibrios ácido-base eran analizados a partir de la variación del área de las señales según las ecuaciones 2:8 y 2:9 (pág. 61). La velocidad de canje del equilibrio ácido-base se calculaba utilizando la ecuación 2:10 (pág. 61), y las velocidades de canje de protones lábiles con el disolvente se determinaron mediante las ecuaciones 2:12 y 2:13 (pág. 62-63, ver también la figura 2:6 en la pág. 63).

Los espectros COSY (espectroscopia de correlación)[35] eran del tipo-n convencional (MCOSY). Los espectros TOCSY (espectroscopía de correlación total)[36] se realizaron utilizando el "tren de pulsos" MELV-17. Los espectros NOESY (espectroscopía de efecto nuclear Overhauser) se registraron utilizando el modo "States-Haberkorn"[37] o el TPPI (incremento de fase proporcional al tiempo)[38]. La secuencia WEFT-NOESY[39] era utilizada para obtener correlaciones entre protones de relajación rápida dentro de la zona diamagnética. Debido a la gran diversidad de resonancias, especialmente desde el punto de vista de su relajación, los espectros bidimensionales (2D) fueron registrados utilizando un amplio abanico de condiciones. Así, los tiempos de reciclo de los espectros NOESY, COSY y TOCSY variaban entre 20 y 300 ms, y los tiempos de mezcla variaban entre 2 y 200 ms para los espectros NOESY y entre 15 y 70 ms para los TOCSY. El número de scans, la ventana espectral, el número de puntos en la dimensión t_2 y el número de incrementos en la dimensión t_1 también variaron considerablemente (64-2048 scans, 10-190 kHz de ventana espectral, 512-2048 puntos en t_2 y 128-512 incrementos).

Para el procesado de los espectros también se utilizaron diferentes condiciones. Los espectros NOESY y TOCSY se transformaban utilizando funciones seno-campana al cuadrado desplazadas 45°, 60° u 80°, dependiendo del carácter paramagnético de las señales observadas. El número de puntos

---

[35]Bax, A. (1982) *Two-dimensional NMR in liquids*, Reidel Publishing Co., Dordrecht, The Netherlands.

[36]Bax, A. & Davis, D.G.J. (1985) *J. Magn. Reson. 65*, 355.

[37]States, D.J., Haberkorn, R.A. & Ruben, D.J. (1982) *J. Magn. Reson. 48*, 286.

[38]Marion, D. & Wütrich, K. (1983) *Biochem. Biophys. Res. Commun. 113*, 967.

[39]Chen, Z., de Ropp, J.S., Hernández, G. & La Mar, G.N. (1994) *J. Am. Chem. Soc. 116*, 8772.

utilizado en el procesado era de 256, 512, 1024 o 2048 en ambas dimensiones, según los casos. Los espectros COSY eran transformados utilizando funciones seno-cuadrado no desplazadas. La línea base de los espectros NOESY y TOCSY fue corregida de la manera convencional y mediante predicción lineal.

Finalmente, para muchos de los espectros realizados en H_2O, la señal del disolvente era sustraída mediante un filtrado digital en el dominio de tiempos de la FID[40].

Cristalografía de rayos X.

La Ni(II)-azurina de *Pae* fue cristalizada utilizando el método de difusión de vapor. Para ello se preparaban gotas que contenían 15 mg/ml de azurina, $(NH_4)_2SO_4$ 1.5 M, $LiNO_3$ 0.25 M y CH_3COONa 0.1 M a pH 5.05, las cuales fueron equilibradas con soluciones de concentración salina creciente al mismo pH. Para concentraciones de $(NH_4)_2SO_4$ 3.1 M, $LiNO_3$ 0.5 M y CH_3COONa 0.1 M, aparecieron cristales de forma prismática y color amarillo brillante de tamaño 0.8 mm x 0.5 mm x 0.4 mm, los cuales difractaban bien hasta una resolución de 2.05 Å.

Los valores de intensidad de difracción de rayos X se recogieron mediante un sistema de imagen Hendrix/Lantfer (Mar Research, Hamburgo), utilizando una distancia cristal-detector de 90 mm. La radiación X era generada por un ánodo rotatorio a 4.0 kW de potencia (Enraf-Nonius, Netherlands). Para la recogida de un conjunto completo de datos, el cristal fue girado 114° con oscilaciones de 1.5° entre cada imagen. Las imágenes de difracción eran procesadas mediante el programa MOSFLM[41]. De un total de 129132 reflexiones medidas hasta 2.05 Å de resolución, se obtenían 32694 reflexiones únicas, con un factor R de convergencia de 0.06. Se utilizaron como coordenadas modelo las de la azurina de cobre(II) de *Pseudomonas aeruginosa*, tomadas del banco de datos de Brookhaven. Los factores estructurales y mapas de densidad electrónica fueron calculados a partir de las fases de la azurina de cobre, omitiendo las moléculas de disolvente, seguido de una inspección y corrección manual en la pantalla gráfica (Evans & Sutherland) con ayuda del programa FRODO[42]. El refinamiento de la estructura cristalográfica se llevó a cabo con restricciones de energía utilizando el programa XPLOR[43]. Sin embargo, los sitios metálicos fueron refinados sin restricciones de energía. La

---

[40]Smallcombe, S.H. (1993) *J. Am. Chem. Soc. 115*, 4776.

[41]Leslie, A.G.W. (1990) MOSFLM Program. Abstract of the *Crystallographic Computing School*. Bischenberg.

[42]Jones, T.A. (1978) *J. Appl. Crystallogr. 15*, 24.

[43]Brünger, A.T. (1990) X-PLOR (version 2.1), Manual Yale University, New Haven, CT.

simetría de los cristales de Ni(II)-azurina y los parámetros de celda: a=57.3 Å, b=80.9 Å, c=110.5 Å, fueron prácticamente los mismos que los encontrados para la azurina de cobre[9]. Otros datos cristalográficos de interés se presentan resumidos en la Tabla 3:4 (pág. 95).

IV.Resultados.

a) Azurina de níquel(II).

Los derivados de Ni(II) de azurina, tanto de las proteínas silvestres de *Pae* y *Ade* como del mutante M121Q de *Ade*, presentan espectros UV-vis característicos, en los cuales destaca la presencia de dos bandas intensas de transferencia de carga S^{γ}_{Cys}-metal entre 300 y 500 nm (ε=600-3300 M^{-1} cm^{-1}) y transiciones d-d moderadas alrededor de 550 nm ($\varepsilon\approx$200 $M^{-1}cm^{-1}$). Estos espectros son prácticamente idénticos para las dos azurinas-wt (Fig. 1:5A, pág. 30 y Fig. 5:2B, pág. 156) y presentan ligeras diferencias con respecto a la azurina M121Q que básicamente se ciñen a un desplazamiento de las bandas de transferencia de carga de ~30 nm hacia valores de mayor energía en el mutante (Fig. 5:2B, pág. 156; Tabla 5:2, pág. 158).

Espectros RMN de protón.

Los espectros ^{1}H RMN de las azurinas de níquel se muestran en la figura II. Como puede observarse, los espectros de las Ni(II)-azurinas silvestres (figura IIA,B) poseen un patrón de resonancias muy similares. Como principales características destacamos la presencia de dos señales anchas desplazadas entre 180 y 240 ppm (a,b), una señal mas estrecha cercana a 100 ppm (c), y una señal de área triple entre 45 y 30 ppm (i)[44]. En el espectro del derivado de Ni(II) de la azurina M121Q (figura IIC) se observa un conjunto muy similar de señales, con la diferencia principal de que dos de las señales mas características en los anteriores (c,i) no aparecen aquí. Por consiguiente, estas señales pueden asignarse sin ambigüedad a protones correspondientes a la Met121.

Son también características de los tres espectros las señales h y j, pues son canjeables por protones del disolvente y por lo tanto no aparecen en D_2O. Ambas deben de corresponder a los protones $N_{\varepsilon 2}H$ de las dos histidinas coordinadas. A pH alto, la primera de ellas pierde intensidad y termina por desaparecer, lo que nos permite asignar esta señal al protón ε2 de la His117, mucho mas expuesto al disolvente que el protón correspondiente de la His46[9b]. Otro efecto importante del pH es una transición en canje lento que se observa sólo en el caso de la Ni(II)-azurina de *Pae*[9b] (Fig. 3:2, pág. 75). A partir de esta transición, y utilizando la ecuación 2:8 o 2:9 (Fig. 3:3, pág. 76), puede calcularse un pK_a=5.9±0.1, que corresponde muy probablemente al equilibrio ácido-base de la His35[9b,26].

---

[44]La denominación de las señales corresponde a la expresada en la figura IIB.

La asignación del resto de las señales se ha realizado utilizando espectros NOE 1D y NOESY, interpretados con la ayuda de información estructural procedente de difracción de rayos X, además de espectros COSY y TOCSY para las señales menos desplazadas isotrópicamente[45]. Así, las señales correspondientes a los $N_{\varepsilon 2}H$ imidazol de las histidinas coordinadas (h,j) pueden relacionarse con los protones vecinales del mismo anillo ($C_{\delta 2}H$ y $C_{\varepsilon 1}H$) a través de conectividades NOE 1D o 2D (Fig. 3:5A y 3:6, pág. 78; Fig. 5:4A, pág. 160; Fig. 5:5C-E, pág. 162). En el caso de los protones $C_{\varepsilon 1}H$, se encuentra una sola conectividad, entre las señales g' y j de la Ni(II)-azurina M121Q. No obstante, las señales de estos protones (g,g') son muy características, por presentar desplazamientos similares a los del resto de protones-imidazol y debido a su gran anchura, indicativa de una distancia al metal de alrededor de 3 Å.

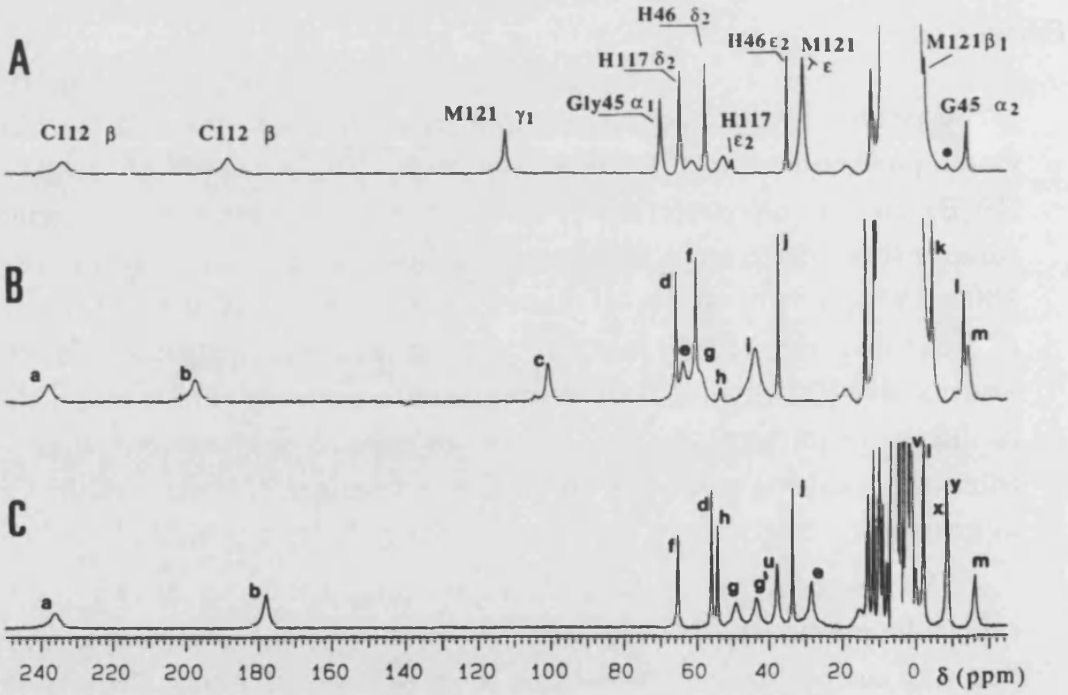

Figura II. Espectros de RMN de protón de los derivados de Ni(II) de la azurina silvestre de *Pseudomonas aeruginosa* (A) y de las azurinas silvestre (B) y mutante M121Q (C) de *Alcaligenes denitrificans*. Estos espectros fueron registrados en un campo de 300 MHz a 30 °C y pH 7.0 (A, B) o pH 5.2 (C) en H_2O.

[45] Presentaremos aquí tan solo un resumen de estas asignaciones. Una explicación detallada de las mismas puede encontrarse en los capítulos 3 y 5.

Las señales a y b se encuentran relacionadas a través de conectividades NOE a pesar de su gran anchura (Figs. 3:5B, 5:4C y 5:5A,B). Ello indica su correspondencia con protones muy cercanos entre sí, como son dos protones geminales. Dado su gran desplazamiento isotrópico, que indica la existencia de una fuerte coordinación al metal, y debido a las conectividades NOE que presentan con protones de la Gln121 en la Ni(II)-azurina M121Q (ver mas adelante), asignamos estas señales a los protones β de la Cys112.

En los espectros NOE 1D y 2D se observa la presencia de conectividades intensas de dos señales a campo bajo con otras dos situadas a campo alto (Figs. 3:5, 3:7, 5:4A, 5:5F y 5:6). Estos pares de señales deben de corresponder a pares de protones geminales. Las señales e y l presentan además conectividades con protones lábiles que se canjean lentamente con el disolvente (Figs. 3:5D,E y 3:7B), por lo que su asignación a los protones alfa de la Gly45, muy cercanos a los protones amida de Gly45 e His46, se presenta como la única posibilidad de acuerdo con la estructura de la azurina. Por otro lado, como ya hemos adelantado, algunas de estas señales corresponden a la Met121, puesto que no aparecen en el espectro del mutante M121Q. La presencia de conectividades NOESY y COSY entre estas señales y las señales q y r (Fig. 3:5 y Fig. 3:8, pág. 81), así como la existencia de otras conectividades NOESY entre alguna de estas señales y la señal característica correspondiente al grupo Met121 $C_\varepsilon H_3$ (Fig. 3:5), está de acuerdo con la asignación de este residuo en base a la comparación de los espectros de las azurinas wt y M121Q, y permite además la asignación estereoespecífica de estas señales (Tabla 5:3, pág. 165).

Las señales u y x de la azurina M121Q presentan un patrón muy parecido al de las señales correspondientes a los protones γ de Met121 en la azurina wt (Fig. 5:6). Además, como ya se ha indicado, estas aparecen relacionadas mediante NOE con las señales de los protones β de la Cys112 (Fig. 5:5A,B). Por lo tanto, las señales u, x, así como otras relacionadas con ellas mediante conectividades NOESY (Fig. 5:6), son asignadas a protones de la Gln121. También es asignada a este residuo la señal canjeable y, que a pesar de no estar conectada mediante NOE con el resto de señales de la Gln121 presenta unas características similares a estas[46]. Estas asignaciones, y otras de residuos no coordinados, se encuentran recogidas en las Tablas 3:2 (pág. 84) y 5:3 (pág. 165).

[46] Para ser probada como cierta esta asignación, debería observarse un NOE entre las señales x e y, lo cual no es posible, dada su proximidad. Sin embargo, un grupo de señales de características similares se observa también en la Co(II)-azurina M121Q, donde sí se encuentra tal conectividad (Fig. 5:10, pág. 170).

Estructura de rayos X.

El análisis cristalográfico de la estructura de la azurina de Ni(II) a 2.05 Å de resolución revela que la estructura global de la proteína no es perturbada por el cambio del metal. Al igual que en la azurina de cobre, hay 4 moléculas cristalográficamente independientes por unidad asimétrica, de manera que los cuatro monómeros están organizados a su vez en un dímero de dímeros[16,9b] (Fig. 3:13, pág. 96). La superposición de las coordenadas de la cadena principal de las azurinas de Ni(II) y Cu(II) dio como resultado un valor de desviación r.m.s de 0.16 Å. El valor final de R para 31439 reflexiones entre 8.0 Å y 2.05 Å de resolución fue 0.179. En el modelo final, las desviaciones r.m.s. de la geometría standard fueron 0.012 Å para las distancias de enlace y 2.7° para los ángulos de enlace.

Las mayores diferencias entre las azurinas de Ni(II) y Cu(II) se sitúan en el centro metálico, tal y como puede observarse en un mapa de diferencia Fourier obtenido con coeficientes y fases de la azurina de cobre[9b] (Fig. 3:14, pág. 97). La diferencia mas significativa la constituyen dos lóbulos de densidad 12σ positiva y negativa vistos por encima y por debajo del plano ecuatorial definido por los ligandos N^{δ}_{His46}, N^{δ}_{His117} y S^{γ}_{Cys112}. El ion níquel(II) se ha desplazado alejándose del ligando S^{δ}_{Met121}, a la vez que se acerca al oxígeno carbonílico de la Gly45, quedando situado a 0.18 Å por enzima del plano ecuatorial. Adicionalmente, la Gly45 contribuye a su acercamiento al metal con un desplazamiento de 0.25 Å (Fig. 3:15, pág. 98). En conjunto, estas pequeñas reorganizaciones producen un acortamiento de la distancia metal-O_{Gly45} desde 2.97 Å en la azurina de Cu(II)[9b] a 2.46 Å en la azurina de Ni(II). Paralelamente, la distancia Ni(II)-S^{δ}_{Met121} se alarga hasta 3.30 Å, 0.15 Å más que en la Cu(II)-azurina[9b] pero 0.1 Å menos que en el caso de la Zn(II)-azurina[11a]. Estas últimas variaciones están próximas al error estimado a partir de una representación de Luzzati (0.2 Å), aunque en el caso de la esfera de coordinación los errores son menores (0.08 Å en las distancias y 3° en los ángulos), según se desprende del análisis de la diferencia entre las cuatro moléculas cristalográficamente independientes. Las distancias del metal a los otros tres ligandos: His46, His117 y Cys112, cambian muy poco con respecto a la azurina de cobre (Fig. 3:16 y Tabla 3:5, pág. 99; Tabla 3:6, pág.103).

Medidas de susceptibilidad magnética.

La variación de la susceptibilidad paramagnética molar χ_M y del momento magnético efectivo μ_{eff} de la Ni(II)-azurina de *Pae* con la temperatura obedecen la ley de Curie entre 120 y 30 K, conduciendo a un valor constante de $\mu_{eff} \approx 2.8$ μ_B, de acuerdo con un estado fundamental $S=1$. Por debajo de 30 K, el

momento magnético disminuye alcanzando un valor de 1.8 μ_B a 5 K. (Fig. 3:17, pág. 107) Esta desviación de la ley de Curie indica la existencia de desdoblamiento a campo cero del estado triplete.

El comportamiento magnético ha sido analizado considerando las ecuaciones 3:1 y 3:2 (pág. 108). Del mejor ajuste de los datos a la curva teórica 3:2 se obtuvo un valor de desdoblamiento a campo cero D_S=17.7 (1) cm^{-1} y un factor g isotrópico g_S=1.98 (0.1). Teniendo en cuenta los valores de *D* determinados para varios complejos pseudo-tetraédricos y octaédricos distorsionados, el aquí obtenido para la Ni(II)-azurina resulta ligeramente bajo con respecto a los valores normales en complejos tetraédricos (30-50 cm^{-1}) y se sitúa entre los correspondientes a simetrías tetraédrica y octaédrica distorsionada[47].

b) Azurina de cobalto(II).

Las azurinas wt de Co(II) de *Pae* y *Ade* presentan prácticamente el mismo espectro UV-vis (Fig. 1:5B, pág. 30 y Fig. 5:2A, pág. 156). Al igual que en los derivados de Ni(II), estos espectros se caracterizan por la presencia de dos bandas intensas de transferencia de carga S^{γ}_{Cys}-metal, en este caso entre 300 y 400 nm, con coeficientes de extinción molar de 1500 a 4000 M^{-1} cm^{-1}. El espectro correspondiente al mutante M121Q de *Ade* es también muy similar, aunque las bandas de transferencia de carga ligando-metal se encuentran desplazadas 15-20 nm hacia valores de energía mas altos (Fig. 5:2A, Tabla 5:1, pág. 157). Las transiciones d-d, situadas entre 500 y 650 nm, son también características y relativamente intensas, con coeficientes de extinción de hasta 600 $M^{-1}cm^{-1}$.

RMN de protón.

Los espectros de RMN de los derivados de cobalto de las azurinas silvestres de *Pae* y *Ade*, así como el correspondiente al mutante M121Q, se muestran en la figura III. Como ya veíamos en el caso de los derivados de Ni(II), los espectros correspondientes a ambas azurinas wt son muy similares, y las diferencias con respecto al espectro de la azurina mutante M121Q han de deberse a la sustitución del aminoácido en posición 121. Por otro lado, también en este caso, el espectro de la Co(II)-azurina de *Pae* varía con el pH en condiciones de canje lento,

---

[47] a) Frydendahl, H., Toftlund, H., Becher, J., Dutton, J.C., Murray, K.S., Taylor, L.F., Anderson, O.P. & Tieking, E.R.T. (1995) *Inorg. Chem. 34*, 4467, and references within. b) Kowal, A.T., Zambrano, I.C., Moura, I., Moura, J.J.G., LeGall, J. & Johnson, M.K. ((1988) *Inorg. Chem.*, *27*, 1162.

encontrándose un pK_a=5.7±0.1 (Figs. 4:4 y 4:5, pág. 119). Los espectros de ambas azurinas de *Ade* (wt y mutante M121Q) no muestran tal transición con el pH, aunque al igual que en la azurina de *Pae*, una de los dos señales intercambiables presentes a campo bajo (la señal b) desaparece a pH alto, por lo que es asignada al protón $N_{\varepsilon 2}H$ de la His 117 como en el caso de los derivados de Ni(II).

El resto de las asignaciones de señales se realizan mediante espectros NOESY, NOE 1D, COSY y TOCSY (Figs. 4:6–4:13, págs. 121–131; Figs. 5:8–5:11, págs. 168–171) , siguiendo un razonamiento paralelo al ya explicado anteriormente para los derivados de Ni(II). Estas asignaciones se resumen en las Tablas 4:2 (pág. 132) y 5:4 (pág. 172) y su seguimiento de forma detallada puede encontrarse en los capítulos 4 y 5.

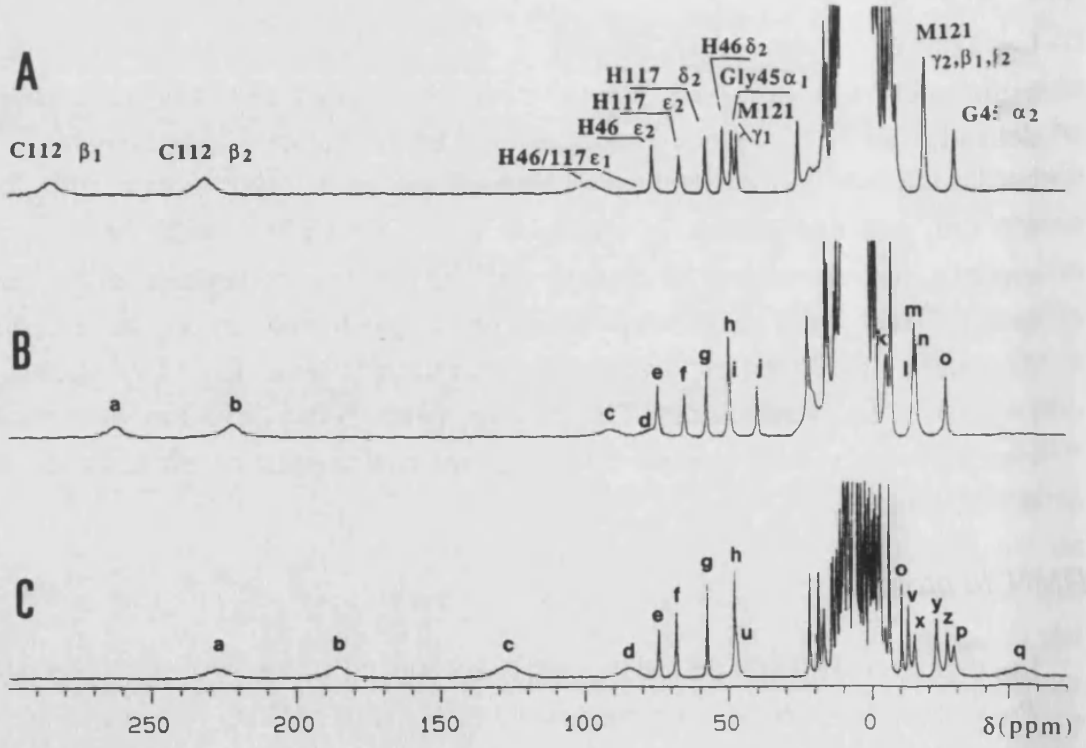

Figura III. Espectros de RMN de protón (300 MHz, H_2O, 37 °C, pH 4.5) de los derivados de Co(II) de la azurina silvestre de *Pseudomonas aeruginosa* (A) y de las azurinas silvestre (B) y mutante M121Q (C) de *Alcaligenes denitrificans*.

Espectros de EPR.

El espectro de EPR a 5K muestra un patrón típico de Co(II) de alto spin con una geometría axial distorsionada, en el cual la señal perpendicular aparece dividida en dos componentes indicando la existencia de distorsión rómbica (Fig. 4:19, pág. 149). Los valores efectivos de g son 5.91 (g_y), 3.77 (g_x) y 2.01 (g_z) a pH 7.5, y 5.20 (g_y), 3.85 (g_x) y 2.0 (g_z) a pH 4.5. Estos espectros son consistentes con un valor de S=3/2 y la existencia de desdoblamiento a campo cero, donde sólo es resonante el doblete de Kramers (±1/2) identificado a partir de los valores efectivos de g. El valor medio de g calculado es ~2.3, de acuerdo con la existencia de acoplamiento spin-órbita de segundo orden y de un estado fundamental orbitalmente no degenerado.

Cuando la temperatura aumenta desde 5 a 20 K, la intensidad de las señales varia encontrándose un máximo de intensidad a 10 K. El hecho de que se observe la misma variación de la intensidad para las tres señales, confirma la existencia de anisotropía rómbica del único doblete (±1/2). Por otro lado, la existencia de un máximo de intensidad muestra que este doblete es el excitado, y por lo tanto, el desdoblamiento a campo cero predominante es negativo. El valor del parámetro de desdoblamiento D puede ser evaluado teniendo en cuenta la dependencia de la intensidad de las transiciones con la temperatura, de acuerdo con la distribución de Boltzman de los dos nivelas de Kramers (±1/2) y (±3/2) asociados con el estado fundamental S=3/2 (ecuación 4:1). Según este tratamiento, se calcula un valor de D=-3.5 cm^{-1} (ver esquema de la página 148).

V. Discusión.

a) Cobalto y níquel como sondas espectroscópicas de las proteínas azules de cobre.

El estudio de los espectros electrónicos de derivados de Ni(II) y Co(II) ha sido frecuentemente utilizado para analizar las propiedades electrónicas y estructurales de los centros de cobre de tipo 1, puesto que las bandas de transferencia de carga y las d-d se encuentran normalmente bien separadas en estos sistemas[5,6]. En este estudio, los espectros UV-vis nos permiten distinguir claramente las azurinas silvestres del mutante M121Q, donde la diferencia fundamental con respecto a las primeras es un desplazamiento de las bandas hacia valores más energéticos. Esta diferencia puede también ser observada en los espectros de los correspondientes derivados "naturales" de cobre[17].

Los estudios de EPR de la azurina de cobalto y de susceptibilidad magnética de la azurina de Ni(II) permiten una descripción de la estructura electrónica de los centros metálicos, que sin embargo, no llega a ser lo suficientemente completa como para ayudar a distinguir entre las geometrías tetraédrica y pentacoordinada de bipirámide trigonal. Los estudios de RMN parecen, sin duda alguna, mucho más significativos por la cantidad de la información que aportan, que puede utilizarse para extraer conclusiones sobre las propiedades estructurales y dinámicas de la proteína. Pero para ello, resulta imprescindible una asignación correcta de las señales del espectro. La utilización de la metodología convencional en sistemas paramagnéticos está sometida a importantes limitaciones, debido a los grandes desplazamientos de las señales y a su elevada velocidad de relajación[7,34b]. Por ello, se han desarrollado durante los últimos años estrategias especiales para estos casos, las cuales han sido utilizadas en este trabajo[7b,34b,48]. Así, dada la dificultad para obtener correlaciones por acoplamientos de contacto entre las señales mas paramagnéticas, estas asignaciones se han llevado a cabo utilizando principalmente conectividades dipolares conseguidas a través de espectros NOE 1D y NOESY. Estos datos pueden interpretarse de forma independiente en algunos casos, como cuando las distancias calculadas por NOE pueden hacerse corresponder con distancias estándar, como son las distancias entre protones geminales o las distancias entre protones vecinales en anillos imidazol de histidina. En otros casos, sin embargo, es necesario disponer de información estructural, procedente en general de difracción de rayos X, de la misma proteína

[48]Luchinat, C. & Piccioli, M. (1995) in *Nuclear Magnetic Resonance of Paramagnetic Macromolecules, seriesC: Mathematical and Physicals Sciences* (La Mar, G.N., ed.) vol. 457, p. 1, Kluwer Accademic Publishers, Dordrecht.

o al menos de una proteína análoga, como puede ser un derivado metálico diferente[9,11,15]. Tal información estructural ayuda a interpretar las conectividades dipolares obtenidas y a asignar los protones implicados. En este caso hemos utilizado las estructura de las azurinas wt de Cu(II)[9] y Ni(II)[15], la segunda de ellas resuelta como parte de este trabajo, así como la estructura de la azurina M121Q de Cu(II)[17]. Otras asignaciones han podido realizarse de forma convencional, es decir, caracterizando sistemas de spin completos a través de espectros TOCSY y asignando éstos específicamente con ayuda de espectros NOESY[49]. La obtención de conectividades dipolares entre alguno de estos sistemas de spin y otros asignados en base sólo a conectividades NOE sirve para contrastar las asignaciones de todos ellos.

Por último, en unos pocos casos se han realizado asignaciones en base a la interpretación de las propiedades de relajación en términos de distancias protón-metal. Tales asignaciones deben considerarse sólo a nivel tentativo, debido al importante margen de error al que está sometida la aplicación de la ecuación de Solomon[50], por el desconocimiento del valor exacto del tiempo de correlación, así como por el error intrínseco en el cálculo de los tiempos de relajación y por la posible existencia de una deslocalización electrónica importante sobre los ligandos del metal.

b) El centro metálico en las azurinas de níquel y cobalto.

Al hablar de la estructura del centro metálico en azurinas metalosustituidas, hemos de empezar analizando la estructura cristalográfica de la azurina de níquel. Como puede observarse si comparamos la estructura de las azurinas de cobre[9] y níquel, el centro metálico es mas tetraédrico en esta última. Así, la distancia metal-O_{Gly45} ha disminuido desde 2.97 Å a 2.46 Å en la azurina de níquel, mientras que la distancia metal-S^{δ}_{Met121} se incrementa hasta 3.30 Å (ver Tabla 3:6 en pág. 103). Según estos resultados, el centro metálico en Ni(II)-azurina sería bastante parecido al de la azurina de cinc[11] (Tabla 3:6), el cual ha sido descrito como tetraédrico distorsionado, y podemos también admitir que la azurina de cobalto presentaría una geometría de coordinación similar a ambos metaloderivados, tal y como se desprende de la comparación de las distancias protón-metal obtenidas a partir de los tiempos de relajación de protones de diversos residuos alrededor del metal (ver Fig. 4:15, pág. 140 y Tabla 4:3, pág. 139).

---

[49] Wüthrich, K. (1986) *NMR of proteins and nucleic acids*, John Wiley & Sons, New York.

[50] a) Bloembergen, N., Purcell, E.M. & Pound, R.V. (1948) *Phys. Rev. 73*, 679. b) Solomon, I. (1955) *Phys. Rev. 99*, 559. c) Bloembergen, N. & Morgan, L.O. (1961) *J. Chem. Phys. 34*, 842. d) Koening, S.H. (1982) *J. Magn. Reson. 47*, 441.

La intensidad de las transiciones d-d en complejos de cobalto puede relacionarse con la geometría de coordinación del centro metálico. Esta intensidad es muy parecida en las azurinas wt y el mutante M121Q, donde los coeficientes de extinción molar se encuentran claramente en el intervalo típico de complejos de Co(II) tetraédricos (ε_{max}>250 $M^{-1}cm^{-1}$)[51]. Esta interpretación está de acuerdo con las estructuras cristalográficas de los derivados de Ni(II) y Zn(II) de la azurina *Pae* wt y con la estructura de la Cu(II)-azurina M121Q[11b,15,17]. Por otro lado, el valor del desdoblamiento obtenido del espectro de EPR de Co(II)-azurina wt de *Pae* (-3.5 cm^{-1}) se encuentra más bien dentro del intervalo típico de los complejos tetraédricos de cobalto (establecido entre -36 y 13 cm^{-1})[52], aunque según ha sido descrito en otros casos, también podría tratarse de un centro con geometría tetraédrica cuya distorsión preserva una simetría próxima a la de bipirámide trigonal[53].

El valor de *D* obtenido del análisis de la dependencia con la temperatura de la susceptibilidad magnética en la azurina de Ni(II) (D =17.7 cm^{-1}) es intermedio entre los esperados para complejos tetraédricos y octaédricos de Ni(II)[47], sugiriendo la posible existencia de pentacoordinación, y por tanto de interacción del metal con la Met121. Una conclusión similar se extrae del estudio de la Ni(II)-azurina por RMN. La presencia de desplazamientos isotrópicos importantes en las señales de los cinco residuos potencialmente coordinados al metal, indica la existencia de contribución de contacto, y por tanto coordinación, en todos ellos. A pesar de que existe una contribución de pseudocontacto importante, tal y como demuestra el comportamiento de los desplazamientos isotrópicos con la temperatura (Fig. 3:4, pág. 76), que sería debido a la presencia de anisotropía magnética en este centro metálico, la magnitud de los desplazamientos isotrópicos de algunas de las señales de la Met121 (111 ppm para el protón γ_1 a 45 °C) parece demasiado grande como para deberse sólo a un efecto dipolar. De la misma forma, en los espectros de RMN de las azurinas wt de cobalto se observa un desplazamiento isotrópico de las señales de Met121, que estarían indicando la posible existencia de coordinación a este residuo. Sin embargo, si comparamos las señales de la Met121 con las de la Cys112, donde la coordinación al metal es sin duda fuerte, queda claro que de existir interacción de contacto en el caso de la Met121, ésta habría de ser muy débil. Una conclusión similar puede extraerse de la comparación de los espectros de RMN

[51] a) Rosenberg, R.C., Root, C.A., Wang, R.-H., Cerdonio, M. & Gray, H.B. (1973) *Proc. Natl. AAcad. Sci. U.S.A. 70*, 161. b) Bertini, I. & Luchinat, C. (1984) in *Advances in Inorganic bBiochemistry* (G.L. Eichorn & L.G. Marzilli, eds) p. 71, Elsevier, New York.

[52] Makinen, M.W., Kuo, L.C., Yim, M.B., Wells, G.B., Fukuyama, J.M. & Kim, J.E. (1985) *J. AAm. Chem. Soc. 107*, 5245.

[53] Banci, L., Bencini, A., Benelli, C., Gattesci, D. & Zanchini, C. (1982) *Structure and Bonding 552*, 37.

de protón de los derivados de cobalto de las azurinas wt con el espectro correspondiente a la Co(II)-amicianina (Fig. 5:12, pág. 177), donde al no existir un oxígeno carbonílico axial en posición opuesta al S^{δ} de metionina, el metal se coordina claramente a este último ligando[54].

A la vista de los presentes resultados, parece evidente la existencia de una cierta contradicción, motivada fundamentalmente por la posibilidad de coordinación de los iones metálicos Ni(II) o Co(II) al S^{δ} de la Met121, siendo a la vez la distancia metal-ligando en estos casos demasiado grande para tal interacción. Un análisis profundo de las contribuciones de contacto y pseudocontacto a los desplazamientos isotrópicos de ambos metaloderivados de azurina podría aclarar este punto. Tal separación de contribuciones puede realizarse si se conocen las componentes y la dirección del tensor de anisotropía magnética, para lo cual sería necesario un estudio de susceptibilidad magnética de monocristal[7a]. Alternativamente, podría utilizarse un conjunto suficiente de desplazamientos isotrópicos únicamente de pseudocontacto, que con ayuda de la estructura de la metaloproteína podrían utilizarse para extraer la información necesaria acerca del tensor de susceptibilidad magnética[7b].

c) Cambio conformacional y otros efectos asociados al pH.

Como se ha indicado, los derivados de Ni(II) y Co(II) de la azurina-wt de *Pae* presentan una transición conformacional con el pH que puede ser observada en los espectros de RMN de ambos metaloderivados y en el espectro de EPR de la azurina de Co(II). El espectro de RMN de la azurina de cobalto muestra que el efecto observado se debe al equilibrio de desprotonación de la His35 y permite calcular, mediante experimentos de transferencia de saturación (Fig. 4:8A, pág. 122; ecuación 2:10, pág.61), una velocidad de canje igual a 3.0 sec^{-1}, de acuerdo con los valores obtenidos en el caso de la azurina nativa de Cu(II) por métodos cinéticos[26]. Por otrol lado, el valor de pK_a determinado en este estudio es ligeramente inferior al de la azurina de Cu(II) (5.9 para la Ni(II)-azurina y 5.7 para la Co(II)-azurina, frente a 6.5 en el caso de la Cu(II)-azurina[55]). Tal diferencia podría interpretarse en el mismo sentido en que ha sido explicada la diferencia en este pK_a entre las azurinas de Cu(II) y Cu(I), es decir, debido a un efecto electrostático[55]. Así pues, el hecho de que la distancia entre el metal y el grupo $N_{\delta 1}H$ de His35, el cual sufre la desprotonación, sea 0.25 Å menor en la azurina de Ni(II) que en la de Cu(II), según la estructura de rayos X de ambas proteínas[9b,15], explicaría la existencia de un menor pK_a en la primera. Por otro lado, la existencia de valores de pK_a similares en las azurinas de Ni(II) y de

[54] Salgado, J. & Kalverda, A., resultados no publicados.

[55] van de Kamp, M., Canters, G.W., Andrew, C.R., Sanders-Loehr, J., Bender, C.J. & Peisach, J. (1993) *Eur. J. Biochem. 218*, 229.

Co(II), puede ser una indicación más de la similitud estructural en ambas proteínas.

A pesar de que la ionización de la His35 afecta a los desplazamientos isotrópicos de las señales de los residuos coordinados, el hecho de que los tiempos de relajación de estas señales no varíen significativamete (Tabla 3:3, pág. 92) indica que las distancias protón-metal permanecen esencialmente constantes al cambiar el pH. Por lo tanto la transición conformacional no se extiende al centro de coordinación del metal. Esta conclusión es concordante con el estudio de la estructura cristalográfica de la azurina a varios valores de pH, donde se observa que el efecto de la desprotonación de la His35 tiene tan solo una consecuencia local y afecta únicamente al entorno más inmediato de este residuo de aminoácido (Fig. 4:16, pág. 143)[9b].

Otro efecto importante del pH en los espectros de RMN de los derivados de Ni(II) y Co(II) de todas las azurinas estudiadas, tanto de *Pae* como de *Ade*, así como del mutante M121Q de *Ade*, es el aumento de la velocidad de canje del protón $N_{\varepsilon 2}H$ de la His117 al aumentar el pH, que conduce a la no observación de éste a pH alto por encontrarse en condiciones de canje rápido con el disolvente. La velocidad de canje de este protón puede calcularse a la temperatura de coalescencia (Fig. 4:18, pág. 145) a partir de la diferencia en Hz entre la posición de su señal y la señal correspondiente agua, teniendo en cuenta además que la concentración de la proteína resulta despreciable frente a la del disolvente[56]. Así, el tiempo de vida τ definido en la relación 2:13 (pág. 63) tendría el valor $\sqrt{2}/\pi\Delta\nu$, y por lo tanto la constante de canje k_A en la dirección del disolvente seria $k_A = P_B/\tau_{cc} = \pi\Delta\nu/\sqrt{2} = 5.3 \times 10^4$ sec^{-1}, siendo $P_B \approx 1$ la fracción molar de protones del disolvente (ver ecuación 2:12, pág. 62 y Fig. 2:6, pág. 63)[56]. La velocidad de canje calculada, a pesar de ser elevada, no invalida el mecanismo propuesto de autotransferencia electrónica en azurina, ya que la velocidad de autotransferencia electrónica es aún dos órdenes de magnitud mayor[57]. Según este mecanismo, el electrón "viajaría" de una molécula de azurina a otra a través de un sistema de puentes de hidrógeno, en el que participan las His117 coordinadas de dos azurinas que interaccionan por sus patch hidrofóbicos y dos moléculas de agua bien definidas en la estructura cristalográfica de la azurina (Fig. 4:17, pág. 144)[16].

---

[56]a) Sandström, J. (1982) *Dynamic NMR spectroscopy*, Academic Press, New York. b) Shanan-Atidi, H. & Bar-Eli, K.H. (1970) *J. Phys. Chem. 74*, 961.

[57]Groeneveld. C.M. & Canters, G.W. (1985) *Eur. J. Biochem. 153*, 559.

d) El mutante M121Q y el centro metálico en estelacianina.

La coincidencia entre los espectros electrónicos y de EPR de la estelacianina y la azurina M121Q fue utilizada como un argumento sólido en defensa de la coordinación de la Gln97 en la estelacianina[17]. Los espectros UV-vis de los derivados de Ni(II) y Co(II) de la azurina-M121Q son también muy similares a los espectros correspondientes de la estelacianina[5a,58]. Los desplazamientos de las bandas de transferencia de carga hacia valores de mayor energía en la azurina mutante, con respecto a las bandas de la azurina-wt, están de acuerdo con una mayor fuerza del campo de ligandos, y por lo tanto con una coordinación de la Gln121 a través del oxígeno carbonílico de la cadena lateral[6c]. Esta misma conclusión se desprende del estudio de los espectros de RMN de los derivados de Ni(II) y Co(II) de esta proteína mutante, donde las señales correspondientes a la Gln121, y en especial la señal de un protón del grupo $N_{\varepsilon 2}H_2$ de este residuo, indican también coordinación a través del carbonilo.

Por otro lado, se aprecian diferencias importantes en las resonancias de los ligandos ecuatoriales entre los derivados metálicos, especialmente los de Co(II), de las azurinas wt y la azurina M121Q. Es de destacar, principalmente, la disminución de los desplazamientos isotrópicos de los protones β de la Cys112 en la azurina mutante, que indicarían la existencia de un menor solapamiento entre los orbitales del metal y del S^{γ}_{Cys112}, como consecuencia de un desplazamiento del ión metálico fuera del plano ecuatorial. Curiosamente, el mismo comportamiento de las señales de la cisteina coordinada es observado en el espectro de RMN de la estelacianina de cobalto[59], lo cual sugiere que ambas proteínas presentan centros metálicos muy similares. Desafortunadamente, no podemos extender la comparación a las señales de la glutamina, pues estas no han sido aún asignadas en el espectro de la estelacianina de Co(II).

---

[58]Lum, V. & Gray, H.B. (1981) *Isr. J. Chem. 21*, 23.

[59]Vila, A.J. (1994) *FEBS Lett. 355*, 15.

VI.Conclusiones.

La utilización de los iones metálicos Ni(II) y Co(II) como sondas del centro metálico en proteínas azules de cobre, a través principalmente de la RMN de paramagnéticos, ha demostrado ser de gran ayuda para la investigación de las propiedades estructurales de estas proteínas. El estudio de las señales isotrópicamente desplazadas proporciona importante información acerca de la primera esfera de coordinación, tal como la identificación de los ligandos coordinados, la geometría de coordinación y la fuerza de la interacción metal-ligando. Por otro lado, el incremento en la sensibilidad de las señales desplazadas isotrópicamente a cualquier cambio en el entorno de sus protones correspondientes, permite detectar y analizar incluso pequeñas variaciones estructurales. Tal y como demuestran los datos presentados aquí, así como los publicados por otros autores[11], la estructura de diversos derivados metálicos de azurina permanece prácticamente invariable con respecto a la estructura de la azurina de cobre, con la excepción de pequeñas diferencias en la geometría de coordinación del metal.

Los espectros de RMN de protón de los derivados de Ni(II) y Co(II) de proteínas azules de cobre con entornos de coordinación similares, tales como las azurinas wt de *P. aeruginosa* y *A. denitrificans*, son también muy parecidos y pueden ser considerados como una "huella dactilar" de dicho entorno de coordinación. Las características más importantes de estos espectros son: i) la presencia de desplazamientos isotrópicos elevados en las señales de los protones β de la cisteina coordinada, que indican la existencia de importante deslocalización de spin desapareado, y por tanto una fuerte coordinación de este residuo al metal; ii) el patrón de resonancia de las señales de grupos CH_2 de los ligandos en posición axial (el grupo $C_\alpha H_2$ de la Gly45 y el $C_\gamma H_2$ de la Met121), en los cuales uno de los protones aparece a campo alto mientras que el otro se desplaza hacia campo bajo; iii) el patrón de resonancia de las señales de las histidinas coordinadas, especialmente la observación de los dos grupos $N_{\varepsilon 2}H$ correspondientes a ambas histidinas a pH bajo, pero tan solo el correspondiente a la His46 a pH alto.

Los centros metálicos con geometrías intermedias entre tetra y pentacoordinación, son difíciles de evaluar y a menudo dan lugar a contradicciones aparentes. El sitio metálico de la azurina representa uno de estos casos, donde la existencia de dos posibles ligandos axiales en posiciones opuestas y tres ligandos ecuatoriales fuertemente coordinados va a condicionar la coordinación del metal. Así, mientras que en la azurina de cobre la Gly45 puede ser considerada fuera de la esfera de coordinación, en las azurinas de Zn(II), Ni(II), y probablemente Co(II), es la coordinación de la Met121 la que resulta

dudosa. De acuerdo con la estructura de la Ni(II)-azurina, el sitio metálico es tetraédrico y la Met121 no estaría coordinada. Sin embargo, tanto en este metaloderivado como en la Co(II)-azurina existen indicios, a través fundamentalmente de los espectros de RMN, de una posible coordinación débil de este residuo. Una interpretación mas precisa requiere de un estudio profundo que lleve a la separación de las contribuciones de contacto y pseudocontacto en los protones de los ligandos supuestamente coordinados.

En cuanto a los efectos del pH en la azurina, podemos distinguir claramente dos: un cambio conformacional local provocado por la desprotonación de la His35 en la azurina de *Pae* y el aumento de la velocidad de canje del protón $N_{\varepsilon 2}H$ de la His117 a pH alto. Del primero calculamos una velocidad de canje consistente con otros valores determinados para la azurina de cobre. En cuanto al segundo, es importante puesto que al conjunto His117 $N_{\varepsilon 2}H$---H_2O se le ha otorgado un papel decisivo como "via de paso" del electrón en el proceso de autotransferencia electrónica. Sin embargo, aún cuando el protón $N_{\varepsilon 2}H$ de la His117 se intercambia rápidamente con el disolvente en la escala de tiempos de RMN, esta velocidad de canje es lenta si se compara con la de autotransferencia electrónica, dos órdenes de magnitud mayor.

Por último, diversas similitudes entre los derivados de Co(II) de la estelacianina y de la azurina M121Q indican que la coordinación del metal en ambas proteínas ha de ser muy similar y apoyan la coordinación de la Gln97 en estelacianina. No obstante, es necesario un estudio mas profundo de la estelacianina de cobalto para alcanzar una conclusión definitiva en este punto.

Agradecimientos • Acknowledgments.

Ciertamente una *Tesis Doctoral* requiere tal esfuerzo de dedicación, durante tanto tiempo, que probablemente termine por cambiarle a uno la vida. Aunque tal vez sea eso lo que se pretende, para llegar a ser finalmente *Doctor*, yo sólo espero que a mí no me haya cambiado demasiado.

Pero como en cualquier otra experiencia vital, sois los que habéis estado a mi lado durante estos largos años los que habéis hecho que todo esto haya valido la pena. Quiero por ello recordaros aquí y expresaros mi más sincero agradecimiento, empezando de forma muy especial por José M. Moratal (*Pepe*), por darme la oportunidad de trabajar con él y por la paciencia y dedicación que siempre ha demostrado conmigo. También quiero agradecer su ayuda a Antonio Donaire, con quien he aprendido tantas cosas, y al resto de los que son o han sido compañeros de grupo: Hermas, Rosario, Josep, Mª José, Fernando, Cristina, Eva y Mikel. Igualmente agradezco a los miembros del *Departamento de Química Inorgánica* su acogida y apoyo, en especial a Juanjo, Rafa, Eduardo, Juan Cano, Carlos Gómez, Marina, Maribel, Delfi, Alicia, J.V. Folgado, Eugenio, Miquel Julve, Quique García-España, Paco Esteban, José Antonio, Pascual Lahuerta y Merche Sanau. A los miembros del *Instituto Agroquímico y de Tecnología de Alimentos* les agradezco el haberme facilitado una "mili" llevadera, muy especialmente a Julio Polaina y a su grupo: Cristina, Marta, Alejo, Juan Luis y José Luis. Y como no, un recuerdo muy especial para mis fieles amigos: Julian, Berni, Luismi, Aurora, Esteve, Ana, Montse, Paco, Sara, Helena, Carlos, Peter, Eraci, Alex, Luis, y a mis sufridos compañeros de piso: Gloria y Carlos.

I also gratefully acknowledge Antonio Romero (Instituto de Química Física "Rocasolano", Madrid) for the X-ray structure of Ni(II)-azurin, Irene Morgenstern-Badarau (Paris-sud-XI University) for the magnetic susceptibility and EPR measurements, Herbert Nar (Max-Planck Institute, Martinsried) for making me available the azurin coordinates, and Gerard Canters, Sandra Kroes, Gertrud Warmerdam, Arnout Kalverda and the whole Metalloprotein Group at Leiden University for their help with the isolation of proteins and their hospitality.

Finally, helpful discussions are acknowledged from J. M. Moratal, H. Jiménez and A. Donaire (Valencia); C. Luchinat and M. Piccioli (Florence); G. Canters, S. Kroes, C. Dennison, A. Kalverda and G. van Pouderoyen (Leiden); and A. Vila (Rosario, Argentina).

UNIVERSIDAD DE VALENCIA FACULTAD DE CIENCIAS QUÍMICAS

Reunido el Tribunal que suscribe, en el día de la fecha, acordó otorgar, por unanimidad, a esta Tesis doctoral de D. JESUS SALGADO BENITO la calificación de APTO "CUM LAUDE"

Valencia, a 17 de Noviembre de 1995

El Secretario,

El Presidente

UNIVERSITAT DE VALÈNCIA BURJASSOT FACULTAT DE CIÈNCIES QUÍMIQUES